TGFβ signalling and cell cycle regulation during early follicle development

By

Sofia Granados Aparici

A thesis submitted in partial fulfilment of the requirements for the degree of Doctor of Philosophy

Department of Oncology and Metabolism

July 2017

Academic Unit of Reproductive and Developmental Medicine

Elles, xiuxiuejen paraules "de-salaes"
Jo, l'inhale i perd la consciència

L'inhale tan fort que sent que mor

Pero en canvi, torne a nàixer
Ella, tot i que la ferim, encara ens engronsa

ABSTRACT

In the mammalian ovary, little is known about the mechanisms that maintain the relatively quiescent phenotype in primordial follicles or trigger primordial follicle activation (PFA). Previous studies in our lab showed the TGFβ mediator and transcription factor SMAD2/3 are detectable in granulosa cells (GCs) of primordial follicles. Since cell proliferation involves cell cycle progression, this thesis sought to investigate whether SMAD2/3 regulates the expression of MYC oncogene and the cell cycle genes CCND2 and p27 in GCs in the mouse ovary, and whether this regulation is associated with the maintenance and activation of primordial follicles. Therefore, the first part of this thesis focused on the expression and localisation of these factors throughout the stages of early follicle development. SMAD3, CCND2 and p27 proteins co-localised in GC nuclei of primordial follicles while expression of each decreased in growing follicles. Furthermore, using co-immunoprecipitation, CCND2 and p27 proteins associated in complexes in samples enriched in primordial follicles, and these complexes were lost in growing follicles, suggesting CCND2/p27 protein dynamics contributes to the maintenance of GC cell cycle arrest. Using ChIP-qPCR on immature mouse ovaries enriched with different proportions of small follicles, SMAD3 bound to the promoter of *Ccnd2* and *Myc*, but not *p27*. Gene expression analysis using qPCR revealed that *Ccnd2* was relatively higher in ovaries containing mostly primordial follicles, while *Myc* was relatively higher in older aged ovaries with many growing follicles. This suggests that SMAD3 promoted and repressed the expression of these genes, respectively. With this evidence, the effect of brief exposure to TGFβ1 ligand and TGFβ-receptor inhibitor on SMAD3-dependent regulation of cell cycle genes and PFA was examined in a validated neonatal mouse ovary culture model. TGFβ1 ligand increased *Ccnd2* and *Myc* genes, while the inhibitor had no effect. SMAD3 binding to both genes was unchanged after any of the treatments; however, elevated pERK and pAKT indicated that changes in gene expression may be due to non-canonical TGFβ signalling. TGFβ1 ligand had a small influence on promoting PFA whereas the inhibitor caused a slight delay in GC proliferation and increased the presence of multi-oocyte follicles. Taken together, these findings suggest that basal TGFβ levels maintain the primordial follicle phenotype via the regulation of *Ccnd2* and *Myc* in GCs. Altering the balance of TGFβ exposure influences the expression of these genes and PFA. Understanding these molecular events may shed some light on the mechanisms leading to age-related infertility and ovarian dysfunctions from conditions such as POI or PCOS.

ACKNOWLEDGEMENTS

The development of this work during these 4 years has been an intense personal and professional learning process. I would like to express my gratitude to all the people who has been somehow involved in this part of my life.

First of all, I would like to thank my supervisor Dr. Mark Fenwick for being a good guide and for inspiring me with his knowledge. I really appreciate your critical thinking and your efforts to always make the most of my capacities. Specially, it has been a pleasure to discuss about real science with you. I would also like to thank my tutor Dr Colby Eaton for his intelligent advice and support during these four years.

To all the people from the AURDM. Special thanks to Sarah, your technical advice and help in the lab has been essential. Daniel, thanks for your company and support during the last year of effort. Nurul, thanks for sharing all the ups and downs of this long ride with me. Mari, it has been a pleasure to collaborate with you and have your help and feedback on the last steps of this experience.

To my Sheffield people. Thanks to Lucie, Silvia, Hannan and kids, Daria, Javier, Kostas, Pablo, Shillo, Pri, Ana, Laura, Jack and Diana. I take anywhere I go a little bit of each of you. Thanks for making this experience unforgettable.

Ara en la meua llengua. Gracies papa i mama. Gracies per creure en mi i educar-me d'una forma tan lliure i plena de valors meravellosos. Me donareu la vida una volta i me la doneu sempre que la necessite. Pablo, la meua gran espineta es estar lluny de tu. Pero sempre pense amb tu i t'estime inmensament. Som quatre!

Per ultim, Juan. Moltes gracies pel teu suport incondicional, en qualsevol forma i estat mental, pero sobretot, desde qualsevol cantonada d'aquest mon. Serem nomades pero "no hi havia a Valencia uns amants con nosaltres".

LIST OF PUBLICATIONS

Oral presentations and short communications

Granados Aparici, S. Foxl2 and Smad transcription factors during early follicle development: Localisation and regulation of target genes (2014). Three-minute thesis competition in Annual Symposium of the Academic Unit of Reproductive and Developmental Medicine. Sheffield, UK.

Granados Aparici, S*. Molecular mechanisms of ovarian follicle activation (2015). Three-minute thesis competition in Annual Symposium of the Academic Unit of Reproductive and Developmental Medicine. Sheffield, UK.

***This presentation was awarded first prize.**

Granados Aparici, S. The sleeping egg waiting for mysterious prince charming (2015). In Ignite Academy 2015. Sheffield, UK.

Granados Aparici, S., Sharum, I., Waite, S., Chapman, N & Fenwick, M. TGFβ signaling and cell cycle control during early ovarian follicle development (2016). In Medical School Research Meeting. Sheffield, UK.

Granados Aparici, S. & Fenwick, M. Evidence for TGFβ regulation of cell cycle genes in granulosa cells of primordial follicles (2016). In Annual Symposium of the Academic Unit of Reproductive and Developmental Medicine 2016. Sheffield, UK.

Granados Aparici, S. & Fenwick, M. Evidence for TGFβ regulation of cell cycle genes in granulosa cells of primordial follicles (2016). In National Ovarian Workshop (NOW) 2016. Cambridge, UK.

Granados Aparici, S.* & Fenwick, M. Evidence for TGFβ regulation of cell cycle genes in granulosa cells of primordial follicles (2016). In Fertility 2017. Edinburgh, UK.

***This presentation was awarded runner-up prize in Fertility 2017.**

Poster presentations

Granados Aparici, S., Sharum, I., Hardy, K., Franks, S., Waite, S., Chapman, N., & Fenwick, M. (2014). Foxl2 and Smad transcription factors during early follicle development: localisation and regulation of target genes. In Society for Reproduction and Fertility (SRF) and World Congress of Reproductive Biology joint meeting 2014 (WCRB). Edinburgh, UK.

Granados Aparici, S., Sharum, I., Hardy, K., Franks, S., Waite, S., Chapman, N., & Fenwick, M. (2015) Regulation of CyclinD2 by Smad3 and Foxl2 during early follicle development. In Society for Reproduction and Fertility (SRF) Annual Meeting. Oxford, UK.

Granados Aparici, S., Sharum, I., Hardy, K., Franks, S., Waite, S., Chapman, N., & Fenwick, M. (2015) Regulation of CyclinD2 by Smad3 and Foxl2 during early follicle development. In Medical School Research Meeting. Sheffield, UK.

Research collaboration

Warrander, F., **Granados Aparici, S.**, Cutting, R., Franks, S., Hardy, K., & Fenwick, M. (2015). Using RNA-interference as a tool to knock down gene expression in ex vivo cultures of small follicles. Oral presentation in Fertility 2015. Birmingham, UK

Sharum, I, S. **Granados Aparici, S.** & Fenwick, M. Serine/Threonine Kinase Receptor Associated Protein (Strap) inhibits early follicle development in mouse ovaries (2015). In Society for Reproduction and Fertility (SRF) Annual Meeting. Oxford, UK.

Novita Z. **Granados Aparici, S**. & Fenwick, M. Identification and regulation of Pmepa1 during early follicle development in the mouse ovary (2017). In Fertility 2017. Edinburgh, UK.

Herigstad, M., **Granados Aparici, S**., Pacey, A., Paley, M., Reynolds, S. Imaging Seminiferous Tubules in a Mouse Model at 9.4 T – Feasibility for In Vivo Fertility Research. Oral presentation in ISMRM 25th Annual Meeting & Exhibition 2017. Honolulu, HI, USA

Papers

Sharum, I., **Granados Aparici, S.**, Warrander , F., Tournant , F. & Fenwick, M. (2016) S*trap* regulates early follicle development in the mouse ovary. *Reproduction,* 153(2), 221-231.

Granados Aparici, S., & Fenwick, M. (2017). Smad3 transcription factor regulates cell cycle genes and modulates pre-granulosa cell proliferation in the mouse ovary (*in preparation*).

Granados Aparici, S., & Fenwick, M. (2017). Increased TGFβ signalling stimulates granulosa cell proliferation and initiates primordial follicle activation (*in preparation*).

TABLE OF CONTENTS

Chapter 2. Materials and Methods

LIST OF FIGURES

LIST OF TABLES

LIST OF ABBREVIATIONS

AFC	Antral follicle count
AKT	Protein kinase B
ALK	Activin like kinase
AMH	Anti-Müllerian hormone
Ap1	Activator protein 1
APS	Ammonium persulfate
BAD	BCL2-associated agonist of cell death
BAMBI	BMP and activin membrane-bound inhibitor
bFGF	Basic fibroblast growth factor 2
BMP	Bone morphogenetic protein
BMP15	Bone morphogenetic protein 15
BSA	Bovine serum albumin
cAMP	Cyclic adenosine monophosphate
CBP	CREB-binding protein
CCND2	Cyclin D2
CDC42	Cell division cycle 42
CDK	Cyclin-dependent kinase
ChIP	Chromatin immunoprecipitation
CKI	CDK inhibitors
cKIT	KIT oncogene receptor
cKO	Conditional knockout

CL	Corpus luteum
Co-IP	Coimmunoprecipitation
CO-SMAD	Common-partner SMAD
DAZL	Deleted in azoospermia-like
DDX4	DEAD (Asp-Glu-Ala-Asp) box polypeptide 4
DPC	Days post-coitum
EGF	Epidermal growth factor
EMT	Epithelial-mesenchymal transition
ERK	Extracellular regulated MAP kinase
FBS	Fetal bovine serum
FIGLA	Folliculogenesis specific basic helix-loop-helix
FKBP12	FK506 binding protein
FOXL2	Forkhead box L2
FOXO	forkhead box , subgroup O
FSH	Follicle stimulating hormone
FSHB	Follicle stimulating hormone beta subunit
FST	Follistatin
GC	Granulosa cell
GDF	Growth differentiation factor
GDNF	Glial cell line derived neurotrophic factor
GSK3	Glycogen synthase kinase 3
HPG	Hypothalamic-pituitary-gonadal
HRP	Horseradish peroxidase

HRT	Hormone replacement therapy
HTRA1	HtrA serine peptidase 1
IP	Immunoprecipitation
I-SMAD	Inhibitory SMADS
IVA	*In-vitro* activation
K4-6	Cyclin-dependent kinase 4/6
KGF	Fibroblast growth factor 7
KIT	KIT oncogene
KO	Knockout
LH	Luteinizing hormone
LHX8	LIM homeobox protein 8
LIF	Leukemia inhibitory factor
MAPK	Mitogen-activated protein kinase
MPF	Maturation promoting factor
mTOR	Mechanistic target of rapamycin (serine/threonine kinase)
MYC	Myelocytomatosis oncogene
NBL1	Neuroblastoma 1, DAN family BMP antagonist
NES	Nuclear export signal
NFKB	Nuclear factor kappa-light-chain-enhancer of activated B cells
NGF	Non-growing Follicles
NOBOX	NOBOX oogenesis homeobox
NPC	Nuclear pore complex
OCT4	Organic cation/carnitine transporter4

OGC	Ovarian germline stem cells
OSE	Ovarian surface epithelium
p107	Retinoblastoma-like 1 protein
p15	Cyclin dependent kinase inhibitor 2B
p21	Cyclin-dependent kinase inhibitor 1A
p27	Cyclin-dependent kinase inhibitor 1B
p300	E1A binding protein
p38	p38 mitogen activated protein kinase
p85-p110	Heterodimeric phosphoinositide 3-kinase
PAR6	Partitioning defective 6 homolog alpha
PBS	Phosphate-buffered saline
PCO	Polycystic ovaries
PCOS	Polycystic ovarian Syndrome
PCR	Polymerase chain reaction
PDGF	Platelet-derived growth factor
PDK1	3-phosphoinositide dependent protein kinase-1
PFA	Primordial follicle activation
PGC	Primordial germ cells
PI3K	Phosphatidyl-inositol-3-kinase
PIP2	Phosphatidylinositol-3,4-biphosphate
PIP3	Phosphatidylinositol-3,4,5-triphosphate
PND	Post-natal day
POI	Primary ovarian insufficiency

PTEN	Phosphatase and tensin homolog
RA	Retinoic acid
Rac	Ras-related C3 botulinum toxin substrate 1
Rb	Retinoblastoma protein
RELA	v-rel avian reticuloendotheliosis viral oncogene homolog A
RhoA	Ras homolog family member A
R-SMAD	Receptor-activated SMAD
RSPO1	R-spondin 1
RTK	Receptor tyrosine kinase
RUNX	Runt-related transcription factor
S6K	Protein S6 kinase
SCP3	Signal peptidase complex subunit 3
SHCA	SHC-transforming protein 1
SOHLH	Ocyte-specific basic helix-loop-helix (bHLH)
SOX9	SRY box 9
SP1	Specificity protein 1
SRY	Sex-determining region Y
STRA8	Retinoic acid gene 8
STRAP	Serine/threonine kinase receptor associated protein
TAZ	Transcriptional coactivator with PDZ-binding motif
TF	Transcription factor
TLP	TRAP-1-like protein
TMPEAi	Prostate transmembrane protein, androgen induced 1

TRAF6	TNF receptor-associated factor 6
TRAP-1	TNF receptor-associated protein 1
TSC1	Tuberous sclerosis 1
WNT4	wingless-type MMTV integration site family, member 4
YAP	Yes-associated protein

Chapter 1.

Introduction

1.1 Social impact of understanding ovarian biology

Concern about female fertility is nowadays a major consequence of a profound social change. Since the late 20th century, changes in lifestyle have had a major influence in the reproductive lifespan of women. Women are born with a limited supply of primordial follicles in their ovaries, the ovarian reserve, which declines naturally with age in number and quality (Hansen et al, 2008; Pellestor et al, 2003). Moreover, the effect of lifestyle factors such as smoking (Sun L 1 2012) or the use of chemo-or radiotherapy (De Vos et al, 2010) seriously compromise the integrity of the follicles from the reserve and therefore accelerate women's reproductive age. This can contribute to ovarian dysfunction, leading to for example, primary ovarian insufficiency (POI), or exacerbate symptoms associated with polycystic ovarian syndrome (PCOS).

PCOS is the most common cause of anovulatory infertility in women and it is often associated with hyperandrogenism and major metabolic disorders, such as Type 2 diabetes, insulin resistance and obesity. According to the Rotterdam criteria 2003, the prevalence of PCOS ranges from 5 to 10% of general female population and 30% of the infertile population (Baird et al, 2012). Although women with PCOS reach menopause at the average age of 50 years they suffer decreased rates of ovulation and higher rates of miscarriages during their reproductive life (Dumesic & Richards, 2013; Kamalanathan et al, 2013; Webber et al, 2003).

POI is a condition associated with amenorrhea for more than 4 months, increased gonadotropin production and decreased levels of oestrogen, and has an incidence of 1% under the age of 40 and 0.1% under the age of 30 (Webber et al, 2016). Depending on the aetiology, it can be classified as spontaneous (caused by genetic or metabolic disorders) or induced (caused by iatrogenic factors such as radio-chemotherapy) (Jin et al, 2012). Spontaneous POI has serious social consequences nowadays. The increased opportunity of women to pursue a career results in a delay in childbearing. Therefore, when women with POI decide whether or not they want to have children, they are often infertile. In the cases with induced POI as a result of ovarian surgery or radio-chemotherapy treatment, major impact exists particularly in young girls, since they suffer the consequences of infertility from an early age and availability of fertility preservation strategies is more limited (De Vos et al, 2015).

Notwithstanding the impact on fertility, PCOS and POI can also precipitate serious consequences on women's health and quality of life. The ovarian follicles are the source of steroid hormones which are necessary for the development and maintenance of the reproductive tissues, but also for the function of cardiovascular cells and maintenance of bone density (Compston, 2001; Knowlton & Lee, 2012). For this reason, the impact of ovarian dysfunctions transcends the fertility potential, since the loss of healthy growing follicles leads to impaired production of steroids hormones which subsequently increases the risk of cardiovascular diseases and osteoporosis (JC1., 2007; Joakimsen et al, 2000). As a consequence, these women often suffer from psychological disorders that seriously affect their quality of life (Acmaz et al, 2013; Jones et al, 2011; van der Stege JG 1 2008).

1.2 Introduction to mammalian follicle development

The mammalian ovary is a heterogeneous organ with interstitial tissue made up of follicles set in stroma. These follicles and corpora lutea are present at various stages of development (McGee & Hsueh, 2000). The ovary is a dynamic organ: its function includes the development and maturation of oocytes for fertilization, the maintenance of menstrual/estrous cyclicity and metabolic activity and the consequential development of female secondary sex characteristics. All of these tasks are possible because of the synthesis and secretion of hormones and also intrinsic ovarian factors that play an important role at all stages of follicle development (Adhikari & Liu, 2009; Li et al, 2010).

1.2.1 Overview of follicle development

The mammalian follicles are the functional units of the ovary. The primordial follicles are the most immature form and constitute the limited supply of follicles, the ovarian reserve (Findlay et al, 2015a). They consist of an immature oocyte surrounded by a layer of flattened granulosa cells (GCs) and eventually activate (primordial follicle activation, PFA) and start growing, in a process independent of gonadotrophins (Abel et al, 2000; Kumar et al, 1997; Peters et al, 1973). At this point, GCs rapidly proliferate and oocyte diameter also increases (McGee & Hsueh, 2000). During early 'preantral' development, GCs become more responsive to gonadotrophins and start expressing receptors for follicle stimulating hormone (FSH) (Figure 1.1). However, they are still able to grow in the absence of gonadotrophins where paracrine signalling between oocyte and GCs is essential (Eppig et al, 2002). Juxtracrine signalling enhances oocyte-GC communications due to the presence of connexin C37-dependent gap junctions, which allows the diffusion of growth factors and other intraovarian factors but also oxygen and nutrients, since follicles are avascular (Gittens & Kidder, 2005; Li et al, 2007; Veitch et al, 2004). As follicles develop, a condensation of ovarian stromal cells forms on the outer basement membrane, the theca cells, which will differentiate in two distinctive layers, theca interna and externa. Theca interna is stimulated by intra-ovarian factors to express luteinising hormone (LH) receptors and at this point follicles become dependent on gonadotrophins from the hypothalamic-pituitary-gonadal (HPG) axis (Edson et al, 2009). LH stimulation from the pituitary in theca interna allows the synthesis of androstenedione from cholesterol, which will be used by GCs for the synthesis of oestrogen in response to FSH.

This cooperation between theca and GCs for producing oestrogen corresponds to the "two-cell two-gonadotrophin" model (Liu & Hsueh, 1986).

Antral follicle development is characterised by atretic degeneration of most of the follicles from the growing pool and is mainly driven by arrest of granulosa cell (GC) proliferation and apoptosis (Matsuda-Minehata et al, 2006). Only a few follicles grow further and reach the preovulatory stage and although the mechanisms of follicle selection are still poorly understood, several intraovarian factors have been involved, favouring high production of oestrogen and competence (Mihm & Evans, 2008). The antrum (Figure 1.1) separates two functionally different GC populations, one promotes steroidogenesis, progesterone production and subsequent ovulation in response to LH surge (mural cells) and the other enhances further oocyte growth and competence (cumulus cells). Meiosis resumption depends on a decrease of cAMP levels in both oocyte and GCs that favours the activation of the maturation promoting factor (MPF) in the oocyte at the LH surge during ovulation (Shimada, 2012). Disruption of juxtracrine signalling between oocyte and granulosa-theca cells will cause the differentiation of follicle cells released after ovulation into lutein cells, the corpus luteum (CL). Supported by progesterone and LH in humans and prolactin in rodents (Malven PV 1966), the CL will eventually regress in absence of pregnancy.

The mechanisms regulating the gonadotrophin-independent follicle growth by intra-ovarian factors is yet to be fully deciphered. In particular, the molecular mechanisms necessary for the activation and maintenance of individual primordial follicles are still poorly understood. Understanding the biology of the primordial follicle pool has significant clinical implications; for instance, a better comprehension of the dynamics of age-related infertility and ovarian dysfunction from conditions such as POI and PCOS (see 1.3.2 below). Therefore, this thesis is focused on the study of the molecular mechanisms operating in primordial follicles during early follicle development.

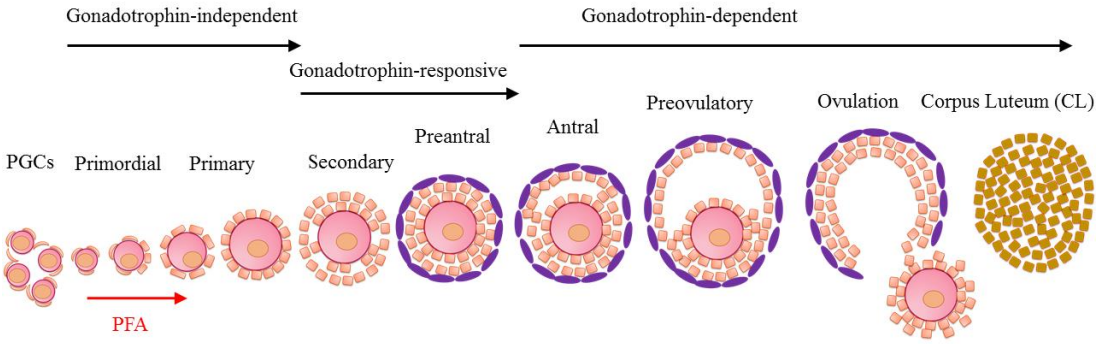

Figure 1.1. Classification of the major stages of follicle development. Primordial follicles formed from primordial germ cells (PGCs) develop to primary follicles. Gonadotrophin-independence takes place from primordial to preantral stage (PFA). At preantral stage, follicles do not require stimulation by gonadotrophins but they are highly responsive. Antral follicle development is dependent on LH and FSH and will produce steroid hormones following the two-cell two-gonadotrophin model.

1.2.2 Embryonic ovarian development and follicle formation

The process of sex determination in the bipotential gonads takes place after formation of the genital ridges, where the pre-supporting somatic cells in XY and XX individuals (termed pre-sertoli and pre-GCs, respectively) differentiate based on the presence or absence of the sex-determining region Y (*sry*) gene (Koopman P 1991). This occurs between 11 to 12.5 dpc (days post coitum) in mice and around 7 weeks in human, and results in the expression or repression of genes such as SRY box 9 (*Sox9*, target gene of *sry*) in the developing testis and wingless-type MMTV integration site family, member 4 (*Wnt4)*, R-spondin 1 (*Rspo1)*, bone morphogenetic protein 15 (*Bmp15)* and forkhead box L2 (*Foxl2)* in the developing ovaries (Harikae et al, 2013; Karkanaki et al, 2007). These testis and ovary-specific genes antagonise one another and a defect in one or more of them has been reported to cause sex-reversal (Maatouk et al, 2008). Between 10.5 and 13.5 dpc in mice and from 6 weeks of gestation in human (Mamsen et al, 2012; Pepling & Spradling, 1998) primordial germ cells (PGCs) migrate from the yolk sac endoderm to the genital ridges.

The migrated PGCs in the developing ovary eventually undergo mitosis with incomplete cytokinesis, creating intercellular bridges (ring canals), giving rise to germ cell clusters that subsequently enter meiosis to become oocytes (Pepling & Spradling 2001) (Figure 1.2). At around 12.5 dpc, pre-GCs become mitotically arrested, expressing high protein levels of the cyclin-dependent kinase inhibitor 1B (p27) and FOXL2 (Gustin et al, 2016).

Right after germ cell cluster formation, mitotically arrested pre-GCs start to invade and surround germ cell clusters (Pepling & Spradling 2001) (Figure 1.2). At this time, up to 98% of germ cells undergo programmed breakdown while only a small fraction survive to become potential mature oocytes (Pepling & Spradling 2001) (Figure 1.2). This process causes a major reduction in the overall oocyte population. As happens in *Drosophila* with "nurse cells" (Cox & Spradling, 2003), it is possible that germ cell clusters create a source of nutrients, a good supply of organelles like mitochondria, and a genome free from defects that favour the quality of the surviving germ cells (Pepling et al, 2007). In the mouse ovary, it is proposed that a similar mechanism exists, with "nurse-like" germ cells providing support to a single oocyte, although this requires further evidence (Lei & Spradling, 2013).

Onset of meiosis in oocytes is a protracted process (approximately 4 days in mice) that begins around 13.5 dpc in mice and around embryonic week 11 in human (Childs et al, 2011) (Figure 1.2). During this time, retinoic acid (RA) acts to induce and repress the expression of stimulated by retinoic acid gene 8 (*Stra8)* and the pluripotency marker organic cation/carnitine transporter4 (*Oct4),* respectively (Bowles & Koopman, 2007; Childs et al, 2011; Le Bouffant et al, 2010; Mu et al, 2013; Pesce et al, 1998). Although the "extrinsic" RA signalling suggests meiosis onset may be induced, there is evidence of "intrinsic" factors that are present during this window in germ cells. For instance, RNA-binding proteins DEAD (Asp-Glu-Ala-Asp) box polypeptide 4 (DDX4) and deleted in azoospermia-like (Dazl) are expressed in germ cells from the time they arrive in the gonad (Medrano et al, 2012). The functional role of DDX4 is not well defined although it is the most well-known germ cell marker and is highly conserved across species (Medrano et al, 2012). In contrast, Dazl is an important mediator of RA signalling and *Stra8* gene induction (Lin et al, 2008).

Onset of meiosis occurs in a rostral to caudal wave in the gonad (Bullejos & Koopman, 2004) and the most cited hypothesis states that the oocytes entering meiosis first are the first to enter follicle development. This is called the "production-line" theory (Henderson SA 1968) and was first demonstrated by studies using [3H]thymidine labelling in rats and mice (Hirshfield, 1992; Polani & Crolla, 1991).

After cluster breakdown, the oocyte arrests meiosis in the diplotene stage of prophase I and pre-GCs start surrounding individual oocytes to be enclosed within a basement membrane that together constitute the fundamental functional unit of the ovary: the primordial follicle (Pepling & Spradling, 1998) (Figure 1.2).

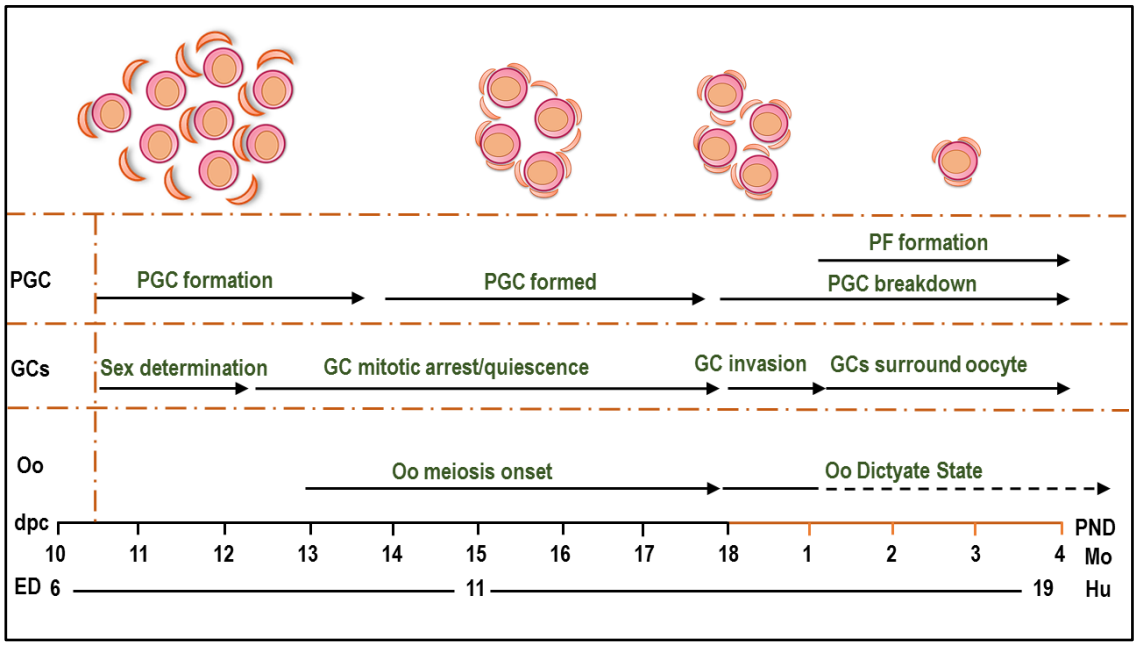

Figure 1.2. Timeline of primordial follicle formation in mice (Mo) and human (Hu). Three different events are depicted, 1) the changes experienced around clusters of primordial germ cells (PGC), 2) the somatic-dependent sex determination, the mitotic arrest and invasion of the surrounding pre-GCs and 3) the onset of meiosis in the oocyte (Oo). Time is referred as ED (months of embryonic development) in human and dpc (days post-coitum) and PND (post-natal day) in mice.

1.2.3 Primordial follicle activation

The term of 'primordial follicle activation' (PFA) is employed to describe the process where individual follicles start growing in an irreversible manner, eventually leading to either atresia or ovulation (Li et al, 2010). Primordial follicles are still capable of developing up to the antral stage in mice deficient for FSH or FSHR (Abel et al, 2000; Kumar et al, 1997); moreover, injection of gonadotrophins into juvenile mice does not alter the rate of primordial follicle growth (Peters et al, 1973). Therefore, the process of PFA is believed to be independent of gonadotrophins and mainly driven by intra ovarian regulation.

The adult ovary consists of a heterogeneous population of follicles at all stages of development. However, and in support of the production-line theory, the distribution of follicles is not random. Interestingly, primordial follicles accumulate in the cortical region and the growing follicles are more concentrated in the medulla. This pattern is particularly well illustrated in prepubertal (immature) mouse ovaries (Figure 1.3). This distribution is conserved among mammals including humans, where two distinct primordial follicle populations are activated at different times otherwise known as "waves" (Zheng et al, 2014a). The first wave corresponds to the primordial follicles in the medulla and the second wave is the pool located in the cortex. By using primordial-follicle specific markers for GCs (e.g. FOXL2; described in section 1.4.2) it has been reported in mice that the difference between the follicles from the two waves relates to the time that the surrounding GCs are specified from their precursors (Mork et al, 2011). Some GCs differentiate during foetal development, giving rise to the first wave in the medulla, while others differentiate perinatally (up to day 7 of age), enclosing follicles from the second wave in the cortex (Figure 1.3) (Capel et al, 2012; Gustin et al, 2016). This finding suggests that the different timing in follicle activation is due to the timing of GC specification during follicle formation and challenged the production-line hypothesis, which is related to the oocyte. Furthermore, it was later observed that the first wave of primordial follicles grew fast and mainly persisted until puberty while the second wave of primordial follicles were slower and developed throughout adult reproductive life (Zheng et al, 2014b) (Figure 1.3).

Based on these results, it was suggested that their differential role was related to the hypothalamic-pituitary-gonadal (HPG) axis, where follicles from the first wave contribute to the establishment of the HPG while the follicles from the second wave maintain the axis during adult life. Another hypothesis suggested growing follicles from the first wave could influence the rate of growth of the second wave to prevent early depletion (Zheng et al, 2014a). For example, primordial follicles from the second wave could receive inhibitory signals from the existing growing follicles from the first wave (Da Silva-Buttkus et al, 2009; Durlinger et al, 1999) (Figure 1.3). Moreover, a stimulatory effect between the growing and the primordial follicles from the first wave has also been reported in immature mice (d4-d12 of age) (Da Silva-Buttkus et al, 2009) and could explain the high-rate of growth of these follicles (Figure 1.3). These spatial mechanisms of activation and inhibition may be key to regulate the rate of activation of the second wave from puberty, favouring the maintenance of the ovarian reserve of follicles that will be recruited to ovulate during adulthood (Zheng et al, 2014a). Whether the differences in rate of growth from the two waves and their initial recruitment is dependent on the temporal differences of their GCs is yet to be demonstrated.

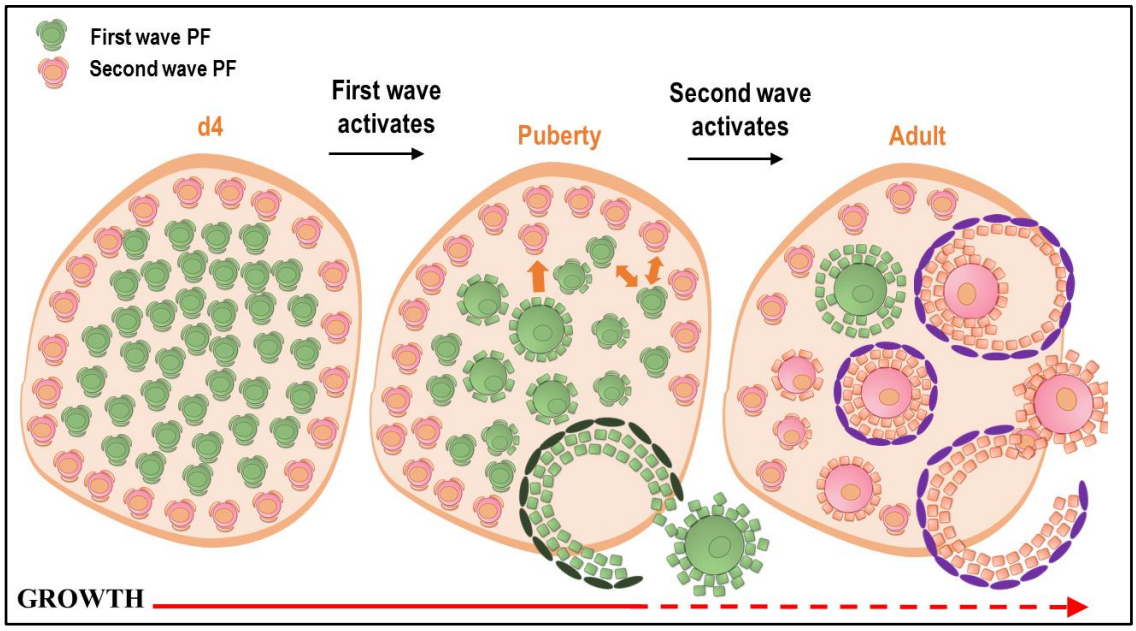

Figure 1.3. Sequential activation of the "two-waves" of primordial follicles in the mouse ovary. Follicles formed in the medulla of the ovary belong to the first wave and activate around day 4 after birth in mice (d4) following a high-rate of growth (solid red line) until puberty. Orange arrows indicate the hypothesised communication between follicles from the first wave and between the two waves (Da Silva-Buttkus et al, 2009; Zheng et al, 2014a). The second wave of primordial follicles, located in the cortex, start activating around puberty and follicles grow in a slow-rate during adult life (dashed red line).

1.3 Clinical implications of investigating the primordial follicle pool

1.3.1 Age-related infertility: Dynamics of follicle depletion

Once primordial follicles are formed, they generally have three fates: to remain quiescent, to die directly by atresia or to activate and enter follicle development (Reddy et al, 2010). Direct primordial follicle loss by atresia is difficult to measure but is proposed to contribute a reduction in the primordial follicle supply (Tingen et al, 2009). Follicle growth through activation contributes to a progressive depletion of the ovarian reserve and it is a major determinant of the reproductive lifespan: when the reserve is near depleted, reproduction ceases and menopause starts. Many research groups have focused on determining the dynamics of follicle depletion by establishing the relationship between the number of remaining follicles and women's age (Block, 1952; 1953; Forabosco & Sforza, 2007; Gougeon et al, 1994; Richardson et al, 1988). Using histological sections from ovaries from females across a range of ages, these studies include both primordial and primary follicles under the term non-growing follicles (NGF) to define the ovarian reserve and were able to show a decline in follicle number with age. However, the limited number of subjects, the use of different counting techniques, statistical analysis and modelling have been the main limitations to obtaining a definitive model (Faddy, 2000; Faddy & Gosden, 1996; Gougeon et al, 1994; Hansen et al, 2008). For example, the mathematical model used to represent the data was first considered to be biphasic-exponential and showed an accelerated depletion in follicle number from 38 years of age (Faddy et al, 1992) (Figure 4, A). More recently, Hansen et al (2008) applied unbiased stereology techniques and an increased number of subjects (n=122) to derive an alternative "power model" in order to improve the description of age-related follicle loss in humans. This model shows that the decline in follicle number occurs at a constant rate throughout life until the onset of menopause (around 50 years) (Figure 4, B).

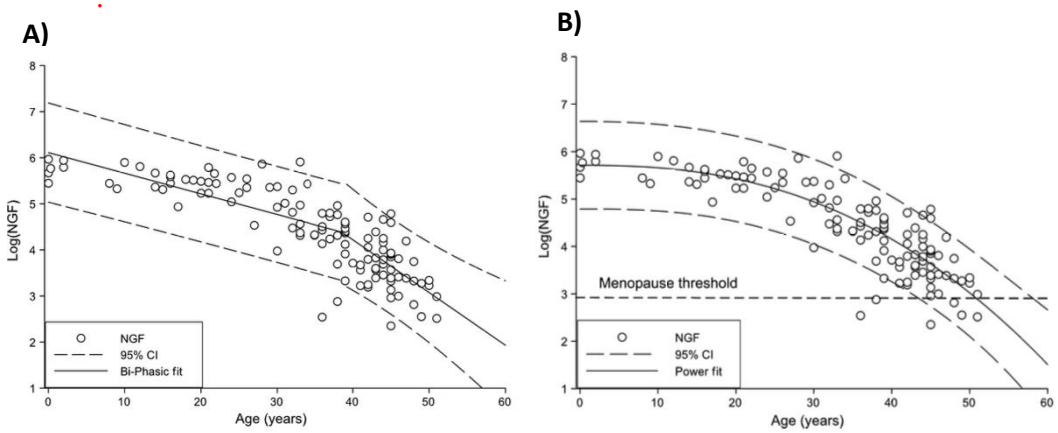

Figure 1.4. Relationship between non-growing follicles (NGF) of women and their age. Each point represents total follicle counts in each woman from the studies. The solid line in A) represents the classical biphasic-exponential model (Faddy et al, 1992) whereas B) represents the fitted power model (Hansen et al, 2008). In comparison with the classical model where there is an abrupt change in follicle depletion rate in late 30s, the power model shows how the number of follicles steadily declines throughout life with the onset of menopause around 50 years when very few follicles remain. Figures are reproduced with permission (Hansen et al, 2008) (Appendix 15).

Apart from histological counts, several putative markers of the ovarian reserve have been studied and only serum levels of anti-Müllerian hormone (AMH) and antral follicle counts (AFC) using ultrasound have shown a similar trend with NGF count and age (Hansen et al, 2011; Rosen et al, 2012). However, AMH is expressed in GCs from primary follicle stage but not in primordials (Weenen et al, 2004). Consequently, any factors affecting the growing follicle population can lead to a change in any of these parameters, (e.g serum AMH levels) that does not necessarily implicate a change in the ovarian reserve (van Dorp et al, 2016). Therefore, although AMH and AFC are of especial interest in clinics as non-invasive diagnostic tools to predict women's reproductive lifespan and assess follicle growth stimulation for assisted reproductive techniques (ART), they are not a direct measure of the primordial follicle population (Findlay et al, 2015b).

In addition to the number, follicle quality could also be an additional variable to consider when evaluating reproductive potential. Aneuploidy is reported to be the main cause of oocyte quality decline with age (Kuliev et al, 2011; Pellestor et al, 2003). For instance, oocytes from adult human ovaries (45 years and above) showed 40% more frequency of chromosomal abnormalities than in younger women (35 years)(Kuliev et al, 2011). Notwithstanding this, the effect that the long-term quiescence of primordial follicles has on their quality and subsequently on their growth potential is still undetermined. Ultrastructural assessment of the human primordial follicle pool using transmission–electron microscopy (TEM) has been proposed as a tool to determine follicle quality (de Bruin et al, 2002). By using ovary sections of young women, several signs of atresia in primordial follicles were studied. Notably, when healthy and atretic primordial follicles were compared, an increased number and ruptured mitochondria in oocyte and GCs from atretic follicles were described, respectively. Moreover, presence of vacuoles and dilatation of Golgi and rough endoplasmic reticulum (RER) were also observed in atretic primordial follicles (de Bruin et al, 2002). In another study, cytoplasmic vacuolization in oocytes of some primordial follicles were also observed in young rats (Devine et al, 2000). The results from these investigations suggest that impaired quality of primordial follicles could contribute to the dynamics of follicle depletion with age. Therefore, the molecular pathways that may be affected in these atretic primordial follicles is still a field worth to be investigated.

1.3.2 POI, PCOS and preservation of fertility

Interestingly, both POI and PCOS have been associated with impaired rate of PFA. Afollicular POI is the result of an accelerated rate of PFA leading to early depletion of the ovarian reserve whereas follicular POI is characterised by follicles that fail to develop (Nelson, 2009). By comparison, induced POI (as a consequence of ovarian surgery, endometriosis or radio-chemotherapy treatments) is characterised by a lack of follicle activation due to a loss of ovarian tissue (De Vos et al, 2015). In the case of anovulatory PCOS, a higher rate of PFA has been observed, mirroring the characteristic arrest of follicle growth that is detected in PCOS at antral stages (Webber et al, 2003). It is then likely that the decreased rates of ovulation may be partially caused by this unbalanced rate of follicle activation and growth (Franks et al, 2008).

Therefore, understanding the molecular factors implicated in the maintenance, activation and early follicle development can provide a range of biomarkers for the early detection and diagnosis of POI and PCOS.

Fertility preservation in women suffering from ovarian dysfunction, particularly with POI, can be considered from different options depending on the patient. In the case of patients with cancer that are planning to have ovarian surgery or chemo-radiotherapy there are two main techniques in the clinical practice: oocyte and embryo cryopreservation. However, none of these techniques are applicable to pre-pubertal girls and embryo cryopreservation is also limited to women with a male partner or sperm donor (Levine et al, 2010; Nyboe Andersen & Erb, 2006). Ovarian cortex cryopreservation and *ex-vivo* retrieval of immature oocytes are the other two alternatives for fertility preservation that can be applied to young women or prepubertal girls (Huang et al, 2008; Kuwayama et al, 2005). However, ovarian cortex transplantation is still experimental and reintroduction of malignant cells is a risk (Rosendahl et al, 2013). *In vitro* maturation of oocytes reduces all those issues but the fertilisation potential of *in vitro* matured oocytes is often compromised by the cryopreservation process (Brambillasca et al, 2013). Cryopreservation of primordial and preantral follicles for later culture have several advantages; firstly, women have relatively more follicles at these stages and secondly, in the case of cancer patients, there is a reduced risk of reintroduction of malignancy (Laronda et al, 2014). Furthermore, this technique could be offered to women with POI that have not planned to have a family at the moment of diagnosis. Although they suffer from follicle depletion, there is a low number of primordial follicles from the reserve and small antral follicles that can be preserved for *in vitro* maturation (IVM) and used for ART (De Vos et al, 2015; Suzuki et al, 2015). Considering these options, knowledge of the factors implicated in maintenance, activation and early follicle development will be extremely useful in developing systems to support viability *in vitro*.

1.3.3 Oocyte renewal

The general dogma of mammalian ovarian reserve consolidated by Zuckerman in 1951 states that the number of primordial follicles originated from primordial follicle formation constitutes the maximum oocyte supply possible in a female mammal.

Since then, it has been generally accepted. However, a study from Johnson et al. in 2004 challenged this dogma when they reported the presence of mitotically active cells in the ovarian surface epithelium (OSE) in mice that also expressed some meiotic markers, such as signal peptidase complex subunit 3 (SCP3), and the germ cell marker DDX4 (Johnson et al, 2004). With these findings, they postulated the existence of oocyte renewal as a mechanisms to supply the ovarian reserve and prevent the premature exhaustion of follicles due to follicle atresia. In order to test this phenomenon *in vivo*, the isolation of putative OGCs from young and adult mice ovaries was performed using the germ cell marker DDX4, and isolated OGCs were able to restore ovarian function and generate new fertilisable follicles and offspring (Zou et al, 2009). In ovarian cortical biopsies from healthy young women, FACS-based techniques using DDX4 antibodies we used to isolate these putative OGCs and successfully propagate them *in vitro* (White et al, 2012). However, the isolation and maintenance of these putative OGCs has been difficult to replicate and whether cytoplasmic DDX4 has a FACS-detectable extracellular domain in OSCs has been also recently questioned (F. Hernandez et al, 2015; Zarate-Garcia et al, 2016; Zhang et al, 2012). Moreover, the studies by Zou et al only demonstrated the potential of OSCs to generate new fertilisable oocytes but did not show their ability to generate primordial follicles in physiological conditions. However, a recent study using the stem cell marker Oct4 developed a tracing system *in vivo* by crossing Oct4 and YFP transgenic mice to generate a tamoxifen-inducible line, where they observed that these cells could become "meiotically active" cells and generate new primordial follicles (Guo et al, 2016).

The extent to which these putative OSCs contribute to the ovarian reserve and their physiological function is still undetermined, however, their use could be a potential alternative strategy for preservation of fertility of women with compromised supply of follicles in their ovaries, for example, in young girls with induced POI.

1.4 Maintenance and activation of primordial follicles

The biology of PFA is one of the major unanswered questions of reproductive biology: How are the individual follicles either maintained in relative quiescence or selected to activate and grow? The morphological and molecular events that a primordial follicle experience during activation have been described during recent decades. Earlier studies in mice suggested two important aspects about PFA, the pre-determined time of PFA and the ability of primordial follicles to grow without gonadotrophins, as explained above (see 1.2.3). Moreover, other studies observed that cuboidalisation and proliferation of GCs in mice were key morphological changes that occur during activation (Hirshfield, 1992; Lintern-Moore & Moore, 1979). This process of transformation in GCs was further confirmed by later studies (Da Silva-Buttkus et al. 2008; Mora et al. 2012; Braw-Tal 2002) and was proposed to be similar to an epithelial-mesenchymal transition (EMT), since GCs from growing follicles lack some of the common epithelial cell markers such as cytokeratin 8 and E-cadherin (Childs & McNeilly, 2012; Mora et al, 2012b; Samy et al, 2014). Oocyte growth occurs alongside this process; however, changes in GCs seem to precede major oocyte growth (Braw-Tal, 2002). The development of *in vitro* culture models has allowed to establish some hypotheses about the activation or maintenance of the primordial pool. First, the increased activation of primordial follicles in cultured bovine cortical biopsies when compared to ovaries *in vivo* suggested that the presence of inhibitory signals *in vivo* may maintain the primordial follicle population (Wandji et al, 1996). It was later demonstrated that insulin in the culture medium is an activator of PFA *in vitro* and therefore the existence of inhibitory factors *in vivo* may exist (Fortune et al, 2011). Moreover, a detailed spatial analysis in immature mouse ovaries allowed to establish some hypotheses about the source of these molecules (Da Silva-Buttkus et al, 2009). It was proposed that primordial follicles are exposed to (i) stimulatory signals from growing follicles or (ii) inhibitory signals from neighbouring primordial follicles located in close proximity. However, the identity of these effectors and their molecular mechanisms are still yet to be clarified.

The mouse ovary as a model of PFA

The neonatal mouse ovary culture was the first system to demonstrate the whole process of follicle development *in vitro* (Eppig & Brien, 1996). Since then, this model has provided a system to investigate in detail the molecular events leading PFA.

The ovarian mouse model is ideal as a preliminary model, since it is easier to culture and a repertoire of novel molecular biology tools and transgenic possibilities can be applied to study in detail the molecular biology under PFA. In mice, primordial follicle formation occurs around 1-3 days after birth with some follicles initiating growth shortly after. This timing provides a short, well-defined window to observe the biological process of PFA. Moreover, a neonatal mouse ovary is approximately 1mm in diameter, meaning the small size allows the entire organ to be maintained in a culture environment. Notwithstanding this, follicle development in mice is different from that in human: they are poly-ovulatory and the follicle morphology, size and the time required for follicle growth are different (Griffin et al, 2006). Hence, the use of non-human primate models is essential to optimise effective culture methods that are more translatable to human (Telfer & Zelinski, 2013). For instance, the ovarian cortex culture has been developed in cattle and provided an improvement of the culture of human ovarian cortical biopsies (McLaughlin & Telfer, 2010; Telfer et al, 2008).

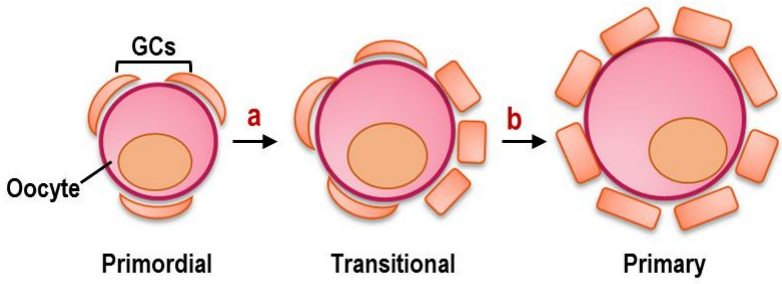

Figure 1.5. Morphological changes associated with primordial follicles during PFA. Primordial follicles with flat GCs start to cuboidalise and proliferate into a transitional follicle (a). At around the same time, or just after, a major increase in oocyte volume occurs as the follicle transitions into a primary follicle (b).

1.4.1 Molecular events in the oocyte

The phosphatidylinositol-4,5-bisphosphate 3-kinase (PI3K) pathway is involved in cell growth, division, survival and migration and has been well characterised in cancer biology (Chalhoub & Baker, 2009; Spoerke et al, 2012; Tran et al, 2013). The role of this signalling pathway during early follicle development, particularly in the activation of the primordial follicle pool has also been studied extensively (Reddy et al, 2005). Forkhead box family (FOXO) family, FOXO3a is a substrate of the PI3K mediator serine/threonine kinase AKT that normally regulates cell cycle arrest (Figure 1.6) (Brunet et al, 1999). Upon stimulation by AKT, FOXO3a relocates to the cytoplasm, triggering cell proliferation (Arden & Biggs, 2002) (Figure 1.6). PI3K pathway is negatively regulated intracellularly by the function of Phosphatase and Tensin Homolog (PTEN). It catalyses the hydrolysis of the phosphate group of Phosphatidylinositol-3,4-triphosphate (PIP3), impeding the recruitment by this factor of PDK1, necessary for AKT phosphorylation (Maehama & Dixon, 1998) (Figure 1.6). *Pten*$^{-/-}$ and *Foxo3a*$^{-/-}$ mice exhibit a similar ovarian phenotype, with an overgrowth of oocytes in all primordial follicles and increased PFA (Castrillon et al, 2003; Jagarlamudi et al, 2009; John et al, 2008). The accelerated growth of oocytes seemed to be promoted by the activation of AKT and mechanistic target of rapamycin (serine/threonine kinase) (mTOR) and its downstream molecules Ribosomal protein S6 kinase (S6K) and ribosomal protein S6 (rps6) (Jagarlamudi et al, 2009). Therefore, PTEN and FOXO3a may be important for maintaining the dormancy of the primordial follicle pool. Pharmacologic inhibition of PI3K in *Pten*$^{-/-}$ suppresses oocyte growth, while treatment with the same inhibitor in *Foxo3a*$^{-/-}$ has no effect on the ovarian phenotype. This result suggests that FOXO3a acts downstream of PTEN which may regulate oocyte growth via PI3K, AKT and FOXO3a (John et al, 2008) (Figure 6) .

The upstream regulator KIT ligand is shown to activate PI3K pathway in mice (John et al, 2008; Liu et al, 2007; Reddy et al, 2005; Thomas & Vanderhyden, 2006b). KIT ligand expression is detectable in GCs while its receptor, KIT proto-oncogene receptor tyrosine kinase (cKIT), is found in oocytes and theca cells in rodents and human (Horie et al, 1991; Merkwitz et al, 2011; Otsuka & Shimasaki, 2002; Tuck et al, 2015).

Mice harbouring non-functional mutations for KIT ligand exhibit growth-arrested follicles at the primary and secondary stage (two layers of GCs) with minimal oocyte growth (John et al, 2009). In addition, the FOXO3a protein is retained in the oocyte nuclei of these mice, suggesting that KIT ligand signalling is crucial for the regulation of the PI3K pathway via FOXO3a. Interestingly, the absence of KIT ligand does not influence GC cuboidalisation and proliferation but affects oocyte growth (John et al, 2009). Since GC proliferation has been proposed to initiate PFA (see 1.4), KIT ligand may be part of the paracrine signalling loop from GCs to the oocyte but once PFA has already taken place.

The ocyte-specific basic helix-loop-helix (bHLH) transcription factor SOHLH1 and SOHLH2, specifically expressed in germ cells and oocytes from primordial follicles in mice (Pangas et al, 2006), are also important for PFA. Both *Sohlh1*$^{-/-}$ and *Sohlh2*$^{-/-}$ mice exhibit accelerated postnatal oocyte loss (Choi et al, 2008). Moreover, microarray analysis indicated that loss of *Sohlh1* promotes down-regulation of other transcription factors, such as the newborn ovary homeobox NOBOX and the basic helix-loop-helix (bHLH) factor FIGLA (Pangas et al, 2006). *Nobox*$^{-/-}$ show arrest in PFA and eventual oocyte loss (Rajkovic et al, 2004). FIGLA controls the oocyte-specific expression of three zona pellucida genes (ZP1, ZP2 and ZP3) that constitute the glycoprotein-rich matrix that surrounds developing oocytes (Gupta et al, 2012). This factor is also important for primordial follicle formation, as increased oocyte loss is found in *Figla*$^{-/-}$ mice (Joshi et al, 2007; Soyal et al, 2000).

Growth factors and cytokines produced by the oocyte also play an important role in early follicle development. Platelet-derived growth factor beta (PDGF) and basic fibroblast growth factor 2 (bFGF) are believed to be important regulators of PFA. PDGF and bFGF are expressed in oocytes and their receptors in GCs and theca cells in rat and pig ovaries (Okamura et al, 2001; Sleer & Taylor, 2007; Taylor, 2000). Treatment of cultured rat ovaries with either bFGF or PDGF leads to an upregulation of KIT ligand expression in GCs (Nilsson et al, 2001; Nilsson et al, 2006; Nilsson & Skinner, 2004).

In addition, oocyte-derived cytokines such as glial cell line derived neurotrophic factor (GDNF) or epidermal growth factor (EGF) are also believed to play a role in early follicle development. However, both may have a role after the primary follicle stage, since in cultured rat ovaries GDNF promotes changes in the expression of factors found in growing follicles (e.g. GDF9 and AMH) and in cultured goat ovarian cortex EGF enhances further oocyte growth after PFA (Dole et al, 2008; Silva et al, 2004). Other factors produced in the stroma or theca cells such as fibroblast growth factor 7 (FGF7, also known as KGF) also have a paracrine effect and influence on PFA by stimulating GC production of KIT ligand in cultured rat ovaries (Kezele et al, 2005).

The characterisation of these molecular pathways in oocytes have been used to develop potential clinical strategies to induce PFA *in vitro* (Li et al, 2010; Reddy et al, 2010). For example, stimulation of early follicle growth using PTEN inhibitors on cultured cortical biopsies with subsequent transplantation has resulted in offspring in women seeking fertility treatment (Kawamura et al, 2013). However, although this clinical tool has a real impact for the production of fertilizable oocytes from women suffering from POI (Kawamura et al, 2013; Suzuki et al, 2015), their use in the *in vitro* activation of follicles still remains uncertain, as treated primordial follicles do not seem to show clear evidence of healthy development beyond the secondary stage (McLaughlin et al, 2014).

A recent report has suggested the initiation of PFA triggered by primordial GCs as the molecular switch that allows further follicle development (Zhang et al, 2014). Therefore, any treatment that only targets the oocyte may enhance a shortcut in the process of activation. As a consequence, GC proliferation may be impaired, affecting further follicle development and oocyte quality (Eppig et al, 2002). Therefore, understanding the molecular events involved in GC transformation may be fundamentally important for developing future strategies that regulate PFA in vitro.

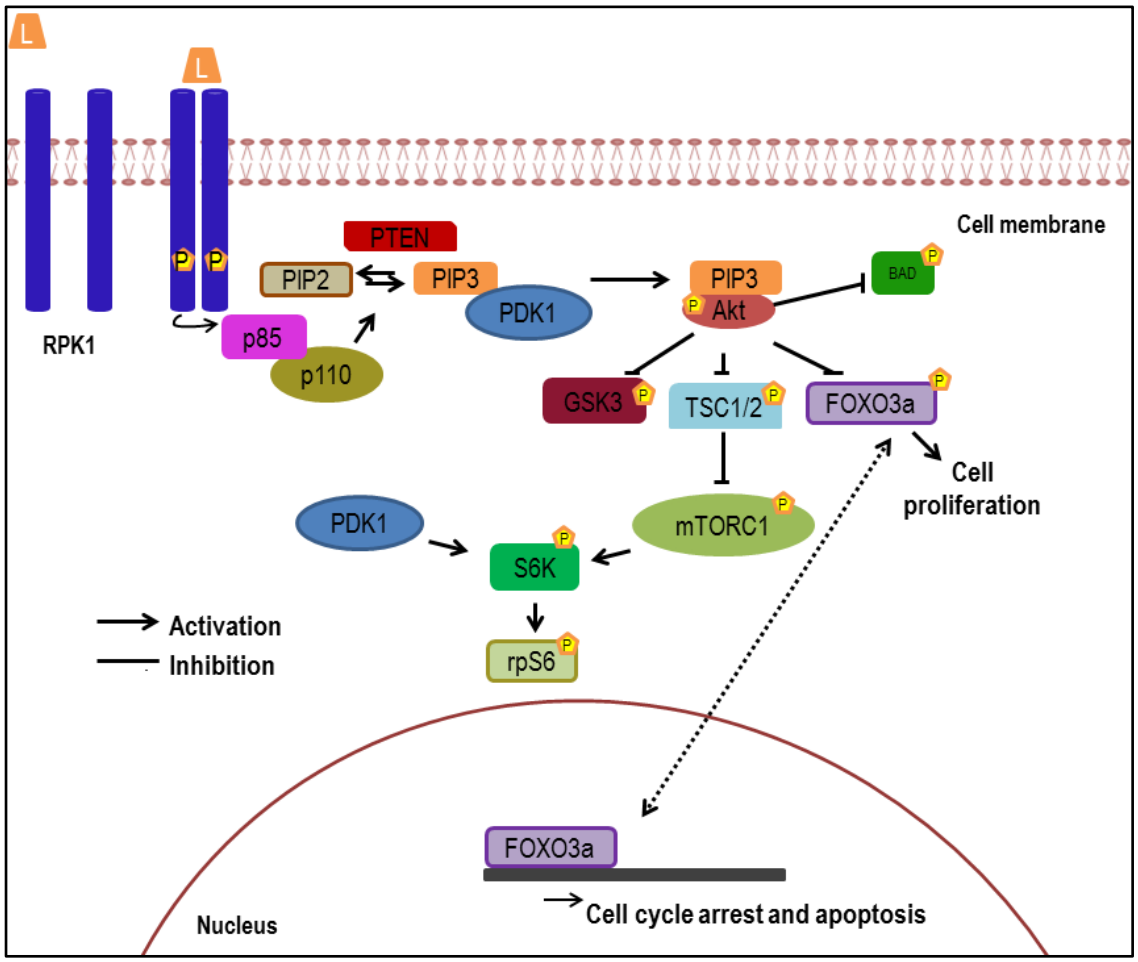

Figure 1.6. PI3K pathway and regulation. Extracellular ligands (L) (e.g KIT ligand) bind to RPK1 receptors, which dimerise, phosphorylate and recruit the p85-p110 heterodimer. p85-p110 converts PIP2 into PIP3 which recruits PDK1. PDK1 phosphorylates AKT which inhibits BAD, GSK3, TSC1/TSC2 (described in 1.4.2), p27 and FOXO3a. As TSC1/TSC2 is inhibited, mTORC1 become phosphorylated and also its downstream molecules (S6K and rpS6). Inhibition of FOXOA3 leads to its relocation to the cytoplasm, promoting cell proliferation.

1.4.2 Molecular events in GCs

Key GC markers and regulators

FOXL2 is a forkhead domain/winged-helix (WH) transcription factor. A mutation in this gene is associated with human blepharophimosis/ptosis/epicanthus inversus syndrome (BPES) type I, an autosomal disorder associated with POI (Crisponi et al, 2001). Due to its specificity in GCs it is often used as GC marker (Capel et al, 2012). The role of FOXL2 in PFA has been also reported (Schmidt et al, 2004; Uda et al, 2004). Foxl2lacZ homozygous mutant mice (obtained by replacing the coding region of *Foxl2* gene by *nlslacZ* cassette) and also *Foxl2*$^{-/-}$ mice showed an absence of GC cuboidalisation during primordial to primary transition (Schmidt et al, 2004; Uda et al, 2004). Furthermore, although oocytes were able to grow, they underwent atresia and a progressive depletion of follicles was observed (Schmidt et al, 2004). These results suggest that a change in GC morphology is an important aspect that supports oocyte growth to later stages of follicle development. FOXL2 regulates the transcription of genes involved in primordial follicle maintenance; for example, p27, expressed in both oocyte and GCs (Garcia-Ortiz et al, 2009). In *p27*$^{-/-}$ mice, the primordial pool was found to be prematurely activated (Rajareddy et al, 2007). Therefore, p27 is considered an important negative regulator of PFA. In other cells, p27 supresses cell growth when it is phosphorylated and excluded from the nucleus (Nakayama, 2004). Although initially believed to be downstream PTEN/PI3K-FOXO3a pathway, double knockout p27$^{-/-}$FOXO3a$^{-/-}$ mice showed more PFA than mice lacking one of them, suggesting that the p27 cell cycle pathway and the PTEN/PI3K-Foxo3a pathway could act independently (Rajareddy et al, 2007).

Since FOXL2 is mostly restricted to GCs, the gene promoter has been used to generate conditional knockout (cKO) mice targeting this lineage. Recent studies have exploited this to specifically study the role of the **mTORC** (mechanismtic target of rapamycin complex) signalling pathway in GCs (Zhang et al, 2014). Conditional deletion of the regulatory-associated protein of mTOR (Rptor) in GCs decreases PFA, while the opposite effect is observed when the mTORC inhibitor protein TSC1 (Tuberous sclerosis 1) is ablated in these cells.

Moreover, a relationship between mTOR and PI3K signalling is evident, since FOXO3a is confined to the oocyte cytoplasm in *Tsc1*$^{-/-}$ female mice. This suggests that constitutive mTOR activation leads to constitutive PI3K pathway inhibition. In addition, using cultured *Tsc1*$^{-/-}$ cKO ovaries, treatment with an inhibitor to KIT ligand prevented the global PFA phenotype, suggesting mTORC1 pathway could be the upstream mechanism upregulating KIT ligand, necessary for the further oocyte growth, as previously reported (John et al, 2009). Despite these findings, the upstream factors stimulating the mTOR pathway in primordial follicles are still unknown. The mTOR pathway is stimulated with factors such as oxygen, other growth factors and energy (Zhang et al, 2014).Whether this is the case for primordial follicles or other intra-ovarian factors are regulating this pathway has yet to be determined. Nevertheless, mTOR seems to play an important role in the initiation of PFA.

Key ligands: TGFβ superfamily

Other factors also play an important role in GCs during PFA. **AMH**, a TGFβ ligand is expressed in GCs of human preantral and small antral follicles in human and mice (Durlinger et al, 2002a; Weenen et al, 2004). AMH$^{-/-}$ mice exhibit an early depletion of primordial follicles within the ovary, with a corresponding increased rate of PFA, suggesting a role for AMH as an inhibitory signal (Durlinger et al, 2002a; Durlinger et al, 1999). Furthermore, exogenous AMH in cultures of human cortical biopsies and the exposure to endogenous AMH of grafted neonatal mouse ovaries and bovine ovarian cortex (beneath the chorioallantoic membrane, CAM) showed an inhibition of PFA (Carlsson et al, 2006; Gigli et al, 2005). By comparison, **GDF9** is an oocyte-derived TGFβ that promotes proliferation of GCs during early follicle development (Dong et al, 1996). Studies have identified that some patients with POI exhibit different variants of the GDF9 gene (Persani, 2011; Qin et al, 2015). GDF9$^{-/-}$ mice show arrest of follicle development at the primary stage due to a failure in GC proliferation (Dong et al, 1996). Moreover, GDF9 plays an essential role in stimulating GCs and theca cell growth by influencing the expression of non-oocyte-derived ligands such as activin or KIT ligand (Dong et al, 1996; Elvin et al, 1999b; Joyce et al, 2000a; Myers et al, 2013; Thomas & Vanderhyden, 2006a).

Since AMH and GDF9 are not expressed in primordial follicles, it is unclear whether they contribute directly to the process of PFA; yet, may instead be important factors promoting transition through the small preantral stages.

Activins and **inhibins** have a well-known role in FSH regulation during follicle development (Bernard, 2004; Ling et al, 1986; Suszko et al, 2005; Suszko et al, 2003; Vale et al, 1986). However, comparatively less is known about their role during the early gonadotrophin-independent phase. In terms of structure, activin and inhibin differ in the dimerization of their subunits: activins are composed by homodimers or heterodimers of beta A or B subunits while inhibins are heterodimers of one beta and one alpha subunit (Rabinovici et al, 1992). Inhibin and activin both bind to the same receptors, therefore they act by competitive binding (Zhu et al, 2012). In human, mutations in inhibin alpha gene (*Inha*) have also been found in POI patients (Qin et al, 2015). In mice, $Inha^{-/-}$ are infertile and show decreased numbers of primordial follicles together with increased numbers of primary and secondary follicles suggesting accelerated PFA, possibly due to increased activin signalling (Matzuk MM 1992). Consistent with this, increased proliferation of GCs is also observed in these mice alongside reduced expression of KIT ligand and AMH (Myers et al, 2009). With regard to activin, activin A (homodimer of beta A subunits) stimulates growth of GCs in preantral follicles (Zhao et al, 2001). However, recent investigations showed that activin A enhances maintenance rather than activates the primordial pool (Childs & Anderson, 2009; Coutts et al, 2008; Ding et al, 2010). Interestingly, mice null for the activin antagonist follistatin, exhibit an increased rate of PFA (Kimura et al, 2011; Yao et al, 2004), supporting the possible role for activins in maintaining the dormancy of primordial follicles. Despite this, the mechanism of action may be indirect, since activin A and its receptors activin A receptor type 2A (Acvr2a) and 1B (ALK4) are expressed in oocytes (Martins da Silva et al, 2004) and GCs of follicles from primary stage, but not in primordial follicles (Coutts et al, 2008; Pangas et al, 2002).

TGFβ1 ligand is detectable in mouse oocytes in follicles at all stages, including primordial follicles (Christopher, 2000; Gueripel et al, 2004). However, TGFβ1 staining in GCs is less clear, being detectable in small follicles in cattle and in large follicles in human but not in mice (Chegini N 1992; Nilsson et al, 2003; Wang et al, 2014b).

Treatment of cultured neonatal mouse and rat ovaries with TGFβ1 results in a reduced rate of PFA compared to controls (Ingman WV 1 2006; Ingman et al, 2006; Rosairo D 2008; Wang et al, 2014b). Conversely, the addition of a TGFβ inhibitor specific to type I TGFβ receptor promotes follicle activation and growth (Wang et al, 2014a). *Tgfβ1*$^{-/-}$ knockout mice maintained until adulthood have a reduced number of oocytes in their ovaries. In addition, the extracellular antagonist *Htra1* is highly expressed in GCs of mouse follicles from early stages of development but not primordial follicles in a pattern similar to follistatin (Fenwick et al, 2011). Therefore, like activin, TGFβ1 in primordial follicles may be important to maintain the primordial follicle pool.

Bone Morphogenetic Proteins (BMPs) are also implicated in PFA. BMP15, belongs to the list of gene candidates implicated in POI (Persani, 2011). BMP15 mRNA and protein are predominantly expressed in oocytes of preantral and larger follicles of sheep and human and mutations in *Bmp15* gene are involved in POI (homozygotes only in sheep and heterozygote carriers in human) (Di Pasquale et al, 2004; Galloway et al, 2000). Although BMP15 is not known to be involved in PFA in mice, it plays an important role in later steps of follicle development, as treatment of preantral follicles with exogenous BMP15 inhibits growth and promotes atresia (Fenwick et al, 2013). BMP4 and BMP7, are both expressed in theca cells of mice and rat ovaries and the addition of exogenous BMP4 and 7 to cultured rodent ovaries is thought to increase the rate of PFA (Ding et al, 2013; Lee et al, 2001; Lee et al, 2004; Nilsson & Skinner, 2003). However, these proteins are not expressed in primordial follicles (Nilsson & Skinner, 2003; Shimasaki et al, 1999) suggesting that the actions of BMPs on primordial follicles may also be indirect.

Smad Knockout mice to study TGFβ function in the ovary

SMAD proteins are the canonical downstream signalling mediators of TGFβ ligands. Like TGFβ1, 2 and 3 or BMP 2, 4 and 7 (Lawson et al, 1999; Memon et al, 2008; Nilsson & Skinner, 2003; Ross et al, 2007; Solloway et al, 1998; Yan et al, 2001; Zhang & Bradley, 1996), knockout mice (KO) for SMAD mediators often show embryonic/perinatal lethality (Pangas, 2012a), thereby impeding the study of their role in PFA (Pangas, 2012b).

Interestingly, from the KO generated for the TGFβ/activin mediators SMAD2/3, *Smad3*$^{-/-}$ mice (by deleting exon 2 from the gene, see table 1.2) often develop colorectal cancer and immune deficiencies but is fertile, whereas an alternative *Smad3* $^{-/-}$ variant (deletion in exon 8) is viable but exhibits a reduced ratio of follicle growth and GC proliferation (Tomic et al, 2004; Zhu et al, 1998). The difference between the two variants resides on the activity of the truncated protein: in the case of exon2-deleted *Smad3*$^{-/-}$, an inactive SMAD3 form is generated whereas exon8-deleted *Smad3*$^{-/-}$ translates a protein that although is not able to be phosphorylated by the receptor, maintains the MH1 active domain and linker region (responsible for its non-canonical activation) (see Figure 1.10). In order to clarify the role of SMADs and other TGFβ factors in follicle development, *in vitro* experiments with cultured ovaries would be a good alternative. The generation of cKO mice have also provided unique models to assess the role of various SMADs in GCs only. Using this approach, *Smad2*$^{-/-}$ and *Smad3*$^{-/-}$ cKO mice show normal fertility whereas double *Smad2/3*$^{-/-}$ cKO are subfertile, with a reduced number of antral follicles, reduced ovulation rates and cumulus cell defects (Li et al, 2008) (Table 1.2). This suggests that SMAD2/3 proteins may compensate for each other when one is absent. This "redundancy" can also explain the differential phenotype observed with the two *Smad3*$^{-/-}$ mice variants. Since SMAD2 may be able to replace the non-functional protein in exon2-*Smad3*$^{-/-}$, the presence of the truncated yet partially functional protein in exon8-*Smad3*$^{-/-}$ may not allow SMAD2 to replace SMAD3 function, hence its infertile phenotype. With regards to the BMP downstream mediators SMAD1/5 and 8; Smad1$^{-/-}$ and 5$^{-/-}$ cKO exhibit relatively normal fertility while triple *Smad 1/5/8* and double *Smad1/5* cKO mice in GCs develop GC tumours and are subfertile (Pangas et al, 2008) (Table 1.2). Interestingly, GCs from these mice show an upregulation of genes associated with SMAD2/3 signalling, suggesting that SMAD1/5 pathway may contribute to normal follicle development as a tumour suppression mechanism in GCs particularly for TGFβ ligands and its downstream effectors (Pangas et al, 2008).

Although the cKO models have demonstrated a clear role for the different SMADs in GCs of growing follicles, these mice were generated using the AMH receptor 2 gene promoter (AMHR2) as the locus for Cre recombinase. AMHR2 is expressed in GCs of growing follicles and therefore any 'floxed' allele is not found in primordial follicles. Therefore, these transgenic models do not address the function of the targeted gene in PFA.

In mice, SMAD1/5/8 is expressed in GCs of growing follicles while SMAD2/3 is predominantly expressed in small, single-layered (primordial and primary) follicles (Fenwick et al, 2013; Xu et al, 2002a). Likewise, SMAD2/3 is found in primordial follicles in the human foetal ovary (Coutts et al 2008). These results complement the findings from cKO mice, where SMAD2/3 signalling may be more involved in PFA whereas SMAD1/5/8 is likely to be more relevant after this initiation, probably as a tumour suppressor mechanism when GCs have a higher proliferative status (Pangas et al, 2008).

Smad variant	**Fertility and ovarian phenotype**	**References**
Smad3$^{-/-}$ (exon 2-3) KO	Fertile	(Zhu et al, 1998)
Smad3$^{-/-}$ (exon 8) KO	Subfertile, decreased follicle growth, GC proliferation and increased follicle atresia	(Tomic et al, 2002)
Smad1/5$^{-/-}$ cKO	Subfertile, GC tumours	(Pangas et al. 2008)
Smad1/5/8$^{-/-}$ cKO	Subfertile, GC tumors	(Pangas et al. 2008)
Smad2$^{-/-}$ cKO (exon 9-10)	Fertile	(Li et al. 2008)
Smad3$^{-/-}$ cKO (exon 2-3)	Fertile	(Li et al. 2008)
Smad2/3$^{-/-}$ cKO	Subfertile, reduced number of antral follicles, reduced ovulation rates and cumulus cell defects	(Li et al. 2008)

Table 1.1. Comparison of the different SMAD$^{-/-}$ KO and cKO mice phenotypes.

Recent immunohistochemistry data from our laboratory showed that there is a translocation of SMAD2/3 from the nucleus to the cytoplasm at the time GCs begin to proliferate (Figure 1.8). This potentially highlights a novel, and very early detectable molecular event in PFA, since it is seen to occur prior to the increase in oocyte size. This finding also suggests that SMAD2/3 is implicated in the maintenance of the primordial pool and initiation of PFA may be triggered by a signal that could either be, as mentioned above (see 1.4), an antagonist of TGFβ signalling. While others have studied the role of PI3K and mTOR signalling pathways in the oocyte and GCs of small follicles respectively, the relationship between TGFβ signalling and these pathways is unknown. As will be explained below, TGFβ signalling is able to modulate these pathways via non-canonical mechanisms. It is then possible that the balance between canonical and non-canonical TGFβ signalling regulates PI3K and mTOR signalling pathways in GCs of primordial follicles and allows the initiation of PFA. Therefore, in order to understand the role of SMADs in the ovary, the mechanisms of SMAD signalling in other cell types will be explained in detail in the next section.

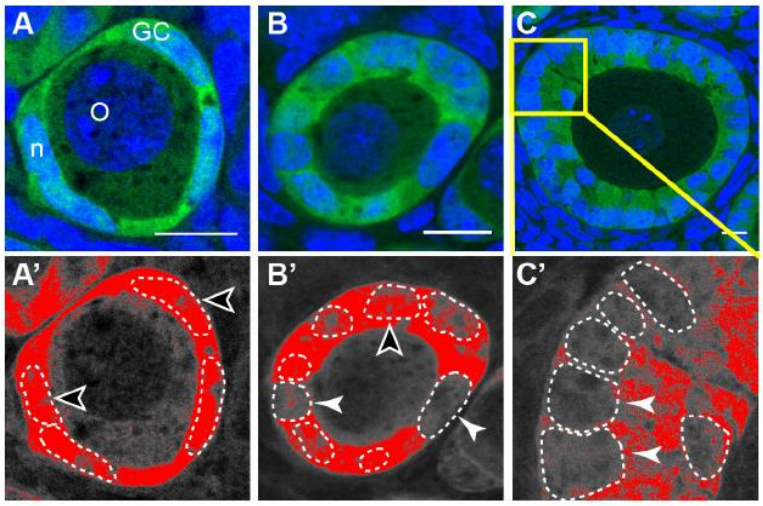

Figure 1.8. SMAD2/3 localisation during PFA. Primordial (A), primary (B) and multilayered (C) follicles labelled for SMAD2/3 (green) and DAPI (blue). (A' –C') ImageJ image of the green channel with a set threshold (red). Dotted lines delineate GC nuclei. SMAD2/3 appears in the nucleus of granulosa cells from primordial follicles, suggesting signalling activity. During PFA, when granulosa cells cuboidalise, SMAD2/3 proteins appear to be excluded from the nuclei (B) and this translocation increases as follicles continue to grow (C).White arrows indicate SMAD-negative nuclei and black arrows show SMAD-positive nuclei.

1.5 TGFβ superfamily pathway and GC proliferation

The canonical TGFβ signalling pathway is well-known for its role in the control of growth arrest (Massague, 2012). To achieve this, the SMAD2/3 intracellular mediators and transcription factors "sense" ligand-receptor binding and form complexes with factors from other pathways to repress or enhance the expression of several genes, such as cell cycle proteins. However, the mechanism by which SMAD2/3 can regulate GC growth is poorly understood. Based on information from other developmental processes, a detailed explanation of SMAD2/3-dependent mechanisms of gene regulation and inhibition will be explained in the sections below. In addition, an overview of the cell cycle and its relationship with SMADs will also be introduced.

1.5.1 Overview of intracellular signalling: SMADs

There are 7 type I (also known as ALKs) and 5 type II TGFβ receptors and they form tetrameric complexes (two type I and two type II) upon ligand binding at the cell surface. These receptors are a family of serine/threonine kinases and activation of the pathway is promoted by phosphorylation of the type I receptor by the type II receptor (Massague, 1998). Once the tetrameric receptor is activated, the type I receptors phosphorylate internal SMAD proteins. There are three subclasses of SMADs: receptor-activated SMADs (R-SMADs; SMAD1, 2, 3, 5 and 8), common-partner SMADs (Co-SMAD; SMAD4) (Moustakas et al, 2001) and inhibitory SMADs (I-SMADs; SMAD6 and 7) (Itoh et al, 2001). SMAD2 and 3 act downstream TGFβ/activin/nodal type I receptors and SMAD1, 5 and 8 act downstream of BMP type I receptors. Once these R-SMADs are phosphorylated, they interact with SMAD4 and form a complex, which enters the nucleus and regulates gene expression by binding to a specific SMAD-binding DNA element (SBE). I-SMADs compete for SMAD4 or associate with different proteins (such as SMAD specific E3 ubiquitin protein ligase Smurf, serine/threonine kinase receptor associated protein STRAP or neural precursor cell expressed, developmentally down-regulated gene 4-like NEDD4-2) to inhibit phosphorylation of R-SMADs by the receptor (Kuo et al, 2011; Moustakas et al, 2001) (Figure 1.9).

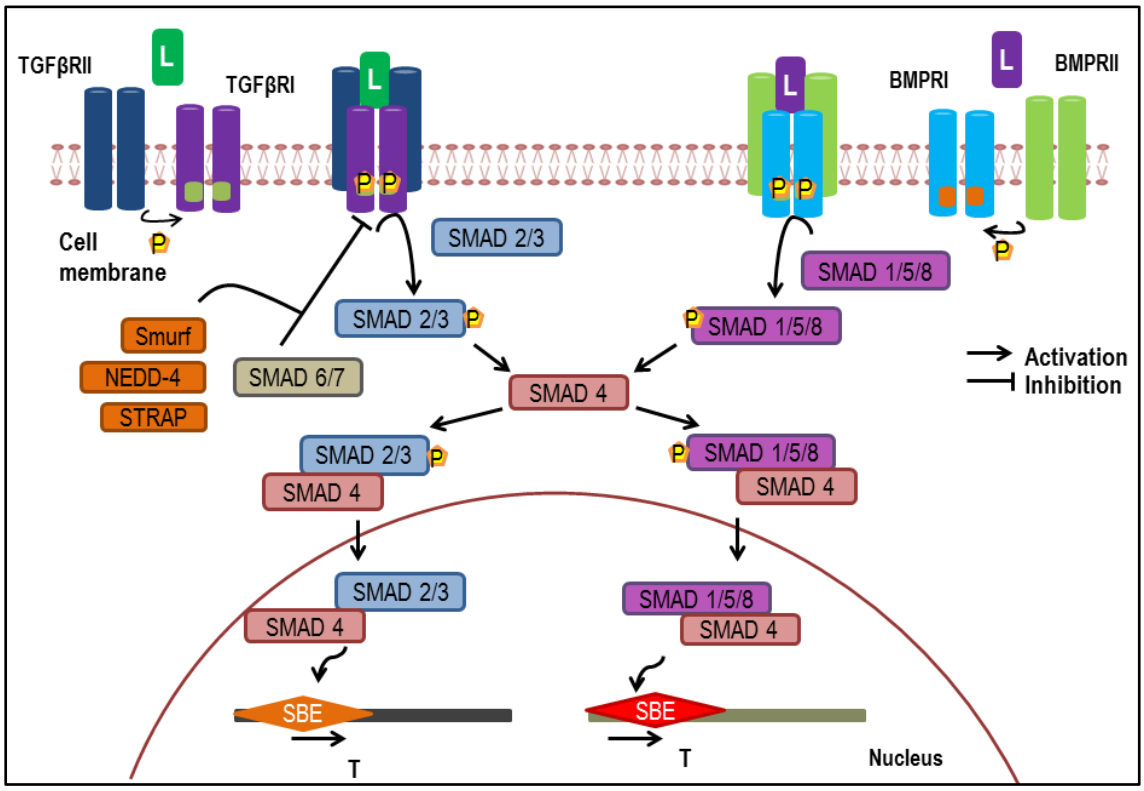

Figure 1.9. Canonical intercellular signalling by SMAD proteins. TGFβ/ activin (green L) and BMP (purple L) ligands bind the type II receptor (TGFβRII, BMPRII) which dimerises with the type I receptor (TGFβRI, BMPRI). The tetrameric receptor complex is then phosphorylated. Upon receptor phosphorylation, either SMAD 2/3 or SMAD 1/5/8 are recruited and phosphorylated and bind SMAD 4, both entering the nucleus and regulating gene expression (T) by binding to a specific SMAD-binding DNA element (SBE).

Structure of Co- and R-SMAD proteins

SMAD proteins are made up of two globular domains (MH1 and MH2) connected by a linker region (Figure 1.10). The MH1 domain corresponds to the N-terminal region and is highly conserved among R- and Co-SMADs and absent in I-SMADs (Massague et al, 2005b). The MH2 domain is located at the C-terminal region and is conserved in all SMADs. The MH1 domain is responsible for DNA binding activity due to its β-hairpin structure with a bound zinc atom, while the MH2 domain is required for the interaction with phosphorylated regions (present in the activated receptor or in the R-SMADs), cytoplasmic proteins and nucleoporins (Hill, 2008). However, both domains facilitate the interaction with other transcription factors and DNA-binding co-factors that stabilise the DNA-binding complex and determine gene regulation activity (Hill, 2008).

SMAD2 protein has a particular difference in the structure amongst the SMADs. Its most abundant isoform has an inserted sequence in exon 3 coding the MH1 domain that prevents its DNA binding activity (Shi et al, 1998; Sylviane et al, 1999). However, it is still capable of entering the nucleus and binding to different co-activators to regulate gene transcription, probably in a different manner to SMAD3 (Xu et al, 2002b). The linker region also has an important role in SMAD function as it harbours phosphorylation sites for the mitogen-activated protein kinase (MAPK) mediators ERK (extracellular regulated MAP kinase) or p38 (p38 mitogen activated protein kinase) (Hough et al, 2012; Matsuura et al, 2005b), Cyclin-dependent kinases (CDKs) (Alarcón et al, 2009), ubiquitin ligases binding sites (Gao et al, 2009) and in the case of SMAD1 and 4, the linker region also contains the nuclear export signal (NES) necessary for its export to the cytoplasm (Massague, 2012; Massague 2012 Oct; Massague et al, 2005b; Moustakas et al, 2001).

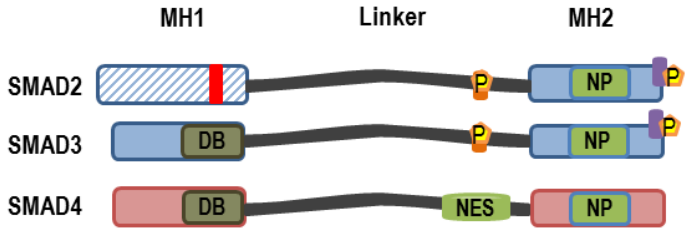

Figure 1.10. Structure of R- and Co- SMADs. Differences between protein domains explain differences in their function. The DNA binding domain (DB) in SMAD3 and SMAD4 is not present in SMAD2 due to the inserted sequence in exon 3 (in red). However both SMAD2/3 have the ability to be phosphorylated (P) by the receptor on their MH2 domain (purple) and also by other stimulatory/inhibitory pathways on the linker region (orange) whereas the linker region in SMAD4 harbours the nuclear export signal (NES). All three proteins have binding sites for different nucleoporins (NP) on their MH2 domain that facilitate their import/export into the nucleus.

SMAD basal subcellular localisation

Non-phosphorylated SMADs are capable of shuttling between the cytoplasm and the nucleus in the absence of receptor stimulation (i.e. basal conditions). However, at any given time, the majority of inactive (non-phosphorylated) SMADs will reside in the cytoplasm. This is the case for SMAD1, 2, 4 and 6 (Imamura et al, 1997; Nicolás et al, 2004; Xiao et al, 2001) whereas some studies have reported the presence of inactive SMAD3 and SMAD7 in the nucleus (Itóh et al, 1998; Schmierer et al, 2008). Furthermore, it is proposed that SMAD2/3 can translocate to the nucleus without being in complex with SMAD4 (Fink et al, 2003; Liu et al, 2016). Therefore, the presence of SMAD3 in the nucleus suggests that it may have transcriptional activity in the absence of a TGFβ signal (Liu et al, 2016), and any stimulation may further enhance or alter its transcriptional activity.

SMAD nucleocytoplasmic shuttling

SMAD import and export from the nucleus is mainly a consequence of receptor activation: as long as there is a ligand activating the receptor, the cascade of phosphorylation will trigger SMAD complex formation and import to the nucleus (Massague et al, 2005b). This SMAD shuttling requires nucleoporins from the nuclear pore complex (NPC) and/or importins/exportins (the transport receptors) that will allow SMAD shuttling via the Ran GTPase system, as passive diffusion of proteins bigger than 30kDa is not possible (Hill, 2008). If the TGFβ signal is maintained, there is an **accumulation of nuclear** SMADs in complex (Hill, 2008). According to the "retention only" model (RO), SMAD binding to several "retention" factors increases their nuclear residence time (Figure 1.11). Moreover, a different translocation rate between SMAD complexes and monomeric SMADs has been observed where SMADs in complex translocate 5 times faster (Schmierer et al, 2008). Therefore, a "retention/enhanced complex import model" (RECI) is proposed to explain the increased nuclear accumulation of SMADs in complex (Schmierer et al, 2008).

Importins are required to translocate SMADs complexes into the nucleus (Kurisaki et al, 2001). However, monomeric SMADs can also enter the nucleus via importin-independent mechanisms, which may explain the difference in import rate between basal and TGFβ-stimulated cells (Kurisaki et al, 2001; Schmierer et al, 2008; Xu et al, 2003). In addition, the role of nuclear and cytoplasmic "adaptor" and "retention" factors play an important role in the rate of nuclear accumulation and therefore, signal maintenance. For instance, **nuclear accumulation enhancers** such as proteins like TNF receptor-associated protein 1 (TRAP-1) or TRAP-1-like protein (TLP), facilitate SMAD2/3-4 complex formation by interacting with the TGFβ receptor (Felici et al, 2003; Wurthner et al, 2001). Also proteins such as the yes-associated protein (YAP) and transcriptional coactivator with PDZ-binding motif (TAZ) from the Hippo signalling pathway bind to complexed SMADs in the nucleus to prevent their export (Figure 1.12) (Varelas et al, 2008). In contrast, **nuclear accumulation inhibitors** such as serine/threonine kinase receptor associated protein (STRAP) acts at the level of receptor, stabilising SMAD7 association to prevent further R-SMAD signalling (Datta & Moses, 2000). In addition, proteins such as SMAD anchor for receptor activation (SARA) or prostate transmembrane protein, androgen induced 1 (PMEPA1) interact with R-SMADs and inhibit their nuclear translocation, playing a role in signal termination (Runyan et al; Watanabe et al, 2010). Termination of TGFβ stimulation also occurs at different levels: from the receptor inhibition to the removal of cytoplasmic and nuclear retention factors, inhibitory phosphorylation by other pathways (Matsuura et al, 2005a), R-SMAD dephosphorylation by phosphatases such as protein phosphatase (Ppm1a) (Lin et al, 2016) and subsequent SMAD degradation mechanisms (Figure 1.11).

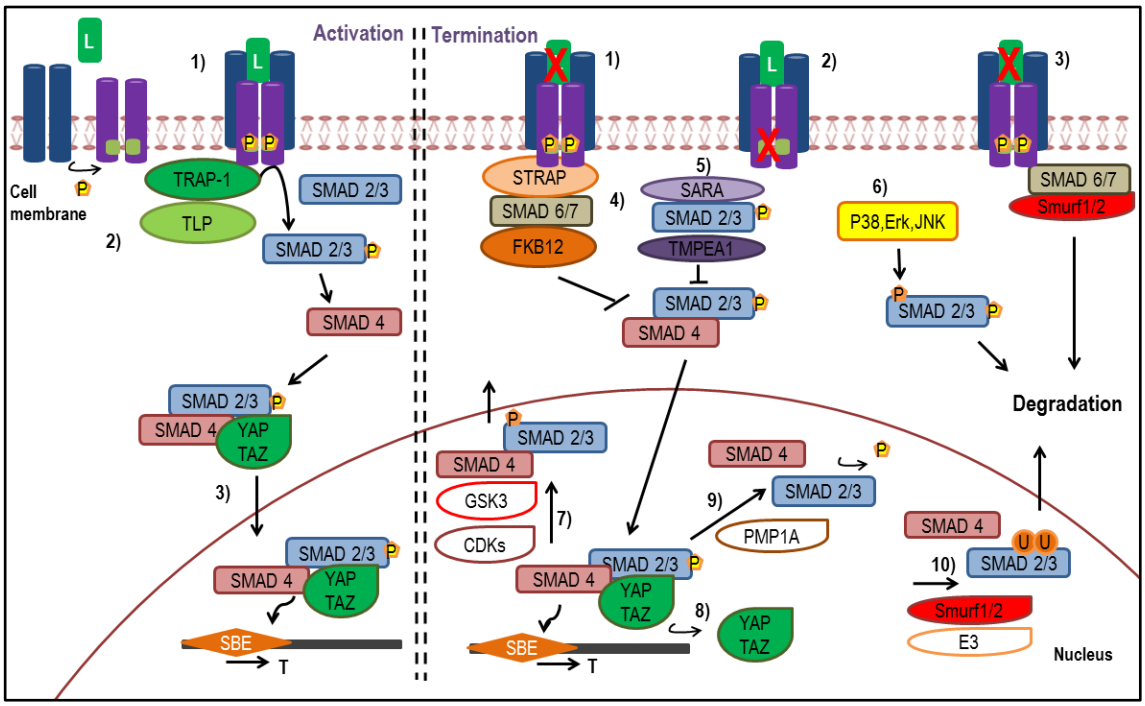

Figure 1.11. TGFβ signal transduction and termination. In the presence of ligand (1), nuclear retention enhancers (such as TRAP-1 or TLP) maintain the signal transduction from the receptor (2) and accumulation of SMADs in the nucleus (such as YAP/TAZ, 3). Several factors contribute to the termination of the signal transduction at three different levels: at the **receptor** level, the absence of ligand stimulation (1) and degradation (3), the role of proteins binding to either TGFβ **receptor I or II** (therefore impeding their phosphorylation, such as FK506 binding protein FKBP12(Yamaguchi et al, 2006), the inhibitory SMAD7 or STRAP) (4) or the effect of decoy receptors interrupting receptor complex formation (e.g BMP and activin membrane-bound inhibitor, BAMBI (not shown) (Onichtchouk et al, 1999)) (2); in the **cytoplasm**, mediators that interact with R-SMADs and block the residues important for nucleoporin interaction and transcriptional complex formation (e.g SARA or TMPEAi) (5) or SMAD inhibitory **phosphorylation** by MAPK pathway mediators (Erks) (6). At **nuclear** level, SMAD export from the nucleus to the cytoplasm may involve the removal of "**retention** factors" (8), SMAD **dephosphorylation** and dissociation of the SMAD complex or viceversa (e.g PPM1A) (9), SMAD inhibitory **phosphorylation** via CDKs and GSK3 (7) and the **ubiquitination** for degradation via proteasome (via Smurf1/2 or E3) (10).

Pathway integration and non-canonical TGFβ signalling

TGFβ signalling is known as an important regulator of epithelial cell maintenance but also has a key role in EMT during processes such as organogenesis throughout embryonic development (Derynck & Akhurst, 2007). During EMT, cells experience a switch from polarised and static to depolarised and migratory with invasive capacities (Kalluri & Weinberg, 2009). Such scenarios are also associated with pathological situations related to fibrosis and cancer progression (López-Novoa & Nieto, 2009). Although the canonical SMAD signalling pathway is a key initiator of EMT, it is proposed that the activation and crosstalk with non-canonical TGFβ signalling is crucial to complete the process (Jian et al, 2009; Massague, 2012).

As well as promoting SMAD signalling, TGFβ receptors can activate MAPK and PI3K signalling pathways. Moreover, these pathways can also independently influence SMAD signalling. (Figure 1.12). Phosphorylation of serine and tyrosine residues of the TGFβRII and TGFβRI can lead to the recruitment of MAPK mediators such as TNF receptor-associated factor 6 (TRAF6), triggering p38/JNK activation (Yamashita et al, 2008) or the activation of Ras-ERK pathway (Xie et al, 2004), both leading to a coordinated transcriptional regulation in conjunction with SMADs (Davies et al, 2005). Moreover, ras homolog family member A (RhoA), cell division cycle 42 (Cdc42) and Ras-related C3 botulinum toxin substrate (Rac) can also be activated by TGFβRII and I, where they influence actin polymerisation and tight junction dissolution, which is an essential requirement for EMT (Bhowmick et al, 2001; Ozdamar et al, 2005; Wilkes et al, 2003). In addition, TGFβ-induced activation of PI3K pathway via AKT and mTOR act to promote an increase in cell size and protein synthesis in epithelial cells undergoing EMT (Lamouille & Derynck, 2007).

Although there is minimal detailed knowledge of the physical interactions between the TGFβ receptors and the non-canonical factors described above (Massague, 2012; Mu et al, 2012), the recruitment of TRAF6 (p38/JNK pathway), PAR6 (RhoA activation), p85 (PI3K signalling) and ShcA (Ras-ERK pathway) can propagate SMAD-independent signals (Figure 1.12) (Jae et al, 2005; Lee et al, 2007; Ozdamar et al, 2005; Yamashita et al, 2008).

Nevertheless, the interaction of intracellular mediators of these pathways with TGFβ signalling is a key event for the spatial-temporal coordination of multiple biological signals (Xing & Xiao-Fan, 2008). For example, the PI3K signalling pathway is known to inhibit the canonical TGFβ pathway by inhibiting the nuclear localisation of Forkhead Box 1 (FOXO1) transcription factor and its interaction with nuclear SMADs (Seoane et al, 2004) or by sequestration of cytoplasmic SMAD3 by AKT during TGFβ mediated apoptosis (Conery et al, 2004). In addition, the Wnt signalling mediator beta-catenin is also known to interact with SMAD2/3 and regulate the expression of common genes (Attisano & Wrana, 2013).

The SMAD2/3 linker region (see Figure 1.9) is the target for the phosphorylation by non-canonical pathways. The MAPK signalling mediators p38/ERK are capable of phosphorylating this region to inhibit SMAD activity (Kretzschmar et al, 1999; Matsuura et al, 2005b). However, recent investigations have also observed a positive induction and maintenance of SMAD2/3 activity via SMAD2/3-linker-phosphorylation (Browne et al, 2013; Hough et al, 2012). The linker region harbours several phosphorylation residues, each having different specificity to different mediators that either activate or inhibit SMAD2/3 activity. For instance, phosphorylarion in residues Ser207 (by ERK), Th179 and Ser 208-213 (by CDKs) often lead to inhibition of SMAD2/3 activity, whereas phosphorylation in Ser 204 (by ERK) has been shown to activate SMAD2/3 activity of target genes (Browne et al, 2013; Matsuura et al, 2005a; Wang et al, 2009).

As described in section 1.4, the initiation of PFA is proposed to show similarities with EMT (Mora et al, 2012b). Whether SMAD signalling with or without cooperation with different pathways is important in this context is currently unknown.

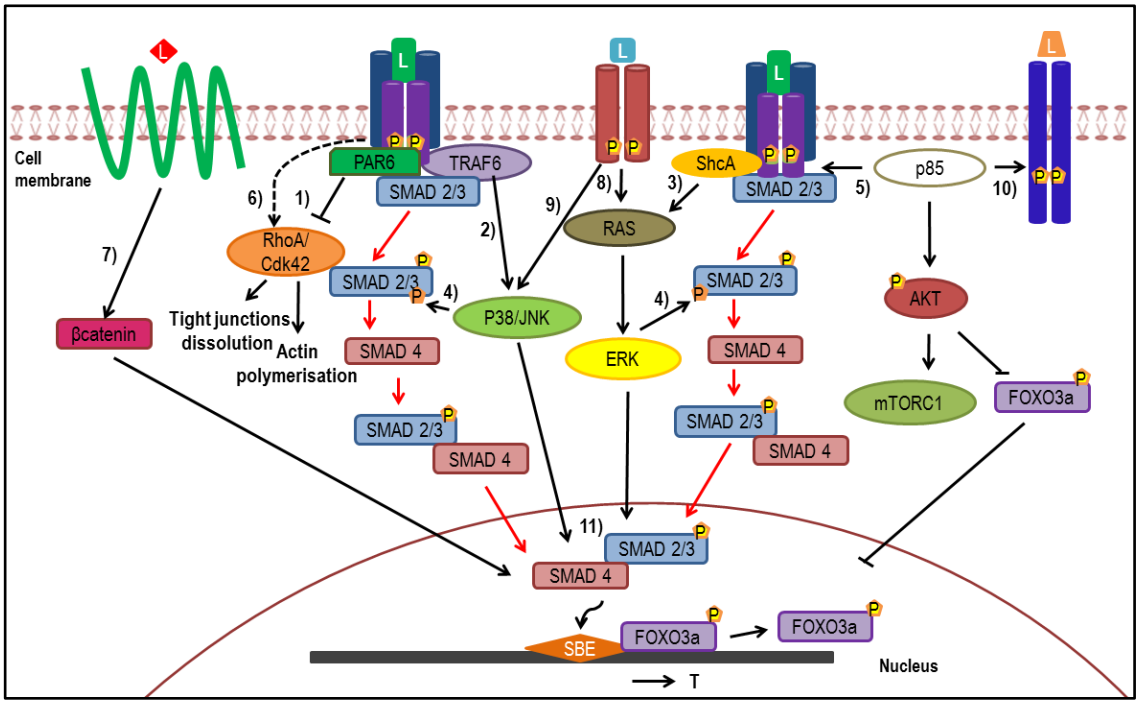

Figure 1.12. Non-canonical TGFβ-driven signalling pathways. After ligand stimulation, TGFβ receptor has the ability to recruit factors from other pathways such as PAR6 (1) which inhibits RhoA/Cdk42 activity; TRAF6 (2) and schA (3), which lead to p38/JNK and ERK phosphorylation and subsequent transcriptional regulation in the nucleus or cytoplasmic phosphorylation of Smad2/3 in the linker region (4); and the regulatory subunit of p85, triggering mTORC activation or Foxo3a inhibition (5). Activation of RhoA by the receptor is also possible (6), promoting actin polymerisation during EMT. In addition, independent canonical pathways activated by their ligands (7,8,9 and 10) can interact with SMADs in the cytoplasm (4) or in the nucleus (11) to regulate common biological processes.

1.5.2 Cell cycle machinery, TGFβ signalling and the primordial follicle ovarian reserve

Overview of cell cycle

In every cell division an interplay of cyclins and their cyclin-dependent kinases (CDKs) allows the transition between G0/G1/S/G2/M phases. In mammalian cells, cyclins can be classified (in the order of their role in cell cycle) as cyclin D, E, A and B. In addition, their corresponding CDKs are CDK4, CDK6, CDK2 and CDK1 (Sherr & Roberts, 1999). During transition from G0 to G1, cyclin D assembles with CDK4 or 6, phosphorylating Retinoblastoma protein (Rb). This allows the release of the E2F transcription factor, which promotes the expression of genes such as cyclin E (Figure 1.13).

During the late G1 phase, CyclinE assembles with CDK2 and promotes again the phosphorylation of Rb with the subsequent E2F transcription promotion of genes such as cyclin A gene. CDK2 binds CyclinA and promotes the initiation of S phase with the phosphorylation of proteins implicated in DNA replication. The transition from G2 to M is regulated by CyclinA-CDK1 and completion of mitosis is dependent on CyclinB action (Sherr & Roberts, 1999) (Figure 1.13). The timing of these transitions is highly dependent on CDK inhibitors (CKIs) that allow the process to be coordinated but also to respond to different biological conditions (such as stress or DNA damage) (Satyanarayana & Kaldis, 2009). Based on their structure and CDK targets, CKIs can be divided in two groups: INK4 proteins (p15, p16, p18, p19), which bind to CDK4 and 6; and Cip/Kip proteins (p21, p27, p57), which bind to either CDKs or cyclins. If p21 or p27 are not bound to CyclinD-CDK, they bind instead to CyclinE-CDK and form an inactive complex that impedes phosphorylation of Rb and further cell cycle progression. Upon mitogen stimulation, assembly of p21/p27 to CyclinD-CDK complexes sequesters its binding to CyclinE-CDK, when Rb can be phosphorylated and cell cycle can progress. In contrast, INK4 proteins are related to cell cycle arrest by binding to CDK4/6 and impeding the CyclinD-CDK assembly (Satyanarayana & Kaldis, 2009).

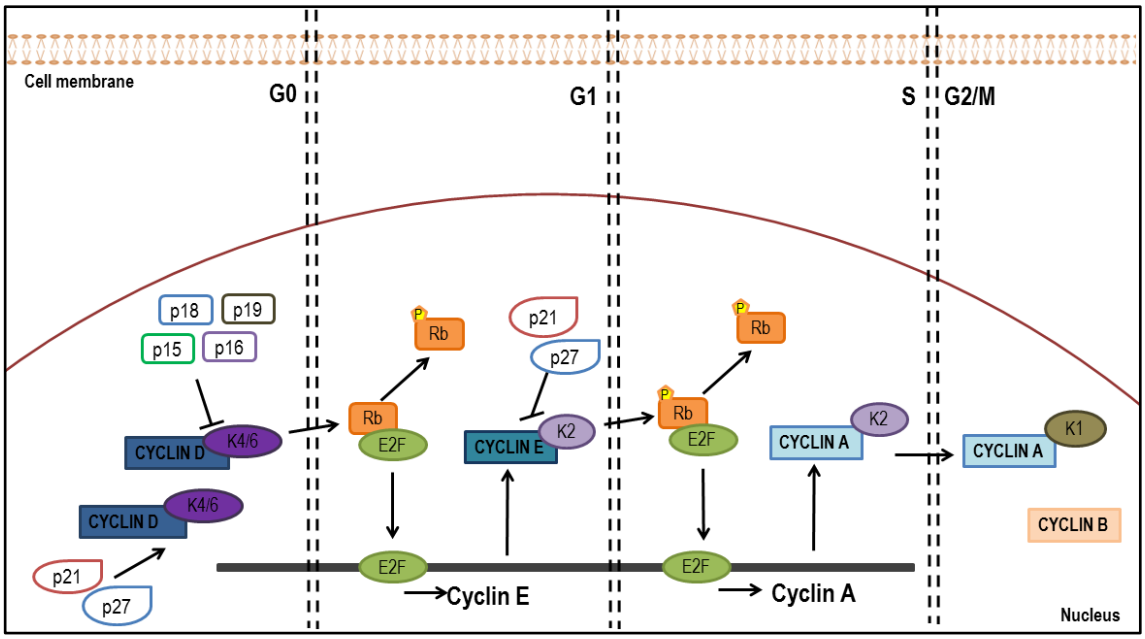

Figure 1.13. Participation throughout the different phases of the cell cycle of Cyclins, CDKs and CKIs. The simplified schematic shows the sequential activation of Cyclins once activated from G0 (quiescence) until M (mitotis entry). Modulation of cell cycle progression is dependent on the different activation and binding of CDKs and CKIs to their corresponding Cyclin.

The role of cell cycle factors in the ovary

Several KO models for cell cycle proteins have been generated and only p27, CyclinD2 (CCND2) and Cdk4 KO mice exhibit impaired fertility (Moons et al, 2002; Rajareddy et al, 2007; Sicinski, 1996). More specifically, *Cdk4*$^{-/-}$ showed normal fertility, however, they presented abnormal CL maintenance due to a deficiency in prolactin production (Moons DS 1 2002). In *Ccnd2*$^{-/-}$ mice, follicles arrest with no more than 3-4 layers of GCs, indicating that the proliferation of GCs during these early stages requires *Ccnd2* gene expression (Sicinski, 1996). By comparison, *p27*$^{-/-}$ mice exhibit premature activation of the primordial follicle pool (section 1.4.2) suggesting that p27 is fundamentally required for the maintenance of follicle quiescence (Rajareddy et al, 2007).

Other cell cycle regulators are also implicated in follicle development. The Cyclin-dependent kinase inhibitor 1A (**p21)** has been reported to control GC proliferation during luteinization in cooperation with p27 (Jirawatnotai et al, 2003). The Cyclin dependent kinase inhibitor 2B (**p15**), one of the more well characterised target genes for SMAD3 (Seoane et al, 2001), has not been investigated in the context of small follicles but is detectable in mouse luteal cells (Burns KH 1 2001) and is up-regulated in cases of ovarian cancer (Arcellana-Panlilio et al, 2002). Therefore, it is unclear whether regulation of p15 expression is important in the context of GC proliferation. Myelocytomatosis (MYC) oncogene has been extensively related to the cell cycle, and its overexpression is often associated with human cancers (Jonas & John, 2003). The *MYC* gene is a target of SMADs and its protein product is a transcriptional suppressor of the SMAD-regulated target genes, p15 and p21 (Seoane et al, 2001; Siqin et al, 2003). There is little information on the role of MYC in the context of the ovary, however, its expression has been observed in GCs of growing follicles, follicles undergoing atresia and luteal cells in human, mice and rat (Li et al, 1994; Nandedkar & Dharma, 2001; Putowski LT 1 1997).

TGFβ signalling and CCND2 in GC proliferation

In GCs obtained from large, gonadotrophin-dependent follicles, activin promotes *Ccnd2* expression via SMAD2/3 (Park et al, 2005). Likewise, *Ccnd2* gene expression is reduced in ovaries of exon 8-*Smad3*$^{-/-}$ mice (Looyenga & Hammer, 2007; Tomic et al, 2004). Furthermore, higher levels of SMAD3 and CCND2 are found in GC tumours (Anttonen et al, 2014a). Together these studies suggest that SMAD3 is an important regulator of *Ccnd2* expression. Moreover, this expression was localised in GCs of follicles from all stages, including primordial follicles (Robker & Richards, 1998a). Since SMAD2/3 proteins are predominantly expressed in GCs of small follicles (Fenwick et al, 2013), it is possible that the TGFβ-SMAD pathway is also inducing *Ccnd2* gene expression in this context. Since CyclinD proteins tend to be expressed in the G0 phase of the cell cycle, the expression and regulation of *Ccnd2* in quiescent primordial follicles may be key towards understanding how these follicles are maintained and subsequently activated to grow.

1.6 Hypothesis and objectives

Within the process of follicle development, the transition between primordial to primary follicles is believed to be gonadotrophin-independent. Intraovarian factors are needed to monitor this transition to coordinate development of the oocyte and GCs. The proliferation of GCs is thought to precede oocyte activation and growth, marking the initiation of PFA. The presence of SMAD2/3 in the nuclei of GCs is clearly evident in primordial follicles and loss of this expression in the nuclei of GCs of growing follicles suggests SMAD2/3 is associated with PFA. SMAD2/3 transcription factors are critical modulators of many cellular processes; however, regulation of growth arrest and EMT transition are believed also to be important (Heldin et al, 2009). For instance, SMAD2/3 regulation of cell cycle genes (such as MYC) is essential to maintain cell proliferation. The cell cycle regulators CCND2 and p27 are detectable in the ovary and have been implicated with GC function. However, the conditions by which these genes are regulated, and their role in primordial follicles are poorly understood. In the studies presented in this thesis it is hypothesised that **SMAD2/3 transcription factors regulate the expression of key cell cycle genes in GCs to allow the maintenance and activation of primordial follicles.** This will be tested by the following objectives:

Objective 1: To determine the expression pattern and map the relationship of SMAD2/3, CCND2 and p27 throughout the different stages of early follicle development (chapter 3).

Objective 2: To establish the relationship between CCND2/p27 protein complexes in primordial and growing follicles and determine how this relates to maintenance and activation of primordial follicles (Chapter 4).

Objective 3: To determine if SMAD2/3 directly regulates key cell cycle genes in different TGFβ conditions and determine how this relates to early follicle growth (Chapter 5).

Chapter 2.

Materials and Methods

2.1 Animals and tissue collection

All mice used in this study were wild-type C57BL/6 genetic background. These mice were tissue donors only and no interventions were carried out on live animals. All mice were maintained, purchased, and killed by Schedule 1 procedures in accordance with UK Home Office regulations and adherence to the Animals (Scientific Procedures) Act, 1986, in the Biological Services Unit, at the University of Sheffield.

In order to study the process of PFA, the molecular and morphological changes during the transition from primordial to large preantral follicle stages were the main focus of this thesis. For this, ovaries from immature (day 4,8 and 16) mice were used, since they contained a high proportion of these follicle stages. Based on estimate numbers from a large cross-section of day 4, day 8 and day 16 ovaries (Appendix 1A), day 4 ovaries mainly consist of primordial and transitional follicles (~45% of each stage), day 8 ovaries contain mostly primordial, transitional and a few small preantral and large preantral follicles (~38%, 27%, 16% and 13% respectively) and day 16 ovaries are exemplified by primordial, transitional and secondary follicles (~38%, 20% and 28% ,respectively) and also include small and large preantral follicles (~14%) (Figure 2.1). This model has been used to profile morphological and gene expression changes during early follicle development previously (Drummond et al, 2002; Fenwick et al, 2011; Sharum et al, 2016).

For total RNA and protein extraction, ovaries from immature (day 4, 8 and 16) mice were dissected from the ovarian bursa and peri-ovarian fat under a dissection microscope in Leibovitz's L-15 medium (Life Technologies) containing 1% (w/v) BSA (Vector Laboratories) before snap freezing in liquid nitrogen and storage at -80 ºC.

For immunostaining, ovaries were immersed in 10% neutral buffered formalin solution (Sigma-Aldrich) for 24 hours and then transferred to 70% ethanol. Ovaries were processed in paraffin blocks (Appendix 1B), which briefly consisted of the following: dehydration in a graded series of ethanol, treatment with a clearing agent (HistoChoice, Sigma) to remove the ethanol and finally, submersion in melted paraffin for embedding. Solid paraffin blocks were removed from the metal molds and sectioned (5µm) using a microtome (Reichert-Jung 1150/Autocut). Wax sections were mounted on positively charged slides (Superfrost® Plus scientific slides, ThermoFisher Scientific) and dried overnight at 37ºC.

2.2 NIH3T3 and PHM1 cell lines

The NIH3T3 fibroblastic cell line (ATCC) derived from a NIH Swiss mouse embryo contains endogenous CCND2 and p27. Therefore, this cell line was used as a positive control for some western blot and co-immunoprecipitation experiments. Cells were maintained in Dulbecco's Modified Eagle Medium (Sigma) containing 10% (v/v) Fetal Calf Serum (FCS) (Sigma), 2mM L-glutamine (Sigma) and 0.01% penicillin/streptomycin (Sigma) and passaged every three days to avoid total confluency. The PHM1 cell line (ATCC) was derived from pregnant human myometrium at 39 weeks of gestation, during cesarean section. This cell line was used to study SMAD3 phosphorylation with Western Blot. PHM1 cells were maintained in Dulbecco's Modified Eagle's Medium (Sigma) containing 10% (v/v) FCS (Sigma), 0.01% penicillin/streptomycin (Sigma) and Geneticin (0.1mg/ml) (Gibco).

2.3 Neonatal mouse ovary culture

As the ovary is an approximately spherical organ, oxygen access to the center of the tissue (ovarian medulla) is limited when a thick layer of culture medium is overlaid. Therefore, the use of permeable membrane inserts into culture plates (24mm Transwell® plates; Corning) was used for all day 4 mouse ovaries. Using these inserts, ovaries are maintained within a thin meniscus of culture medium, which permits oxygen and nutrient access to the whole organ. Ovaries were cultured in Waymouth medium 752/1 (Life Technologies) supplemented with 10% of fetal bovine serum (FBS) (Sigma), 0.23mM pyruvic acid (Sigma), 10µg/L streptomycin sulfate (Sigma), 75µg/L penicillin G (PENK; Sigma) and 0.3mg/mL BSA. Medium (1.5ml) was filtered with a 0.2µm sterile syringe filter and added below the membrane insert. Ovaries were maintained in a 37ºC incubator (5% CO2) for 24h with either serum or serum-free medium, prior to any experiment.

2.4 Histological analysis

2.4.Haematoxylin and Eosin (H&E) staining

In order to evaluate the morphology of follicles at different developmental stages, sections from paraffin embedded ovaries from mice at 4, 8 and 16 days of age were dewaxed with HistoChoice (2x 5 minutes) and rehydrated with gradient series of industrial methylated spirit (IMS) solutions (99%, 99%, and 70%, 1x 5 minutes each). Then, sections were

washed with tap water (1x 5 minutes), nuclei were stained with Gill's haematoxylin (Surgipath Europe LTD, Peterborough, UK) for 120 seconds and immediately washed in tap water for 3 minutes in order to increase the nuclear staining contrast with the cytoplasm. Cytoplasm was stained (1x 5 minutes) with 1% aqueous eosin (Surgipath) and washed in tap water for 30 seconds. Sections were dehydrated using gradient series of IMS solutions (70% and 95% for 10 seconds each and 99% for 1 minute) and finally placed in HistoChoice to ensure total removal of IMS. Sections were mounted with DPX (Merck, Darmstadt, Germany), left to dry under the hood and imaged using an Olympus CKX41 microscope (Figure 2.1).

2.4.2 Immunofluorescence staining

Immunofluorescence staining was performed to localise all factors of the study within the ovary. Sections from paraffin embedded ovaries (5 μm) were dewaxed with HistoChoice (2x5minutes) and rehydrated with gradient series of IMS solutions (100%, 95%, and 70%, 1x3 minutes each) and washed in distilled water (1x5 minutes) and microwaved in 0.1M citrate buffer (pH6.0) for antigen retrieval (20 minutes). Sections were washed in 0.1M PBS pH7.4 (2x 5 minutes) and blocked with CAS universal blocking reagent (Invitrogen) for 20 minutes at room temperature to reduce non-specific binding. Primary antibodies (Table 2.1) were diluted in blocking solution at a concentration previously optimised by titration and incubated overnight at 4ºC in a humidified chamber. Negative controls for the primary antibody (by using an isotype control IgG antibody at the same concentration) and secondary antibody (absence of primary antibody) were included in each experiment (Table 2.2). Sections of adult ovaries were used as a positive control for optimisation experiments.

The following day, sections were washed in PBS (3x10 minutes) and incubated with secondary antibodies (Table 2.2) for 45 minutes at room temperature in the dark. Sections were washed in PBS (2x 5 minutes) and coverslips were mounted with a drop of Prolong® Gold anti-fade reagent with DAPI (ThermoFisher Scientific) onto each section. Specimens were analysed using an inverted fluorescence microscope Olympus IX73 and for better resolution, high quality images were obtained using an inverted Leica SP5 confocal laser-scanning microscope (Leica Microsystems, Wetzlar, Germany).

For TUNEL labelling, tissues were permeabilised for two minutes with a solution containing 0.1% (w/v) tri-sodium and 0.1% (v/v) triton X-100 in distilled water and were washed in PBS (2x2 minutes) prior to blocking. The TUNEL label mix (Roche) was applied to the slides and incubated for 1 hour at 37 ºC prior to secondary antibody incubation.

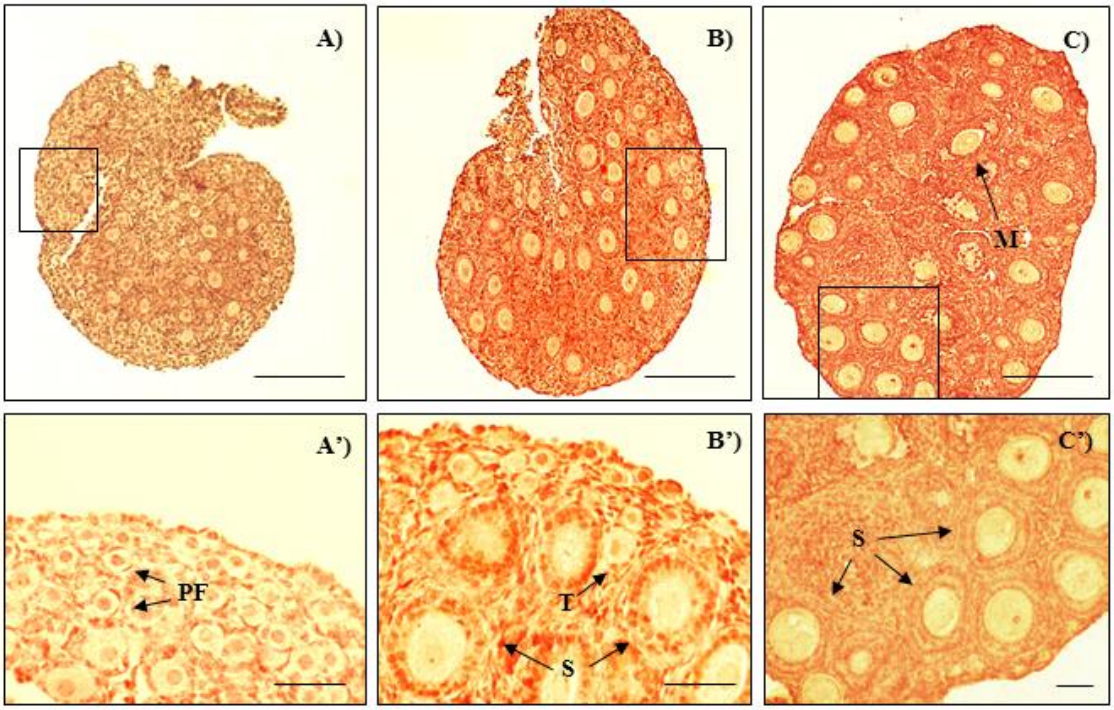

Figure 2.1. H&E staining of day 4 (A), day 8 (B) and day 16 (C) mouse ovaries. The proportion of growing follicles increases with age due to progressive follicle activation (PFA). Higher magnification (A', B' and C') shows primordial follicles (PF) with a few flat granulosa cells (GCs), transitional follicles (T) with a few cuboidalised GCs and secondary follicles (S) with two layers of cuboidalised GCs and multilayered follicles (M) with an antrum starting to form. Scale bar is 200µm (A, B, C) and 50 µm (A', B', C') with magnification of 10X and 40X, respectively.

2.4.3 Classification of small follicles for image analysis

In order to perform image analysis of immunofluorescently-labelled ovary sections, a follicle classification system was used. As explained in chapter 1, a change in granulosa cell (GC) number and shape are key morphological events observed during PFA. Many of the factors studied in this thesis are mainly present in GCs; therefore, localisation was related to the morphological changes associated with PFA. Figure 2.2 shows the classification criteria considered for the analysis. As will be explained in more detail in chapter 3, sections of day 8 ovaries were used in the analysis. The ROI manager tool of Image J software was used to carefully select individual GC nuclei in follicles to quantify the percentage of specific staining (chapter 3).

Follicles were classified as primordial (PF) when 1 to 3 flat GCs were enclosing the oocyte; transitional (T) when follicles contained from 4 to 7 flat and cuboidal GCs; small primary (P) when a clear ring of cuboidalised GCs was observed (from 9-14); large primary (P+) when more than 14 cuboidalised cells were observed in a single layer and secondary (S) when a second layer of cuboidalised GCs started to form (Figure 2.2). For better accuracy in the classification, only follicles that contained a clear outline of the oocyte nucleus (indicating largest cross-section of the follicle) were selected for analysis. The classification criteria applied is similar to the previously reported for mouse follicles (Pedersen & Peters, 1968), however, the additional group of transitional follicles (T) was considered (different from primordial follicles, PF) as the PFs that have started or are in the process of activation.

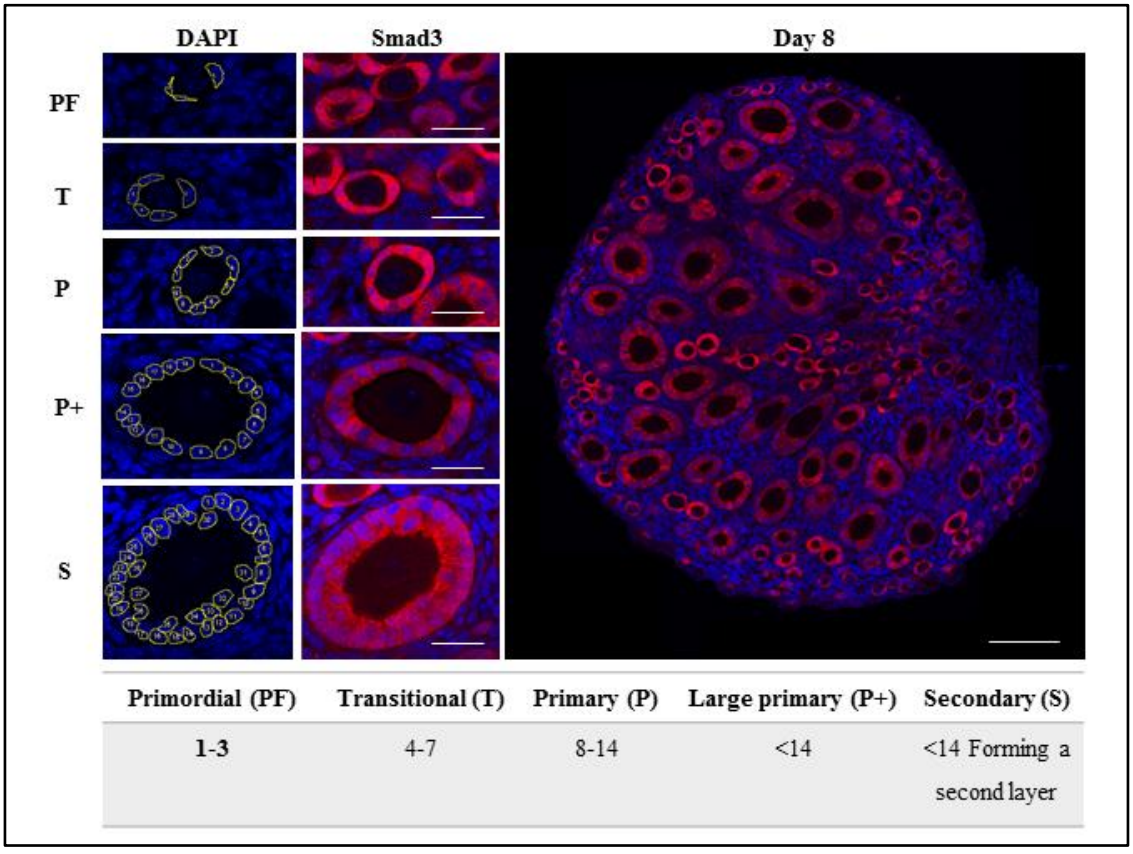

Primordial (PF)	Transitional (T)	Primary (P)	Large primary (P+)	Secondary (S)
1-3	4-7	8-14	<14	<14 Forming a second layer

Figure 2.2. Classification of follicles according to GC number. First two columns show a representative example of each follicle stage, where individual GC nuclei are selected using the DAPI channel (blue). The staining for SMAD3 protein is shown in red for the same follicles. An example of a section from a day 8 ovary that was employed for the image analysis is also shown. Numbers shown in the table correspond to the number of GCs included for each group of follicles. Scale bar is 25µm for the two first columns and 100µm for the day 8 ovary section, with magnification of 63X and 20X, respectively.

2.5 Protein extraction, co-immunoprecipitation and western blot

2.5.1 Protein extraction from cell lines

For protein extraction, cells were washed in ice-cold PBS and the monolayer was removed with a cell scraper with a specific volume of Pierce IP lysis buffer (ThermoFisher Scientific) depending on the surface area (1ml for 75mm2 flask and 150µl for 6 well-plate culture dish). IP lysis buffer contained protease inhibitors (cOmplete ™ Mini ULTRA tablets; Roche) and phosphatase inhibitors (PhosSTOP™, Roche) to prevent protein/phosphate degradation. Cells were placed in 1.5ml Eppendorf tubes, vortexed briefly and placed on ice for 15 minutes. After centrifugation at 13,000x rpm for 10 minutes at 4 ºC, the supernatant containing total protein was collected and stored at -20ºC.

2.5.2 Protein extraction from mouse ovaries

Ovaries from day 4, 8 and 16 mice were used for total protein extraction. In order to obtain enough protein content, two ovaries per sample were used for day 4 and day 8 and one ovary for day 16. After washing with lysis buffer, samples were further disrupted with 25G needles. Different volumes of IP lysis buffer (ThermoFisher) were optimised and used to lyse the ovaries: 70µl for day 4, 100µl for day 8 and 80 µl for day 16 ovary samples. Samples were vortexed 6 times for 1 minute before leaving on ice for 15 minutes and finally centrifuged at 13,000x rpm for 10 minutes at 4 ºC. Supernatant containing total protein was collected and stored at -20ºC.

2.5.3 Subcellular fractionation of proteins from day 4 and day 16 mouse ovaries

In order to study the location of candidate proteins at the cellular level in primordial and growing follicles, a protein extraction protocol based on sequential cell lysis with three different extraction buffers containing increasing detergent strengths (Appendix 7) was used. The combination of the different extraction buffers and the different centrifugal forces to collect the subcellular fractions were based on a recent report (Baghirova et al, 2015).

The key components from each buffer are digitonin (buffer A), a saponin that binds mainly to cholesterol on the plasma membrane and permeabilises it by pore formation, leaving the organelle membranes intact; igepal (buffer B), a non-ionic and non-denaturing agent that allows the disruption of endoplasmic reticulum membranes, golgi and mitochondria but not the nucleus and finally, the combination of sodium deoxycholate/SDS (buffer C) which increases nuclear membrane solubilisation and treatment with benzonase, an enzyme that digests DNA and RNA to allow the release of nuclear protein content.

The protocol used for day 4 and day 16 mouse ovaries was adapted from the mentioned report (Baghirova et al, 2015) and was based on a combination of mechanical disruption of mouse ovaries (by brief vortexing) with the extraction buffers (containing proteases and phosphatases inhibitors) followed by the centrifugation at 4ºC and collection of each fraction. First, three ovaries/sample from day 16 and six ovaries/sample from day 4 of age were disrupted with needles with 100 µl buffer A and incubated for 10 minutes with 10 second vortex intervals (every 2 minutes). After centrifugation for 10 minutes at 4000xg, supernatant containing the cytoplasmic fraction was collected. The pellet was resuspended in 100 µl of buffer B and incubated for 30 minutes with 5 second vortex intervals (every 5 minutes). After centrifugation for 10 minutes at 6000xg, the supernatant containing the membrane/organelle fraction was collected. Two µl (500 units) of benzonase (Sigma) were added with 20 µl of water to the pellet and incubated at room temperature for 15 minutes. The pellet was then resuspended in 100 µl of buffer C and incubated for 10 minutes with 10 seconds vortex intervals (every 2 minutes). The nuclear fraction was obtained by collecting the supernatant after centrifugation at 6800xg for 10 minutes and stored at -20 ºC. Equal amounts of the cytoplasmic, membrane and nuclear protein fractions (from a range of 3-5µg) were used for analysis by western blotting.

2.5.4 Protein concentration determination

Protein concentration from whole cell lysates, whole ovary lysates and subcellular fractions were measured according to the manufacturer's guidelines using the Pierce BCA (bicinchoninic acid) protein assay kit (ThermoFisher Scientific).

Briefly, reagent B was diluted 1 in 50 with reagent B and 200 µl of the solution were added to each well in a 96-well plates. Then, 10 µl of protein standards (known concentrations of BSA from 25µg/ml to 2000µg/ml), negative control (lysis buffer) and protein lysate samples were added in duplicate to each well, incubated at 37 ºC for 30 minutes and allowed to cool at room temperature. Protein absorbance was measured on a POLARstar Galaxy microplate reader (BMG Labtech) at the wavelength of 562nm. A standard curve by plotting the absorbance vs. the concentration of each BSA sample was generated in GraphPad Prism using a second order polynomial (quadratic) curve-fitting algorithm and the concentration of the protein lysate samples was determined by interpolation of their absorbance with the standard curve.

2.5.5 Co-immunoprecipitation

In order to study protein interactions, isolation of protein complexes was performed following protein extraction with Pierce IP lysis buffer containing protease inhibitors (cOmplete ^{TM} Mini ULTRA tablets; Roche) and phosphatase inhibitors (PhosSTOP^{TM}, Roche). Twenty-five µg (ovaries) and 80µg (NIH3T3 cell line) of total protein extract were diluted up to 500µl with IP buffer. This facilitates the interactions with the immunoprecipitating antibody (2µg) which was incubated with the proteins for 1.5 hours at 4 ºC with rotation. Equal amounts of total protein and antibody concentration were used for the specific immunoprecipitated antibody and non-specific IgG to evaluate non-specific binding (Table 2.2). After antibody incubation, 20 µl of Protein G magnetic beads (Millipore) were added to each aliquot and incubated with rotation for an additional hour. Magnetic beads with attached protein complexes were washed with 500ml of IP buffer 3x 30 seconds at room temperature. Beads were collected each time by mild centrifugation at no more than 1000rpm. First and last unbound samples were saved for analysis. After the last wash, 35 µl of 5x loading buffer (EC-887, National Diagnostics) was used to elute the beads. Samples were boiled for 10 minutes at 100 ºC and stored at -20 ºC for further analysis with SDS-page electrophoresis.

2.5.6 SDS-page electrophoresis and semi-dry transfer of proteins from gel to membrane

Protein samples were diluted to a final concentration of 20µg (NIH3T3 cell line) or 15µg (ovaries) with 5x loading buffer (EC-887 National Diagnostics), boiled at 100ºC for 10 minutes and briefly centrifuged for 30 seconds at 4000 rpm in a Sigma 1-14 microcentrifuge. Proteins were separated in polyacrylamide gels (12% for separating gel and 4 % for concentrating gel from the stock solution 1.5M Tris-HCl pH 8.8, 1M Tris-HCl pH 6.8, H2O, APS and TEMED). Electrophoresis was performed at 150V for 1.5 hours at room temperature and proteins were transferred to a nitrocellulose membrane using a semi-dry transfer for 40-45 minutes at 20V. Membranes were stained using PonceauS solution (Sigma) to determine if the transfer was successful.

2.5.7 Western blotting

Membranes were washed with TBS-Tween and blocked in either 5% (w/v) BSA (Sigma) for phospho-protein detection or 5% (w/v) non-fat dried milk at room temperature for 2 hours. Blots were washed in TBS-Tween for 3x 7 minutes each. Primary antibodies (Table 2.1) were incubated overnight at 4ºC. Blots were washed in TBS-Tween for 3x7 minutes and HRP-conjugated secondary antibodies (Table 2.1) were applied for 1 hour at room temperature. Blots were developed using ECL reagents (Westar Supernova enhanced chemiluminescent HPR substrate; Cyanagen, Bologna, Italy) according to the manufacturer's guidelines and imaged using the G:BOX iChemi and associated GeneSnap and GeneTools software (Syngene).

2.6 Proximity Ligation Assay (PLA)

The Proximity Ligation Assay (PLA) is immunostaining-based technique that allows the detection of closely associated proteins (maximum distance 30-40nm) on fixed tissue sections. Protein complexes were labelled using the Duolink In Situ Red Starter Kit (Sigma) according to the manufacture's guidelines. Briefly, following incubation with primary antibodies as described in section 2.4.2 and after washing with PBS, secondary antibodies conjugated to specific PLA probes were applied at 37ºC for 1 hour.

After washing with Buffer A (provided with the kit) 2x 5 minutes each, ligation solution (containing oligonucleotides that will hybridise the PLA probes) and ligase enzyme were incubated at 37ºC for 30 minutes to allow the ligation of PLA probes that are in close proximity, creating a ligated product. After washing 2x2 minutes with Buffer A, amplification solution (containing fluorescently labelled nucleotides) and polymerase enzyme were incubated at 37ºC for 100 minutes. This allowed the amplification of the ligated product. Sections were imaged using an inverted Leica SP5 confocal laser-scanning microscope (Leica Microsystems, Wetzlar, Germany).

2.7 Chromatin immunoprecipitation (ChIP) - qPCR

2.7.1 Crosslinking, lysis and sonication of ovary samples.

Isolated ovaries were directly fixed with 1% formaldehyde (1/4 dilution of 10% neutral buffered formalin solution containing 4% formaldehyde; Sigma) in either Waymouth medium 752/1 (Life Technologies) or Leibovitz's L-15 medium (Life Technologies) for 30 minutes.

An EZ- Magna ChIP™ G kit (Millipore) was used according to manufacturer's instructions. Briefly, 10x glycine was added to a final concentration of 125mM for 10 minutes to quench any unreacted formaldehyde. The quenching solution was removed and ovaries were washed with PBS. Then, 150 µl of cell lysis buffer containing protease inhibitors was added to each sample and ovaries were further disrupted with 25G needles and vortexed 6x for 1 minute each. Disrupted ovaries were centrifuged at 800g for 5 minutes at 4ºC and then supernatant was discarded. Nuclear lysis buffer (170µl) was used to resuspend the disrupted ovaries and samples were transferred to 0.5ml tubes for sonication. Sonication was carried out using an ultrasonic liquid processor (vibra cell 150, Sonics) with an exponential probe at maximum amplitude for 3 times with 5-10 second intervals. Samples were transferred to 1.5ml tubes and then centrifuged at 10,000g for 10 minutes at 4ºC to remove any insoluble material. To analyse the size of sheared chromatin, 5µl of the sample was loaded into a 1.5 % agarose gel and separated by electrophoresis. If the sonication was successful, sheared chromatin was then aliquoted (50-70µl), snap frozen in liquid nitrogen and then kept at -80 ºC. A detailed description of the optimisation of the starting material and sonication of the chromatin is shown in Appendix 2.

2.7.2 Immunoprecipitation (IP) of crosslinked protein/DNA

Aliquots were diluted 1 in 10 with ChIP dilution buffer containing protease inhibitors (provided by the kit) and two % of the initial volume (undiluted) was taken as control for the IPs (Input). Then, 20 µl of Protein G magnetic beads (Millipore) were added to each aliquot along with 1.0 µg of immunoprecipitating antibody and non-immune mouse IgG (Table 2.1) as negative control for non-specific binding (1.0 µg). Samples were left to incubate overnight at 4ºC with rotation. After incubation, protein G beads were captured with a magnetic separator (Magna Grip Rack 8 Well)(Invitrogen) and complexes were washed for 5 minutes each with wash buffers (Millipore) containing increasing amount of salts (low salt buffer, high salt buffer, lithium chloride buffer and final wash with TE buffer).

2.7.3 Elution of protein/DNA complexes and reverse crosslinking of protein/DNA to free DNA

Chromatin:antibody:magnetic bead complexes were resuspended in 100µl ChIP elution buffer (Millipore) containing 1µl Proteinase K (Millipore) and incubated at 62ºC for 2 hours followed by a 10 minute incubation at 95ºC using a standard PCR thermal cycler . After cooling samples to room temperature, the magnetic beads were captured using the magnetic separator and the supernatant containing the chromatin was removed to a fresh tube. The chromatin was purified using spin filters with collection tubes (provided by the EZ- Magna ChIP^{TM} G kit). Briefly, 500 µl of Bind Reagent A was added to each 100µl ChIP sample (immunoprecipitations and inputs), mixed, added to the spin filter, centrifuged for 1 minute and flow through was discarded. Then, 500 µl of wash Reagent B was added, centrifuged and flow through was discarded. The spin filter was then re-centrifuged to remove any residual solution and then placed in a clean collection tube. DNA was eluted from the filter by applying 50 µl of Elution Buffer C and centrifuged. Eluted DNA samples were stored at -20 ºC. All centrifugations were performed at 12,500 x g.

2.7.4 Preparation of primers

Primers were designed to detect the promoter of different mouse target genes using the Primer 3 Plus software (*http://primer3plus.com/web_3.0.0/primer3web_input.htm*), NCBI (*https://www.ncbi.nlm.nih.gov*) and Ensembl Genome Browser (*www.ensembl.org)* databases. If the sequence of the promoter region was not available in GenBank (NCBI), it was predicted by selecting 2000bp upstream of the first exon with ENSEMBL and GenBank genome databases.

Specific binding regions of SMADS and FOXL2 to the target promoters were selected according to literature (Tran et al, 2011) and by using a predictive tool for transcription factor binding sites (TRANSFAC® software) (Appendix 3). The predicted promoter region with the highlighted binding sites was then introduced in Primer-3 Plus Software and at least two primer sets were designed for each promoter according to standard parameters including the product size (100-250bp), melting temperature TM (55-56ºC), primer GC content (40-60%) and a maximum self-pair complementarity of 4. Primer-Blast tool *(http://www.ncbi.nlm.nih.gov/tools/primer-blast)* was used to check primer specificity.

Primers were reconstituted in RNase/ DNase free water (Roche) to obtain a concentration of 100 µM stock solution and heated at 65ºC for 15 minutes. Then, primers were diluted to a working solution of 20µM with RNAse/DNAse free water, aliquoted in 50µl aliquots to avoid freeze/thaw cycles and stored at -20ºC.

Conventional PCR (section 2.7.5) using genomic DNA followed by 2% agarose electrophoresis was performed in order to assess the specificity of the primers. If primers showed single products of correct size, quantitative real-time PCR was then used to determine primer efficiency (section 2.7.7).

2.7.5 Conventional PCR of ChIP samples

In order to detect the presence of all gene promoters in the immunoprecipitated sample, conventional PCR was used. A PCR mixture was prepared in a reaction volume of 25µl consisting of 2µl of DNA template, 12.5µl of TaqRed Mix DNA polymerase (Bioline), 0.5µl (20µM) of primers (forward and reverse) and 10µl of RNase/DNase water. Samples were incubated in a standard PCR thermal cycling and PCR products were analysed using 2% (w/v) agarose gel electrophoresis.

2.7.6 Quantitative real-time PCR (qPCR) of ChIP samples

For quantitative purposes, qPCR was performed to detect subtle differences in binding between immunoprecipitated samples (IPs), positive controls (input) and negative control (IgG) samples. SensiFAST™ SYBR® Hi-ROX kit (Bioline) was used according to manufacturers' guidelines. Each reaction (20µl) contained 1xSensiFAST SYBR HI-Rox Mix (10 µl), 500nM of the premixed primer set (0.5 µl) and RNAse/DNAse free water (5.5 µl). An equal volume (4µl) of IP sample, control samples or RNAse/DNAse free water (additional negative control) was included in duplicate in 384 well-plates. The cycling conditions were set as follows: Activation step at 95°C for 3 minutes and then 40 cycles of amplification (3 seconds at 95°C for DNA denaturation, 20 seconds at 60°C for primer annealing and 10 seconds at 72°C for primer extension) in a 7900HT Fast Real-Time PCR System (Applied Biosystems). Fluorescence signals were collected after each cycle and also after a DNA melting/dissociation step to assess the identity of the products amplified.

2.7.7 Primer efficiency

Optimal efficiency of the primers is necessary for the quantitative analysis to be valid, especially when using low concentrations of DNA (e.g. ChIP-DNA). To determine efficiency, a sample of genomic DNA was extracted from two day 4 ovaries according to manufacturer's guidelines (RNA/DNA/protein purification Plus Kit; Norgen Biotek Corp). This sample was used to prepare five, 5x dilutions (from a stock concentration of 4.3 ng/µl; 1:1, 1:5, 1:25, 1:125, 1:625), which were then amplified by qPCR according to the protocol above. Values were plotted using the log concentration versus mean Ct value of three replicates and the % efficiency for each set of primers was calculated from the slope with the equation (Ginzinger, 2002):

$$E\ (\%) = [-1+ (10^{[-1/slope]})]*100$$

Primers with efficiencies ranging from 80-120% were considered optimal for quantitative analysis.

2.7.8 Analysis of qPCR data for ChIP samples

Input, IPs and IgG control samples were analysed using the '% input' method (*http://www.thermofisher.com)* where the mean Ct value of each IP and IgG sample was normalised against the input sample. The starting input sample was 2% of the initial chromatin, therefore a dilution factor of 50 or 5.64 cycles (log 2 of 50) needs to be subtracted. Calculations were performed as follows:

1) Mean Ct INPUT – 5.64

2) Mean Ct IP (or IgG) - Mean Ct INPUT= ΔCt

3) % INPUT= $(2^{(-\Delta Ct)})$ x 100

% input represents the % of initial chromatin in the IP and IgG control samples where the transcription factor was bound at the time ovaries were fixed. For an alternative description of the results, % input was categorised as low, medium and high. This classification was based on the full range of % input values for each target gene obtained with the specific (e.g SMAD2/3) antibodies. For example, if the full range of % INPUT was between 0 and 0.15%, values would be classified as low (≤0.05), medium (0.05-0.10) and high (≥0.15).

2.8 Gene expression analysis

2.8.1 Total RNA extraction from mouse ovaries

Ovaries at different developmental stages (day 4, 8 and 16) were used for total RNA extraction using Qiagen RNeasy® Micro Kits (QIAGEN, Crawley, UK) according to manufacturer's instructions. Briefly, 75µl of Buffer RLT (β-ME -RLT) was added to each of the ovary samples and vortexed for 1-2 minutes to lyse the samples. Pre-diluted carrier RNA (5µl) was added to each sample to enhance capturing low concentrations of RNA and vortexed for 1-2 minutes. Ovaries from day 4 and 8 mice were previously disrupted by using 25G needles. Seventy-five µl of 70% ethanol was added to each sample to precipitate the RNA before adding to a micro-column. After brief centrifugation, samples were washed with Buffer RW1, centrifuged, and treated with DNase I for 15 minutes at room temperature to remove genomic DNA. Samples were washed again in Buffer RW1 followed by Buffer RPE to remove traces of salts and then centrifuged.

Membranes were washed by 80% ethanol and centrifuged at maximum speed for 5 minutes. RNase/ DNase free water (14µl) was added to the membrane and centrifuged at maximum speed for 1 minute to elute the RNA sample. To concentrate RNA content, samples of day 4 and day 8 ovaries were additionally centrifuged under negative pressure for 4 minutes and 2 minutes at 23 degrees, respectively. Samples were stored at -80ºC. Concentration and purity of all RNA samples was assessed using the Agilent 2100 Bioanalyzer. Samples with an RNA integrity number (RIN) between 8 and 10 were used for gene expression analysis.

2.8.2 Reverse transcription PCR

For reverse transcription of RNA samples into first strand DNA (cDNA), the SuperScript III Reverse Transcription kit (Invitrogen) was used according to the manufacturer's instructions. Briefly, the reaction mixture consisted of RNA from each of the ovary samples (50ng), random hexamers (50ng/µl) and dNTP Mix (10mM). RNase/DNase free water was added to complete a final volume of 10 µl. The mixture was incubated at 65°C for 5 minutes and then kept in ice for one minute. The complementary DNA Synthesis Mix was prepared by adding each of the following components per reaction in order: 10X RT Buffer (2µl), 25mM MgCl2 (4µl), 0.1M DTT (2ul), RNaseOUT, 40U/µl (1µl) and SuperScript® III RT, 200 U/µl (1µl). The synthesis Mix (10 µl) was added to each 10 µl RNA mix sample, mixed gently, and collected by brief centrifugation. Then, the mixture was incubated at 25°C for 10 minutes, followed by 50 minutes at 50°C and 85°C for 5 minutes. Negative controls (without adding SuperScript® III RT) were included in each experiment. Samples were stored at -20°C. Conventional PCR using primers to detect mRNA for the reference gene *Htrp1* (hypoxanthine phosphoribosyltransferase 1) was used to ensure cDNA synthesis was successful in all samples.

2.8.3 Quantitative real-time PCR (qPCR) and analysis of qPCR data

Primers were designed using Primer-3 Plus Software with the same parameters as explained in section 2.7.4. However, primer location was set to span an exon/exon boundary in order to reduce the likelihood of amplifying any residual genomic DNA. Primer efficiencies were calculated (section 2.7.7) using cDNA from a single day 4 or day 16 ovary sample.

SensiFAST™ SYBR® Hi-ROX kit (Bioline) was used, the cycling conditions were the same as in section 2.7.6 and samples (1µl per reaction) were also run in duplicate in a 384 well-plate. Primers for the reference gene *Atpb5* (PrimerDesign, Southampton, UK) were included in the analysis to normalise the amount of total cDNA in the different samples. This reference gene was chosen based on previous studies using similar ovary samples (Fenwick et al, 2011; Fenwick et al, 2013). Fold changes were calculated relative to one of the ovary samples (reference sample) using the $2^{-\Delta\Delta Ct}$ method below (Livak & Schmittgen, 2001):

1) Mean Ct Target gene - Mean Ct Reference gene = ΔCt per sample

2) Mean ΔCt Target sample - Mean Ct Reference sample= ΔΔCt

3) Fold change= $2^{-\Delta\Delta Ct}$

2.9 Statistical analysis

In order to compare the geometric mean of % intensities of the different factors across the different follicle stages, data from the image analysis of immunofluorescently-labelled ovary sections was analysed using a non-parametric Kruskal-Wallis test with a post-hoc Dunn's multiple comparisons test. Fold changes ($2^{-\Delta\Delta Ct}$ method) obtained from gene expression analyses by qPCR were evaluated using one-way ANOVA with Bonferroni multiple comparisons post-hoc tests to determine differences between the mean values for each group. For the analysis of ChIP-qPCR data, non-parametric tests were used to compare the median value of % SMAD3 binding to the different target genes (Mann-Whitney U test for two groups and Kruskal-Wallis test with post-hoc Dunn's multiple comparisons test for more than two groups). To compare the geometric mean of oocyte areas measured for the different treatments in cultured ovary sections, a Kruskal-Wallis test with post-hoc Dunn's multiple comparisons was used. Graphpad Prism 7.03 was used to calculate and represent the data and differences were considered statistically significant when $P < 0.05$.

Primary antibody	Company	Stock conc.	IF	WB	ChIP
Goat anti-FOXL2 sc-55655	Santa Cruz Biotechnology	200mg/ml	1:100 (2µg/ml)	-	1µg
Goat anti-FOXL2 NB100-1277	Novus biologicals	0.5mg/ml	1:2000 (0.25µg/ml)	1:2500	-
Rabbit anti-Smad3 #9523	Cell Signalling	75mg/ml	1:100 (0.75µg/ml)	1:1000	-
Rabbit anti-phospho-Smad3 ab52903	Abcam	-	-	1:1000	-
Rabbit anti-CyclinD2 sc-593	Santa Cruz Biotechnology	200µg/ml	1:400 (0.5µg/ml)	1:500	-
Rabbit anti-p27 sc-528	Santa Cruz Biotechnology	200µg/ml	1:200 (1µg/ml)	1:300	-
Mouse anti-p27 sc-1641	Santa Cruz Biotechnology	50µg/ml	1:100 (0.5µg/ml)	-	-
Rabbit anti-Smad2 #5339	Cell signaling	237µg/ml	1:400 (0.59µg/ml)	1:1000	-
Mouse anti-Smad2/3 sc-133098	Santa Cruz Biotechnology	200µg/ml	1:800 (0.25µg/ml)	1:1000	1µg
Rabbit anti-NFκB p65 sc-372	Santa Cruz Biotechnology	200µg/ml	-	-	1µg
Rabbit anti-beta Actin ab8227	Abcam	0.5mg/ml	-	1:2500	-
Rabbit anti-DDX4 ab13840	Abcam	0.9mg/ml	-	1:1000	-
Rabbit anti-ki67 #12202	Cell signalling	-	1:200	-	-
Rabbit anti-caspase3 #9664	Cell signalling	-	1:200	-	-
Rabbit anti-GADPH (6C5) sc-32233	Santa Cruz Biotechnology	200µg/ml	-	1:1000	-

Table 2.1 List of primary antibodies used for immunofluorescence staining, ChIP assay and Western Blot. Optimised working dilutions and concentrations for each antibody are shown. IF: Immunofluorescence; WB: Western blotting; ChIP: Chromatin immuno-precipitation.

Secondary antibody	Company	IF (dilution)	WB (dilution)
Alexa fluor® 555 Donkey- Anti-mouse	Santa Cruz Biotechnology	1:400	-
Alexa fluor® 488 Donkey-Anti-Rabbit	Cell Signalling	1:400	-
Alexa fluor® 488 Donkey-Anti-Goat	Santa Cruz Biotechnology	1:400	-
Alexa fluor® 555 Donkey-Anti-Rabbit	Cell signalling	1:400	-
Anti-rabbit HRP P0448	DAKO	-	1:20.000
Anti-goat HRP P0449	DAKO	-	1:20.000
Anti-mouse HRP P0447	DAKO	-	1:40.000
Protein A (HRP) 18-160	Millipore	-	1:5000

Controls	Company	Stock (conc.)
Normal mouse IgG sc-2025	Santa Cruz Biotechnology	200µg/ml
Normal mouse IgG I-200	Vector laboratories	2mg/ml
Normal rabbit IgG I-1000	Vector laboratories	5mg/ml
Normal goat IgG I-5000	Vector laboratories	5mg/ml

Table 2.2 List of secondary and control antibodies used for immunofluorescence staining, ChIP assay and Western Blot. Optimised working dilutions and concentrations for each antibody are shown. IF: Immunofluorescence; WB: Western blotting.

Chapter 3.

Localisation and expression of key TGFβ factors and cell cycle regulators during early follicle development

3.1 Introduction

The mechanisms that lead to the activation of primordial follicles are still not well understood. Although primordial follicles have an oocyte in a state of meiotic arrest as well as a complement of GCs with relatively low rates of proliferation, the cells still express the molecular machinery that at some point will be necessary to respond to intra-ovarian signalling and allow activation and growth. Why some primordial follicles respond to these signals and others remain unresponsive may partly be explained by the fact that GCs may be derived from different cell precursors (Mork et al, 2011). Several morphological changes are associated with PFA; however, it is generally believed that GC proliferation precedes oocyte growth (Braw-Tal, 2002; Da Silva-Buttkus et al, 2008; Mora et al, 2012a). Therefore, the "production line" hypothesis where PFA only depends on the time oocytes enter meiosis (Hirshfield, 1992) may not be supported and GCs could be functioning as drivers of follicle activation. Therefore, revealing the molecular mechanisms regulating GC proliferation may be key to understanding this initial proliferation and PFA.

The TGFβ signalling pathway, well known for its role in growth arrest and EMT, has been implicated in GCs during early follicle development and PFA (Pangas, 2012b). The intercellular mediators of the canonical TGFβ signalling pathway, SMAD2/3, have been previously localised in GCs of primordial follicles in mice and implicated in the regulation of GC proliferation (Fenwick et al, 2013). However, as yet, it is not known whether SMAD2, SMAD3 or both are important. Cell proliferation involves cell cycle progression and in this context the cell cycle regulators CCND2 and p27 have been found in the ovary with specific functions during early follicle development (Rajareddy et al, 2007; Sicinski, 1996).

As well as proliferation, GCs also undergo a change in cell shape during PFA. The transcription factor FOXL2 is a lineage specific marker of GCs and mice deficient in this gene exhibit impaired GC proliferation and cuboidalisation during PFA (Uda et al, 2004). Moreover, FOXL2 has been reported to regulate the expression of some cell cycle genes, such as *Ccnd2* and *p27* (Bentsi-barnes et al, 2010; Garcia-Ortiz et al, 2009). Interestingly, Foxl2 and SMAD3 are known to interact and regulate common target genes in other systems, such as the pituitary, where they regulate the expression of follistatin (Blount et al, 2009).

Whether Foxl2 and SMAD3 cooperate to regulate the expression of genes in the ovary is not known, although some evidence has been reported in GC tumours for *Ccnd2* gene (Anttonen et al, 2014a).

Despite the associated roles of these factors in GC proliferation, their expression and role in regulating cell cycle genes has not been clearly mapped with early follicle development. Therefore, the following aims will be addressed:

- To analyse the mRNA and protein expression pattern of Smad2, Smad3, Ccdn2, p27 and Foxl2 using ovaries from different ages containing different proportions of small (primordial and early growing) follicles by qPCR, Western blotting and immunofluorescence staining.
- To analyse the relationship between GC number and oocyte area in small follicles and quantify the expression of the above proteins in GCs during early follicle development in immunofluorescently-labelled sections.
- To determine whether the transcription factors FOXL2 and SMAD3 interact using an in situ proximity ligation assay (PLA).
- To determine whether FOXL2 and SMAD3 bind to promoters of *Ccnd2* and *p27* (and the SMAD3 positive control *Myc*) in primordial and growing follicles.

3.2 Materials and Methods

3.2.1 The ovary model and tissue collection

Ovaries from postnatal age 4 (day 4) are mainly enriched in primordial/transitional follicles while ovaries from day 16 contain higher proportion of activated/growing follicles (see 2.1). Therefore, for molecular analysis, day 4 ovaries were used as a model of primordial/transitional follicles and day 16 ovaries represented the growing preantral follicle population. Ovaries from postnatal day 8 containing a balanced proportion of primordial/transitional and small/large preantral follicles (see 2.1) were mainly used to perform localisation studies and image analysis.

Ovaries from day 4, 8 and 16 mice were dissected and either immersed in formalin for immunostaining purposes or flash frozen in liquid nitrogen for protein, RNA extraction and ChIP experiments as described in Chapter 2 (see 2.2).

3.2.2 Western blotting

Whole ovaries from day 4, 8 and 16 mice were used for protein analysis. Two ovaries were pooled from each age (day 4 and day 8) and 1 ovary from day 16 were used for each sample. The entire procedure was repeated twice (n=2). Protein extraction was performed using Pierce ^{TM} IP lysis buffer as described (see 2.5.1). The protein expression of SMAD2 (#5339, Cell Signalling), SMAD3 (#9523, Cell Signalling), phospho-SMAD3 (ab52903, Abcam), CCND2 (sc-593, Santa Cruz), p27 (sc-528, Santa Cruz) and FOXL2 (NB100-1277, Novus Biologicals) was analysed by using specific primary antibodies listed in Table2.1 and the loading control protein beta-actin was used to normalise protein content between samples (15µg). Optical density (OD) of the observed bands was measured using Ingenius Bioimaging software "GeneTools" with G:BOX iChemi (Syngene). The mean pixel value of specific bands and background were normalised against the pixel area. Background was then subtracted to the specific band value and referred as "OD value". For each sample, the ratio between the OD value of each specific protein and beta-actin was used for normalisation and represented in graphs.

3.2.3 RNA extraction and qPCR

For gene expression analysis, whole ovaries from day 4, 8 and 16 mice were used as biological replicates (five ovaries per age group, n=5). As one ovary per sample was used, additional vacuum centrifugation was necessary to concentrate day 4 and day 8 ovary samples (see 2.8.1). RNA concentration and quality was measured (RIN number) by using the Agilent 2100 Bioanalyser (Appendix 4, A) and cDNA synthesis was performed with SuperScript III Reverse Transcription kit (see 2.8.2). Conventional PCR using the housekeeping gene *Htrp1* was employed to check the quality of cDNA prior to qPCR (Appendix 5, A). Quantitative PCR using primers for *Smad2*, *Smad3*, *Ccnd2*, *p27*, *Foxl2* and the TGFβ receptor Type I (*Alk5*) were used (Table 3.1) with the SensiFAST™ SYBR® Hi-ROX kit (Bioline) according to manufacturers' guidelines (see 2.8.3). Samples (1µl per reaction) and the same volumen of distilled water (negative control) were run in duplicate in a 384 well-plate. PCR conditions were as follows: Activation step at 95°C for 2 minutes and then 40 cycles of amplification (3 seconds at 95°C for DNA denaturation, 20 seconds at 60°C for primer annealing and 10 seconds at 72°C for primer extension) in 7900HT Fast Real-Time PCR System (Applied Biosystems). Ct values were normalised against *Atpb5* (PrimerDesign, Southampton, UK) and fold changes relative to day 4 ovaries were calculated for each gene according to the $2^{-\Delta\Delta Ct}$ method (see 2.8.3).

Primers	Sequence (5'➤3')	bp	Primer efficiency (%)
Smad3	F: GTCAAAGAACACCGATTCCA R: TCAAGCCACCAGAACAGAAG	154	91
Smad2	F: CGTCCATCTTGCCATTCAC R: GTCCATTCTGCTCTCCACCA	102	113
Foxl2	F: TCATAGCCAAGTTCCCGTTCTA R:GTAGTTGCCCTTCTCGAACATG	179	89
Ccnd2	F: CTTGTAGCCCATTCAGACACAG R:TATCATCCACGTGTGCTGTAGA	165	93
p27	F: AGTCAGCGCAAGTGGAATTT R: AGTAGAACTCGGGCAAGCTG	100	130
Alk5	F: CAGCAATAGAACAGCGTCGCG R: ATTGCTCCAAACCACAGAGTA	157	-
Htrp1	F: GTTGTTGGATATGCCCTTGAC R: GCGCTCATCTTAGGCTTTGTA	105	-

Table 3.1. Primers sequences, amplification product size (bp) and primer efficiency (%) for qPCR assays.

3.2.4 Immunofluorescence staining and image analysis

After embedding formalin-fixed tissues in paraffin (see 2.1), ovaries from day 4, 8 and 16 were sectioned (5µm) and immunostained as described (see 2.4.2) with specific antibodies against SMAD2 (#5339, Cell Signalling), SMAD3 (#9523, Cell Signalling), CCND2 (sc-593, Santa Cruz), p27 (sc-528, Santa Cruz), FOXL2 (sc-55655, Santa Cruz) and Ki67 (#12202, Cell Signalling) (Table 2.1). Image analysis was performed for each protein using one of the largest cross sections per ovary from a total of 7 ovaries from different litters (four day 4 and three day 8 ovaries, n=7). Images were obtained with an inverted Leica with confocal laser SP5 scanning microscope (Leica Microsystems, Wetzlar, Germany). All sections were imaged at high power using a 63X oil immersion objective and the 488 and 555 laser lines. For each high power image, the digital gain and offset settings were maintained consistently for all sections.

Images were stitched together using DoubleTake (http://echoone.com/doubletake/), which maintains the scale of all individual images to create a high resolution composite of each section (Figure 3.1).

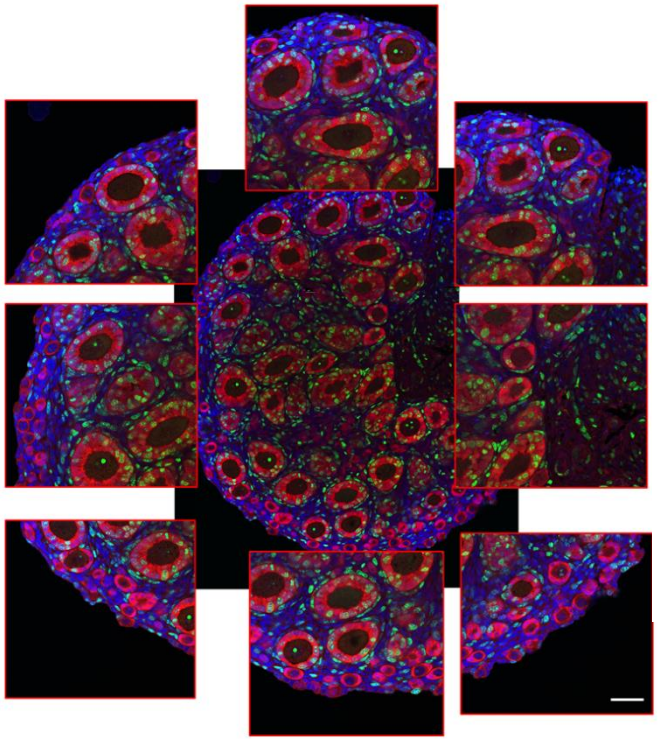

Figure 3.1. Representation of a composite image of a day 8 ovary section from high power images using DoubleTake. Immunofluorescent localization of SMAD2/3 (red) and Ki67 (green) is shown. Scale bar is 25µm and magnification is 63X.

Threshold setup, selection of follicles and measurement parameters

Images were obtained as 8 bit RGB stack file. The threshold for each channel in every composite section was set up with the same criteria across the different sections of the same staining (Figure 3.2). In general, the threshold was manually adjusted until the thresholded image matched with the original image from the analysis. In the case of FOXL2, where non-specific ooplasm staining was observed, absence of this staining was used to establish the threshold (Figure 3.2, B). This created a binary image for quantification; for example, pixels highlighted in red showed the pixels above the threshold and were considered as "positive pixels", while the remaining pixels were registered as negative.

Follicles with a visible outline of the oocyte nucleus were carefully selected across the 7 sections with the region of interest (ROI) manager tool of Image J software. The number of follicles considered for analysis was variable between the different sections and therefore protein analysed (Figure 3.3A). The classification criteria for each follicle stage, according to GC number, was as described in Chapter 2 (see Figure 2.2). In order to quantify and compare the presence of each of the candidate proteins in different ROIs, such as different follicles or nuclei, the area of positive pixels "Area fraction" was calculated (Number of red positive pixels/Area of ROI) and referred as "Intensity" for simplicity. For the description of the results, intensities were considered low, medium and high when median intensities were 0-30%, 30-60% and 60-100%, respectively.

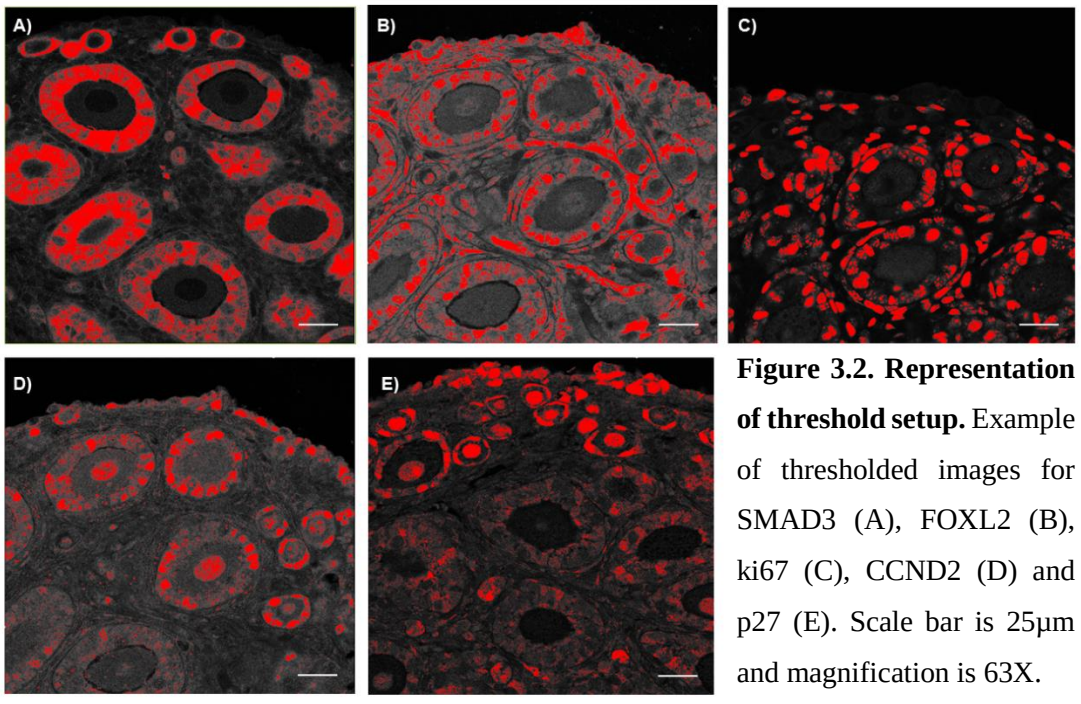

Figure 3.2. Representation of threshold setup. Example of thresholded images for SMAD3 (A), FOXL2 (B), ki67 (C), CCND2 (D) and p27 (E). Scale bar is 25µm and magnification is 63X.

ROIs from each follicle were selected manually using the DAPI channel and the "measure and label" tool, which allowed the intensity of each ROI to be quantified (Figure 3.3). For each follicle, measurements were recorded for the intensities of individual GC nuclei (Figure 3.3B) and the intensity of the entire somatic (GC) cell compartment (Figure 3.3C). In any given follicle, the ratio between the geometric mean of the intensities for the GC nuclei, and the entire GC compartment were calculated as a measure of nuclear:cytoplasm expression.

As the distribution of the data obtained was generally skewed (Shapiro-Wilk test) the geometric mean was plotted to determine the central tendency of the intensities obtained from each group of follicles.

A)

	Day 4				Day 8			Total
Protein	4.1	4.2	4.3	4.4	8.1	8.2	8.3	
SMAD3	42	41	24	41	40	72	42	302
FOXL2	26	52	24	48	39	32	53	274
CCND2	30	51	25	47	39	34	48	275
p27	19	27	30	38	37	90	57	298
ki67	17	33	-	-	35	36	34	155

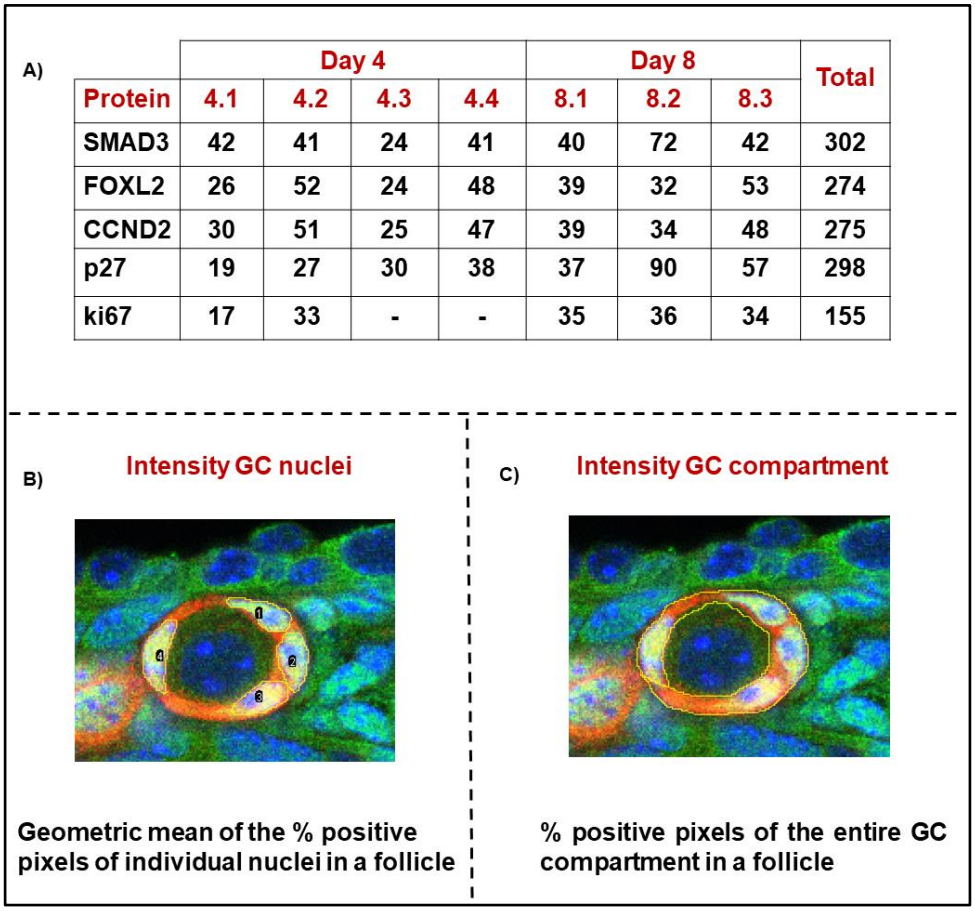

Figure 3.3. Number of follicles counted per section for each protein and example of the different ROI selections in a follicle. A) Total number of follicles counted across the 7 ovary sections from day 4 and day 8 ovaries. In B) and C) selection shows individual GC nuclei and the entire GC cell compartment. Definition of the different intensities calculated and plotted in graphs is also shown.

3.2.5 Chromatin Immunoprecipitation immunoprecipitation (ChIP)

Whole ovaries from day 4 (2 ovaries/sample) and day 16 (1 ovary/sample) mice were used with SMAD2/3 (sc-133098, Santa Cruz) and FOXL2 (sc-55655, Santa Cruz) antibodies (Table 2.1) to study the level of binding of these factors to the promoter of *Ccnd2*, *Myc* and *p27* genes. Sheared chromatin was analysed with a 1.5% agarose gel to visualise fragment size range (Appendix 6, C). Conventional PCR was performed using promoter specific primers (Table 3.2). A non-immune isotype (IgG) antibody (sc-2025, Santa Cruz) was used as negative control to determine the level of non-specific binding. Protocol used was as described (see 2.7).

Primer set	Sequence (5'➔ 3')	bp	Primer efficiency (%)
Ccnd2.1	F:TTCTGCAGGAGGGTCATATTCT R:AATGAGGAACAAGGAAAGGCTT	207	102
Myc.3	F:GGCATATTCTCGCGTCTAGC R:TGAAGACAAACGGATGAACAGT	154	92
p27.2	F:TTAGTGTCTGGGACGGCTCTAA R:GACCCCAGAAGTCTCTGCTATG	175	93

Table 3.2. Primer sequences, amplification product size (bp) and primer efficiency (%) for ChIP-PCR of the promoter region of *Ccdn2*, *Myc* and *p27* target genes.

3.2.6 Proximity ligation assay (PLA)

Sections of ovary from day 4 mice were used to study the putative interaction between SMAD3 and FOXL2 by localising both proteins using antibodies to SMAD3 (#9523, Cell Signalling) and FOXL2 (sc-55655, Santa Cruz) (Table 2.1). Protein complexes were labelled using the Duolink In Situ Red Starter Kit (Sigma) with anti-goat and anti-rabbit secondary antibodies conjugated to specific PLA probes (see 2.6). Two sections were used as negative controls to determine the level of the specificity of the antibodies and assay: One negative control was used with two antibodies raised against DDX4 and FOXL2 as putative non-interactive proteins, and another control contained only FOXL2 primary antibody to check the level of background staining for the assay.

3.2.7 Statistical analysis

Data from the image analysis (section 3.1.2) was deemed to be not normally distributed (based on Shapiro-Wilk test in all groups); therefore, a non-parametric Kruskal-Wallis with post-hoc Dunn's multiple comparisons test was used to compare the central tendency between % intensities of the different follicle stages. For gene expression analyses by qPCR, fold changes ($2^{-\Delta\Delta Ct}$ method) relative to day 4 ovary samples were evaluated using one-way ANOVA with Bonferroni multiple comparisons post-hoc tests to determine differences between age groups. Graphpad Prism 7.03 was used to calculate and represent the data and differences were considered statistically significant when $P < 0.05$.

3.3 Results

3.3.1 Gene and protein expression of TGFβ factors and cell cycle proteins in day 4, day 8 and day 16 mouse ovaries.

Gene expression analysis with qPCR was used to study the differences in steady state mRNA expression between each age group relative to day 4 (Figure 3.4). For the TGFβ factors, *Smad2* expression did not vary between the three groups, while *Smad3* decreased in older ovaries (day 8 and day 16) relative to day 4 ($P<0.05$). Although *Alk5* expression also decreased in day 8 and day 16 ovaries, expression relative to day 4 was more reduced in day 8 ovaries ($P<0.01$).

For the cell cycle factors, *p27* expression was reduced in day 8 and day 16 ovaries ($P<0.0001$), whereas *Ccnd2* expression was only decreased in day 16 ovaries relative to day 4 ($P<0.01$). *Foxl2* transcript expression was not different between the three ages.

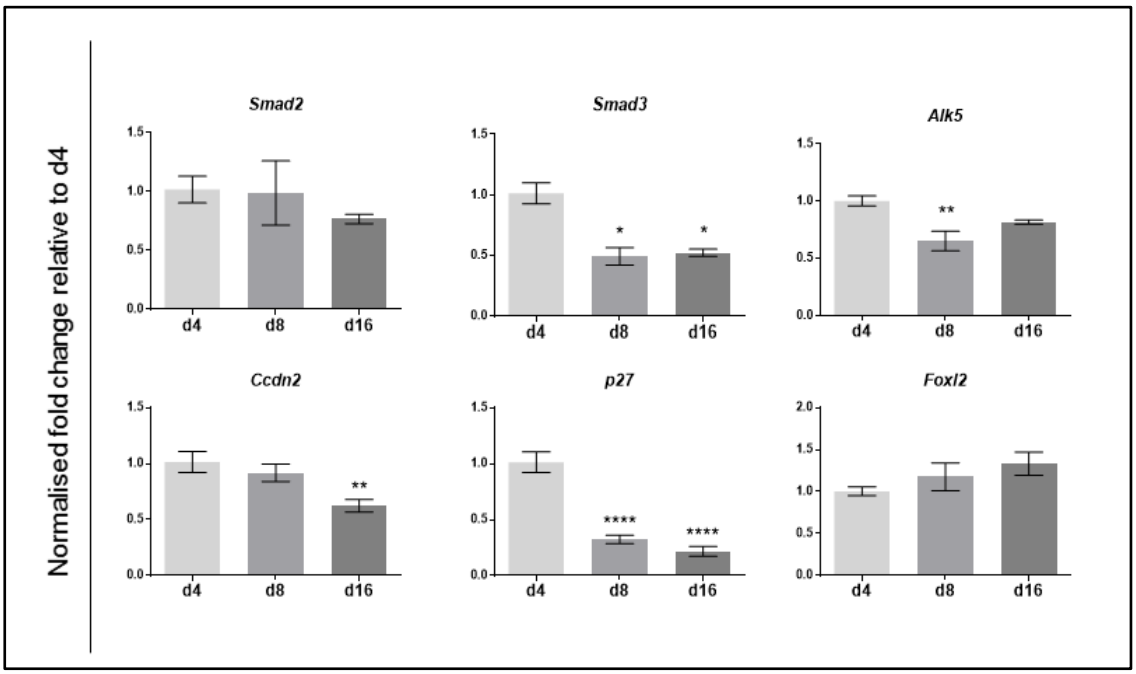

Figure 3.4. Expression of candidate TGFβ and cell cycle gene transcripts in juvenile mouse ovaries. Transcript levels were determined by quantitative PCR and were normalised against the endogenous reference *Atpb5*. Fold changes were calculated relative to day 4 using the $2^{-\Delta\Delta Ct}$ method as described in the methods. Each group contained 5 samples (n=5). Data are means ±SEM and significant differences are relative to day 4 (*P<0.05, **P<0.01 and ****P< 0.0001).

Next, total protein expression was analysed with western blotting (Figure 3.5). SMAD3 did not show any major changes in protein expression across ages, while phosphorylated SMAD3 (p-SMAD3) increased with age. This expression pattern was confirmed when bands were normalised against the loading control beta-actin. Based on visual inspection, CCND2 and p27 expression did not vary across ages, however, they showed decreased protein expression in day 16 ovaries when normalised against beta-actin and compared to other ages. Although SMAD2 also showed higher expression in day 16 ovaries, normalisation against loading control did not show major differences in protein expression. Moreover, FOXL2 showed a clear increase in expression across ages.

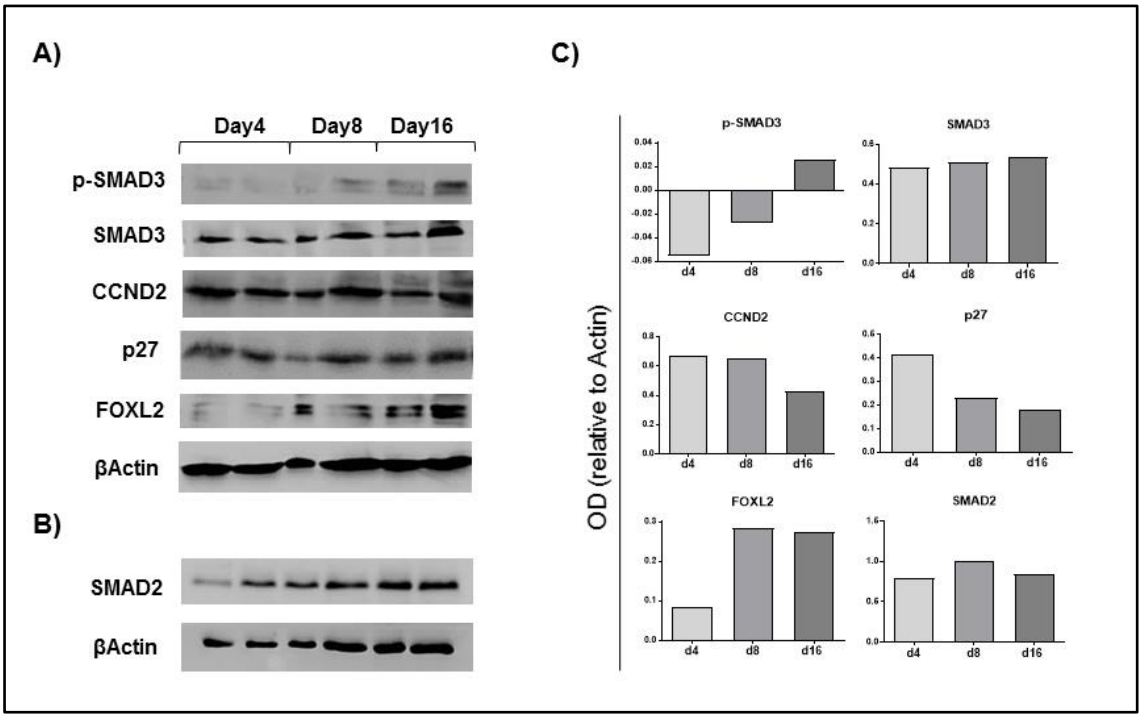

Figure 3.5. Expression of candidate TGFβ and cell cycle proteins in juvenile mouse ovaries. A) Protein expression of SMAD3, CCND2, p27, FOXL2 and phospho-SMAD3 were analysed by western blotting (15µg). B) SMAD2 was analysed in a separate blot (10µg). C) OD values were normalised against beta-actin as described in the methods and means plotted (n=2).

3.3.2 GC proliferation and oocyte growth during early follicle development

GC proliferation is a key morphological event during PFA, and some reports have proposed that GCs initiate proliferation before the oocyte starts its growth (Braw-Tal, 2002; Da Silva-Buttkus et al, 2008; Mora et al, 2012a). Therefore, another objective was to examine this using the classification criteria applied in this thesis (see 2.4.3). Follicles from day 4 and day 8 were selected according to the criteria explained in the methods (see 3.2.3) and oocyte area and number of their surrounding GCs were measured. As expected, when follicles were classified according to GC number, oocyte areas increased from primordial to secondary follicle stages (Figure 3.6A). A significant increase in the oocyte area was observed from the transitional stage when compared to primordial follicles ($P<0.0001$). Then, oocyte areas from follicles up to small primary stage were calculated for each follicle with a specific GC number. Only a significant increase in the oocyte area was observed in follicles containing six GCs or more when compared to follicles with 3 GC ($P<0.01$) (Figure 3.6B).

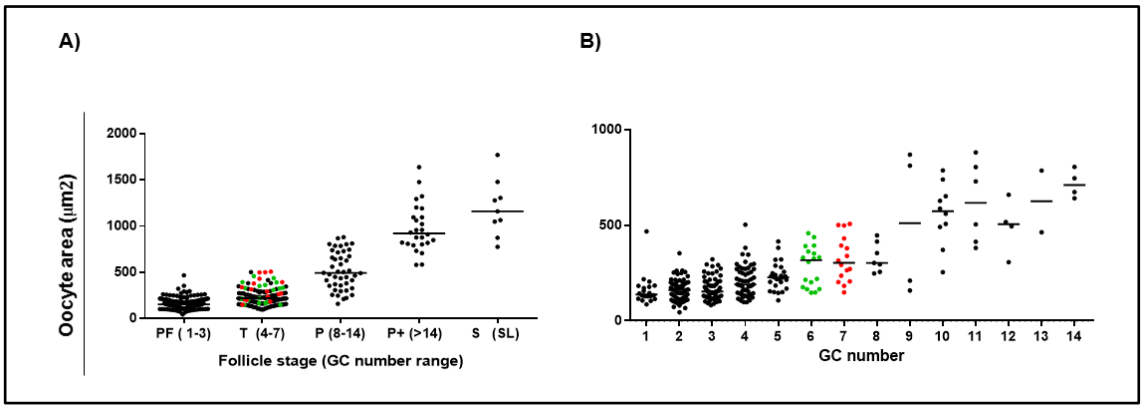

Figure 3.6. Relationship between oocyte area and GC number in small follicles. Oocyte areas of classified follicles according to GC number were measured. Each dot represents a follicle with specific GC number. Red and green dots in both graphs represent the follicles surrounded by 6 and 7 GCs, respectively. Follicles were measured from day 8 (n=3) and day 4 (n=4) ovary sections. In A) all groups are significant relative to PF ($P< 0.0001$). In B) all follicles containing 6 GCs or more are significant relative to the group of follicles containing 1 to 3 GCs ($P<0.01$ for the group with 6 GCs). Data are medians. PF, primordial; T, transitional; P, primary; P+, large primary; S, secondary follicle stages.

3.3.3 Localisation of SMAD2, SMAD3, FOXL2, CCND2, and p27 proteins in immature mouse ovaries.

SMAD3 and SMAD2 protein localisation

In all mouse ovary ages examined, SMAD3 was detectable in GCs in all follicle stages, but was absent in oocytes and other somatic compartments (Figure 3.7). In between the ovary ages, SMAD3 expression was reduced in day 8 and day 16 ovaries when compared to day 4 ovaries. In primordial and transitional follicles, SMAD3 expression was strong in the nucleus and cytoplasm of GCs. In growing follicles, a decrease in nuclear SMAD3 was observed. The negative control section did not show any staining in any follicle.

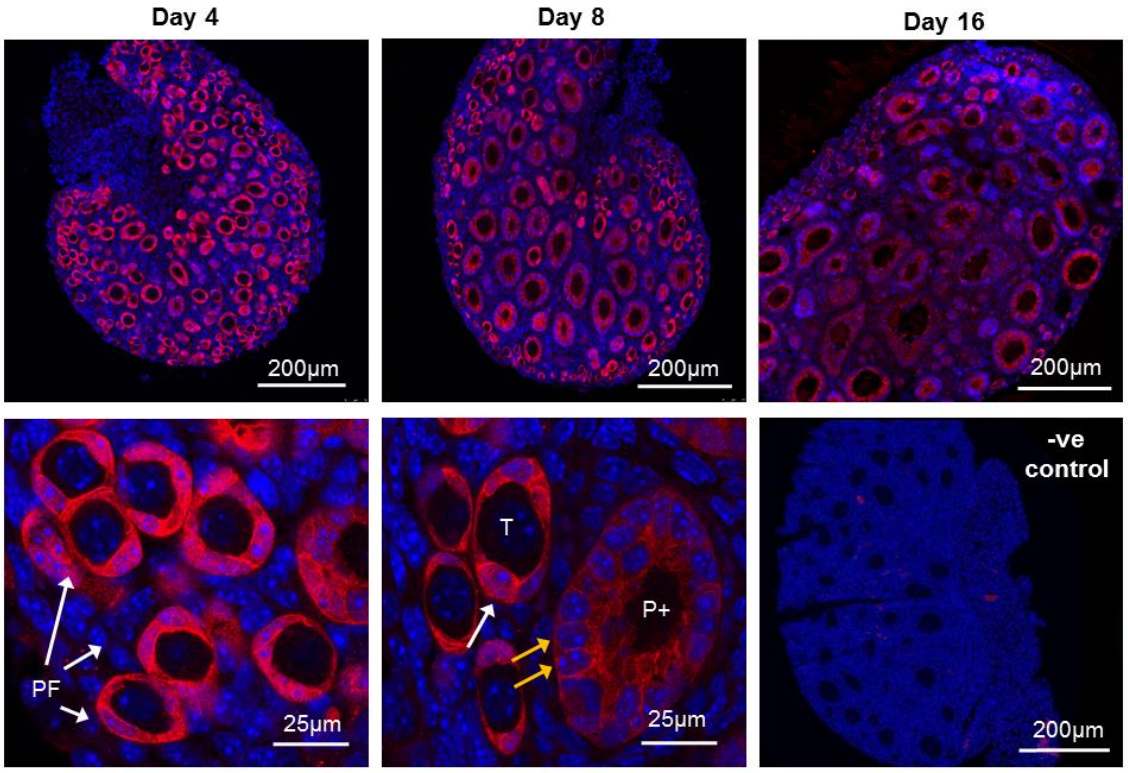

Figure 3.7. Immunofluorescent localisation of SMAD3 in juvenile mouse ovaries. High power images of day 4 and day 8 ovaries show SMAD3 expression (red) in GC nuclei and cytoplasm (white arrows), while absence of nuclear SMAD3 in GCs of growing follicles (yellow arrows). Nuclei are counterstained blue with DAPI. A negative control with a non-immune rabbit IgG antibody is shown. PF, primordial; T, transitional; P+, large primary follicle stages. Low and high power images (20X and 63X magnification) from day 4 and day 8 ovaries are shown in the upper and lower panels, respectively.

In contrast to SMAD3, weak SMAD2 staining was observed in the cytoplasm of GCs, oocyte and other somatic compartments (stromal cells) in all mouse ovary ages (Figure 3.8). Moreover, no difference in staining was observed between ovary ages. In primordial follicles, SMAD2 expression was not detected in GCs, while weak expression was observed in growing follicles. Oocyte staining was observed in all follicles stages, with similar intensity. No staining in any follicle stage was detected in the negative control section.

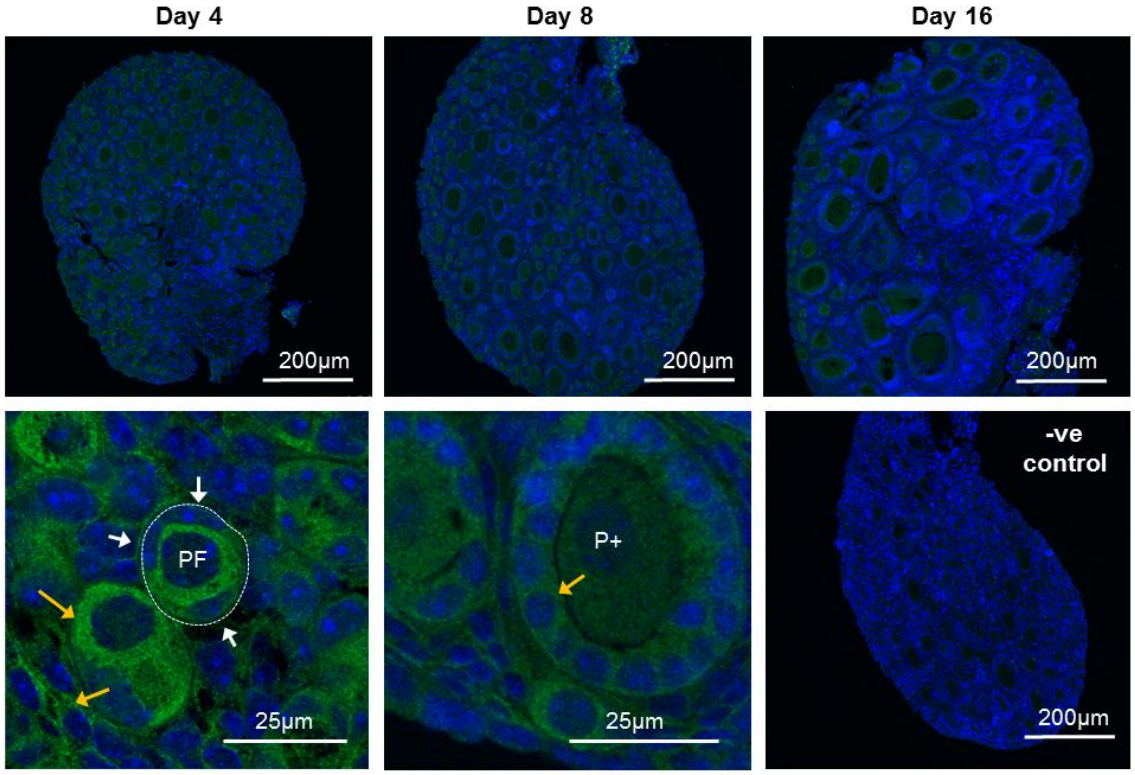

Figure 3.8. Immunofluorescent localisation of SMAD2 in juvenile mouse ovaries. High power image of a day 4 ovary shows a primordial follicle with no SMAD2 staining (green) in GCs (white arrows) while cytoplasmic staining is observed in the GCs of larger follicles (yellow arrow, day 8). Staining in oocyte and stromal cells is also detected (yellow arrows, day 4). Exposure of the day 4 high power image was increased for better visualization of the staining. Nuclei are counterstained blue with DAPI. A negative control with a non-immune rabbit IgG antibody is shown. PF, primordial; P+, large primary follicle stages. Low and high power images (20X and 63X magnification) from day 4 and day 8 ovaries are shown in the upper and lower panels, respectively.

FOXL2, CCND2 and p27 protein localisation

FOXL2 expression was observed in all ovary ages examined and was detectable in the nuclei of GCs, the ovarian surface epithelium (OSE) and stromal cells (Figure 3.9). FOXL2 was strongly expressed in GCs from all follicle stages and epithelial cells from OSE whereas stromal cells showed weaker staining. The ooplasm also showed weak FOXL2 staining, however, similar staining in the ooplasm was also found in the negative control.

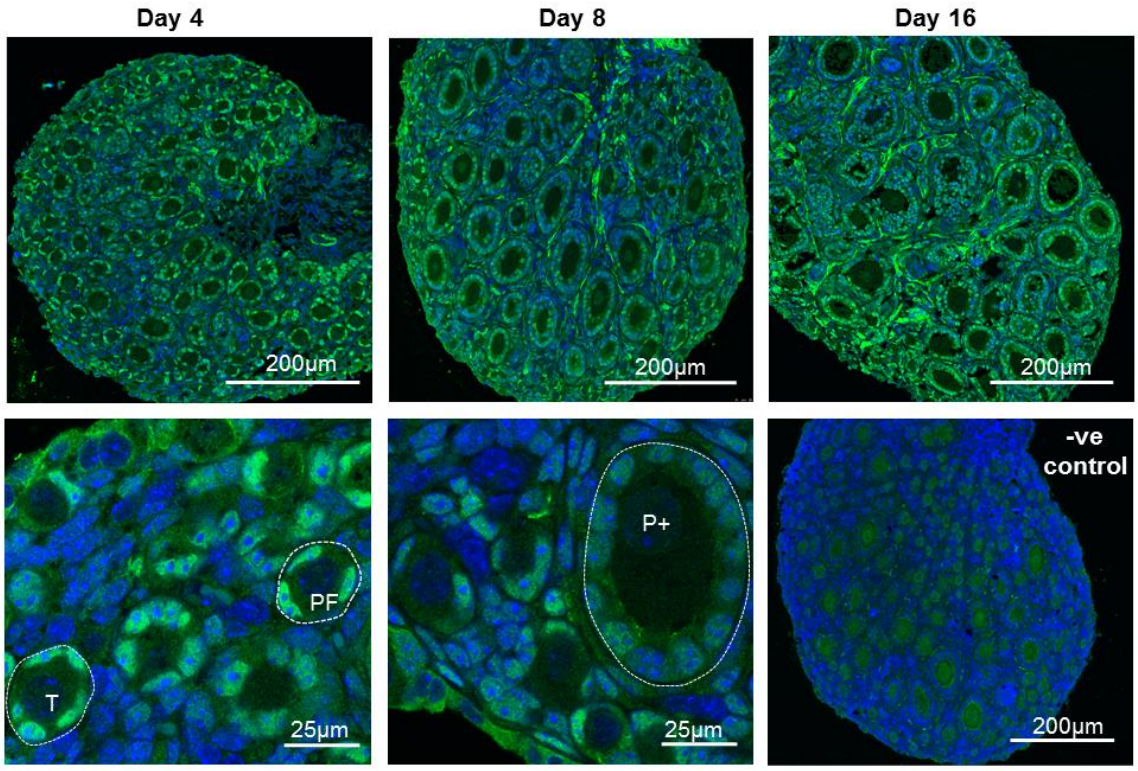

Figure 3.9. Immunofluorescent localisation of FOXL2 in juvenile mouse ovaries. High power images show nuclear FOXL2 staining (green) in GCs of primordial and transitional follicles (day 4) and large primary follicles (day 8). Nuclei are counterstained blue with DAPI. A negative control with a non-immune rabbit IgG antibody is shown. PF, primordial; T, transitional; P+, large primary follicle stages. Low and high power images (20X and 63X magnification) from day 4 and day 8 ovaries are shown in the upper and lower panels, respectively.

CCND2 expression was detected in all ovary ages analysed, however, a decrease in day 8 and day 16 ovaries was observed when compared to day 4 ovaries. CCND2 was present in the nucleus of GCs and oocyte in all follicle stages but not in other somatic compartments (Figure 3.10). In primordial follicles, CCND2 expression was strong in all GCs. In transitional follicles, CCND2 expression was also strong in GCs, however, GCs with decreased expression were detected in some of these follicles. In larger follicles, CCND2 expression was generally reduced in GCs although the expression pattern was more variable between individual nuclei. Oocyte staining was observed in all follicles stages, with similar intensity. No staining was detected in the negative control section.

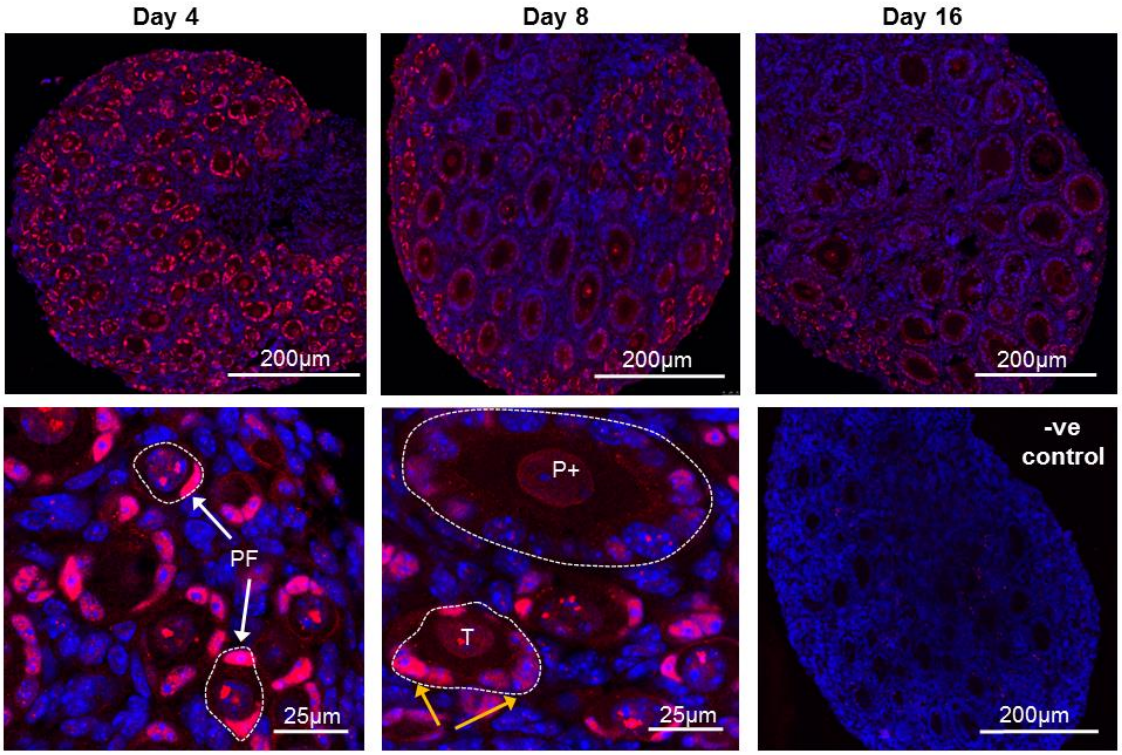

Figure 3.10. Immunofluorescent localisation of CCND2 in juvenile mouse ovaries. High power images show strong nuclear CCND2 staining (red) in GCs of primordial follicles (white arrows). Transitional follicles show nuclei with strong and reduced CCND2 (yellow arrows) whereas larger follicles show decreased CCND2 expression (P+). Nuclei are counterstained blue with DAPI. A negative control with a non-immune rabbit IgG antibody is shown. PF, primordial; T, transitional; P+, large primary follicle stages. Low and high power images (20X and 63X magnification) from day 4 and day 8 ovaries are shown in the upper and lower panels, respectively.

p27 expression was detectable in day 4 and day 8 ovaries whereas weak staining was observed in day 16 ovaries. p27 was observed in the nucleus and the cytoplasm of GCs and oocyte in all follicle stages (Figure 3.11). In primordial and transitional follicles, p27 expression was strong in the nucleus of GCs while reduced expression was observed in growing follicles. From primary stage, p27 expression was not detectable in the nucleus of some GCs and in larger follicle stages, p27 was only detected in the cytoplasm of all GCs. Oocyte staining was observed in all follicles stages, with similar intensity. Negative control showed no detectable staining.

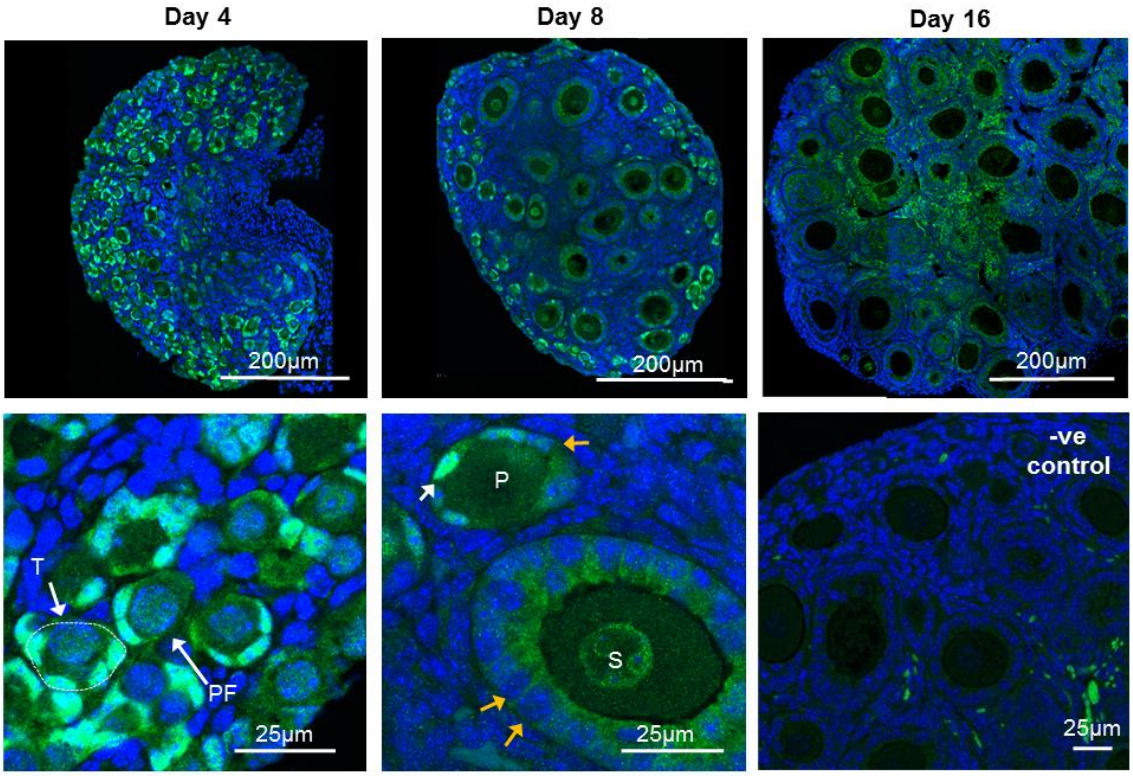

Figure 3.11. Immunofluorescent localisation of p27 in juvenile mouse ovaries. High power image of day 4 ovaries shows strong nuclear p27 staining (green) in GCs of primordial and transitional follicles (white arrows). In day 8 ovaries, primary follicles show GC nuclei with strong and decreased p27 expression (white and yellow arrow, P), whereas in larger follicles p27 in GC nuclei is lost (S). Nuclei are counterstained blue with DAPI. A negative control with a non-immune rabbit IgG antibody is shown. PF, primordial; T, transitional; P, small primary; P+, large primary follicle stages. Low and high power images (20X and 63X magnification) from day 4 and day 8 ovaries are shown in the upper and lower panels, respectively.

3.3.4 Image analysis: Detailed quantification of protein expression

Since all factors described above are detectable in GCs and GC proliferation has been shown to initiate before oocyte growth (see Figure 3.6), another objective was to establish whether there was a relationship between protein expression of these factors and GC proliferation. Image analysis of immunofluorescently-labelled ovary sections from day 4 and day 8 ovaries (n=4 and n=3, respectively) was used to quantify their expression pattern in GCs of follicles classified according to GC number (see 2.4.3).

Expression pattern of GC factors throughout early follicle development

Since SMAD2 expression was very weak in small follicles (see Figure 3.8), image analysis was not carried out for this protein.

SMAD3 in GCs

When SMAD3 intensities in the whole GC compartment (including nuclei and cytoplasm) were measured, primordial follicles showed medium GC staining while transitional and primary follicles showed high GC staining (Figure 3.12B). Large primary and secondary follicles showed high and medium GC staining, respectively. When different follicles were compared, SMAD3 staining in transitional follicles was significantly increased when compared to primordial follicles ($P<0.0001$). Moreover, secondary follicles showed a significant decrease in staining when compared to primordial, transitional and primary follicle stages ($P<0.05$, $P<0.0001$ and $p<0.01$, respectively).

SMAD3 in GC nuclei

A decrease in nuclear GC staining was evident from primordial to secondary follicles (Figure 3.12A). Median values for primordial, transitional and primary follicles showed high nuclear SMAD3 staining whereas large primary and secondary follicles showed medium nuclear SMAD3 staining. When the different stages where compared, a significant decrease in nuclear SMAD3 intensity was observed in large primary and secondary follicles when compared to primordial follicles ($P<0.001$ and $P<0.05$, respectively). A significant decrease in large primary and secondary follicles were also observed when compared to transitional ($P<0.01$ and $P<0.05$) and primary follicle stages (both $P<0.05$).

When the ratio of SMAD3 intensities between GC nuclei and whole GC compartment were measured, a decrease in the ratios were observed across the different ages (Figure 3.12C). Specifically, a significant decrease was observed from primary stage when the ratio was compared to primordial follicles ($P<0.05$) and in large primary and secondary follicles when compared to primordial ($P<0.001$ and $P<0.0001$, respectively) and transitional stages ($P<0.001$ and $P<0.05$; respectively).

As expected with FOXL2, staining in GC nuclei was high in all follicle stages and no significant differences where observed when the different groups were compared (Figure 3.12D).

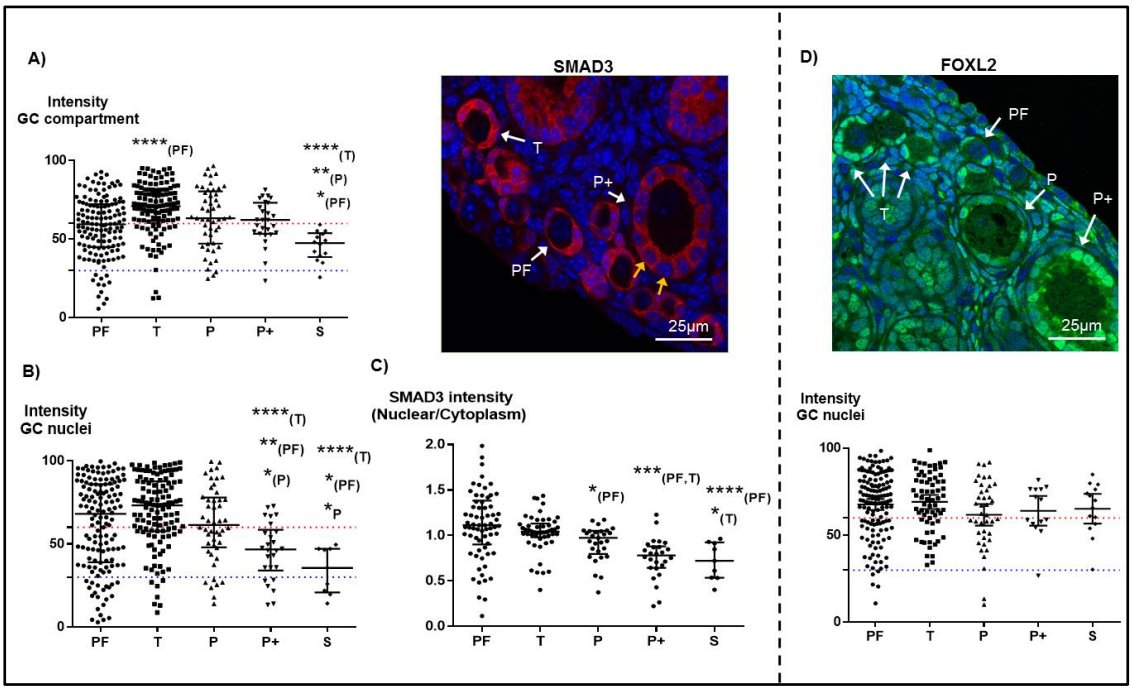

Figure 3.12. Quantification of SMAD3 and FOXL2 staining in GCs during early follicle development. A) and B) show the measured intensities for SMAD3 in the whole GC compartment and in GC nuclei for each follicle stage, respectively. C) shows the ratio of both intensities across follicle stages. Image of SMAD3 staining (red) shows an example of primordial, transitional and large primary follicle stages, where SMAD3 nuclear exclusion is observed in large primary follicles (yellow arrows). D) shows FOXL2 staining (green) with examples of primordial, transitional, primary and large primary follicles. Measured intensities in GC nuclei are shown for the different follicle stages. Dashed lines in graphs delimit medium (blue line and above) and high (red line and above) intensities. Nuclei from the images are stained blue with DAPI. Data are medians ±interquartile range and significant differences for each group are relative to the follicle stage in parentheses (*P<0.05, **P<0.01, ***<P<0.001, ****P< 0.0001). PF, primordial; T, transitional; P, primary; P+, large primary; S, secondary follicle stages.

The intensity of cell cycle regulators CCND2 and p27 in GCs from the different follicle stages was also measured. For CCND2, a decrease in nuclear GC staining was observed across follicle stages (Figure 3.13A). However, median values in all stages showed high CCND2 staining with the exception of medium intensity in secondary follicles. When the different stages were compared, CCND2 intensity was significantly decreased in primary, large primary and secondary follicles when compared to primordial follicles ($P<0.01$, $P<0.0001$ and $P<0.0001$, respectively). When compared to transitional follicles, only large primary and secondary follicles showed significant differences (both $P<0.0001$). Only secondary follicles showed a significant decrease in CCND2 when compared to primary follicles ($P<0.05$).

p27 nuclear staining in GCs showed an abrupt decrease across follicle stages. Median values in primordial and transitional follicles showed medium p27 staining whereas primary, large primary and secondary follicles showed low p27 staining. When follicle stages were compared, large primary and secondary follicle stages showed a significant decrease in p27 staining when compared to primordial and transitional follicle stages ($P<0.0001$).

For each follicle stage, all GC factors analysed showed variability of intensities. When comparing the interquartile range of the different follicle stages, the primordial follicle population showed the highest variability for all factors. When the minimum and the maximum values of the interquartile range of the different factors was compared in primordial follicles, SMAD3 (39-85.9%) and p27 (28.7-74.1%) showed the highest variability in comparison to CCDN2 (69.1-88.1%) and FOXL2 (56.7-88.2%).

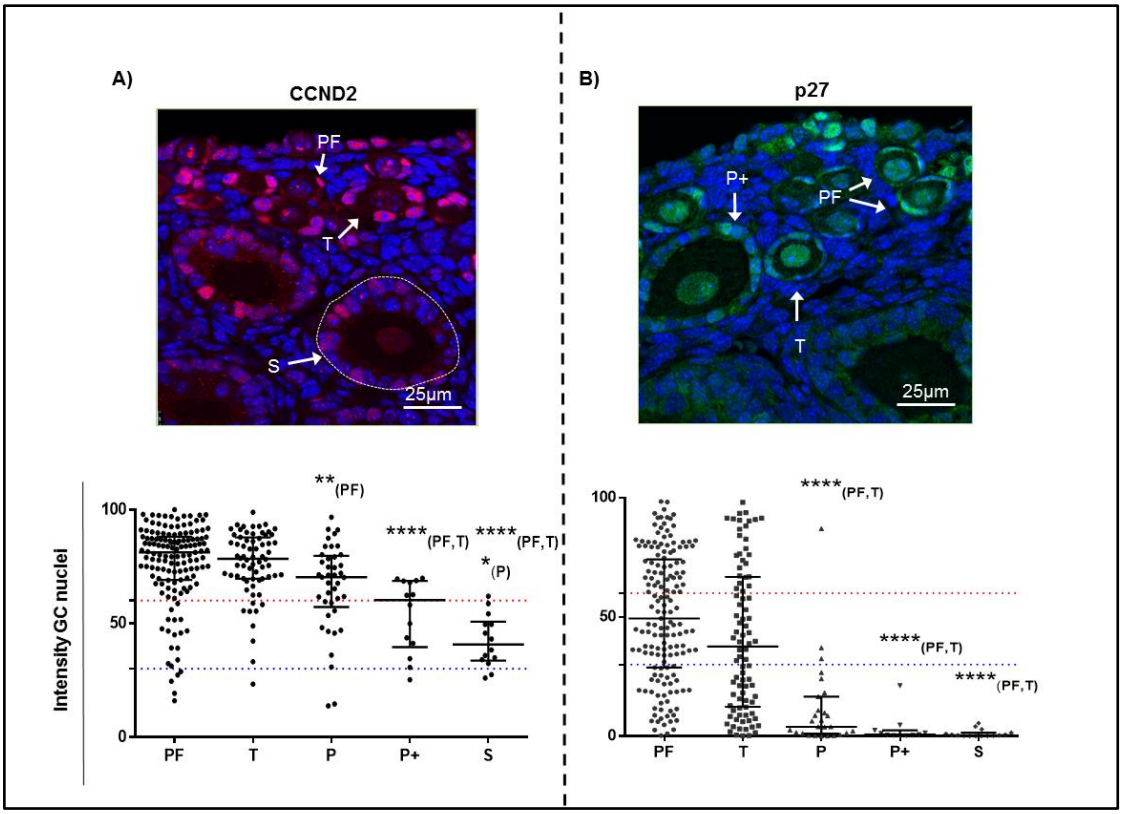

Figure 3.13. Quantification of CCND2 and p27 staining in GCs during early follicle development. A) and B) show the measured intensities for CCND2 and p27 in GC nuclei for the different follicle stages, respectively. Image of CCND2 staining (red) shows an example of primordial, transitional and secondary follicle stages. Image for p27 staining shows an example of primordial, transitional and large primary follicle stages. Dashed lines in graphs delimit medium (blue line and above) and high (red line and above) intensities. Nuclei from the images are stained blue with DAPI. Data are medians ±interquartile range and significant differences for each group are relative to the follicle stage in parentheses (*P<0.05, **P<0.01, ***<P<0.001, ****P< 0.0001). PF, primordial; T, transitional; P, primary; P+, large primary; S, secondary follicle stages.

Association between SMAD3 expression and GC proliferation

The expression of the proliferative marker Ki67 was also measured as a control to determine the proliferative state of the different follicles. As expected, an increased Ki67 staining was detected from primordial to secondary follicle stages. In primordial and transitional follicles, absence of staining with the exception of few cells was observed, whereas in primary, large and primary follicles, more GCs Ki67 positive cells were observed but Ki67 staining was still low.

Therefore, when the different follicle stages were compared, a significant increase in Ki67 staining was observed in primary, large primary and secondary follicles when compared to primordial and transitional follicles (P<0.0001).

When sections were co-stained with SMAD3 and Ki67, very few Ki67 positive cells were observed in GCs of primordial and transitional follicles, the same cells that were positive for SMAD3 protein (Figure 3.13B). The incidence of Ki67 positive GCs increased in growing follicles around the same stage when SMAD3 is excluded from the GC nuclei.

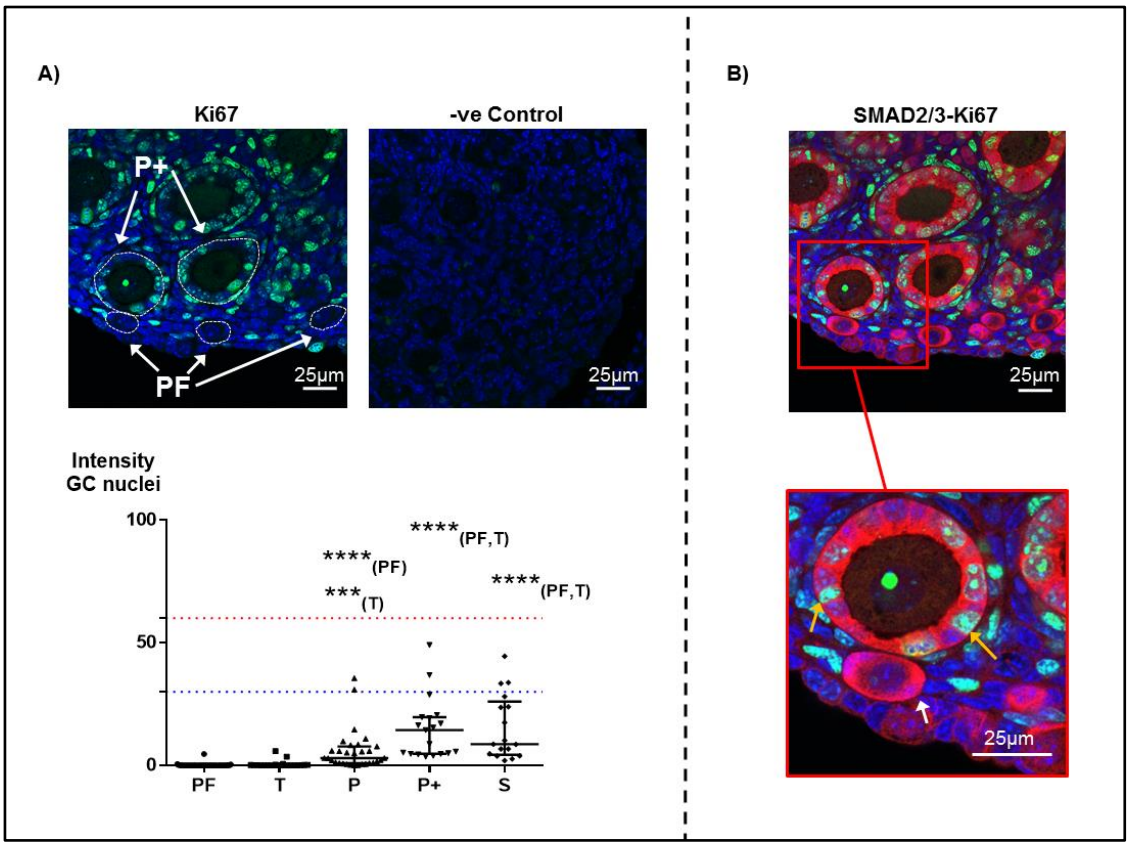

Figure 3.14. Quantification of Ki67 and co-localisation with SMAD3 during early follicle development. . A) shows the measured intensities for Ki67 in GC nuclei for the different follicle stages, respectively. Image of Ki67 staining (green) shows an example of primordial and large primary follicle stages (white arrows). A negative control with a non-immune rabbit IgG antibody is shown. B) shows the localization of SMAD2/3 (red) and Ki67 (green). White arrow shows a primordial follicle stained for SMAD2/3 but negative for Ki67. Yellow arrows show nuclear Ki67 cells where SMAD3 is excluded from the nucleus in growing follicles. Dashed lines in graphs delimit medium (blue line and above) and high (red line and above) intensities. Nuclei from the images are counterstained blue with DAPI. Data are medians ±interquartile range and significant differences for each group are relative to the follicle stage in parentheses (P<0.05, **P<0.01, ***<P<0.001, ****P< 0.0001). PF, primordial; T, transitional; P, primary; P+, large primary; S, secondary follicle stages.

3.3.5 FOXL2 and SMAD3 as transcriptional regulators of *Ccnd2* and *p27*

Although FOXL2 is expressed in GCs of follicles from all stages, its role in PFA has not been reported. Since FOXL2 and SMAD3 are both transcriptional regulators, the aim was to determine first whether these proteins co-localise and interact in GC nuclei of primordial/transitional follicles and secondly, whether they individually regulate the expression of *Ccnd2* and *p27*.

Foxl2 and SMAD3 co-localisation and protein interactions

As expected from the image analysis and individual staining above, FOXL2 and SMAD3 co-localised in GCs of primordial/transitional follicles (Figure 3.15A). To determine if they interact in situ, a proximity ligation assay was used. This assay works by ligating a molecular complex between two antibodies that are in close proximity. The complex is then labelled (indicated as red dots) to highlight protein interactions. Using FOXL2 and SMAD3 antibodies on day 4 ovary sections, no labelling/interactions were observed in any specific follicle cell type (Figure 3.15B). When FOXL2 was co-localised with the oocyte protein DDX4 as a negative control (since each factor is located in a different cell type), a signal was observed in the ooplasm. The negative control with only FOXL2 primary antibody showed no red dots.

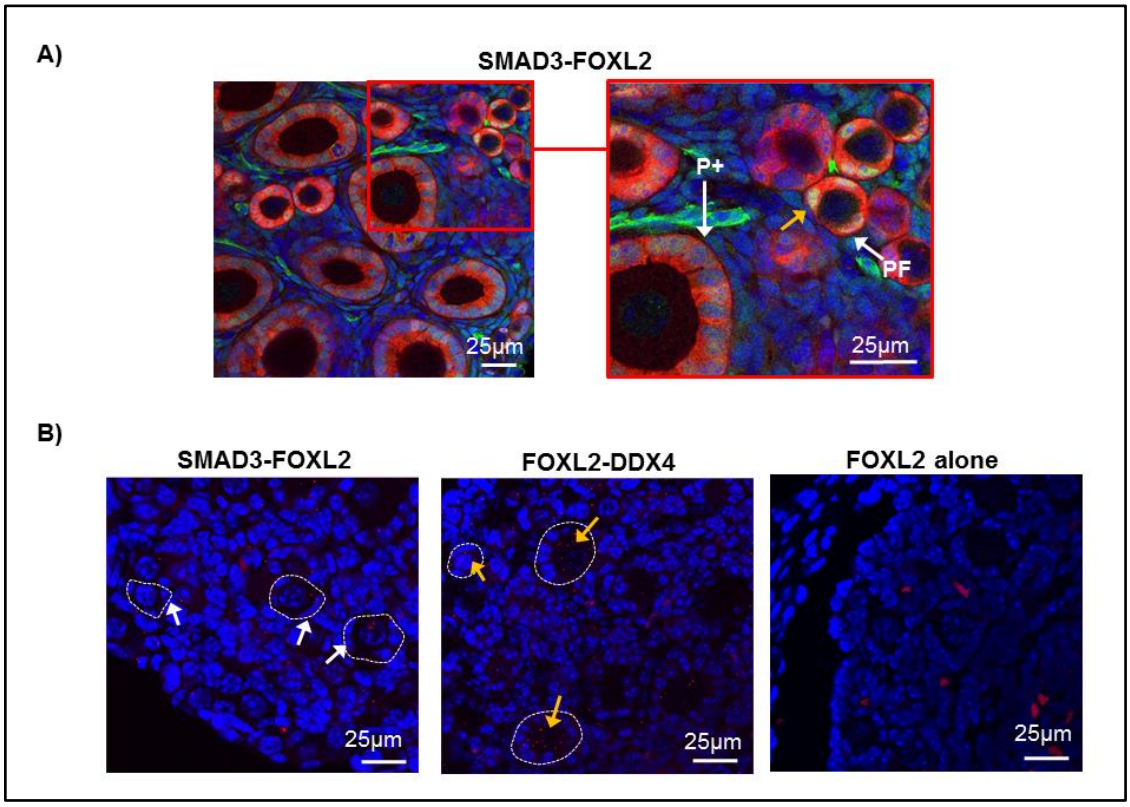

Figure 3.15. Co-localisation and interaction of FOXL2 and SMAD3 proteins in small follicles. A) shows the localisation of SMAD3 (red) and FOXL2 (green) in an example of primordial and large primary follicles. Yellow arrow indicates co-localisation in GC nuclei in primordial follicles. B) shows the results from the PLA assay with FOXL2 co-localised with SMAD3, DDX4 and FOXL2 alone, respectively. White arrows show no signal in GCs from any follicle. Yellow arrows show red dots on the oocyte cytoplasm. Nuclei from the images are stained blue with DAPI. PF, primordial; P+, large primary follicle stages.

Foxl2 and SMAD3 binding to Ccnd2 and p27 gene promoters

The next aim was to determine whether FOXL2 and SMAD3 have the ability to bind and regulate the expression of *Ccnd2* and *p27* cell cycle genes in GCs, since they are all expressed in GCs primordial/transitional follicles. *Ccnd2* and *p27* are known targets of Foxl2 (Garcia-Ortiz et al., 2009; Bentsi-Barnes et al, 2010). SMAD3 regulation of *Ccnd2* gene has been proposed but direct SMAD3 binding has not been demonstrated (Park et al, 2005), therefore, the oncogene *Myc* was used as a positive control target gene for SMAD3 (Warnet et al., 1999).

Samples of day 4 and day 16 ovaries (enriched in primordial/transitional and large primary follicles, respectively) were subjected to ChIP with SMAD2/3 (sc-133098, Santa Cruz) and FOXL2 antibodies (SC-55655, Santa Cruz) (Table 2.1), and a different binding pattern was observed (Figure 3.16A). In day 4 ovaries, SMAD3 bound to the promoter of *Ccnd2* and *Myc*, but not *p27*, while in day 16 ovaries, SMAD3 bound to all three genes. By comparison, FOXL2 binding to *Ccnd2* and *Myc* was not observed whereas binding to *p27* was detected in day 4 ovaries. In day 16 ovaries, FOXL2 bound to all three genes.

When gel images were quantified by optical densitometry, SMAD3 binding to *Ccnd2* was higher in day 4 ovaries (relative to IgG control) whereas reduced to *Myc* and *p27* (relative to IgG control) when compared to day 16 ovaries (Figure 3.16). In contrast, Foxl2 binding to *Ccnd2* and *Myc* (relative to IgG control) was reduced in day 4 ovaries while higher to *p27* (relative to IgG control) when compared to day 16 ovaries (Figure 3.16).

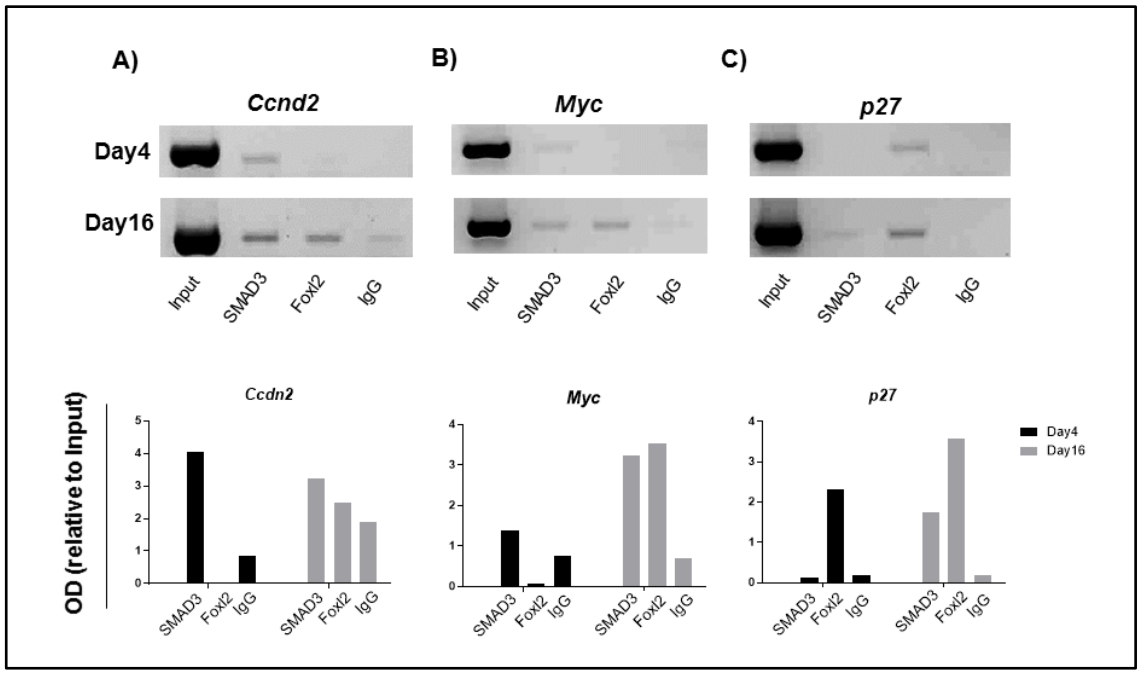

Figure 3.16. ChIP with SMAD3 and FOXL2 antibodies in day 4 and day 16 mouse ovaries.A) B) and C) show amplification by conventional PCR of *Ccnd2*, *Myc* and *p27* gene promoters with SMAD3, FOXL2, non-immune IgG antibodies and input (chromatin sample prior to ChIP). Data was obtained from 1 sample from each ovary age (n=1). Graphs represent the OD values relative to input sample.

3.4 Discussion

GCs show a slow proliferative state in primordial follicles and their escape from this state and further proliferation marks the onset of the initiation of primordial follicle activation and growth. The TGFβ intermediates SMAD2/3, the cell cycle regulators CCND2 and p27 and FOXL2 are also key factors in the ovary; however, their specific function and expression pattern throughout early follicle development have not been mapped out in the context of PFA. The first aim of this chapter was to study the localisation and differential expression of these factors in detail in small follicles. Since GC proliferation has been previously proposed to precede oocyte growth during PFA (Braw-Tal, 2002; Da Silva-Buttkus et al, 2008), the second aim was to establish the relationship between GC proliferation and oocyte growth using the classification criteria applied in this thesis. The next aim was to measure the expression pattern of the candidate factors across follicle stages. Finally, the last aim was to investigate whether there was a molecular link between them, specifically, whether SMAD3 and FOXL2 were able to interact and bind to the promoter of the candidate cell cycle regulators.

SMAD3 but not SMAD2 may play an important role in primordial follicles

The TGFβ mediators SMAD2/3 were previously localised in GCs of primordial follicles (Fenwick et al, 2013); however, whether SMAD2 or SMAD3 have a compensatory role in the ovary have solely been reported with double cKO (Li et al, 2008), where SMAD2 and SMAD3 had the ability to overtake each other's role when one of them is absent. As discussed in Chapter 1, it is important to note that these deletions were generated using the AMHR2 promoter, which is not expressed in primordial follicles (Durlinger et al, 2002b). Therefore, whether SMAD2 and SMAD3 have the same function in primordial follicles *in vivo* remains undetermined. Interestingly, the level of *Smad2* mRNA, although detectable, did not vary between the different ovary ages, and SMAD2 protein expression was low/absent in small follicles. By comparison, *Smad3* mRNA expression was higher in day 4 ovaries (with higher proportion of primordial follicles) in comparison to older ages, whereas total protein levels by western blot did not show differences between ages, indicating that post-transcriptional/translational regulation of SMAD3 may help maintaining enough protein levels in all follicle stages.

However, a detailed image analysis of immunostained sections revealed that SMAD3 protein was highly expressed in GC of primordial follicles with a slight reduction in these cells in more advanced stages. More specific analysis showed that SMAD3 was found in GC nuclei of primordial follicles, followed by a nuclear exclusion as follicles grow, specifically from primary stage (P). The strong presence in the nucleus and its exclusion in growing follicles may indicate that SMAD3 has a key role as transcription factor in primordial follicles. Moreover, the lack of co-localisation with the proliferative marker Ki67 indicates that SMAD3 may contribute to the maintenance of the slow-proliferative state of GCs in primordial follicles.

Increased SMAD3 expression in transitional follicles may be essential for PFA

Higher mRNA expression of TGFβ receptor I (*Alk5*) was observed in day 4 ovaries compared to day 8 ovaries, suggestive of TGFβ signalling in primordial follicles. In a recent study with the same ovary ages (Sharum et al, 2016), relative mRNA levels of TGFβ inhibitors *Smad7* and *Strap* were significantly increased in day 4 ovaries compared to day 8 ovaries. Therefore, these findings suggest that levels of TGFβ signalling may be strictly controlled and regulated in primordial follicles. The low levels of phosphorylated SMAD3 in day 4 ovaries were an unexpected finding. However, it has been recently reported that SMAD3 can be located in the nucleus in basal conditions (Schmierer et al, 2008) and another recent report has shown that transcriptionally active SMAD3 can reside in the nucleus in a low-phosphorylated form (Liu et al, 2016).

When SMAD3 expression in GC nuclei was compared between primordial and transitional stages, no differences were observed. This was also confirmed when the nuclear/cytoplasmic SMAD3 ratio was calculated, where no significant differences in the nuclear exclusion were observed until primary stage. However, when SMAD3 expression of the whole GC compartment was measured, the transitional follicle stage showed an increased presence of SMAD3 protein when compared to primordial follicles, suggesting that the cytoplasm contains an increased presence of SMAD3 in transitional follicles. This increased cytoplasmic expression may be an indicative of increased canonical TGFβ signalling. At primary stage, significant nuclear exclusion was observed. Interestingly, a significant reduction in *Alk5* gene expression in day 8 ovaries was also detected, coinciding with a decrease in *Smad3* relative gene expression.

Since day 8 ovaries are more enriched in activated/growing follicles, a mechanism of inhibition of TGFβ signalling during or after PFA may be necessary to decrease the levels of expression of TGFβ factors and allow follicle growth. Since the transitional stage showed increased SMAD3 expression in the cytoplasm, it can be then proposed that an increase in TGFβ signalling is important to allow subsequent TGFβ inhibition. Whether the increase in TGFβ signalling and subsequent inhibition is the cause or the consequence of PFA (and therefore the GC escape from the slow proliferative state) is still undetermined with these results, therefore, the last chapter of this thesis (Chapter 5) aims to clarify this aspect.

SMAD3, CCND2 and p27 have a common protein expression pattern during early follicle development

The detailed image analysis of immunofluorescently-labelled ovary sections for all the candidates provided a better characterisation of their expression pattern. SMAD3, CCND2 and P27 where highly expressed in the nuclei of GCs of follicles up to the small primary stage (P) and their expression was reduced in nuclei of larger follicles. This expression pattern agrees with the mRNA data, where all factors show higher mRNA levels in day 4 ovaries when compared to day 16 ovaries. In contrast, the proliferative marker Ki67 was detected in only few GCs of primordial and transitional follicles, indicating that GCs have a slow proliferative phenotype. Increased Ki67 is observed as follicles grow and confirms that GCs in these follicles are highly proliferative (Figure 3.17). Interestingly, increased number of GCs of some transitional follicles with no increased oocyte size was observed (particularly those with less than 6 surrounding GCs) indicating that GCs start proliferating before the oocyte grows. Since SMAD3, CCND2 and p27 protein expression is strong in GCs from primordial stage (containing 1-3 GCs) and reduced from transitional stage (4-7 GCs), these findings further implicate these factors in PFA.

Variability between the intensities for all these factors was observed in all follicle stages, however, the primordial follicle population showed the highest variability. This is suggestive of differences between follicles from the primordial follicle pool. Whether there is a relationship between differences in the expression of these factors in primordial follicles and their ability to activate is worth to be investigated.

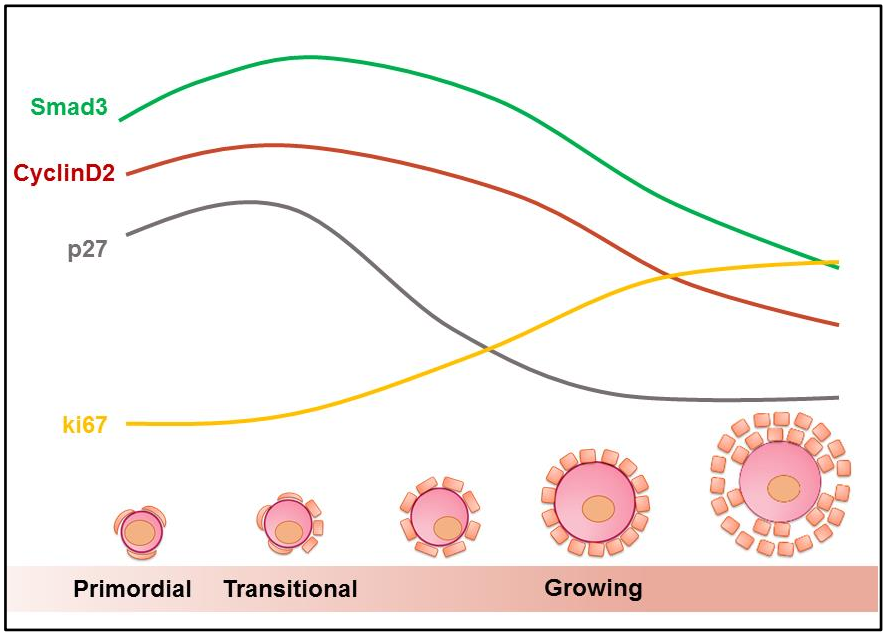

Figure 3.17. Diagram summarising the protein expression pattern in GC nuclei during early follicle development of SMAD3, CCND2, p27 and Ki67. Based on the intensities obtained from image analysis and in comparison with the proliferation marker Ki67**,** all proteins show high presence in GCs of primordial and transitional follicles, where their proliferation is either absent or slow, and expression decreases as follicles grow where GCs proliferate rapidly.

High levels of Ccnd2 are maintained in primordial follicles

Results showed that Ccnd2 mRNA and protein levels were higher in day 4 ovaries compared to older ages. Moreover, image analysis showed that CCND2 protein expression was particularly strong in GCs of small follicles (primordial and transitional stages), followed by a decrease in growing follicles.

Consistent with these results, high mRNA levels of *Ccnd2* in primordial follicles have been observed before in mice, however, the molecular mechanisms regulating these levels were not further studied (Robker & Richards, 1998b).

CyclinDs are the main cyclins regulating cell cycle re-entry in quiescent cells and G1/S transition in proliferative cells (Sherr & Roberts, 1999). They can be regulated at transcriptional level by different pathways, such as the MAPK signalling pathway via RAS or the direct binding of MYC to *Ccnd2* gene (Albanese et al, 1995; Bouchard et al, 2001; Mathew et al, 2004; Meloche & Pouysségur, 2007).

In the ovary, the combination of FSH stimulation and TGFβ ligands has been reported to induce the expression of *Ccnd2* gene in GCs of growing follicles, however, direct binding of SMAD3 was not studied (Looyenga & Hammer, 2007). In this chapter, binding of SMAD3 to *Ccnd2* gene was detected in day 4 ovaries. Since these ovaries contain a high proportion of primordial follicles, it is proposed that TGFβ signalling is a potential regulator of *Ccnd2* gene in these follicles.

Apart from transcriptional regulation, CCND2 levels can also be regulated post-translationally. Inhibitory phosphorylation by GS3K or p38 (from PI3K and MAPK signalling pathways) have been determined as the main mechanisms to allow ubiquitination and degradation of CCND2 protein (Casanovas et al, 2000; Diehl et al, 1998; Kida et al, 2007). However, although the inhibition of the mechanisms of CCND2 degradation may be also important to maintain high CCND2 levels in primordial follicles, the same expression pattern observed for Ccnd2 mRNA and protein levels indicates that regulation of *Ccnd2* gene may be primarily regulated transcriptionally during early follicle development.

It has been proposed that induction of *Ccnd2* expression may be an essential event in quiescent cells prior to cell proliferation. Interestingly, high *Ccnd2* mRNA levels were reported in growth-arrested GC cultures in rat (Robker & Richards, 1998a) and CCND2 protein was localised in proliferative and growth-arrested cells from hamster preantal follicles *in vitro* (Yang & Roy, 2004). In human primary cells and mouse fibroblastic cell lines, *Ccnd2* levels are also abundant in contact-inhibited cells (Meyyappan et al, 1998) and specific molecular mechanisms based on the protein complex dynamics of CCND2 with K4 and p27 have been proposed as determinants of the G0/G1 phase transition in mouse epithelial cell lines (Susaki E 1 2007). These findings together with the observations in this chapter suggest that high levels of Ccnd2 mRNA and protein may be necessary to provide the primordial follicle GCs with the cell cycle machinery necessary to allow follicle activation.

Ccnd2 and p27 expression levels are reduced in growing follicles

In growing follicles, reduction in Ccnd2 mRNA and protein levels were observed in GCs. Overexpression of *Ccnd2* has been found in GC tumours (Anttonen et al, 2014b), suggesting that a decrease in these levels may be necessary to control the level of proliferation in GCs of growing follicles after PFA. In a model of quiescent β-cells, high Ccnd2 protein and mRNA levels also decreases as cells acquire a high proliferative state (Salpeter et al, 2011). The exact mechanism by which these levels are reduced in proliferative β-cells was not determined, however, it was demonstrated that a decrease in glucose levels linked with low calcium influx and NFAT transcription factors downregulated *Ccnd2* gene expression (Salpeter et al, 2011). In the ovary, growing follicles seem to be calcium-dependent to maintain the oocyte-GC interactions necessary for development (Mora et al, 2012a), therefore, it is possible that calcium signalling and NFATs participate in the regulation of *Ccnd2* gene in growing follicles.

p27 gene and protein levels were also high in GCs of primordial follicles and decreased as follicles grow. p27 has been reported to participate in the maintenance of the primordial follicle population, since *p27-/-* mice show premature PFA (Rajareddy et al, 2007). However, although increased kinase activity (specifically, Cdk2/Cdc2-CyclinA/B1) was reported in these mice, it was not determined whether these molecular mechanisms are triggered in the oocyte or GCs. From the results in this chapter, p27 in the oocyte showed no specific pattern across follicle stages. In GCs, p27 showed a clear nuclear reduction after primary stage whereas growing oocytes still expressed p27. Therefore, the decrease in p27 expression and degradation in GCs may be an essential mechanism to allow cell cycle progression after PFA. As mentioned above, the dynamics of CCND2/CDK4/p27 complexes are key to allow entry to G1 phase, and translocation to the cytoplasm has been proposed as a mechanism that involves p27 degradation and subsequent cell cycle progression (Nakayama, 2004). The co-localisation and characterisation of the protein dynamics of these factors in primordial and growing follicles will be explained in the next chapter in order to determine whether this mechanism also operates in the ovary (Chapter 4).

SMAD3 and FOXL2 differentially regulate common cell cycle genes

Image analysis and localisation study did not relate the presence of FOXL2 to any particular stage of early follicle development. At the transcriptional level, *Foxl2* did not show any difference in the mRNA levels between the ovary ages. However, total FOXL2 protein levels were found to be elevated in older ovaries, suggesting a mechanism of post-translational regulation may account to maintain high FOXL2 protein levels high in larger follicles. In fact, different FOXL2 protein isoforms can be generated by sumoylation, phosphorylation or acetylation and determine its binding to target genes and transcriptional activity (Benayoun & Veitia, 2009).

Since transcription factors SMAD3 and FOXL2 are present in the nucleus of GCs, they can be involved, together or independently, in the regulation of cell cycle genes, such as *Ccnd2* and *p27*. Although both genes are well-known targets of FOXL2 (Bentsi-Barnes et al, 2010; Garcia-Ortiz et al, 2009), SMAD3 binding to these genes has only been suggested for *Ccnd2* (Park et al, 2005) and never demonstrated for *p27*. FOXL2 and SMAD3 have been reported to be transcriptional partners in the gonadotrope-derived αT3-1 cell line, a cell model used to study the pituitary (Blount et al, 2009). Therefore, the last aim of this chapter was to investigate first whether this was the case in primordial follicles and secondly, whether they had the ability to regulate *Ccnd2* and *p27* genes. Results from PLA assay did not show any relevant interaction between SMAD3 and FOXL2 in primordial follicles. Although the presence of some "dots" were observed, they were randomly localised. Moreover, the increased presence of signal in the ooplasm of the negative control section indicated that FOXL2 antibody binds in a non-specific manner to a protein in close proximity to DDX4 protein, also present in the ooplasm. Next, the results from the ChIP experiment using samples of day 4 and day 16 ovaries showed that FOXL2 and SMAD3 had a different binding pattern to the target genes *Ccnd2* and *p27* relative to IgG control. Binding of FOXL2 to *p27* gene promoter was detected in these models of primordial and growing follicles and is consistent with the findings by other studies whereby FOXL2 regulates and maintains p27 gene expression levels in mice (Garcia-Ortiz et al, 2009; Mork et al, 2011).

Moreover, reduced FOXL2 binding to *Ccnd2* was observed in primordial follicles whereas binding was increased in growing follicles. FOXL2 has been reported to bind and repress *Ccnd2* gene in transfected ovarian cell lines (Bentsi-barnes et al, 2010). As the findings described in this chapter revealed that Ccnd2 levels (both mRNA and protein) are decreased in growing follicles, a mechanism of transcriptional repression via FOXL2 can be proposed in these follicles.

In contrast, SMAD3 binding was detectable in primordial follicles for *Ccnd2* but not *p27* gene promoter, suggesting SMAD3 may not directly regulate *p27* gene in primordial follicles. However, SMAD3 binding to *Ccnd2* was evident in primordial follicles, indicating *Ccnd2* may be a novel transcriptional target of SMAD3 in primordial follicles. SMAD3 binding to *Myc* oncogene was also detected in both primordial and growing follicles. *Myc* is a common target gene of SMAD3, where SMAD3 acts as a transcriptional repressor and therefore impedes *Myc* from repressing its target gene *p15* (CKI) (Joan et al, 2001), resulting in cell cycle arrest. The role of Myc in primordial follicles has not been reported before. Although SMAD3 binding to *Myc* gene was observed in day 4 and day 16 ovaries, higher binding was detected in day 16 ovaries. Therefore, a more detailed analysis of SMAD3 binding to *Myc* is worth to be investigated in order to determine whether this binding is also necessary in GCs to maintain the quiescent phenotype of primordial follicles.

The differential binding pattern of FOXL2 and SMAD3 to the candidate target genes *Ccnd2* and *p27* in primordial and growing follicles indicates that they act independently in the regulation of these genes in the context of PFA. FOXL2 binds in both primordial and growing follicles whereas SMAD3 binding in primordial follicles is increased. Nevertheless, these findings suggest that FOXL2 and SMAD3 regulation of *p27* and *Ccnd2* genes in primordial follicles may have an essential role as transcription factors in the slow proliferative state of GCs in primordial follicles.

In summary, the descriptive analysis of SMADs and cell cycle factors in this chapter has revealed the following key findings:

- SMAD3 is nuclear in cell cycle-arrested GCs of primordial follicles and is excluded as GCs proliferate in growing follicles. In the transitional stage, increased SMAD3 in the cytoplasm may indicate increased TGFβ signalling during PFA.
- p27 and CCND2 are highly expressed in GC nuclei of primordial and transitional follicles and expression decreases in primary follicles, suggesting an important role of these proteins in PFA.
- SMAD3 is a transcriptional regulator of *Ccnd2* and *Myc* whereas *p27* and *Ccnd2* are targets of FOXL2 in primordial and growing follicles.

Since CCND2 and p27 have been found in primordial follicles and they are known to create a protein complex which is crucial for cell cycle re-entry in other models (Susaki E 1 2007); the next chapter aims to determine whether this also applies to the ovary, by examining CCND2/p27 co-localisation and determining whether these proteins exist in bound complexes in primordial and growing follicles.

Chapter 4.

CCND2/p27 protein dynamics during early follicle development

4.1 Introduction

Cell proliferation is strictly dependent on growth factor signalling and nutritional supply that will allow cell cycle factors to function towards four different phases: Gap phase 1(G1), DNA synthesis phase (S), Gap phase 2 (G2) and mitosis (M). When cells are deprived of growth factors, they have the ability to exit the cell cycle and enter G0 phase, also known as quiescence (Mathew et al, 2004). Cells can only enter quiescence during G1 phase at two restriction points (also known as checkpoints). The first checkpoint (R1) is located in early G1 and is dependent on adequate supply of growth factors while the second checkpoint (R2) occurs later in G1 and relies on a good nutrient supply. After the second checkpoint, cells commit to enter the cell cycle in an irreversible manner (Figure 4.1)(Foster et al, 2011).

Figure 4.1. G1 phase checkpoints in the cell cycle. After mitosis (M), cells enter the first restriction point (R1) of G1 phase, where a good supply of growth factors ensures G1 progression. A second restriction point (R2) exists before entering S phase, where cells with a good supply of nutrients (amino acids, fatty acids, energy, oxygen) enter irreversibly S phase towards M. If the cell lacks any of the requirements for R1 and R2, it exits the cell cycle and enters a reversible state of quiescence (G0).

Cyclin Ds are the main cyclins at R1 and they are regulated transcriptionally and post-translationally (Kida et al, 2007; Sherr & Roberts, 1999; Yen & Pardee, 1978). From all D- type Cyclins, CCND2 is expressed earlier in the cell cycle, being highly expressed in mid-G1 phase while CCND1 and 3 appear later during late G1 phase (Nakayama, 2004; Susaki et al, 2007).

At the transcriptional level, Ras is a well-known inducer of the *Ccnd2* gene, which maintains high CCND2 levels during R1 to avoid exit from the cell cycle (Mathew et al, 2004). At the post-translational level, Cyclin D association with Cdks and CKIs also determines G1 progression. TGFβ signalling arrests cells in R2 via the repression of *Myc* gene and induction of CKIs such *p15*, which inhibits Cyclin D/K4-6 assembly (Warner et al, 1999). CCND2 complex formation with Cdk4/6 (K4-6) has both catalytic and non-catalytic actions (Blain, 2008). The catalytic function is important to allow the G1/S phase transition via the phosphorylation of Rb, subsequent release of E2F and induction of Cyclin E. The non-catalytic role involves assembly with p27, creating an "inactive" CCND2/K4-6/p27 ternary complex that confers the stability necessary to eventually allow cell cycle progression (Nakayama, 2004; Ray et al, 2009).

Degradation of p27 has been related to its translocation to the cytoplasm during G1 phase, therefore allowing G1/S phase transition (Bagui TK 2003; Nakayama, 2004). Although initial hypotheses suggested that phosphorylation of p27 is key for this translocation (Ishida et al, 2002), it has been reported in epithelial cell lines that not only p27 but the whole ternary complex is exported and dependent on the phosphorylation of CCND2 on the Thr^{280} residue (Nakayama, 2004; Susaki et al, 2007) (Figure 4.2). However, the kinases triggering this phosphorylation and therefore their signalling pathways are still unknown. Notwithstanding this, it is also proposed that high levels of CCND2 also result in the nuclear export of the ternary complexes (Nakayama, 2004). The results described in Chapter 3 showed SMAD3 binding to the gene promoters of *Myc* and *Ccnd2* in GCs of primordial follicles, characterised by a non-proliferative phenotype. Therefore, *Ccnd2* was identified as a new transcriptional target of SMAD3, probably regulating its levels during G1 phase progression. In addition, image analysis performed in Chapter 3 showed that high CCND2 protein expression levels in GCs of primordial follicles coincided with p27 protein expression levels. Moreover, abrupt reduction in p27 expression was observed in growing follicles (particularly from primary stage). p27 is a well-established marker of G0/ early G1 phase, where it is expressed at maximum levels, immediately decreasing until total absence during G1/S transition (Toshihiko et al, 2014). Therefore, expression of p27 may be an important switch for the transition from a slow proliferative GC phenotype in primordial follicles to a high proliferative phenotype in growing follicles.

From previous reports, it is proposed that the signalling pathways inducing *Ccnd2* may also participate in the regulation of CCND2/K4-6/p27 complex dynamics (Foster et al, 2011). This chapter is focused on CCND2 and p27 protein expression dynamics in primordial follicles. Based on the findings in the previous chapter and the model for CCND2/K4-6/p27 complex dynamics (Figure 4.2), **it is hypothesised that dissociation of CCND2 and p27 protein complex (and subsequent p27 degradation) in GCs of primordial follicles is associated with PFA.** Therefore, the first aim of this chapter is to determine whether CCND2 and p27 create a complex in primordial follicles. For this purpose, co-localisation with immunofluorescence staining and co-immunoprecipitation will be performed for both proteins using immature mouse ovaries. The second aim is to determine the subcellular localisation of these factors in order to determine whether the complexes are formed in the nucleus or in the cytoplasmic compartment of GCs in primordial and growing follicles.

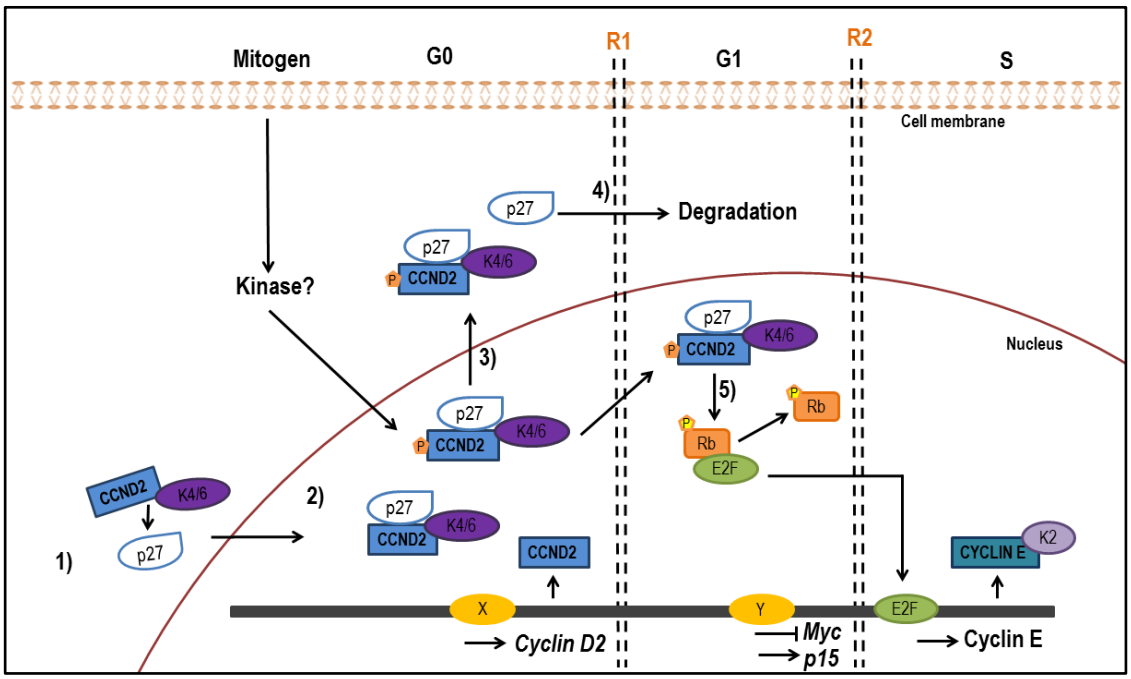

Figure 4.2. Model of CCND2/K4-6/p27 complex dynamics in epithelial cell lines. The ternary complex resides in the nucleus in G0/G1 after nuclear import by p27 (1 and 2) and after mitogen stimulation, the phosphorylation of CCND2 and p27 by yet unknown protein kinases is the trigger for the translocation of the whole complex to the cytoplasm (3), driving p27 towards degradation and entry to G1 (4) and eventually allowing the progression towards the S phase of the cycle (5). Transcriptional control is essential during this time, where CCND2 levels are regulated around R1 (X factor, such as Ras) and *Myc* and *p15* expression is regulated around R2 (Y factor, such as SMAD3).

4.2 Methods

4.2.1 Culture of NIH3T3 cell line and protein analysis

The NIH3T3 cell line was maintained as described (see section 2.3) and used as a control to study the protein dynamics and complex formation of CCND2 and p27 during cell cycle entry. For that, cells were cultured to 80 % confluence, serum-deprived for 24h and then replaced with media supplemented with 10% FCS. Whole protein content was extracted at different time points and western blot with CCND2 (sc-593, Santa Cruz) and p27 (sc-528, Santa Cruz) antibodies (see Table 2.1) were performed as explained (see 2.5). Results were obtained from three independent experiments (n=3). Co-immunoprecipitation (using 80µg of total protein as starting material) was also performed with some of these time points. Half of the volume of the IP samples was loaded on the western blot and input samples (control for the IP) contained 5 times less protein than the initial amount used for the IPs.

4.2.2 Ovary tissue collection and protein analysis

Ovaries from day 4 and 16 mice were dissected as described (see 2.2) and either immersed in formalin for immunostaining purposes or flash frozen at -80ºC for protein extraction. Co-immunoprecipitation and western blot was performed as explained above for the cell line, instead using 25-30µg from a pool of three ovaries from different litters for each sample of day 4 and day 16 ovary ages. Results were obtained from one sample for each age (n=1). Moreover, to study in detail the location of CCND2 and p27 in the follicles contained in day 4 and day 16 ovaries, the protocol of subcellular fractionation described (see 2.5.3) was applied with six ovaries/sample (day 4) and three ovaries/sample (day 16) and equal amounts (3-5µg) of the cytoplasmic, membrane and nuclear fractions were analysed by Western blot. Results were obtained from one sample for each age (n=1). SMAD3 antibody (#9523, Cell Signalling) was used as control of nuclear fraction enrichment and GADPH antibody (sc-32233, Santa Cruz) was used as control for nuclear fraction purity (see Table 2.1).

4.2.3 Visualisation and analysis of western blot images

In order to obtain a better visualisation of the results from western blots, optical densitometry (OD) of the gel bands was measured with the Ingenius Bioimaging software “GeneTools” (Syngene). Mean pixel values of target bands and background were

normalised against the pixel area selection, and background was then subtracted from the target band value. Background subtracted values were referred as “OD value”.

When a comparison of the protein content between samples was required, OD values of CCND2 and p27 were normalised with the loading control beta-actin (by calculating the ratio) (see Figure 4.3). For the immunoprecipitated samples with no loading control, only OD values of CCND2 and p27 were represented (see Figure 4.4).

4.2.4 Immunofluorescence staining and image analysis

In order to determine whether CCND2 and p27 co-localise across the different follicle stages; day 4, day 8 and day 16 ovary sections (one section per age group, n=1) were immunofluorescently-stained as described (see 2.4.2) and the “Colocalization threshold” pluggin from Image J software was used to obtain co-localised images from the different channels showing specific staining for CCND2 (green) and p27 (red). A minimum of 20 individual GC nuclei from primordial (PF) and transitional (T) follicles (only from follicles with a clear oocyte nucleus outline) were selected from a single day 4 and day 8 ovary section, thresholded and the area of positive pixels was measured and referred as “Intensity” of CCND2 and p27 (as explained in Chapter 3 (see 3.2.4). As CCND2 was normally the highest value, difference of intensities between CCND2 and p27 was represented as the increment relative to CCND2 ($\frac{CCND2-p27}{CCND2}$) and referred as “ratio intensities”. Values exceeding 1 or -1 where given the values of 1 or -1. Moreover, values >0.5 were considered to have >50% decreased p27.

4.2.5 Statistical analysis

In order to compare the change in protein expression of CCND2 and p27 at different time points after serum stimulation, OD values (with subtracted background and normalised against a beta-actin) of CCND2 and p27 western blot bands from three independent experiments (n=3) were compared using a two-way ANOVA with Bonferroni multiple comparisons post-hoc test (Graphpad Prism 7.03). Differences were considered statistically significant when $P<0.05$.

4.3 Results

4.3.1 CCND2 and p27 protein expression in NIH3T3 cells during cell cycle entry

As previously reported, NIH3T3 cells express CCND2 and p27 proteins, and these proteins are key modulators of cell cycle progression (Susaki et al, 2007). Therefore, this cell line was used as a positive control for the experiments aiming to understand the complex dynamics of these two proteins in early follicle development. When serum was added to starved cells, p27 protein levels significantly decreased after 9 hours (Figure 4.3). By comparison, CCND2 protein levels remained steady and did not change in all time points analysed (Figure 4.3).

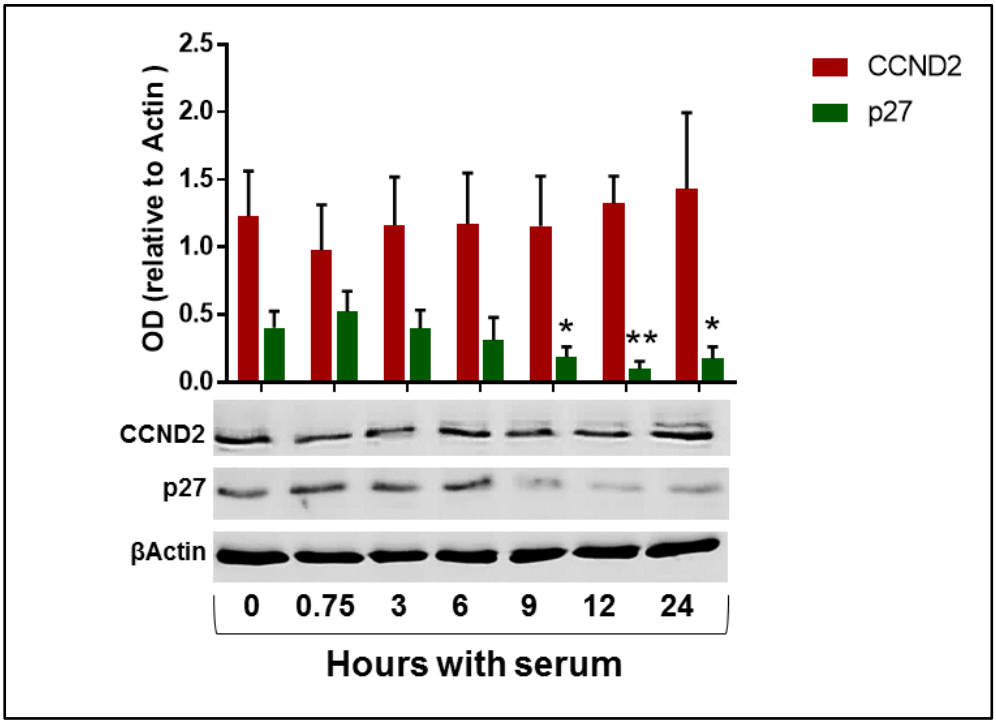

Figure 4.3. Western blot of CCND2, p27 and beta-actin (loading control) expression after serum stimulation in NIH3T3 cells. Cells were serum- deprived for 24 hours and then stimulated with 10% FCS for the stated times (hours). OD values for each protein are normalised against beta-actin as described in the methods. The bar chart in the upper panel represents mean normalized OD values (±SEM) from three independent experiments (n=3) for CCND2 and p27 following serum stimulation. Significant differences are relative to 0 hours of serum stimulation (*P<0.05). A representative blot at each time point is shown in the lower panel.

When whole protein lysates were immunoprecipitated with a p27 antibody, CCND2 protein was detected in the same protein complex in all time points (Figure 4.4). Moreover, the amount of the bound CCND2 protein decreased after serum stimulation alongside the decrease in immunoprecipitated p27 protein. When CCND2 antibody was used for the immunoprecipitation, almost no p27 protein was found to be bound (Figure 4.4).

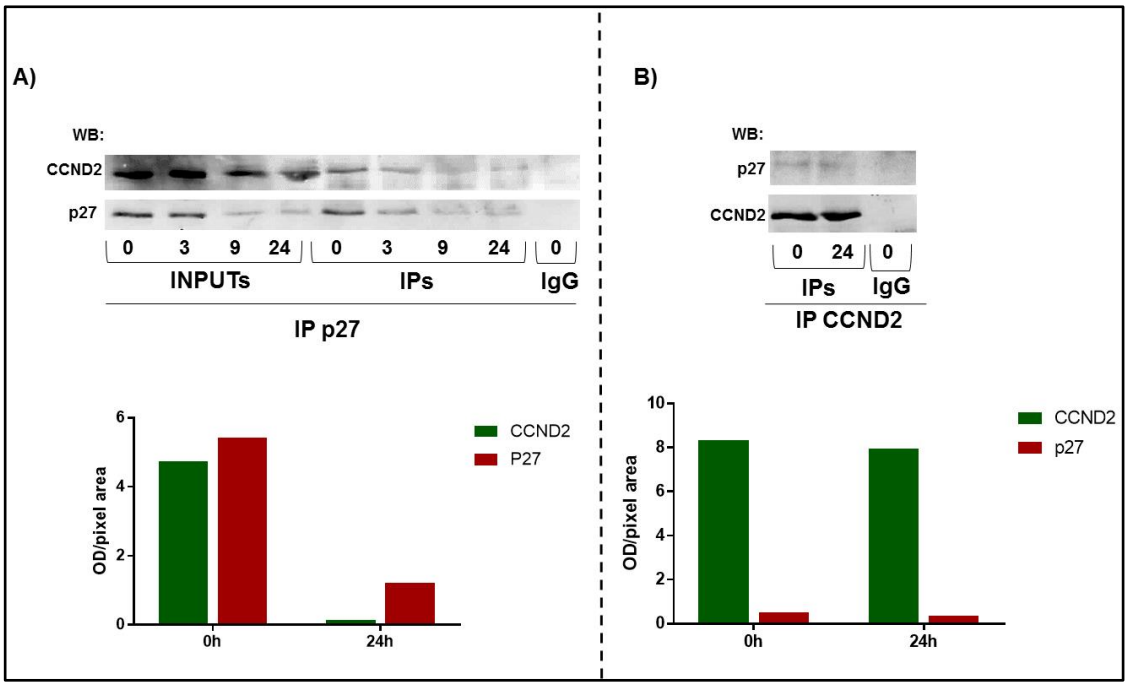

Figure 4.4. Western blot showing immunoprecipitation of CCND2 and p27 in NIH3T3 cells after serum stimulation. Whole cell lysates from different time points after treatment with serum were immunoprecipitated with a p27 antibody and probed with an antibody to CCND2 and p27 (upper panel; A) The opposite was also performed, in that whole cell lysates were immunoprecipated with a CCND2 antibody and probed with an antibody to p27 and CCND2 (upper panel; B). OD values for the bands from A and B corresponding to time points 0 and 24h are plotted in the lower panels. Eighty µg of total protein was used as starting material for the immunoprecipitated samples (IP) and half of the volume was loaded on a western blot. Input samples on the western blot contained 5 times less protein than the initial amount used for the IPs. Non-immune rabbit IgG control (IgG) is used as a control for immunoprecipitations.

4.3.2 CCND2-p27 co-localisation and comparison of intensities across follicle stages

When immunofluorescence staining for both proteins was performed in day 4, day 8 and day 16 ovary sections, they were co-localised in GC nuclei of primordial follicles. From transitional stage, both CCND2 and p27 protein levels showed a progressive decrease in expression. The decrease in p27 was abrupt from the primary stage, where a loss of co-localisation was observed in GCs of larger growing preantral follicles (Figure 4.5). Both CCND2 and p27 proteins were also weakly detected in the nucleus of the oocyte; however, no specific pattern of staining was observed in this cell type and co-localisation of both proteins was difficult to detect (Figure 4.5).

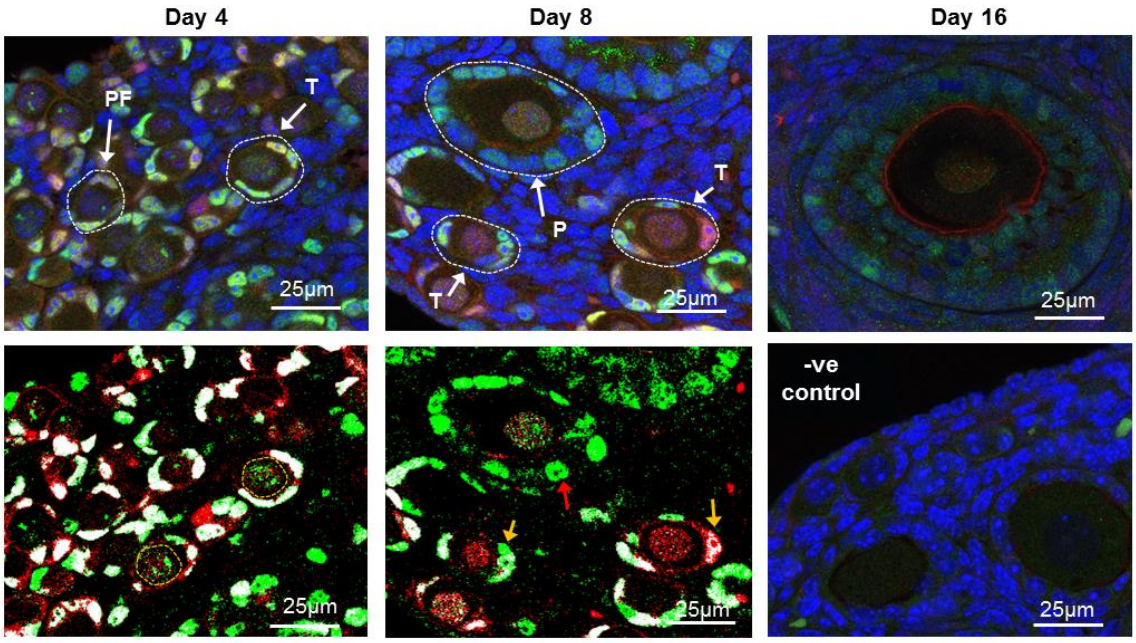

Figure 4.5. Co-localisation of CCND2 and p27 in small follicles in juvenile mouse ovaries. High-power confocal images of day 4, day 8 and day 16 ovary sections show CCND2 (green) and p27 (red) staining. Primordial and transitional follicles show co-localisation of both proteins in GC nuclei (white arrows). Some GC nuclei from transitional follicles show loss of co-localisation (yellow arrows). Primary follicles (red arrow) and secondary follicles (shown in day 16 section) show an abrupt reduction of p27 expression. The oocyte nucleus shows no co-localisation of proteins in any follicle (yellow dashed circle). Images are counterstained blue with DAPI. The lower panels in day 4 and day 8 ovaries show the co-localised pixels of the thresholded image for the individual channels (in white). Negative control with combined non-immune rabbit and mouse IgGs is also shown. PF, primordial; T, transitional and P, primary follicle stages. Magnification is 63X for all images.

When the ratio of the intensities of CCND2 and p27 of individual GCs from primordial, transitional and primary follicles were measured, similar intensities of both CCND2 and p27 (ratios close to 0) were observed in primordial follicles with only 28 % and 23% of GCs with ratio values >0.5 and >-0.5, respectively (Figure 4.6). As explained in the methods, GCs with ratios >0.5 or >-0.5 have >50% decreased p27 or CCND2 expression relative to CCND2, respectively. By comparison, approximately 80% and 12% of the GCs from transitional and primary follicles had a ratio > 0.5 and >-0.5. However, positive ratios in primary follicles are higher than in the rest of the groups.

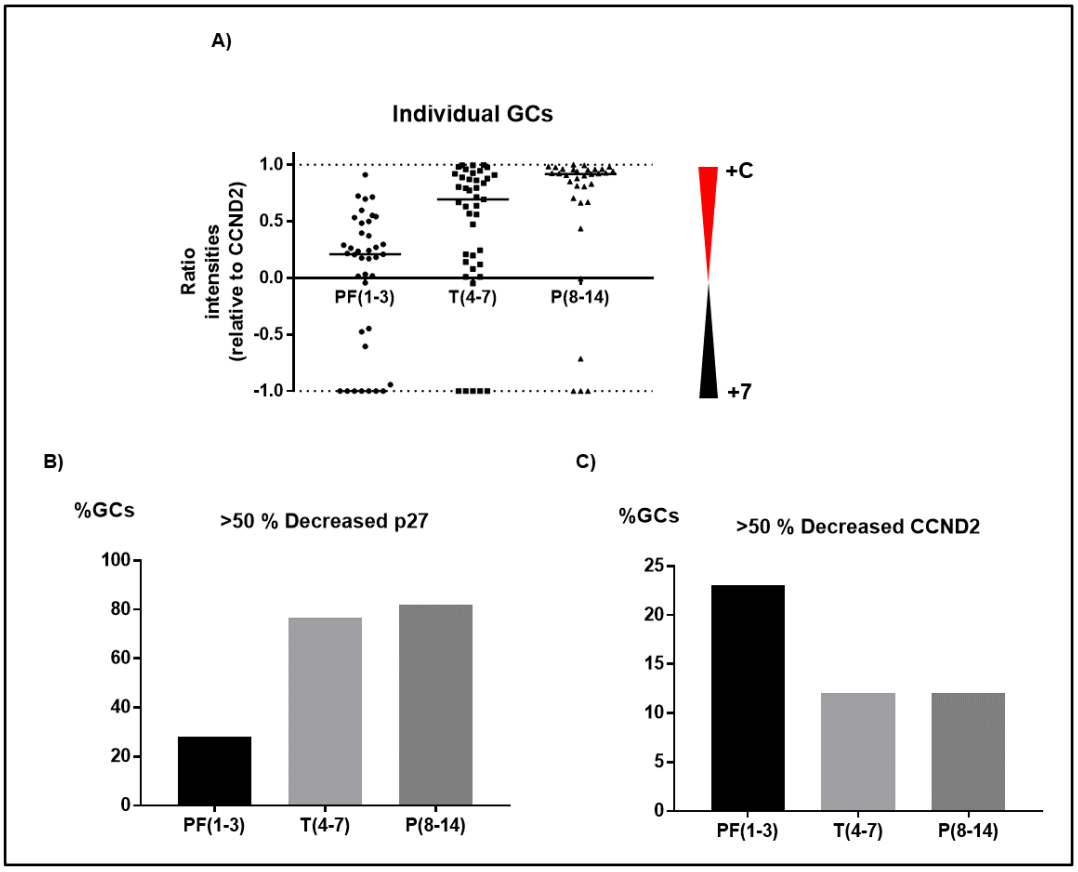

Figure 4.6. Quantification of the ratio CCND2:p27 staining in GCs of small follicles of the mouse ovary. A) shows the ratio of intensities in individual GC nuclei for the different follicle stages. B) and C) show the percentage of GCs with ratios above 0.5 (decreased p27) and -0.5 (decreased CCND2), respectively. Black and red bars in A) refer to increased p27 (+7) and increased CCND2 (+C), respectively. PF, primordial; T, transitional and P, primary follicle stages. Numbers in parentheses refer to the GC number range for each follicle stage.

4.3.3 CCND2 and p27 complex dynamics in day 4 and day 16 ovaries

In order to determine whether p27 and CCND2 were present in the same protein complex in the ovary, immunoprecipitation was performed. When whole protein lysates were subjected to IP using a CCND2 antibody, the amount of bound p27 was low. When samples from day 4 and day 16 ovaries were compared, higher amount of p27 was detectable in day 4 ovaries. By comparison, when p27 antibody was used for immunoprecipitation, the amount of bound CCND2 was high. When samples from day 4 and day 16 ovaries were compared, higher amount of CCND2 was also detected in day 4 ovaries.

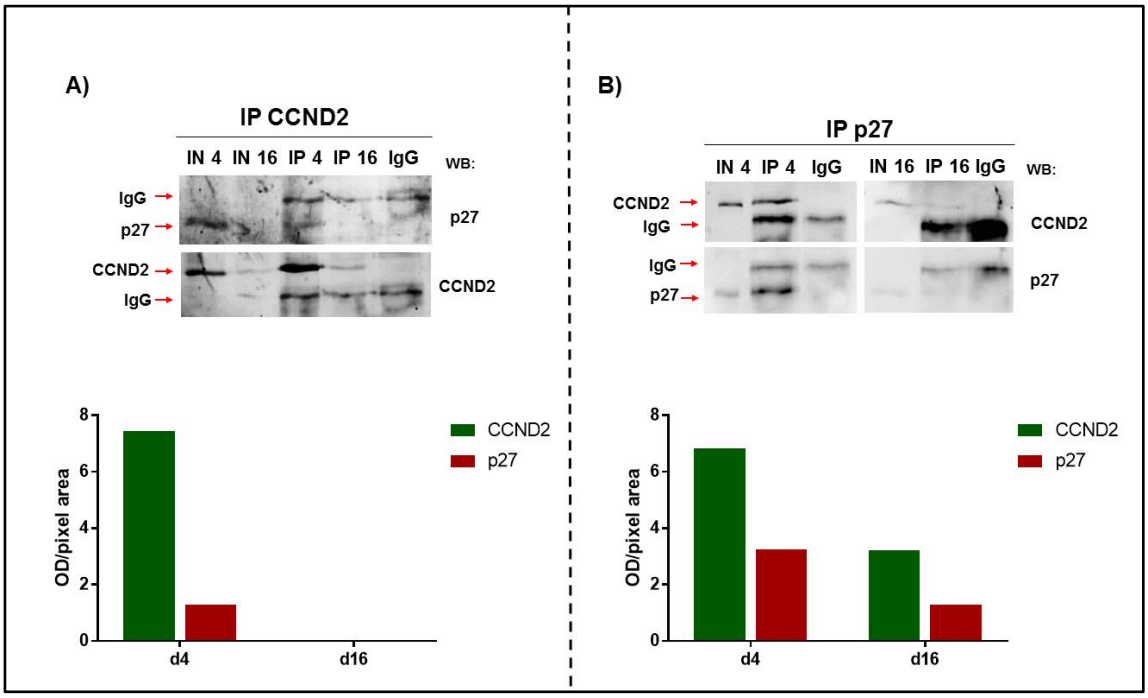

Figure 4.7. Western blot showing immunoprecipitation of CCND2 and p27 in mouse ovaries. Day 4 and day 16 ovaries were immunoprecipitated with a CCND2 antibody and probed with an antibody to p27 and CCND2 (A). The opposite was also performed, in that mouse ovaries were immunoprecipitated with a p27 antibody and probed with an antibody to CCND2 and p27 (B). OD values for the bands from A and B are plotted in the lower panels. Thirty (A) and 25ug (B) were use as starting material for the IPs and half of the volume was loaded on the western blot. Input samples (IN) on the western blot contained 5 times less protein than immunoprecipitated samples (IP) as described in the methods. Input sample of day 16 ovaries contained 10 times less amount of protein than the used for the IP, due to a technical mistake. Non-immune rabbit IgG control (IgG) is used as a control for immunoprecipitations.

4.3.4 CCND2 and p27 subcellular localisation in primordial and growing follicles

In order to determine whether both proteins are localised in the same subcellular compartment where they would create the protein complex, a subcellular fractionation of proteins from day 4 and day 16 ovaries was performed (Figure 4.8). GADPH protein was used as a positive control for the cytoplasmic fraction and as a negative control for nuclear fractions. In the fractions obtained from day 4 ovaries, GADPH showed a strong band in the cytoplasmic fraction whereas it was barely detectable in the nuclear fraction, indicating that the nuclear fraction was mostly free of cytoplasmic content. By comparison, protein fractions from day 16 ovaries showed higher levels of GADPH in the membrane fraction whereas the presence in the cytoplasmic fraction was reduced, suggesting that part of the cytoplasmic fraction may have been isolated with the membrane fraction. The presence of GAPDH in the nuclear fraction of day 16 samples also suggested a degree of contamination in this compartment.

Considering the above, sub-cellular localisation of CCND2 and p27 was determined. In day 4 ovaries, both CCND2 and p27 were found to be enriched in the cytoplasmic fraction whereas in day 16 ovaries, strongest presence in the membrane fraction was observed (probably due to cytoplasmic enrichment in this fraction).

Localisation of SMAD3 protein was also analysed. In day 4 ovaries, SMAD3 was relatively stronger in the nuclear fraction when compared to the cytoplasmic and membrane fraction. By comparison in day 16 ovaries, SMAD3 was also detected in the nuclear fraction, however, it was also observed with the same intensity as the membrane fraction.

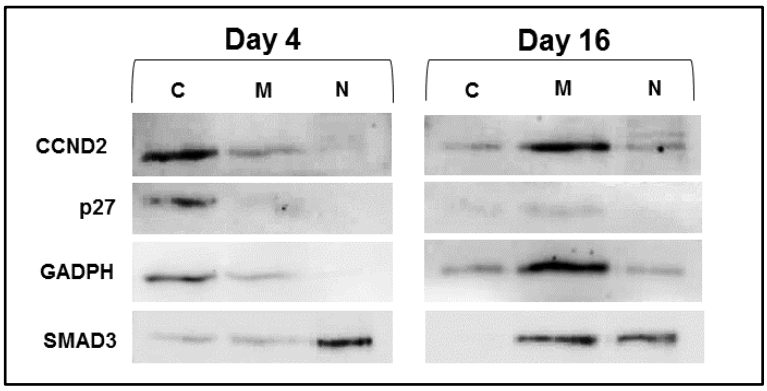

Figure 4.8. Subcellular fractionation of CCND2, p27, SMAD3 and GADPH proteins in mouse ovaries. Day 4 and day 16 ovaries were pooled and total protein lysates were separated by subcelullar fractionation as described in the methods. Cytoplasmic (C), membrane (M) and nuclear (N) fractions were then subjected to western blotting. Three and 4µg of total protein from day 4 and day 16 ovaries was used, respectively. A representative blot is shown for CCDN2, p27, and SMAD3. GADPH is shown as cytoplasmic marker.

4.4 Discussion

CCND2 and p27 have been shown in the image analysis in Chapter 3 to be expressed at high levels in GCs of primordial follicles. Since these factors are key regulators of the G0/G1 transition in the cell cycle and GCs from primordial follicles showed a slow proliferative phenotype, this chapter has aimed first to investigate whether CCND2/p27 system functions in the ovary to regulate GC proliferation in primordial follicles and secondly to determine the subcellular compartment where these proteins are most likely to create a complex in these follicles.

CCND2 and p27 co-localise in GCs of primordial follicles and co-localisation is lost when p27 is degraded in growing follicles

When CCND2 and p27 are co-stained, it was apparent that both proteins co-localise in the nuclei of GCs of primordial follicles. When the ratio of CCND2 and p27 intensities was measured in some individual GC nuclei, the primordial follicles usually showed similar and high levels of both proteins, suggesting non-proliferative GCs are most likely present in G0/early G1 phase. As soon as follicles start growing in the transitional stage, GCs start proliferating and p27 was reduced relative to CCND2, in some but not all cells. Immunolocalisation of proteins represents a snapshot of their localisation at the time the ovaries are fixed. Therefore, if GCs are not synchronised, it would be expected to observe a variable pattern of phase-specific proteins where some GCs are highly stained while others show no presence of the proteins. Therefore, the variation observed between GCs of growing follicles indicates that GCs are not synchronised: while some cells are still in G0 (high p27), others are in mid-late G1 phase (decreased p27 and high CCND2). In primary follicles, the amount of p27 is mostly reduced relative to CCND2 and in larger follicles with highly proliferative GCs (e.g secondary follicles), CCND2 and p27 do not co-localise. p27 is mostly absent in these follicles, suggesting it is downregulated or degraded. Although CCND2 is still present in small growing follicles, a decrease was observed in highly proliferative GCs from larger follicles.

These findings are supported with the results from chapter 3, where protein and mRNA levels for CCDN2 and p27 in day 16 ovaries (containing high proportions of large preantral follicles) are significantly decreased relative to day 4 ovaries (containing mainly primordial and transitional follicles).

CCND2 and p27 are in complex in primordial follicles

The previous results showed that CCND2 levels are highly present in the GCs with high p27 and therefore, it is likely that CCND2/K4-6/p27 complexes are present in GCs of primordial follicles. Since CCND2 is a binding partner of K4-6 and p27 facilitates CCND2/K4-6 assembly (Cheng et al, 1999), the results referring to CCND2/p27 complexes assume the presence of K4-6 protein. When the epithelial NIH3T3 cell line was used as a model, the CCND2/p27 complex was found in serum-starved conditions and was lost alongside the decrease in p27 expression, which was evident after 9 hours with serum. When CCND2/p27 complexes were compared between day 4 and day 16 ovaries, a stronger signal was detectable in day 4 ovaries compared to day 16 ovaries. This suggests that the GCs of primordial follicles contain CCND2/p27 complexes and that these complexes are lost in growing follicles.

Interestingly, the amount of p27 in complex with CCND2 was found to be the limiting step for the presence of the complex in both epithelial cells and ovary samples. When immunoprecipitation was performed with a p27 antibody, a high amount of CCND2 was found to be in complex. By comparison, when CCND2 was immunoprecipitated, only a limited amount of p27 was detectable. These findings suggest that a high amount of CCND2 is not present in complex with p27 (appendix 10). This p27-free CCND2 was detected in non-proliferative and proliferative epithelial cells (0 and 24h with serum) but also in both day 4 and day 16 ovary samples. Therefore, a fraction of non-catalytically active CCND2 exists in these follicles/ovaries. It is well-known that other cyclin kinase inhibitors (CKI) such as p15 can also bind to K4-6 and inhibit CCND2/K4-6 actions in G1 phase. In fact, SMAD3 has been reported to induce p15 gene, becoming one of the mechanisms by which TGFβ signalling allows cell growth arrest, as p15 binds to K4 therefore impeding CCND2/K4 catalytic activity in cell cycle progression (Warner et al, 1999). Interestingly, *p15* mRNA levels were also found to be highly expressed in day 4 ovaries compared to other ovary ages (appendix 9). Therefore, it is likely that other cell cycle inhibitors such as p15 also contribute towards maintaining inactive CCND2 levels in G0/G1 cells.

With the exception of few cells, a strong presence of CCND2 protein was generally observed in all GCs of primordial follicles. The levels of CCND2 in G0/G1 cells are tightly controlled transcriptionally and post-translationally in order to allow the G0/G1 transition when the cell has synthesised all the necessary factors to allow its proliferation (Foster et al, 2011). However, a mechanism to prevent the GCs to become activated at the same time should exist. This mechanism may implicate p27. It has been reported that although non-complexed CCND2 can be imported into the nucleus, the import of CCND2/K4-6 complexes is more enhanced by the assembly with p27 in the cytoplasm (Labaer et al, 1997). In the nucleus, phosphorylation of p27 determines whether the ternary complex is catalytic or non-catalytic (Nakayama, 2004). Non-catalytic complexes have been found in early G1 phase, where p27 confers stability to the ternary complex. The catalytic ternary complex appears more in late G1, and it releases Cyclin E from the inhibitions of p27, therefore allowing a more rapid G1/S transition (Nakayama, 2004). The presence of CCND2/p27 complexes were found in day 4 ovaries. Since most of their GCs in primordial follicles are not proliferative, it is likely that the CCND2/p27 complexes are mostly non-catalytic.

In *p27 -/-* mice, premature activation of primordial follicles was observed (Rajareddy et al, 2007). In cell lines were the p27 gene was deleted, the assembly and catalytic activity of CCND2/K4-6 complex was reduced (Cheng et al, 1999). Therefore, it seems that p27 is important to prevent over activation of primordial follicles. It can be then proposed that the balance between appropriate levels of CCND2 and the formation of non-catalytic CCND2/K4-6/p27 complexes determines the time that a non-proliferative GC re-enters the cell cycle after a change in the extracellular mitogen. Whether GCs with more association of inactive ternary complexes have the ability to maintain their G0/early G1 state for longer time that the GCs with less complexes remains unclear.

Subcellular localisation of p27 and CCND2 in the nucleus is not clear

When subcellular fractionation of whole protein extracts was performed in day 4 and day 16 ovary samples, both CCND2 and p27 proteins were not present in the nucleus, contrasting the immuno-localisation analysis of both proteins. The reduced amount of total protein used in the analysis is a limitation, as only abundant proteins in each fraction will be detected. Therefore, the absence of bands visualised with the western blot is not an indicative of a total absence of the protein in a particular fraction but is suggestive of low abundance.

However, although the immunofluorescence staining appears to be in the nucleus, it is possible that the location of these proteins is not exactly inside the nucleus, but instead is surrounding the nuclear membrane, where CCND2/K4-6/p27 complexes reside in a non-catalytic state (Wang et al, 2008). Although this possibility is consistent with the results in day 4 ovaries, where the CCND2/K4-6/p27 complexes in primordial follicles are non-catalytic, the clear localisation of CCND2 and p27 in the nucleus of GCs in immunostained ovary sections argues with their presence out of the nucleus. Therefore, a more detailed analysis of their localisation by specific markers of nuclear envelope such as lamin, may help clarify their localisation (Holaska et al, 2002).

Interestingly, SMAD3 was found in the nuclear fraction of day 4 ovaries, and supports the image analysis described in Chapter 3, where GCs of primordial follicles contain more nuclear presence of SMAD3. TFGβ signalling has been previously involved in cell cycle arrest via *Myc* repression in late G1 phase (Warner et al, 1999) and SMAD3 binding to Myc was observed in day 4 and day 16 ovaries in the previous chapter. However, SMAD3 binding to *Ccnd2* gene was also observed in these samples, where SMAD3 binding was higher in day 4 ovaries when compared to day 16 ovaries. Since CCND2/p27 complexes were also strongly detected in day 4 ovaries and increased levels of CCND2 have been proposed to regulate the formation of the complexes, it is likely that TGFβ signalling also contributes to the maintenance of CCND2/p27 complex dynamics though transcriptional regulation of *Ccnd2* expression (Figure 4.9).

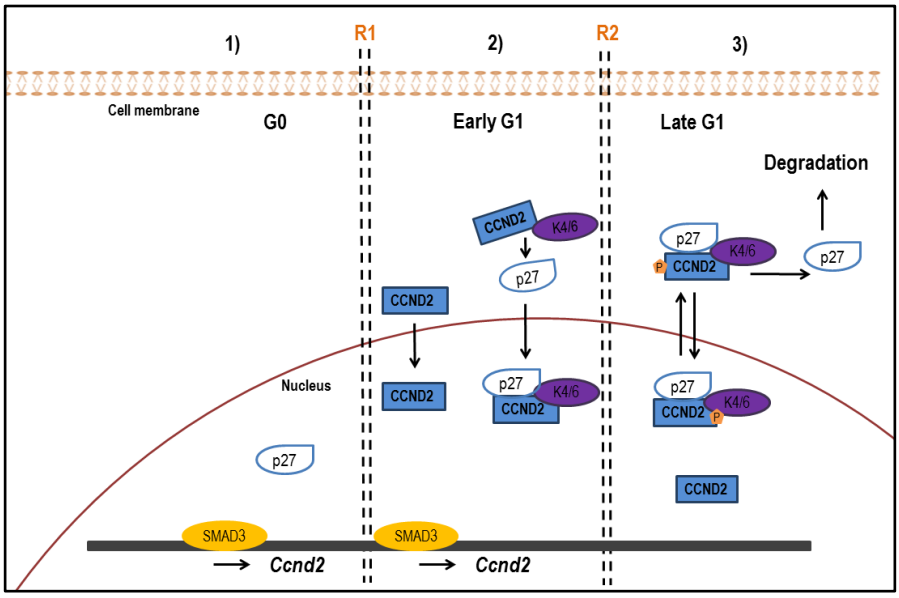

Figure 4.9. Model of CCND2/K4-6/p27 complex dynamics in non-proliferative GCs during G0/G1 phase. If levels of p27 protein in the nucleus are high, GCs are mainly present in G0 and *Ccnd2* gene expression levels are maintained transcriptionally by the binding of transcription factors such as SMAD3 (1). At early G1, an increase in CCND2 protein levels allows both CCND2 alone and the ternary complex CCND2/K4-6/p27 to translocate to the nucleus (2). If levels of CCND2 are still increasing, the ternary complex translocates out from the nucleus, where p27 is degraded allowing transition towards S phase and initiating GC proliferation and PFA (3).

In summary, the results obtained in this chapter have highlighted the following key findings:

- CCND2 and p27 proteins co-localise in GC nuclei of primordial follicles, where they are bound in a complex. This complex (probably non-catalytic) is reduced in GCs of growing follicles.
- CCND2 and p27 were detected in the cytoplasmic compartment of primordial and growing follicles, suggesting that the complex is being formed in this compartment rather than in the nucleus.
- SMAD3 protein was localised in the nuclear compartment of primordial and growing follicles, although it was relatively stronger in the nuclear fraction of primordial follicles, consistent with the findings in Chapter 3.

This chapter has shown evidence of the putative role of CCND2/p27 protein complexes as cell cycle regulators during GC proliferation in primordial follicles. Transcriptional regulation of these factors is essential for their complex formation (Foster et al, 2011). Since SMAD3 binding to *Ccnd2* gene was also detected in primordial follicles, the next chapter is focused on SMAD3 transcriptional regulation of *Ccdn2*, *Myc* and other candidate genes under different conditions of TGFβ signalling, and how this regulation finally relates to follicle activation and growth.

Chapter 5.

Functional role of TGFβ in primordial follicles: Cell cycle regulation and early follicle growth

5.1 Introduction

The mechanisms regulating the relative quiescence of the primordial follicle or conversely, its activation, still remain unclear. In the previous chapter, the TGFβ mediator SMAD3 was detected in the nuclear fraction of day 4 ovaries, supporting the results of Chapter 3, where SMAD3 was expressed in the nuclei of GCs of primordial follicles. These findings implicate SMAD3 as an essential transcription factor in these cells. In support of this, ChIP-PCR experiments revealed that SMAD3 bound to the promoter of *Myc* and *Ccnd2* genes in samples of day 4 ovaries, presumably repressing *Myc* and promoting *Ccnd2*. In other cell types, TGFβ inhibitory actions on cell proliferation have been reported through the repression of *Myc* gene during late G1 phase (Warner et al, 1999). During early G1 phase, direct regulation by TGFβ ligands has not been determined, however, the results in Chapter 3 and 4 revealed that high levels of CCND2 and CCND2/p27 complexes in GCs of primordial follicles are likely to be important for maintaining the non-proliferative state of GCs. Collectively, these findings suggest that TGFβ signaling is necessary to regulate *Myc* and *Ccnd2* levels in GCs of primordial follicles to control their proliferation.

It has been proposed that the TGFβ signaling switches from inhibitory to inducer of cell proliferation (and viceversa) and is related to the different repertoire of factors partnering with SMAD3 in the nucleus, creating alternative transcriptional complexes with different transcriptional activity (Massague, 2012). The identity of the different complexes, their mechanisms of gene regulation and the conditions that drive their formation (such as duration/dose of TGFβ ligand exposure) still remain under investigation, but are crucial to understand the reason why the same TGFβ ligands can trigger either growth arrest or cell proliferation.

Several studies using different exogenous TGFβ ligands in cultured ovaries of different species including human have reported both stimulation and inhibition of follicle development (Childs & Anderson, 2009; Ding et al, 2010; Rosairo D 2008; Telfer et al, 2008; Wang et al, 2014a; Zhao et al, 2001). However, it has been also demonstrated in cultured human cortical biopsies and cell line models that the length of exposure and dose of TGFβ ligand may provide a reasonable explanation for this apparent paradoxical effect of TGFβ signalling in follicle development (Ding et al, 2010; Zi et al, 2011).

Based on these findings and considering the "dual" role that TGFβ signaling has in growth arrest and induced cell proliferation in other models, **it is hypothesised that a brief exposure to increased TGFβ signaling may initiate a change in SMAD3 regulation of cell cycle genes that allows primordial follicles to activate.** Therefore, this chapter has the following aims:

- To study in detail whether SMAD3 induces or represses *Ccnd2* and *Myc* expression by comparing SMAD3 binding in primordial and growing follicles using ChIP-qPCR (binding) and qPCR (target gene expression) in biological replicates.
- To validate a neonatal mouse ovary culture as an *in vitro* model of primordial follicle activation to be used in the subsequent aims.
- To determine with the techniques above how SMAD3 binding and gene regulation changes with experimental modulation in TGFβ signaling using the *in vitro* model of cultured ovaries.
- To identify the activation of non-canonical TGFβ signaling mechanisms.
- To establish the relationship between the TGFβ-associated molecular events with follicle growth, using a quantitative morphological analysis of immunofluorecently labelled ovary sections.

5.2 Materials and Methods

5.2.1 Tissue collection

Ovaries from day 4 and 16 mice were dissected as described (see 2.2) and either placed in culture (day 4 only) or flash frozen in liquid nitrogen and stored at -80ºC for protein, RNA extraction and ChIP experiments.

5.2.2 ChIP-qPCR and qPCR of day 4 and day 16 mouse ovaries

Immunoprecipitation of fixed chromatin using a SMAD2/3 antibody (sc-133098; Santa Cruz) from day 4 and day 16 ovaries was performed as described (see 2.7.6) from five biological replicates (n=5) containing 2 ovaries/sample (day 4) and 1 ovary/sample (day 16). Quantitative PCR (qPCR) was used to quantify the amount of DNA bound to SMAD3 protein for the promoter regions of *Ccnd2* and *Myc* genes with specific primers (see Table 3.3) and the SensiFAST™ SYBR® Hi-ROX kit (Bioline) according to manufacturers' guidelines (see 2.7.6). Non-immune IgG antibody (sc-2025, Santa Cruz) was also used to determine the amount of non-specific binding. An equal volume of unknown concentration (4µl) of input, IP, IgG control or distilled water (negative control) was included in duplicate in 384 well-plates and the cycling conditions were set as follows: Activation step at 95°C for 3 minutes and then 40 cycles of amplification (3 seconds at 95°C for DNA denaturation, 20 seconds at 60°C for primer annealing and 10 seconds at 72°C for primer extension) in a 7900HT Fast Real-Time PCR System (Applied Biosystems). Fluorescence signals were collected after each cycle and also after a DNA melting/dissociation step to assess the identity of the products amplified. The analysis of the results was based on the % input method previously described (see 2.7.8).

5.2.3 PHM1 cultures

Although the main aim of this chapter is to evaluate the effects of modified TGFβ signalling in an ovary culture model, it was important first to determine if the reagents to be used are biologically active. For these preliminary optimisation experiments, the PHM1 cell line (derived from pregnant human myometrium) was used and maintained as described (see 2.2), since evidence of phosphorylaled SMAD3 was obtained in previous experiments.

In order to stimulate TGFβ signalling, the TGFβ1 ligand (R&D systems, 240-B-002) was chosen from all TGFβ ligands activating the canonical SMAD2/3 pathway, since it is widely used and has been previously associated with PFA (Rosairo D 2008; Wang et al, 2014b). To reduce TGFβ signalling, the small molecule inhibitor A 83-01 (MedChem Press, 2939) with specificity for the type I receptors ALK5, ALK4 and ALK7 was used to block SMAD2/3 phosphorylation (Joseph et al, 2014; Tojo et al, 2005). Based on results from a meta-analysis for TGFβ1 ligand (see appendix 11), a range between 5 and 10ng/ml was found for GC cultures and isolated follicle cultures whereas 10ng/ml was the most frequent dose for whole ovary cultures. Since short treatments in cell cultures may need lower amount of ligand than whole organ cultures for optimal stimulation, the amount of 10 ng/ml was considered appropriate for all experiments with neonatal ovary cultures. Therefore, no other concentration was optimized. With reference to the time of the treatments, two different early time points were used with 10 ng/ml of TGFβ1 ligand (30 min and 2 hours). By comparison, three different doses of A 83-01 (0.1 μM, 1μM and 10 μM) were tested to assess TGFβ signalling inhibition. A 83-01 inhibitor showed no major p-SMAD3 inhibition in basal conditions at different time points (appendix 12). Therefore, based on the findings from previous reports (Tojo et al, 2005; Yamamura et al, 2012), the 30 minutes time point was chosen to optimise the three different doses of A 83-01 inhibitor (0.1 μM, 1μM and 10 μM). To assess inhibitor specificity for the receptor, TGFβ1 ligand was added to some wells after the incubation with A 83-01 inhibitor. Protein extraction was performed and 20μg were used for western blotting as previously described (see 2.5.2 and 2.5.5, respectively) with antibodies against p-SMAD3 (ab52903, Abcam) (see Table 2.1).

5.2.4 Neonatal ovary cultures

Effect of culture conditions in the molecular biology of the ovary

Preliminary experiments to assess the viability and protein expression pattern in neonatal (day 4) ovaries were performed under serum and serum-free conditions. For this, ovaries were cultured (using the culture conditions described in 2.3) in serum-free medium (without FBS) for one and three days. Two ovaries were used for each time point and the largest section per ovary (two ovary sections per time point, n=2) was used for immunofluorescence staining with specific antibodies for CCND2 (sc-593; Santa Cruz),

SMAD2/3 (sc-133098; Santa Cruz) and anti-CASPASE3 (#9664; Cell Signalling) as explained (see 2.4.2).

In addition, the effect of serum on pathway activation was also analysed in ovaries cultured during 2, 4, 6 and 24 hours in culture medium with or without 10% FBS. Two ovaries/sample were used for protein extraction and 15µg were used for western blotting with antibodies against p-SMAD3 (ab52903, Abcam) and p-AKT (#4060, Cell Signalling) as described previously (see Table 2.1). One sample per time point and treatment was used for this experiment (n=1).

Optimisation of the time point for short increased and decreased TGFβ signalling

Based on the results obtained with PHM1 cells, 10ng/ml of TGFβ1 ligand and 1µM of A 83-01 inhibitor were chosen for neonatal ovary cultures. However, a preliminary experiment was used to further optimize the time points for the treatments. Day 4 ovaries were cultured and exposed to TGFβ1 ligand during two different time points (30 minutes and 2 hours) to detect the best time for maximum SMAD3 phosphorylation. The same time points were used for A 83-01 inhibitor alone. Moreover, the specificity of A 83-01 inhibitor to the TGFβ receptor I was also assessed by adding TGFβ1 (for 30 minutes and 2 hours) to two wells previously supplemented with A83-01 for 30 minutes. Protein extraction from samples containing 2 ovaries was performed and 15µg were used for western blotting as previously described (see 2.5.2 and 2.5.5, respectively) with antibodies against p-SMAD3 (ab52903, Abcam) (see Table 2.1). Only one sample per time point and treatment was used for this experiment (n=1).

Experimental design to evaluate molecular and morphological changes after treatments

Based on the results obtained from the preliminary experiments described above (see 5.2.4), ovaries were cultured for 24 hours in media containing 10% FBS and treatments were added to the ovaries in fresh serum-free media as indicated on the timeline in Figure 5.1. A single time point (2 hours) and concentration for TGFβ1 ligand (10ng/ml) and A 83-01 inhibitor (1µM) were selected.

For the assessment of the molecular changes under different TGFβ conditions (SMAD3 binding and gene regulation) cultured ovaries were classified in four groups: Control, TGFβ1 ligand, A 83-01 and A 83-01 + TGFβ1 ligand, according to the layout shown in Figure 5.1A and treated for 2 hours. Ovaries were collected (after 2 hours) and either

fixed and processed for ChIP-qPCR (see 2.7.1) or flash frozen in liquid nitrogen for gene expression analysis (see 2.8.1).

For the assessment of the phenotypical changes (effect on follicle activation and growth) under different TGFβ conditions, cultured ovaries were classified as unstimulated (control), stimulated with TGFβ1 ligand and A 83-01 inhibitor alone (Figure 5.1) and treated for 2 hours. In the TGFβ1 treatment group, the addition of A 83-01 inhibitor for an extra 1 hour was used to block further TGFβ1 signalling as previously described (Clarke et al, 2009). After treatments, ovaries were left in culture for two additional days and collected after a total culture time of 72 hours. After this time, ovaries were collected, fixed in formalin and replaced next day with 70% ethanol until paraffin embedded. Six ovary sections (n=6) from 4 ovaries were used per treatment group in this experiment. Immunofluorescence staining with antibodies against DDX4 (ab13840, Abcam) and Smad3 (#9523, Cell Signalling) was performed as described previously (see 2.4.2). Image analysis of immunostained sections was performed with image J by counting and measuring the oocyte area of follicles with a clear and visible outline of the oocyte nucleus (Figure 5.1B). When more than one section from the same ovary was used, a minimum span of 2 sections (10µm) from the largest cross-section was considered to avoid double counting, Follicles were staged using the mean oocyte area as determined in Chapter 3 (see Figure 3.6) as follows: Primordial (0-200µm^2), transitional (200-400µm^2), small primary (400-800µm^2) and large primary (>800µm^2). The proportion of the different follicle stages was also calculated for each treatment group. An additional morphological analysis by GC number of all classified follicles was also performed to validate the follicle stage classification.

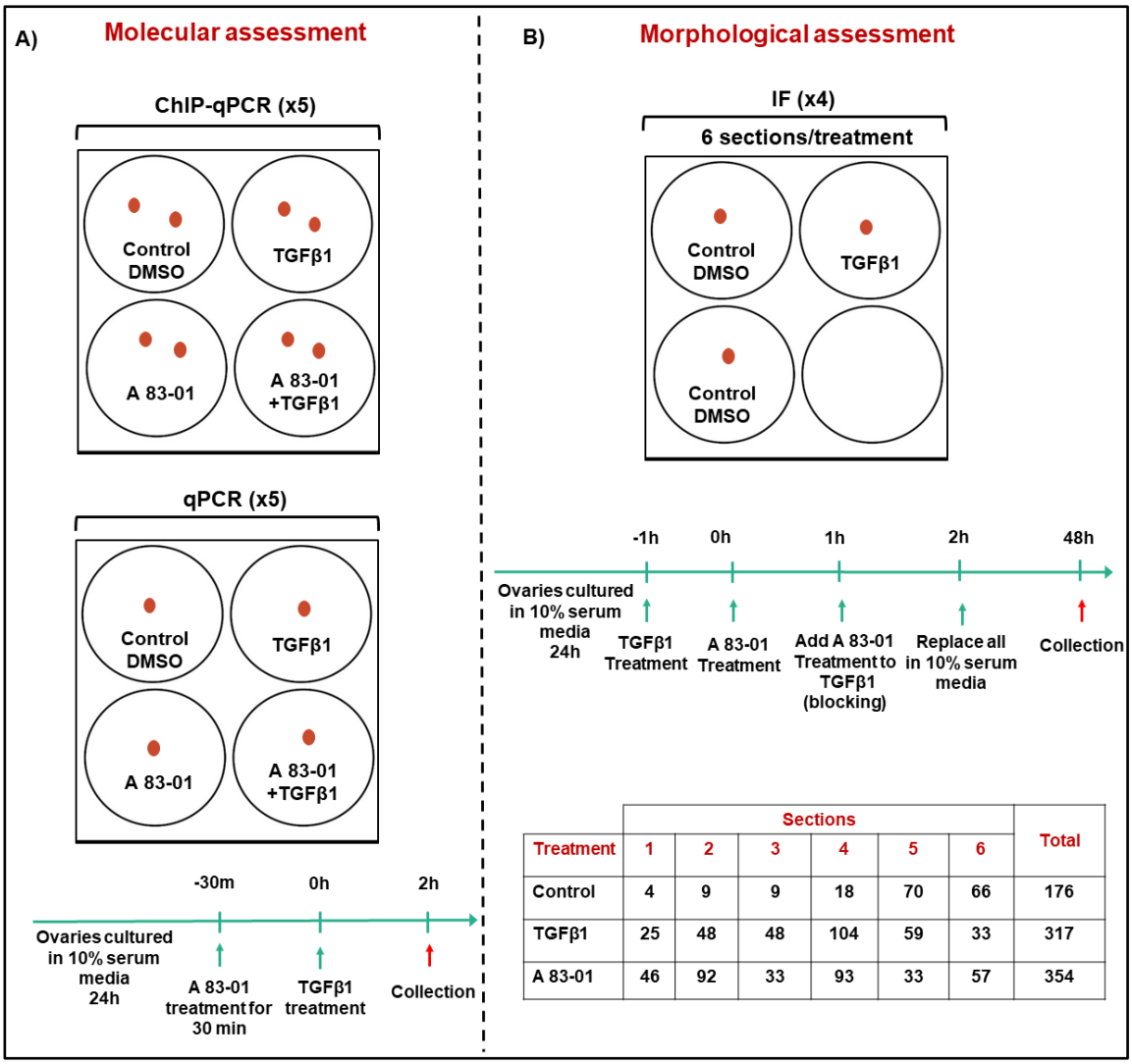

Treatment	Sections						Total
	1	2	3	4	5	6	
Control	4	9	9	18	70	66	176
TGFβ1	25	48	48	104	59	33	317
A 83-01	46	92	33	93	33	57	354

Figure 5.1. Layout of the experimental design with whole neonatal ovary culture. A) For ChIP-qPCR experiments, five samples per treatment (two ovaries per sample) were used (n=5). For qPCR, five samples per treatment (one ovary in each sample) were used (n=5). B) For morphological assessment with immunofluorescence staining (IF), six large cross-sections per treatment (obtained from four ovaries) were used (n=6). Total number of follicles counted per section and treatment are shown in the table. Timeline with treatments (green arrows) and collection of ovaries (red arrows) is also shown at the specified time points.

Gene expression analysis: qPCR

RNA was extracted from 1 ovary/sample as described previously (see 2.8.1). All samples were concentrated by vacuum centrifugation for 4 minutes at 23 degrees before evaluating quality and concentration using the Agilent 2100 Bioanalyser (Appendix 4, B). First strand DNA (cDNA) synthesis was performed followed by conventional PCR (see 2.8.2) with primers for the housekeeping gene *Htrp1* to confirm that the cDNA samples were of sufficient quality to use for qPCR (Appendix 5, B). Quantitative PCR was performed to study the effect of the different treatments on the gene expression of *Smad2*, *Smad3*, *Foxl2*, *p27*, *Myc* and *Ccnd2*. The TGFβ inhibitor *Smad7*, an intracellular regulator of SMAD signalling (Itóh et al, 1998) and *Gdf9,* a gene expressed specifically in growing oocytes (Dong et al, 1996), were also used as controls for TGFβ signalling activation and PFA, respectively (Table 5.1). SensiFAST™ SYBR® Hi-ROX kit (Bioline) was used and cycling conditions were the same as described above (see 5.2.2). Samples (1µl per reaction) and negative control with distilled water were also run in duplicate in a 384 well-plate. Ct values were normalised against the endogenous gene *Atpb5* (PrimerDesign, Southampton, UK) and fold changes relative to the control group were calculated for each gene according to the $2^{-\Delta\Delta Ct}$ method (see 2.8.3).

Primer set	Sequence (5'→ 3')	bp	Primer efficiency (%)
Smad3	F: GTCAAAGAACACCGATTCCA R: TCAAGCCACCAGAACAGAAG	154	91
Smad2	F: CGTCCATCTTGCCATTCAC R: GTCCATTCTGCTCTCCACCA	102	113
Foxl2	F: TCATAGCCAAGTTCCCGTTCTA R:GTAGTTGCCCTTCTCGAACATG	179	89
Myc	F: AAATCCTGTACCTGGTCCGATT R:CCACAGACACCACATCAATTTCT	184	104
Ccnd2	F: CTTGTAGCCCATTCAGACACAG R:TATCATCCACGTGTGCTGTAGA	165	93
p27	F: AGTCAGCGCAAGTGGAATTT R: AGTAGAACTCGGGCAAGCTG	100	130
Smad7	F: AGTCAAGAGGCTGTGTTGCTGT R: CATTGGGTATCTGGAGTAAGGA	130	-
Gdf9	F:TCACCTCTACAATACCGTCCGG R:GAGCAAGTGTTCCATGGCAGTC	139	-
Htrp1	F: GTTGTTGGATATGCCCTTGAC R: GCGCTCATCTTAGGCTTTGTA	105	-

Table 5.1. Primers sequences, amplification product sizes (bp) and primer efficiency (%) for qPCR assays.

ChIP-qPCR analysis

Sheared chromatin from 2 ovaries/sample was isolated as explained previously (see 2.7.1). All samples were analysed with 1.5% agarose gel electrophoresis to visualise fragment size range (Appendix 6). Quantitative PCR was used to quantify the amount of SMAD3 binding to *Ccnd2* and *Myc* genes in the different groups. PCR conditions were as previously described (see 4.2.3) and primers used were Ccnd2.1 and Myc.3 (see table 3.2). The analysis of the results was based on the % input method described in the methods (see 2.7.8).

Western blotting

In order to study the activation of canonical and non-canonical signalling pathways after the treatments, samples containing 2 ovaries/sample (n=1) were used for protein extraction and 15µg of total protein were used for western blotting as previously described (see 2.5.2 and 2.5.5, respectively). Antibodies against p-SMAD3 (ab52903, Abcam) (canonical activation), p-ERK1/2 (#4370, Cell Signalling) and p-AKT (#4060, Cell Signalling) (non-canonical activation of MAPK and PI3K signalling pathways, respectively) were used (see Table 2.1).

5.2.5 Statistical analysis

To compare the central tendency between groups from the ChIP-qPCR data, non-parametric tests were used. In day 4 and day 16 ovaries, a Mann-Whitney U test was performed to compare the differences in % input between the two groups. To compare the differences in % input between the four different treatments in cultured ovaries, a Kruskal-Wallis test with post-hoc Dunn's multiple comparisons was used. For qPCR analysis of day 4, 8 and 16 ovaries and the four different treatment groups in cultured ovaries, means were compared between groups by one-way ANOVA with Bonferroni multiple comparisons post-hoc test. To compare the central tendency of oocyte areas measured for the different treatments in cultured ovary sections, a Kruskal-Wallis test with post-hoc Dunn's multiple comparisons was used. Finally, significant differences in the mean number of multi-oocyte follicles (MOFs) between the three treatment groups were compared by one-way ANOVA with Bonferroni multiple comparisons post-hoc test. Graphpad Prism 7.03 was used to calculate and represent the data and differences were considered statistically significant when $P < 0.05$.

5.3 Results

5.3.1 SMAD3 binding to *Ccnd2* and *Myc* genes in day 4 and day 16 ovaries

In order to quantify the amount of SMAD3 binding to *Ccnd2* and *Myc* target genes *in vivo*, biological replicates of day 4 and day 16 ovary samples (n=5) were used and qPCR was performed instead of standard PCR (as presented in Chapter 3). The results obtained showed significant increased binding of SMAD3 to both target genes in day 4 ovaries when compared to IgG control ($P<0.05$). For Myc, SMAD3 binding in 16 ovaries was not significant when compared to IgG control whereas for *Ccnd2* gene, significant differences in day 16 ovaries were observed when compared to IgG control ($P<0.05$) (Figure 5.2A). When the amount of SMAD3 binding was compared between day 4 and day 16 samples, no significant increased binding in day 4 ovaries was detected for *Myc* or *Ccnd2* (Figure 5.2 B). However, more day 4 ovary samples contained medium and high SMAD3 binding for both *Myc* and *Ccnd2* genes compared to day 16 ovaries, which was reduced for both genes (Figure 5.2B).

In order to determine whether SMAD3 is a repressor or an activator of the genes in primordial follicles, qPCR was used to measure *Ccnd2* and *Myc* mRNA expression in day 4, 8 and 16 ovaries (Figure 5.2 C). Results showed a significant increase in *Myc* gene expression in day 8 and day 16 ovaries relative to day 4 ovaries ($P<0.01$ and $P<0.001$, respectively), whereas *Ccnd2* was decreased in day 16 ovaries relative to day 4 ($P<0.01$).

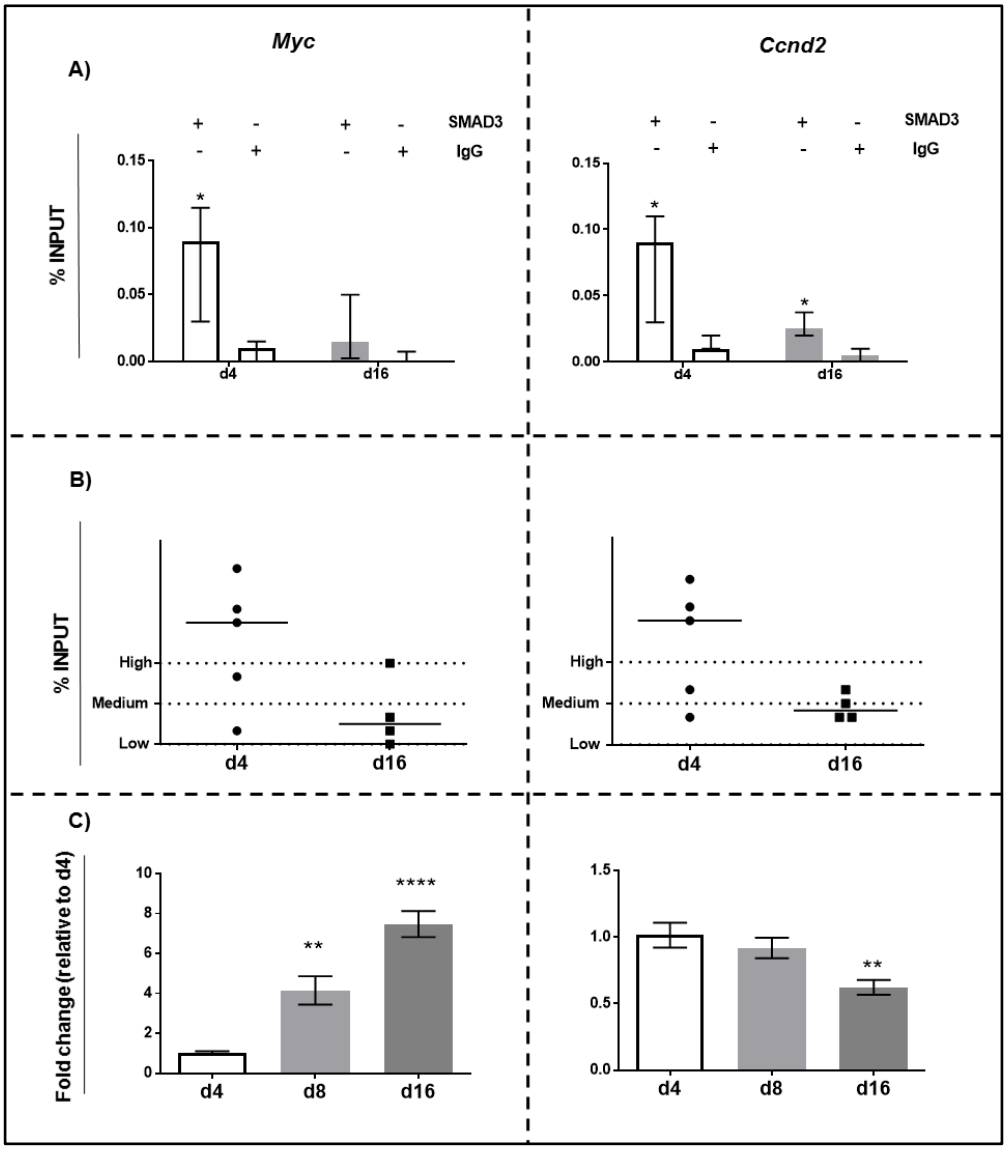

Figure 5.2. **ChIP-qPCR with SMAD3 antibody and qPCR data in juvenile mouse ovaries.** A) shows qPCR amplification of *Myc* and *Ccnd2* gene promoters in day 4 and day 16 ovaries after ChIP with SMAD3 and non-immune IgG antibodies. % input was calculated using the "% input" method. Each group contained 5 samples (n=5). Data are medians ± interquartile range and statistical differences are relative to IgG control (*P<0.05). B) represents the % input of SMAD3-ChIP samples categorised as low (≤0.03), medium (0.03-0.06) and high (≥0.06) and medians plotted. C) shows transcript levels determined by qPCR and normalised against the endogenous reference *Atpb5*. Fold changes were calculated relative day 4 using the $2^{-\Delta\Delta Ct}$ method as described in the methods. Each group contained 5 samples (n=5). Data are means ± SEM and statistical differences are relative to day 4 (*P<0.05, **P<0.01, ****P<0.0001).

5.3.2 Optimisation and validation of TGFβ1 ligand and A3-801 inhibitor in PHM1 cells

TGFβ1 ligand

PHM1 cells were cultured in 6-well plates and 10 ng/ml of TGFβ1 ligand was used to study SMAD3 phosphorylation at 30 minutes and 2 hours (Figure 5.3). The earliest time point (30 minutes) showed higher SMAD3 phosphorylation and was therefore used for the optimisation of the concentration of the A 83-01 inhibitor.

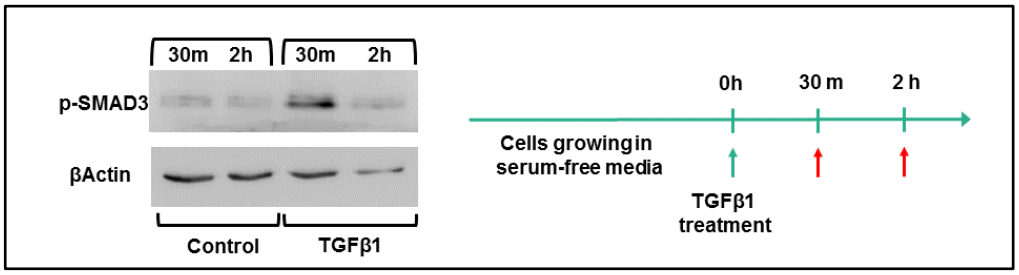

Figure 5.3. Western blot showing SMAD3 phosphorylation in PHM1 cells treated with TGFβ1. PHM1 cells were grown in serum free media and were exposed for 30 minutes or 2 hours in the presence or absence of 10ng/ml TGFβ1. Cells were collected at these time points and protein extracts (20µg) were assayed for p-SMAD3 by western blotting. Beta actin is shown as a loading control. Data was obtained from 1 sample from each group (n=1). Timeline with treatments (green arrow) and collection of cells (red arrows) is shown at the specified time points.

A 83-01 inhibitor

To determine the minimal amount of A3-801 inhibitor that can be used to block the TGFβ receptor and prevent TGFβ signalling, three different doses of inhibitor were used alone (0.1, 1 and 10µM) and with additional incubation with TGFβ1 ligand for 30 minutes. The amount of SMAD3 phosphorylation was used to assess the amount of TGFβ pathway inhibition after 30 minutes (Figure 5.4). All time points maintained the amount of phosphorylated SMAD3 under basal conditions even after the addition of TGFβ1 ligand, with the exception of the lowest concentration (0.1µM), which showed a slight increase after ligand addition (Figure 5.4). Based on these experiments in PHM1 cells, a concentration of 1µM of the A 83-01 inhibitor was considered for the neonatal ovary cultures.

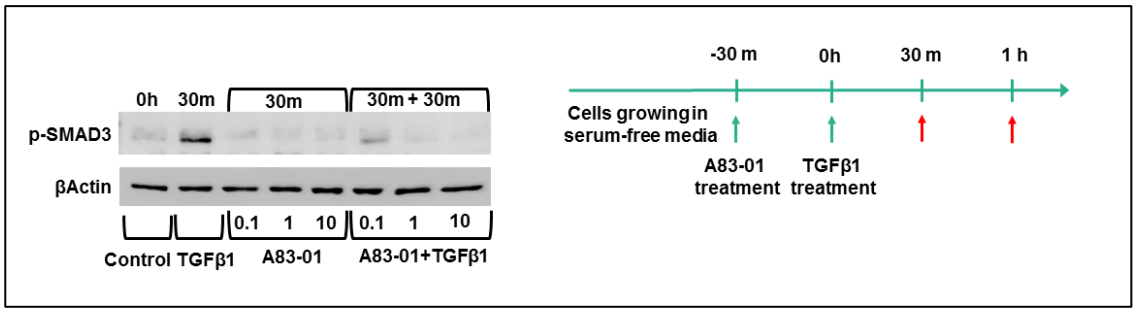

Figure 5.4. **Western Blot showing SMAD3 phosphorylation in PHM1 cells treated with A 83-01 inhibitor.** PHM1 cells were exposed for 30 minutes to 10ng/ml of TGFβ1 ligand and for 30 minutes to 0.1µM, 1µM and 10 µM of A83-01 inhibitor. Samples were collected at these time points and protein extracts (20µg) were assayed for p-SMAD3 by western blotting. Beta actin is shown as a loading control. Control with DMSO was also included. Data was obtained from 1 sample from each group (n=1). Timeline with treatments (green arrows) and collection of cells (red arrow) is shown.

5.3.3 Effect of A 83-01 and TGFβ1 on cultured neonatal mouse ovaries.

Morphological evaluation of cultured ovaries and protein expression pattern under serum-free conditions

Immunofluorescent staining of day 4 ovaries cultured during one and three days in serum-free conditions was performed in order to determine the effects of the *in vitro* environment on the normal protein expression of CCND2 and SMAD2/3 in small follicles. The staining pattern for both of these proteins was retained (Figure 5.5), suggesting that the culture system does not have an observable impact on the molecular biology and normal function of the ovaries, making its use suitable for functional studies.

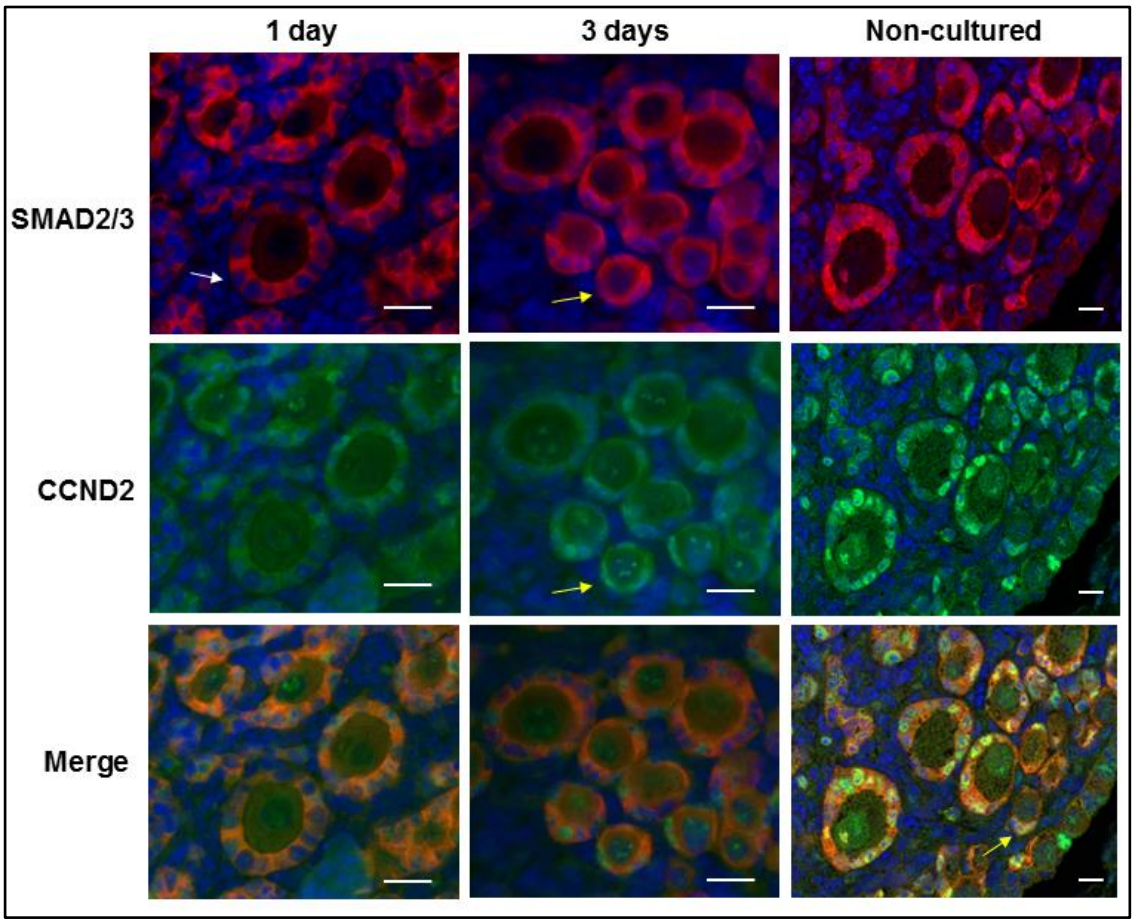

Figure 5.5. Expression of CCDN2 and SMAD2/3 in the mouse ovary after culture. Day 4 cultured ovaries in serum-free conditions for one and three days were immunofluorescently stained for SMAD2/3 (red) and CCND2 (green) and compared with non-cultured ovaries. Nuclear staining is evident in GCs of primordial follicles for both proteins (yellow arrows) while growing follicles (white arrow) show cytoplasmic SMAD2/3 in GCs. Merge of channels show co-localisation of both proteins in primordial follicles. Nuclei are counterstained blue with DAPI. Cultured ovaries were imaged with an inverted fluorescence microscope Olympus IX73 at magnification 60X while non-cultured ovary sections were obtained with an inverted Leica SP5 confocal laser-scanning microscope at magnification 63X. Scale bar is 20µm.

In addition, viability under serum-free conditions was assessed with anti-active Caspase3 staining. A limited amount of apoptosis was observed in stromal cells and some GCs from primary follicles but not in primordials (Figure 5.6).

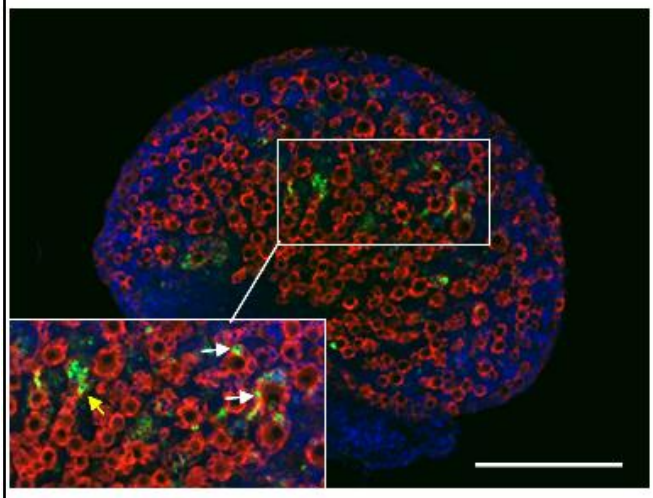

Figure 5.6. Expression of Caspase 3 and SMAD2/3 in the mouse ovary after culture. Day 4 cultured ovaries in serum-free conditions during one day were immunofluorescently stained for SMAD2/3 (red) and CASPASE 3 (green) Apoptosic GCs are observed in primary follicles (white arrows), and the surrounding stromal cells (yellow arrow). Scale bar is 200μm and magnification is 20X.

Effect of serum on SMAD3 and AKT phosphorylation in cultured neonatal ovaries

In order to study the effect of serum on SMAD3 and AKT phosphorylation, day 4 ovaries were cultured for 24 hours under serum-free conditions and after this time, serum was added to some wells and ovaries were collected after different time points. No differences were observed in phosphorylation levels of SMAD3 and AKT at any time point between serum and serum-free conditions (Figure 5.7A). Phosphorylation levels of SMAD3 were also studied after treatment for 24 hours in serum conditions, where no differences were observed when compared to 6 hours and control treatment groups. These findings suggest that serum does not have a major influence on TGFβ and PI3K signalling pathways in this culture model. Thus, it was decided that the inclusion of serum to support long-term cultures may be more beneficial and will be used in all experiments for consistency.

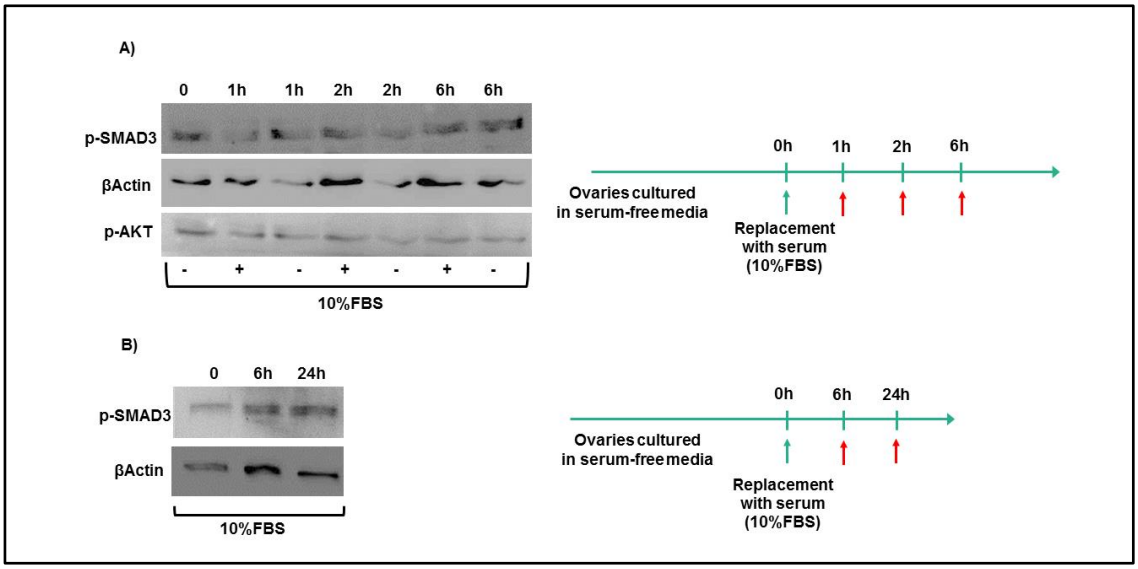

Figure 5.7. Western Blot showing SMAD3 and AKT phosphorylation in the mouse ovary after culture. Day 4 ovaries were cultured in either 10%FBS or serum-free conditions at different times**.** In A) ovaries were collected at these time points and protein samples (15µg) were assayed for p-SMAD3 and p-AKT by western blotting. In B) ovaries were left for 24 hours with 10%FBS and assayed for p-SMAD3 only. Beta actin is shown as a loading control. Data was obtained from 1 sample from each group (n=1). Timeline with treatments (blue arrow) and collection of ovaries (red arrows) is shown.

Time point optimisation of A 83-01 and TGFβ1 treatments in neonatal ovary cultures

Since no effect on SMAD3 phosphorylation was observed in ovaries cultured under serum-free or serum (10% FBS), ovaries were allowed to settle in the culture plates for 24 hours with 10% FBS prior to supplementation with either TGFβ1 ligand or A 83-01 inhibitor. Phosphorylated SMAD3 levels did not appear to differ from control levels after 30 minutes with exogenous TGFβ1. By 2h, p-SMAD3 levels were elevated in TGFβ1 treated ovaries. When ovaries were supplemented with A83-01, p-SMAD3 were reduced after 2 hours, even after addition of TGFβ1, indicating that A 83-01 inhibits and impedes canonical TGFβ stimulation with TGFβ1. Based on these findings, 2 hours was considered sufficient time to either stimulate or inhibit canonical TGFβ signalling and was therefore applied in the next experiments (Figure 5.8).

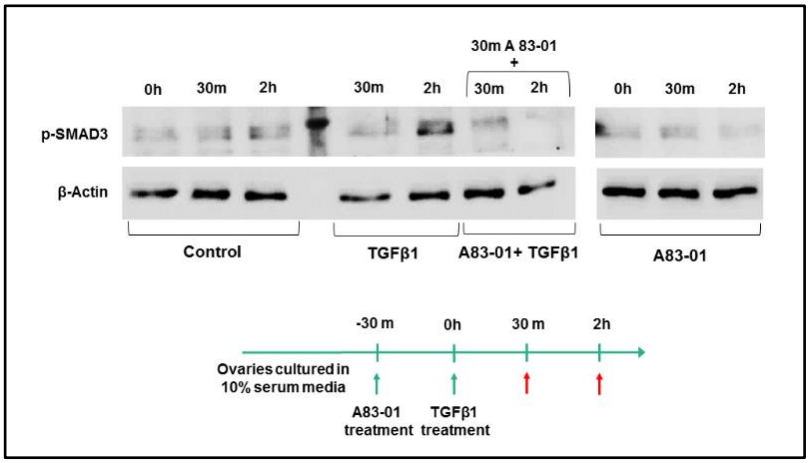

Figure 5.8. Western Blot showing SMAD3 phosphorylation in culture ovaries treated with TGFβ1 ligand and A83-01 inhibitor. Ovaries were treated for 30 minutes and 2 hours with 10ng/ml of TGFβ1 ligand and 1μM A83-01 inhibitor alone and 30 minutes with 1μM A83-01 inhibitor followed by 30 minutes and 2 hours with 10ng/ml TGFβ1. A control with 1 μM DMSO for 30 minutes and 2 hours was also included. Ovaries were collected at these time points and protein extracts (15μg) were assayed for p-SMAD3 by western blotting. Beta actin is shown as a loading control. Data was obtained from 1 sample from each group (n=1). Timeline with treatments (green arrows) and collection of ovaries (red arrow) is shown.

5.3.4 Effect of TGFβ1 ligand and A 83-01 inhibitor on day 4 cultured neonatal mouse ovaries

SMAD3 binding to Ccnd2 and Myc genes

When SMAD3 binding to *Myc* was compared with the IgG control for all treatments, only SMAD3 binding in the control group was significantly increased ($P<0.05$), whereas the treatment with TGFβ1 ligand and A 83-01 inhibitor (alone or with TGFβ1) did not significantly increase SMAD3 binding (relative to IgG control) (Figure 5.9). When SMAD3 binding to *Myc* was compared between treatments, no significant differences were detected. However, more samples containing high and medium SMAD3 binding to *Myc* were observed in the control and TGFβ1 ligand groups in comparison with the low SMAD3 binding observed in the A 83-01 Inhibitor groups (Figure 5.9). When steady state mRNA expression levels of *Myc* gene were compared between the treatment groups, a significant increase in transcript levels were detected with the TGFβ1 treatment group when compared to control and A 83-01 treated groups ($P<0.05$). No significant differences were observed in A 83-01 inhibitor-treated groups when compared to control (Figure 5.9).

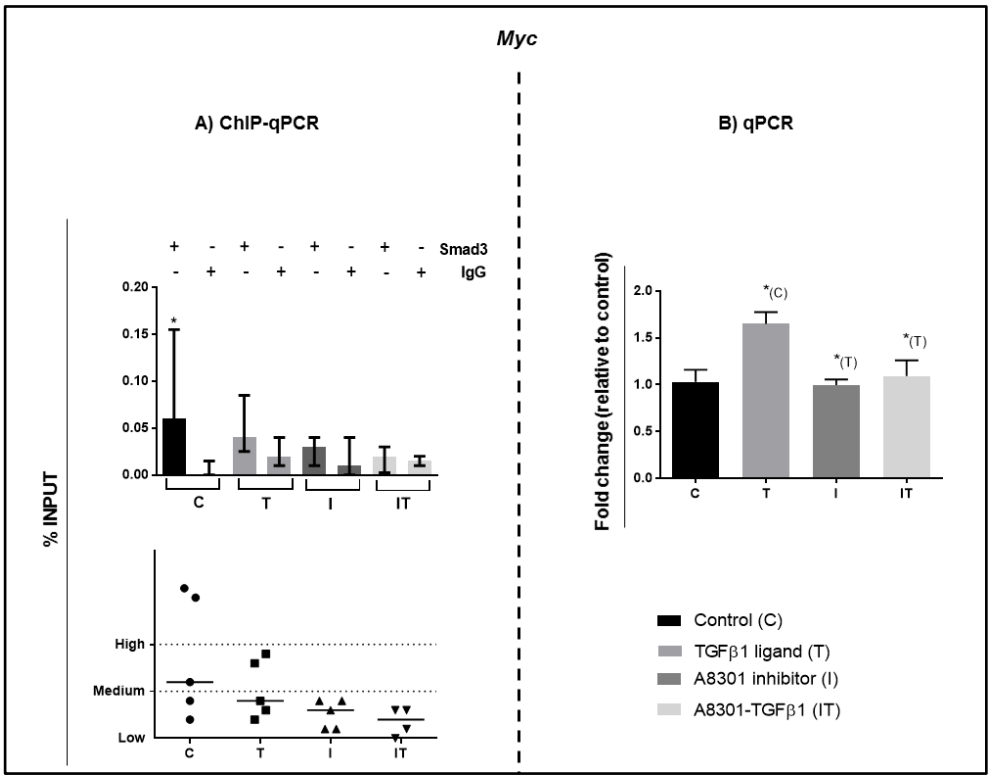

Figure 5.9. **ChIP-qPCR with SMAD3 antibody and qPCR data for *Myc* gene in neonatal mouse ovaries after culture.** Ovaries were treated with 10ng/ml of TGFβ1 ligand, 1 μM A83-01 inhibitor, 1μM A83-01 inhibitor followed by 10ng/ml TGFβ1 and non-treated (control). Upper panel in A) shows qPCR amplification of *Myc* gene promoter after ChIP with SMAD3 and non-immune IgG antibodies. Lower panel represents the % input of ChIP samples categorised as low (≤0.05), medium (0.05-0.010) and high (≥0.10). % input was calculated using the "% input" method described in the methods. Each group contained 5 samples (n=5). Data are medians ± interquartile range and differences are relative to IgG control (*P<0.05). B) shows transcript levels determined by qPCR and normalised against the endogenous reference *Atpb5*. Fold changes were calculated relative to control (non-treated) group using the $2^{-\Delta\Delta Ct}$ method as described in the methods. Each group contained 5 samples (n=5). Data are means ± SEM and differences are relative to the treatment group in parentheses (*P<0.05). C, control; T, TGFβ1 ligand; I, A83-01 inhibitor; IT, A83-01 inhibitor + TGFβ1 ligand.

By comparison, when SMAD3 binding to *Ccnd2* was compared with the IgG control for all treatments, SMAD3 binding in the control group was significantly increased (P<0.01) while the treatment with TGFβ1 ligand and A 83-01 inhibitor (alone or with TGFβ1) did not significantly increase SMAD3 binding relative to IgG control (Figure 5.10). When SMAD3 binding to *Ccnd2* was compared between treatments, no significant differences were detected and SMAD3 binding was generally low (Figure 5.10).

However, medium and high values were observed in control and TGFβ1 treatment groups, while all samples in the A 83-01 inhibitor groups contained low SMAD3 binding values (Figure 5.10). When steady state mRNA expression levels of *Ccnd2* gene were compared between the treatment groups, a significant increase in transcript levels were detected with the TGFβ1 treatment group when compared only to A 83-01 treated group (inhibitor alone) ($P<0.05$). No significant differences were observed in A 83-01 inhibitor-treated groups when compared to control (Figure 5.10).

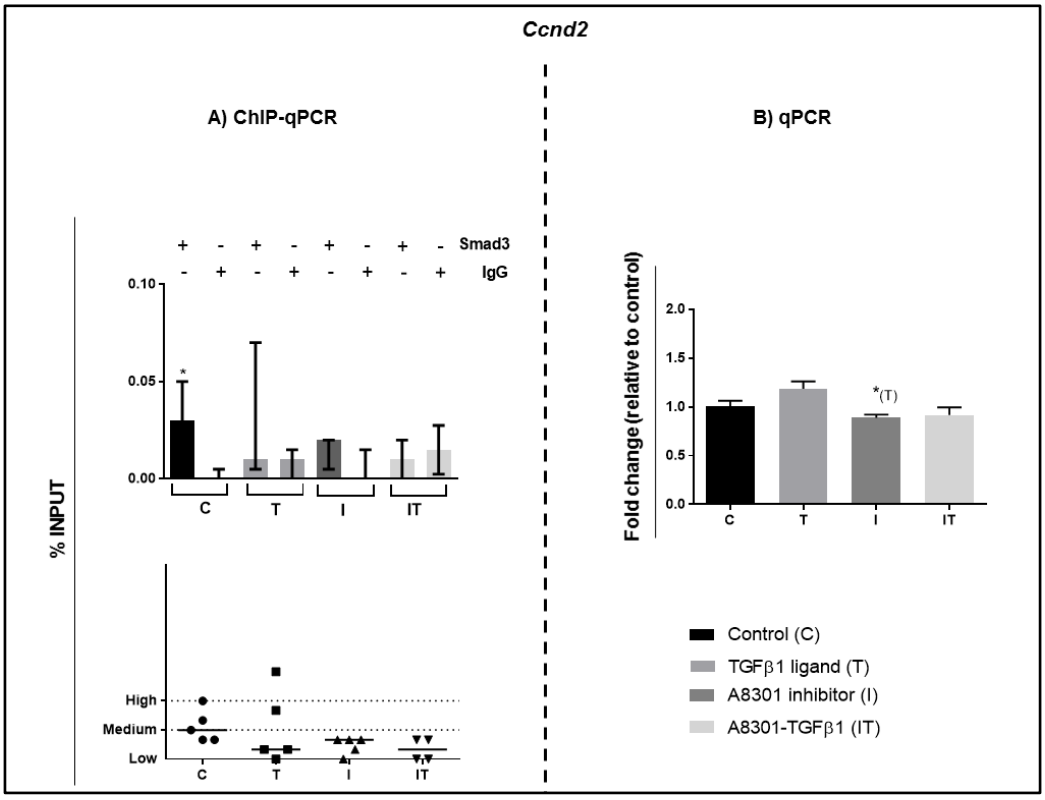

Figure 5.10. **ChIP-qPCR with SMAD3 antibody and qPCR data for *Ccnd2* gene in neonatal mouse ovaries after culture.** Ovaries were treated with 10ng/ml of TGFβ1 ligand, 1 μM A83-01 inhibitor, 1μM A83-01 inhibitor followed by 10ng/ml TGFβ1 and non-treated (control). Upper panel in A) shows qPCR amplification of *Ccnd2* gene promoter after ChIP with SMAD3 and non-immune IgG antibodies. Lower panel represents the % input of ChIP samples categorised as low (≤0.03), medium (0.03-0.06) and high (≥0.06). % input was calculated using the "% input" method described in the methods. Each group contained 5 samples (n=5). Data are medians ± interquartile range and differences are relative to IgG control (*$P<0.05$). B) shows transcript levels determined by qPCR and normalised against the endogenous reference *Atpb5*. Fold changes were calculated relative to control (non-treated) group using the $2^{-\Delta\Delta Ct}$ method as described in the methods. Each group contained 5 samples (n=5). Data are means ± SEM and differences are relative to the treatment group in parentheses (*$P<0.05$). C, control; T, TGFβ1 ligand; I, A83-01 inhibitor; IT, A83-01 inhibitor + TGFβ1 ligand.

Effect of TGFβ1 and A83-01 on expression of TGFβ factors and cell cycle genes

Steady state mRNA levels of *Smad3, Foxl2, Smad2, p27 and Gdf9* remained unchanged between control and treatment groups. By comparison, mRNA levels of the early response TGFβ inhibitor *Smad7* were significantly increased with TGFβ1 treatment relative to all other groups (P<0.0001) (Figure 5.11).

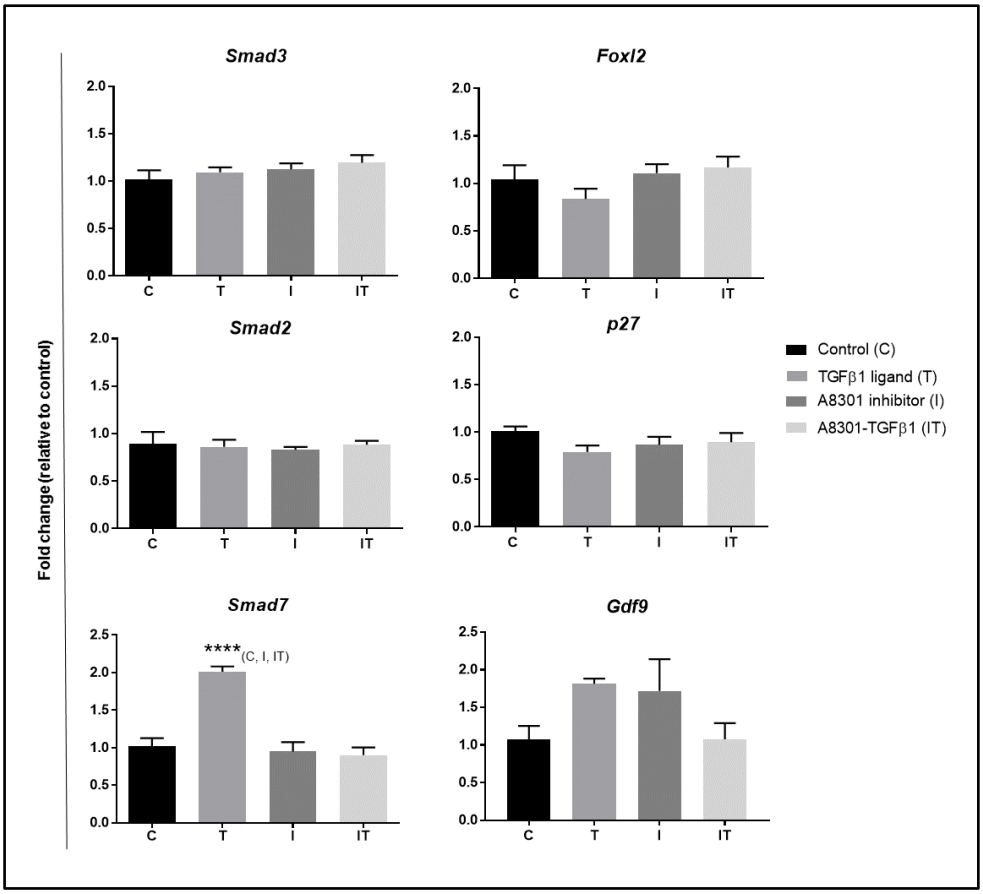

Figure 5.11. Expression of candidate TGFβ and cell cycle gene transcripts in neonatal mouse ovaries after culture. Ovaries were treated with 10ng/ml of TGFβ1 ligand, 1 μM A83-01 inhibitor, 1μM A83-01 inhibitor followed by 10ng/ml TGFβ1 and non-treated (control). Transcript levels were determined by quantitative PCR and were normalised against the endogenous reference *Atpb5*. Fold changes were calculated relative to the control group using the $2^{-\Delta\Delta Ct}$ method as described in the methods. Each group contained 5 samples (n=5). Data are means ±SEM and differences are relative to the treatment group in parentheses (****P< 0.0001). C, control; T, TGFβ1 ligand; I, A83-01 inhibitor; IT, A83-01 inhibitor + TGFβ1 ligand.

Effect of TGFβ1 and A83-01 on non-canonical TGFβ signalling

It is well acknowledged that TGFβ ligands have the ability to activate non-canonical, SMAD-independent signalling pathways (Zhang, 2009). Therefore, to test this hypothesis in neonatal ovaries, a western blot analysis of the non-canonical mediators p-ERK and p-AKT (belonging to MAPK and PI3K signalling pathways) was performed (Figure 5.12). Phosphorylation of both mediators was increased in TGFβ1 treated groups compared to control and inhibitor treated group, indicating that increased TGFβ signalling in neonatal ovaries also activates alternative pathways alongside the SMAD canonical pathway (Figure 5.12).

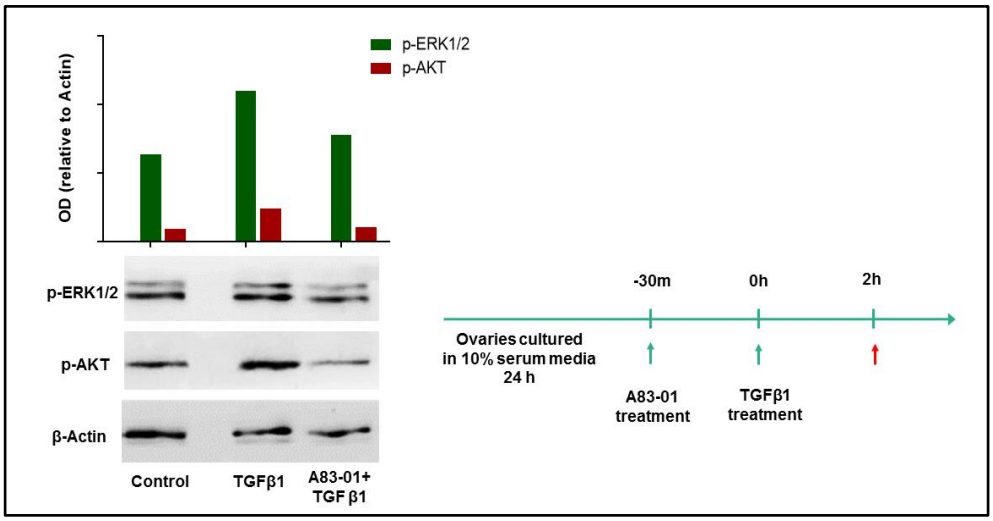

Figure 5.12. Western Blot showing ERK1/2 and AKT phosphorylation in neonatal mouse ovaries in culture. Ovaries were treated 2 hours with 10ng/ml of TGFβ1 ligand, 30 minutes with 1μM A83-01 inhibitor followed by 2 hours with 10ng/ml TGFβ1 and 2 hours with 1 μM DMSO (control). Timeline with treatments (green arrows) and collection of ovaries (red arrow) is shown. Ovaries were collected at these time points and protein extracts (15μg) were assayed for p-SMAD3 by western blotting. Beta actin is shown as a loading control. Data was obtained from 1 sample from each group (n=1). OD values for each protein are represented in the bar chart in the upper panel and are normalised against loading control beta-actin as described in the methods.

Effect of TGFβ1 and A83-01 on follicle activation and growth

Immunofluorescence staining of day 4 cultured ovaries for a total of 3 days in culture of 2 hours-treated with either TGFβ1 ligand or A 83-01 inhibitor (n=6 per treatment group) and control (non-treated) was performed for SMAD3 and DDX4 factors in order to visualise both oocyte and GCs. After measuring the oocyte area of all follicles with visible oocyte nucleus outline, the presence of a few large primary follicles (>800μm^2) in all cultured ovaries confirmed their ability to grow in culture and in comparison with non-cultured day 4 ovaries showed a significant increase in mean oocyte areas (Figure 5.13, A). A similar distribution of follicle stages was observed between all treatments groups.

However, when the proportions of the different follicle stages in each group were calculated, an increase in the proportion of transitional/activated follicles in both TGFβ1 ligand and A 83-01 inhibitor treatment groups was observed when compared with the control group (Figure 5.13, B). When oocyte areas of primordial and transitional follicle stages were compared between groups, only significant differences for the TGFβ1 treated ovaries were observed compared to the control group (Figure 5.13, C).

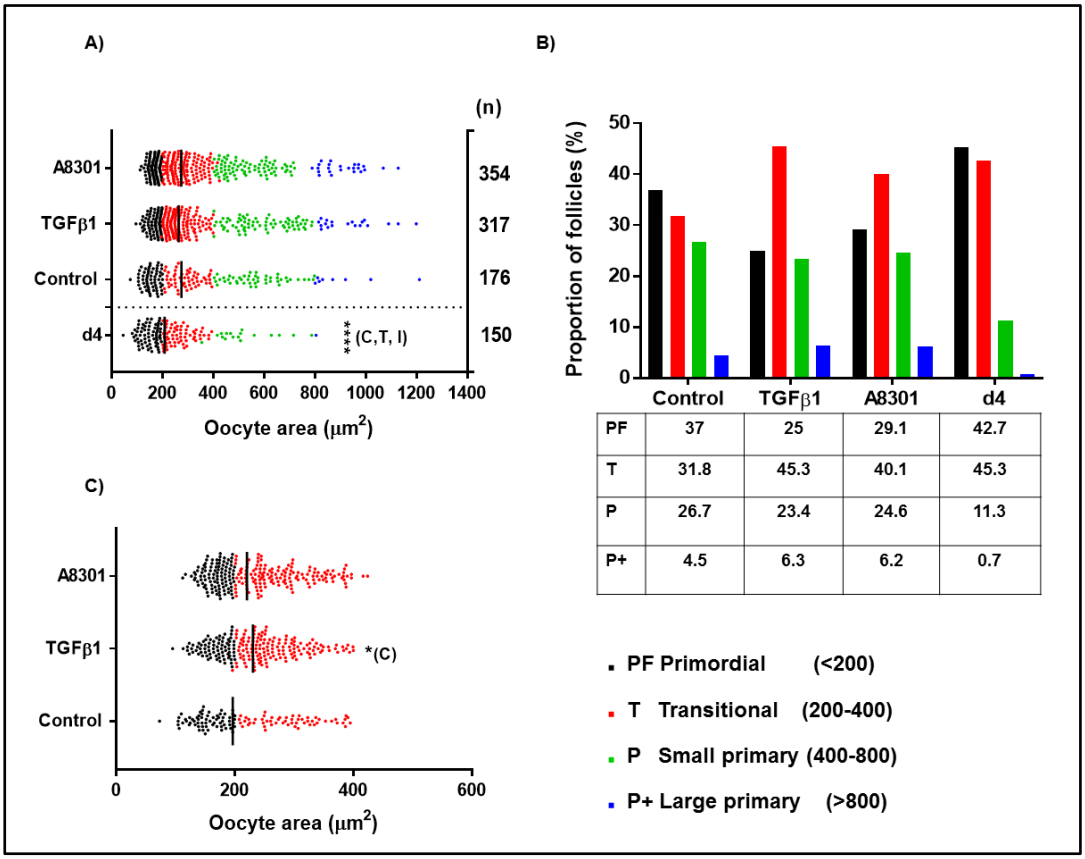

Figure 5.13. Oocyte areas and proportion of different follicle stages in mouse ovaries treated with TGFβ1 ligand and A 83-01 inhibitor. Ovaries were exposed for 2 hours with 10ng/ml of TGFβ1 ligand followed by 1 hour with 1µM A83-01 inhibitor, 2 hours with 1µM A83-01 inhibitor and 2 hours with 1 µM DMSO (control) and left for two additional days in culture. A) shows the distribution of all measured oocyte areas for the treatment groups and the non-cultured day 4 ovaries, where (n) shows the total number of follicles measured. In B) the proportion of the different follicle stages in the treatment groups and non-cultured day 4 ovaries is plotted and numbers are shown in the table. In C) the distribution of oocyte areas in primordial and transitional stages (areas up to 400µm) is shown. Data from cultured ovaries was obtained from six different ovary sections per treatment group (n=6). Four sections from 4 different non-cultured ovaries (n=4) were used as a reference for the non-cultured control. Data in A) and C) are medians and significant differences are relative to the group in parentheses (*P<0.05, ****P< 0.0001). C, control; T, TGFβ1 ligand; I, A83-01 inhibitor.

Follicle morphology assessment and validation of the follicle classification criteria

In order to confirm that every classified follicle belonged to the correct follicle stage, additional morphology assessment by considering the number of surrounding GCs was applied in all sections. Classified follicles from control, TGFβ1 ligand and A 83-01 treated ovaries according to oocyte area showed in general a good correlation with the classification taking into account the GC number (R^2=0.83, R^2=0.85 and R^2=0.80, respectively)(Figure 5.14). However, the A 83-01 group showed increased oocyte area but decreased GC number in some follicles (Figure 5.14, C). Some follicles classified as primary (P) or large primary (P+) according to the oocyte area appeared to be similar to transitional (T) and primary (P) follicle stages (GC criteria) due to their low GC number (Figure 5.15). Moreover, the presence of small multi-oocyte follicles (MOFs) with a defined surrounding GC layer in A 83-01 treated ovaries were also observed and significantly more abundant that in control and TGFβ1 ligand treated ovaries (Figure 5.16, A and C). In order to differentiate MOFs from a fusion of follicles as a side effect of the ovary culture conditions (loss of 3D structure), only follicles with fused ooplasm where considered as MOFs (Figure 5.16, B).

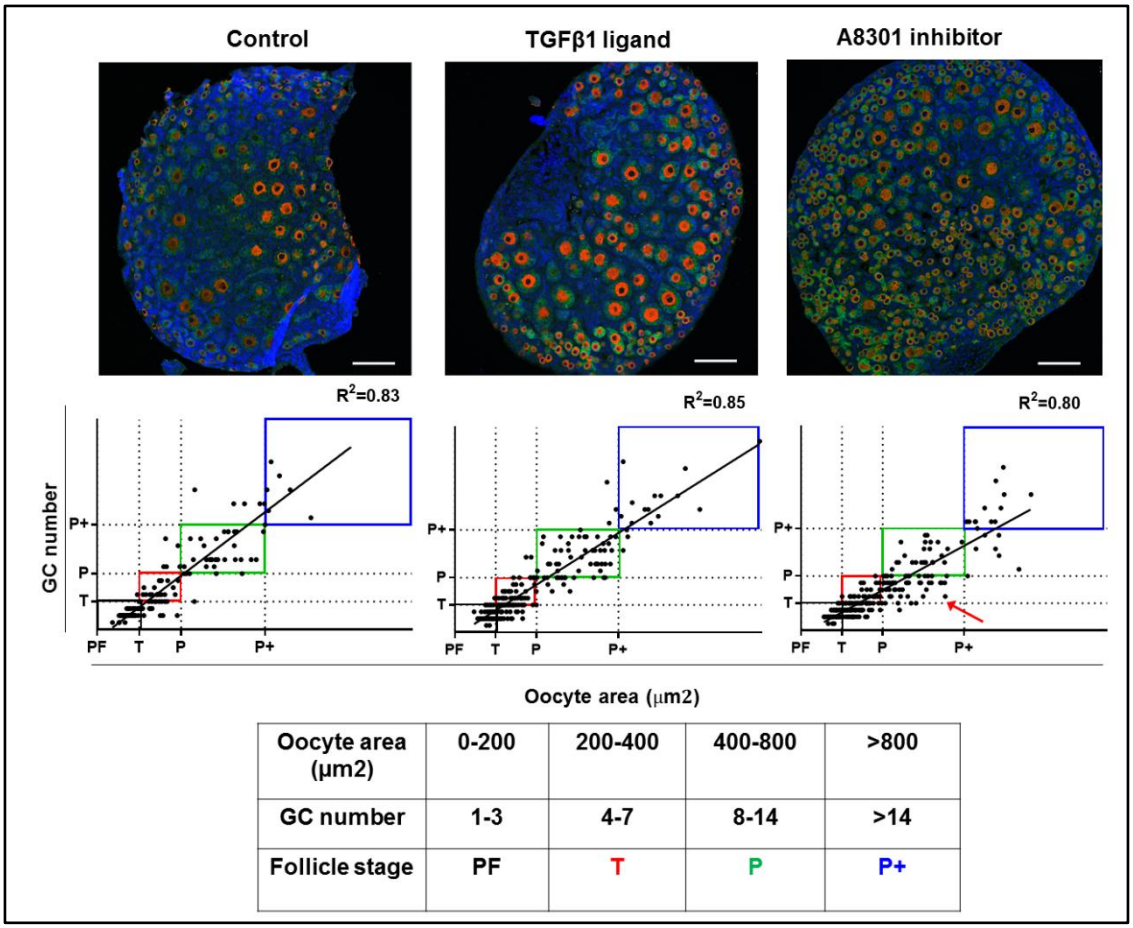

Oocyte area (µm2)	0-200	200-400	400-800	>800
GC number	1-3	4-7	8-14	>14
Follicle stage	PF	T	P	P+

Figure 5.14. Relationship between oocyte area and GC number in small follicles from ovaries treated with TGFβ1 ligand and A 83-01 inhibitor. Ovaries were exposed for 2 hours with 10ng/ml of TGFβ1 ligand followed by 1 hour with 1µM A83-01 inhibitor, 2 hours with 1µM A83-01 inhibitor and 2 hours with 1 µM DMSO (control) and left for two additional days in culture. X and Y values for each dot on the graphs correspond to its classification according to the oocyte area (y-axis) and its classification according to its GC number (x-axis). Horizontal and vertical dashed lines delimit the classification between follicle stages shown in the table. Correlation between these classifications for all measured follicles is shown as R^2 value. The A 83-01 inhibitor group shows some follicles with increased oocyte and decreased GC number (red arrow). Oocytes are stained in red (DDX4) and GCs in green (SMAD3). Nuclei are counterstained blue with DAPI. Scale bar is 100µm and magnification is 20X. PF, primordial; T, transitional; P, small primary; P+, large primary follicle stages.

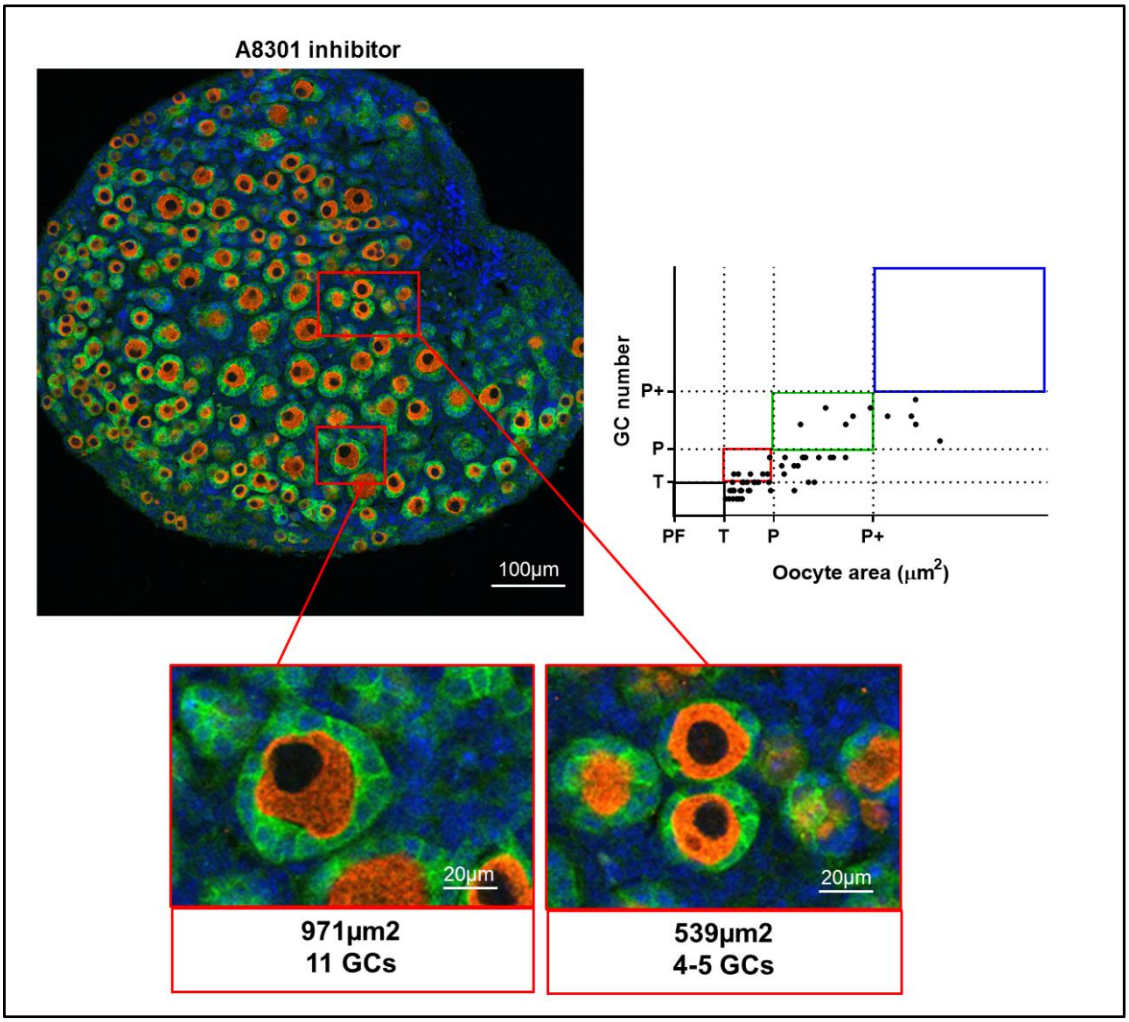

Figure 5.15. Relationship between oocyte area and GC number in small follicles from ovaries treated with A 83-01 inhibitor. Ovaries were exposed for 2 hours with 1µM A83-01 inhibitor and left for two additional days in culture. X and Y values for each dot on the graph correspond to its classification according to the oocyte area (horizontal dashed lines in y-axis) and its classification according to its GC number (vertical dashed lines in x-axis). High power images (magnification of 63X) show an example of follicles classified as large primary (left panel) and small primary (right panel) with decreased number of surrounding GCs (indicated below the images). Oocytes are stained in red (DDX4) and GCs in green (SMAD3). Nuclei are counterstained blue with DAPI. PF, primordial; T, transitional; P, small primary; P+, large primary follicle stages.

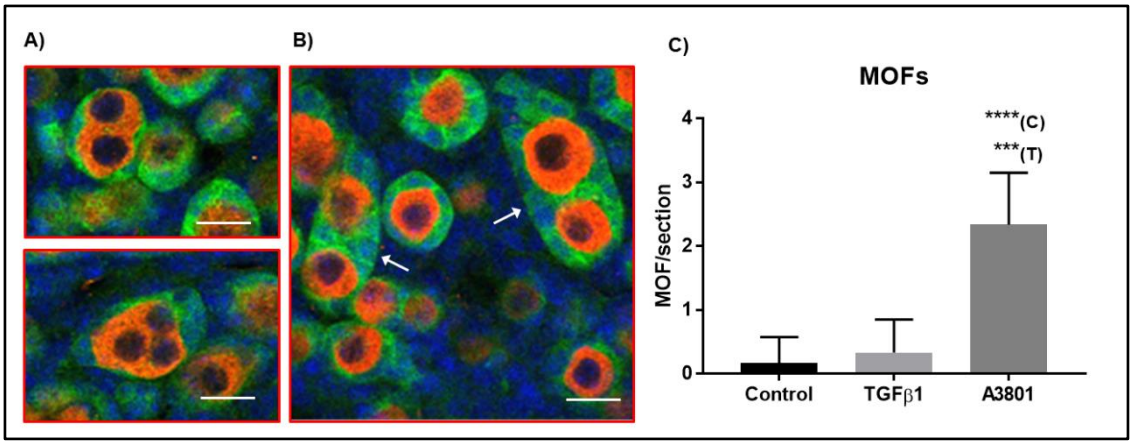

Figure 5.16. Presence of small multi-oocyte follicles (MOFs) in mouse ovaries treated with TGFβ1 ligand and A 83-01 inhibitor. A) shows an example of the structures considered as MOFs, where two or three oocytes are enclosed in a unique layer of GCs. B) shows an example of fused follicles not considered as MOFs, where each oocyte is enclosed by a layer of GCs (white arrows) C) Total number of MOFs across six ovary sections (n=6) per treatment group were counted. Data are means ±SEM and differences are relative to the group in parentheses (***P<0.001, ****P< 0.0001). C, control; T, TGFβ1 ligand; I, A83-01 inhibitor. Oocytes are stained in red (DDX4) and GCs in green (SMAD3). Nuclei are counterstained blue with DAPI. Scale bar is 20µm and magnification is 63X.

5.4 Discussion

SMAD3 binding to *Ccnd2* and *Myc* genes detected in primordial follicles suggested the existence of an endogenous mechanism of control of GC proliferation and further implicated TGFβ signalling in the maintenance of the quiescent phenotype of primordial follicles. Both stimulation and inhibition of follicle development has been previously shown using different exogenous TGFβ ligands in cultured ovaries of different species (Childs & Anderson, 2009; Ding et al, 2010; Rosairo D 2008; Telfer et al, 2008; Wang et al, 2014a; Zhao et al, 2001). However, some studies in human ovaries and cell line models, reported a differential effect of TGFβ signalling depending on the length of exposure/dose to the TGFβ ligand, providing an explanation for this apparent paradoxical effect (Ding et al, 2010; Zi et al, 2011). From the repertoire of TGFβ ligands, TGFβ1 was used for the experiments in this chapter, as it is a well-studied TGFβ ligand. It has been implicated in the maintenance of the primordial follicle pool in several reports, where long-term treatments with the ligand preserved the amount of primordial follicles, suggesting its inhibitory actions (Rosairo D 2008; Wang et al, 2014a). However, the reduced proportions of growing follicles and increased apoptosis in TGFβ1-treated ovaries in both oocyte and GCs was also observed in one these studies (Wang et al, 2014a). This was probably due to a detrimental effect of long exposures to the ligand. These observations contradict the suggested role of TGFβ1 as inhibitor of the primordial follicle pool and suggest instead that sustained TGFβ1 exposure induces follicle atresia, which could finally decrease the population of growing follicles. Therefore, this chapter aimed to investigate the effect of a short two hour exposure to TGFβ1 ligand and also A 83-01 (TGFB1 receptor I inhibitor) in primordial follicles. In order to test this, differences in SMAD3 binding and gene regulation after treatment of day 4 ovaries in culture were investigated for *Ccnd2* and *Myc*. Furthermore, in order to associate these molecular events with morphological changes, the assessment of follicle growth by measuring the proportions of the different follicle stages after the treatments was performed.

Molecular analysis of *in vivo* conditions

SMAD3 binding is reduced in Ccnd2 and Myc genes as follicles grow

The findings obtained in Chapter 3 where SMAD3 binding to *Ccnd2* and *Myc* genes was more evident in samples of day 4 ovaries compared to day 16 ovaries led to the hypothesis that this binding may be related to the maintenance of the quiescent phenotype of the primordial follicle population. In contrast, no evident binding to p27 gene promoter was observed, therefore, SMAD regulation of this gene was not further studied in this chapter. Therefore, in order to take the preliminary observation further, the SMAD binding pattern to *Ccnd2* and *Myc* genes in primordial and growing follicles was compared and quantified using ChIP-qPCR with an increased number of samples (n=5). As expected, increased SMAD3 binding to *Ccnd2* and *Myc* gene promoters was observed in day 4 ovary samples relative to IgG control, which was associated with reduced levels of *Myc* mRNA expression and elevated *Ccnd2*, suggesting that SMAD3 acts as repressor and activator of *Myc* and *Ccnd2* genes in primordial follicles, respectively. Although repression of *Myc* gene by TGFβ signalling during late G1 phase is a well-described mechanism to maintain cell cycle arrest (Warner et al, 1999), there is little evidence about its specific role in the ovary (Li et al, 1994; Nandedkar & Dharma, 2001; Putowski LT 1 1997). Moreover, although TGFβ regulation of Ccnd2 levels has been suggested (Anttonen et al, 2014b; Looyenga & Hammer, 2007), the role of SMAD3 as transcriptional regulator of *Ccnd2* gene has never been reported before.

Molecular and morphological analysis *in vitro*

SMAD3 binding to Ccnd2 and Myc target genes is not affected *after short TGFβ stimulation but gene expression is induced*

SMAD3 regulation of target genes is dependent on increased/decreased TGFβ stimulation (Massague et al, 2005a). By using day 4 ovaries in culture (a model to treat primordial follicles *in vitro*), short exposure to TGFβ1 ligand did not show any significant changes in SMAD3 binding to *Myc* and *Ccnd2* genes, however, a significant upregulation in mRNA expression was observed for both genes.

As SMAD3 binding was not significantly changed after treatment, their induced gene expression was an unexpected finding. However, one possible explanation is that non-SMAD signalling pathways may have contributed to the expression of both *Ccnd2* and *Myc* genes. Several transcription factors acting as binding partners with SMADs have been reported to act as activators and repressors of *Myc* and *Ccnd2* genes (Figure 5.17, C). Interestingly, ERK1/2 targets such as ETS proteins for *Myc* gene or Ap1 complex for *Ccnd2*, are transcriptional activators (downstream MAPK signalling pathway) that maintain high gene expression levels while transcriptional repressors such as the Inhibitors of differentiation (Id) factors or Foxo1 (inhibited by PI3K pathway) bind and repress the expression of *Myc* and *Ccnd2* genes, respectively (Figure 5.17, C). It can be then proposed that the enhanced binding of activators and the release of repressors after TGFβ stimulation may be necessary to induce the expression of *Ccnd2* and *Myc* genes (Figure 5.17, A). Therefore, in order to investigate non-canonical activation, the PI3K and MAPK signalling mediators p-AKT and p-ERK1/2, were analysed in a TGFβ treated sample (n=1). An increased detection of both factors was observed after TGFβ treatment, suggesting that the activation of non-canonical pathways can induce *Myc* and *Ccnd2* gene expression through the recruitment of different transcription factors to the SMAD transcription factor complex) (Figure 5.17, A). However, a detailed experiment with more protein samples (n≥3) from TGFβ treated ovaries is necessary to confirm the activation of non-canonical mechanisms.

Other mechanisms can also account for the induction of *Myc* and *Ccnd2* under TGFβ stimulation. The family of calcium-binding transcription factors, the NFATs, have been reported to have an activating role on *Myc* gene promoter through the displacement of SMAD3 from its TGFβ inhibitory elements (TIE) after TGFβ stimulation. This displacement results in *Myc* gene upregulation (Figure 5.17, B). Although no significant changes in SMAD3 binding to *Myc* gene were detected with TGFβ stimulation, less amount of SMAD3 binding was observed in all samples compared to control. Presence of NFATs and their binding partner Calcineurin have been detected in day 4, 8 and 16 ovaries (Appendix 14) suggesting that this mechanism can also contribute to *Myc* gene upregulation in the ovary.

The increase in *Ccnd2* gene was not as evident as *Myc* gene. *Myc* gene belongs to the group of early response genes (Lau & Nathans, 1987) and after stimulation, *Myc* mRNA expression reaches maximum levels after 2-3 hours (Persson et al, 1985). In contrast, the induction of *Ccnd2* mRNA expression has been reported to peak around 4 hours (Park et al, 2005). Interestingly, Myc protein is well-known to act as transcription factor of *Ccnd2* (Bouchard et al, 2001). Therefore, it is likely that upregulation of *Myc* gene expression contributes to the induction of *Ccnd2* gene but later than 2 hours. Future studies could therefore focus on additional time points to determine the optimal time necessary to promote a significant induction of *Ccnd2* gene.

SMAD3 binding to Ccnd2 and Myc genes is reduced with A 83-01 inhibitor but gene expression is not altered

In contrast to TGFβ treated ovaries, a short exposure to A 83-01 inhibitor showed reduced SMAD3 binding to both *Myc* and *Ccnd2* genes, indicating that the inhibitor is able to disrupt SMAD3 nuclear translocation and binding to target genes. When gene expression was analysed after A 83-01 treatment, relative mRNA levels of *Myc* and *Ccnd2* genes showed no significant differences relative to control. One explanation of this is that short disruption of basal levels of TGFβ signalling does not have a major effect on *Myc* and *Ccnd2* gene expression as other transcription factors also binding to the gene promoter (e.g transcriptional repressors/activators, Figure 5.14, C) would still be bound to the promoters, maintaining basal *Myc* and *Ccnd2* expression levels. However, *Ccnd2* levels showed a slight decrease since differences were significant relative to the TGFβ-treated group. Therefore it is likely that more time of inhibition is required to detect a decrease in *Ccnd2* gene expression levels. Based on the above findings, a hypothetical model of TGFβ regulation of target genes in GCs is proposed in Figure 5.17 below.

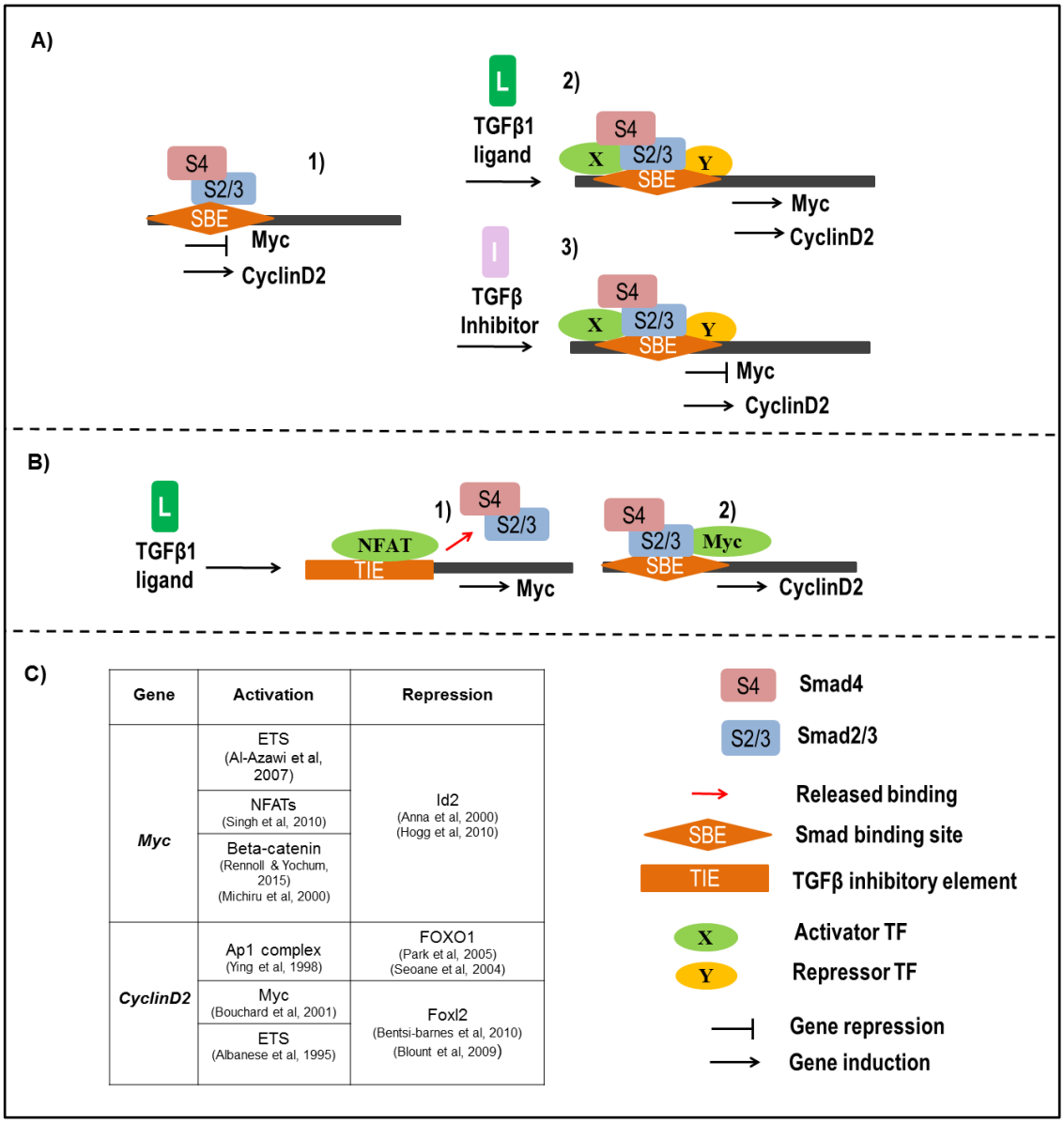

Figure 5.17. Hypothetical molecular model of the effect of short TGFβ stimulation (A, 2) and TGFβ inhibition (A, 3) on SMAD3 binding (and co-factors) and regulation of target genes. In basal conditions, the association of SMAD3 binding partners allows the repression of *Myc* and activation of *Ccnd2* genes. Upon TGFβ1 ligand binding (A, 2), the association of SMAD3 binding partners with activating roles or the release of repressors allows the upregulation of both *Myc* and *Ccnd2* genes. SMAD2/3 binding can also be reduced and displaced by NFATs to activate *Myc* gene (B, 1). Activation of *Myc* can act as transcriptional activator of *Ccnd2*, upregulating its expression (B, 2). When TGFβ pathway is inhibited (A, 3), SMAD2/3 binding is released but also the binding of transcriptional activators, allowing the repressors to maintain *Myc* and *Ccnd2* expression levels. Table in C) summarises some examples of *Myc* and *Ccnd2* transcription factors (also reported as SMAD binding partners) and their role as activators and repressors.

Smad7 and Gdf9 gene expression is not affected by the A 83-01 inhibitor but is induced after TGFβ stimulation

In neonatal ovaries, *Smad7* gene expression was increased with TGFβ1 ligand, indicating that TGFβ signalling was active after treatment with the ligand. By comparison, *Smad7* remained unchanged in the presence of the inhibitor possibly suggesting poor disruption of canonical TGFβ signalling in these conditions. The *Smad7* gene is also a target gene for SMAD3 and its co-factors (Nagarajan et al, 1999), therefore increased expression of *Smad7* confirms that short treatment with the TGFβ1 ligand is able to induce a genomic effect and also the activation of a negative feedback loop to control excessive TGFβ signalling. Moreover, SMAD7 is also known to have a function as a transcription factor to control cell proliferation. For instance, it has been reported that SMAD7 has the ability to form a transcription factor complex with beta-catenin (activator of *Myc*) to induce *Myc* gene promoter (Edlund et al, 2005). This is consistent with the observed *Myc* and *Smad7* induction in the TGFβ1-treated group.

Interestingly, *Gdf9*, expressed in oocytes of all follicle stages except primordial follicles (Dong et al, 1996) showed no significant differences in transcript levels in TGFβ1 ligand and A 83-01-treated groups when compared to controls. Since it is not a GC factor, it is likely that TGFβ treatment does not affect the expression of the gene after a short treatment with either TGFβ or A 83-01 inhibitor. However, insignificant upregulation in the TGFβ treated group was observed. An increase in *Gdf9* gene expression is suggestive of enhanced follicle activation, as *Gdf9* has been reported to promote GC proliferation of growing follicles (Dong et al, 1996; Joyce et al, 2000b) but also to contribute to the primordial to primary follicle transition (Vitt UA, 2000). Increasing the number of samples would help understanding whether there is significant Gdf9 upregulation or not. Nevertheless, significant changes in *Gdf9* gene expression after TGFβ stimulation/inhibition would then be a direct consequence of uncharacterised TGFβ signalling in the oocyte or alternatively, an indirect paracrine or juxtacrine effect from GCs.

Smad2, Smad3, p27 and Foxl2 do not show significant differences between treatments

Smad2 and *Smad3* relative mRNA expression levels remained unchanged between treatment and control groups, indicating that short exposure to both TGFβ and inhibitor affects SMAD phosphorylation but does not have a genomic effect that alters the expression of both genes. In addition, *Foxl2* and *p27* mRNA levels neither showed any significant differences when compared to control, however, a subtle but insignificant downregulation in the TGFβ treated group was observed for both genes. FOXL2 has been reported to be a repressor of *Ccnd2* (Frank et al, 2007) and therefore, the observed upregulation of *Ccnd2* can be a consequence of the release from FOXL2 repressive actions. Moreover, a decrease in p27 protein and mRNA levels is observed *in vivo* after primary stage (Chapter 3, image analysis), therefore, the small downregulation after treatment with TGFβ1 ligand may be an indicator of follicle growth. However, the differences were not significant, probably because only detectable differences on the proportion of activated follicles were observed in TGFβ treated group when compared to controls but any differences were observed in primary follicles (as explained below). Alternatively, insignificant differences detected in these genes can also be due to the short time point employed for the treatments. Therefore, it is worth considering the addition of an increased time point in future experiments.

<u>*In vitro* treatments: Morphological assessment of follicle growth</u>

Short TGFβ1 treatment induces PFA

In order to determine the effects on follicle activation and growth of a short two hour exposure to TGFβ ligand/inhibitor, ovaries were left in culture for two additional days in non-treated serum media. In order to avoid longer action of TGFβ1 ligand and inhibit the increased TGFβ signalling, treatment with A 83-01 inhibitor for one hour was used after the treatment with TGFβ1 ligand. The proportions of the different follicle populations in the different groups revealed a significant increased proportion of transitional/activated follicles in the TGFβ ligand group (Figure 5.18, A) whereas no differences in the proportions of larger follicles was detected when compared to controls.

Increased proportions of transitional follicles in the A 83-01 inhibitor group was also observed, however it was not significant when compared to the control group. These results suggest that short exposure to TGFβ1 ligand targets the primordial follicle population to enhance the molecular machinery necessary to favour the ratio of activated follicles.

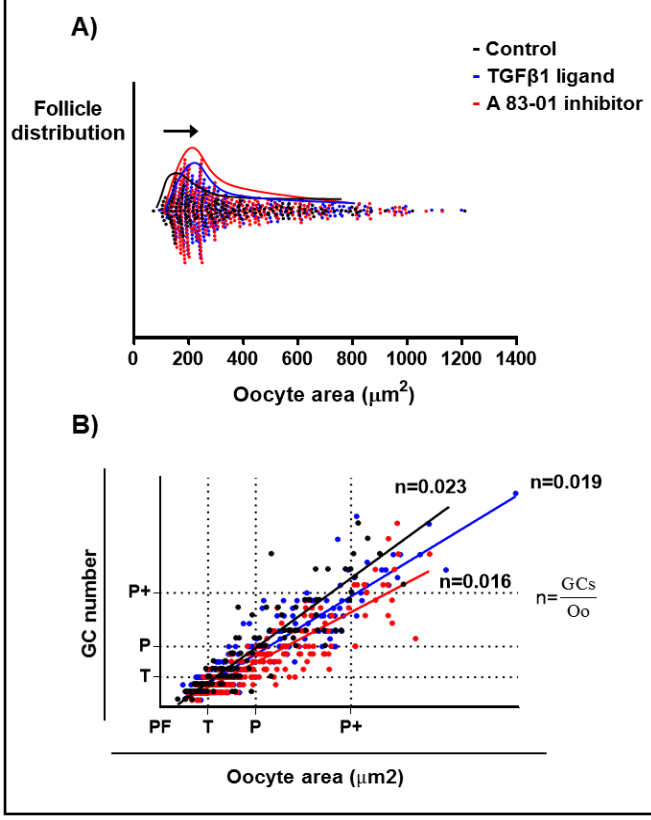

Figure 5.18. Overlayed graphs of follicle distribution according to oocyte area (A) and correlation between GC number and oocyte area classification (B) of control, TGFβ1 and A 83-01-treated ovaries. Graph in A) shows a shift on the follicle distribution towards oocyte areas >200um (transitional follicles, T) in TGFβ1 and A 83-01-treated ovaries compared to control (A, black arrow). Graph in B) compares the slopes of the different treatment groups, where a decreased slope in A 83-01-treated group indicates a reduced number of GCs in enlarged oocytes.

The absence of differences between the proportions of larger follicles between groups can be explained by the short culture period after the treatments which may only allow to detect the growth of the activated primordial follicles to the transitional stage. These findings are supported by gene expression data, where *Ccnd2* and *Myc* genes are upregulated with a short TGFβ treatment, indicating that this upregulation may be necessary to enhance the initiation of GC proliferation during follicle activation. Moreover, these observations suggest that a difference between short and sustained TGFβ exposure have different effects on follicle growth: while a short TGFβ exposure followed by TGFβ inhibition enhances follicle activation, sustained and long-term exposures reverses the effect towards primordial follicle maintenance and follicle atresia (Rosairo D 2008; Wang et al, 2014b) (Figure 5.19).

Overexpression of SMAD3 has been found in GC tumours in mice (Pangas et al, 2008) and TFGβ-induced apoptosis have been reported in some cell types as a mechanism to prevent excessive cell proliferation (Schuster & Krieglstein, 2002). Therefore it is likely that sustained canonical TFGβ signalling overactivates the canonical SMAD3 pathway and accelerates growth of GCs of growing follicles, triggering GC apoptosis and later follicle atresia (Figure 5.19).

Short TGFβ inhibition promotes impaired follicle activation and germ cell nest breakdown

When the GCs of all measured oocytes were counted in each treatment group, a decreased number of GCs in some primary and large primary follicles was observed in the ovaries treated with A 83-01 inhibitor (Figure 5.18, B). As no differences in the proportions of the growing follicles was observed between treatment groups when oocyte area was measured, the impaired oocyte area/GC number can only be due to a reduced proliferation of GCs rather than accelerated oocyte growth. These findings further suggest that a short disruption of TGFβ signalling targets GCs by reducing their proliferative potential while the oocyte grows normally. However, long TGFβ inhibition has been reported to increase oocyte size (Wang et al, 2014a), suggesting that sustained disruption of TGFβ signalling releases the oocyte from a controlled growth (Figure 5.19). Although GCs showed some proliferation, the number of GCs surrounding the enlarged oocytes was reduced, indicating that increased TGFβ signalling might have been necessary at some point in GCs to allow sufficient GC proliferation.

The presence of small multi-oocyte follicles (MOFs) was also observed in the samples treated with the A 83-01 inhibitor, where some somatic cells failed to enclose individual primordial follicles and therefore fused oocytes without separating basement membrane were observed (containing two or three oocytes). These findings further indicate that a disruption in TGFβ signalling affects the proliferation of pre-GCs and therefore reduces the number of cells necessary to encapsulate individual primordial follicles.

The presence of MOFs was also observed when the activin antagonist follistatin was used in day 0 mouse ovaries (Wang et al, 2015), supporting the essential role of active TGFβ signalling in GC proliferation. Interestingly, although GC proliferation was reduced, *Ccnd2* and *Myc* gene expression levels were not significantly changed after treatment with A 83-01. The consequences of this forced maintenance of low levels of these cell cycle regulators in GCs during this period of time can therefore explain the lack of molecular competence necessary in primordial follicles to have a normal growth when ovaries were further maintained in culture without any treatment. These findings are also supported by the observations using PTEN inhibitors in primordial follicles, where PFA takes place but follicles showed atresia after secondary stage (McLaughlin et al, 2014). It is possible in this model, that oocytes were stimulated to grow before GCs had all the required molecular machinery to allow normal proliferation and follicle development. The consequences of short vs sustained TGFβ stimulation in primordial follicles are proposed in the depicted in Figure 5.19 below.

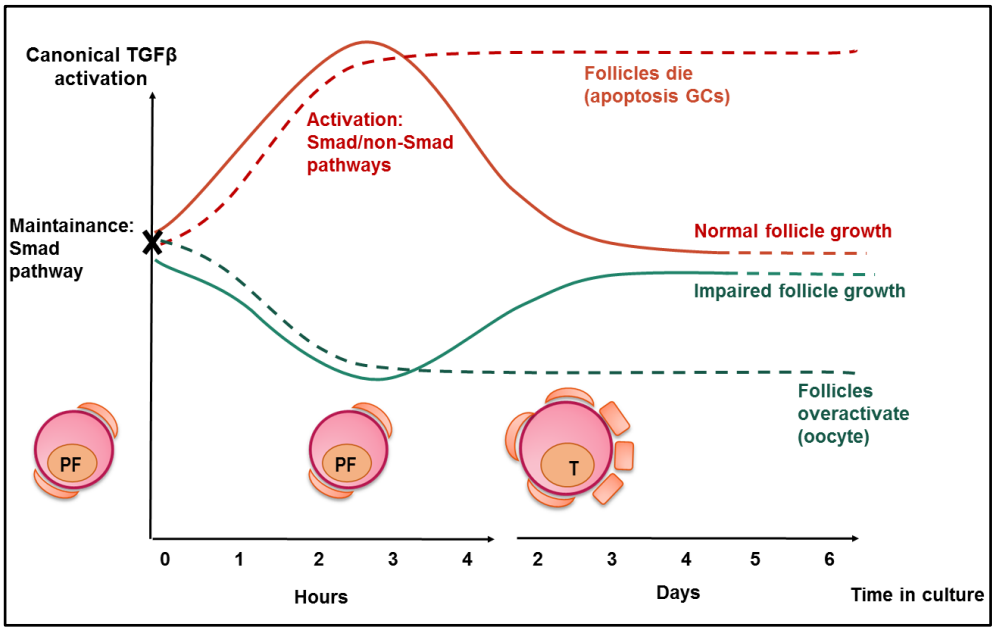

Figure 5.19. Hypothetical model of the effect of short vs. sustained TGFβ stimulation (red) and TGFβ inhibition (green) during early follicle development. In basal TFGβ conditions, the population of primordial follicles is maintained. An increase in TGFβ levels allows PFA through the contribution of SMAD and non-SMAD signaling pathways (solid red line). A decrease in canonical TGFβ signalling avoids increased follicle atresia by preventing GC apoptosis (dashed red line). If primordial follicles are deprived of TGFβ signaling for a short time before PFA, follicles grow but GCs do not proliferate normally (solid green line). If TGFβ inhibition is sustained, oocyte increases in size but GCs show impaired proliferation (green dashed line).

From the results presented in this chapter and the discussion above, the following key findings can be summarised:

- SMAD3 induces the expression of *Ccnd2* and represses *Myc* by direct binding to their gene promoters in primordial follicles *in vivo*.
- Short increase in TGFβ signaling increases the expression of *Ccnd2* and *Myc* genes, probably through the contribution of non-canonical mechanisms, since SMAD3 binding remains unchanged. A decrease in TGFβ signaling does not alter their expression.
- Short increase in TGFβ signaling promotes a subtle enhancement of PFA, while decreased TGFβ signaling delays GC proliferation and affects paired germ cell cyst breakdown.

Chapter 6.

General discussion

6.1 Rationale of the thesis

Primordial follicles are the most precious structures in the ovary. They constitute the ovarian reserve and although they can remain in a non-growing state for many years, they remain metabolically active and eventually activate and grow (Gallardo et al, 2007). The molecular events that trigger the switch from the non-growing to the growing state still remain poorly understood. For more than two decades, the development of *in vitro* cultures of ovarian cortex for different species including human (Telfer et al, 2008) or whole neonatal ovaries in mice (Eppig et al, 1996) have allowed researchers to study the effect of several candidate factors on primordial follicles. Since it was demonstrated that gonadotropins are dispensable for primordial follicles to grow (Abel et al, 2000; Kumar et al, 1997), the effect of a range of intraovarian factors such as the members of the PI3K and TGFβ signalling pathways has been broadly studied *in vitro* and most of them have been related to the maintenance and activation of the primordial follicle pool (Liu, 2010). Some of these candidates and signalling pathways have been further evaluated *in vivo* through the use of transgenic models, which provided a better physiological model to determine specific effects on early follicle development, including the morphological and/or molecular changes in the oocyte and granulosa cells (GCs). It is well established that the cross-talk between the oocyte and the surrounding GCs is essential for early follicle development (Eppig, 2001). However, since primordial oocytes can be induced to grow *in vitro* and *in vivo* (Jagarlamudi et al, 2009; Suzuki et al, 2015) less attention has been directed on the role of GCs during the primordial stage. Furthermore, primordial GCs are difficult to isolate and limited information is known about their molecular phenotype. Several reports have demonstrated that GC proliferation is one of the first morphological events observed during PFA (Braw-Tal, 2002; Da Silva-Buttkus et al, 2008; Mora et al, 2012a). Most recently, the promoter of the GC marker FOXL2 (expressed in all follicle stages including primordial follicles) has been employed as the locus for Cre recombinase to develop GC specific cKO mice and study the role of some factors from the mTOR pathway in GCs of primordial follicles. Interestingly, stimulation of the mTOR pathway (*Tsc1*$^{-/-}$ mice) in primordial follicles increased GC proliferation and promoted PFA, demonstrating for the first time *in vivo* that the initiation of GC proliferation is essential to allow PFA (Zhang et al, 2014).

In addition, *in vitro* treatment of human cortical biopsies with PTEN inhibitor, bpV(HOpic), showed unclear development beyond secondary stage (McLaughlin et al, 2014). Since PTEN is a key regulator of PI3K signalling in oocytes, it can be proposed that the initiation of growth by the oocyte is not sufficient to allow a healthy follicle development. Therefore, a better understanding of the molecular events that initiate GC proliferation in primordial follicles may provide some insight about the mechanisms that allow individual follicles to activate and grow. Previous unpublished studies in our lab have identified the presence of SMAD2/3 in GCs of primordial follicles and loss of this expression in growing follicles suggested that SMAD2/3 is associated with PFA. Interestingly, SMAD2/3 transcription factors are essential regulators of cell proliferation and survival and have been also related with the EMT transition (Heldin et al, 2009). Since it has been proposed that GCs of primordial follicles experience partial EMT during PFA, SMAD2/3 may therefore be an important regulator of GC phenotype. Therefore, this thesis sought to investigate whether canonical TGFβ/SMAD signalling regulates the expression of target genes in GCs, specifically, cell cycle genes in primordial follicles. The cell cycle regulators p27 and CCND2 have been detected in the ovary and are involved in GC proliferation during PFA and early follicle development (Rajareddy et al, 2007; Sicinski, 1996). They are important factors for the maintenance of the quiescent state in many cell types, and their regulation and function is essential to trigger cell cycle re-entry. Therefore, by using molecular techniques at all levels (pathway activation, TF binding to the chromatin, gene and protein expression) and detailed image analysis for the assessment of protein localisation and follicle growth, the expression pattern of SMAD2/3 and the cell cycle regulators CCND2 and p27 was analysed throughout the different stages of early follicle development (Chapter 3). Then, the analysis of CCND2/p27 complexes in primordial follicles was performed to better determine their role in the maintenance and activation of these follicles (Chapter 4). Finally, the development of an *in vitro* model (whole neonatal ovary culture) provided an approach to investigate the role of TGFβ signalling on cell cycle genes and the relationship of this regulation with PFA (Chapter 5).

6.2 Key findings

The repertoire of techniques performed in this thesis has demonstrated the possibility of studying the function of different candidates during early follicle development in mice. Specifically, this work has included both descriptive and functional analysis of key factors from TGFβ signalling and the cell cycle using neonatal mouse ovaries *in vivo* and *in vitro* and has provided a better understanding of their relationship, as described by the main findings below.

6.2.1 Smad3 is present in GC nuclei from primordial follicles and regulates *Ccnd2* gene

In Chapter 3, the protein expression pattern of SMAD3 but not SMAD2 was observed to be specific to GCs and changed as follicles developed, indicating that although both SMADs may compensate each other when one is absent (Li et al, 2008), SMAD3 likely plays a primary role during early follicle development. SMAD3 has the ability to bind to DNA acting as a transcription factor, and its nuclear presence was detected in GCs of primordial follicles. Moreover, higher mRNA expression of *Smad3* and *Alk5* (Type I TGFβ receptor) was detected in day 4 ovaries compared to older ovary ages, complementing the results from a recent study showing similar expression of TGFβ/SMAD2/3 pathway inhibitors SMAD7 and STRAP (Sharum et al, 2016). These results provide further evidence that TGFβ signalling is active and self-regulated in primordial follicles. Interestingly, co-localisation of SMAD3 with the proliferation marker Ki67 confirmed that SMAD3 is present in mitotically-arrested GCs from primordial follicles. Therefore, TGFβ signalling and SMAD3 regulation of target genes in GCs may be related to the maintenance of the slow proliferative phenotype of primordial follicles.

TGFβ signalling is well-known for its role in cell growth inhibition through the regulation of *Myc* and *p15* genes. There is also evidence that TGFβ signalling can influence the expression of *Ccnd2* gene (Anttonen et al, 2014b; Looyenga & Hammer, 2007); yet, SMAD3 direct binding and regulation of the gene has not been studied. ChIP-PCR analysis described in Chapter 3 indicated that SMAD3 bound to the promoter of *Ccnd2* and *Myc* genes in day 4 ovaries and a more detailed analysis in Chapter 5 showed that relatively more SMAD3 binding was present in day 4 ovaries when compared to day 16 ovaries, suggesting that SMAD3 regulated the gene expression of both genes in primordial follicles.

Since *Myc* mRNA levels are low in day 4 ovaries compared to day 16 ovaries whereas *Ccnd2* was relatively higher in day 4 ovaries, suggests that SMAD3 is contributing to the repression of *Myc* while inducing *Ccnd2* in GCs of primordial follicles.

6.2.2 CCND2/p27 complexes in GCs of primordial follicles are lost in growing follicles

SMAD3, CCND2 and p27 proteins were found to share a common expression pattern during early follicle development, since all three factors were highly expressed in the nucleus of GCs from primordial follicles and their expression decreased as follicles grow. As mentioned in the previous section, it is likely that SMAD3 regulates the expression of *Ccnd2* gene, constitutively increasing its protein levels. CCND2 and p27 proteins are key regulators of the G0/G1/S cell cycle transition and their actions depend on the formation and dissociation of a protein complex together with the cyclin-dependent kinase K4/6.

In Chapter 4, CCND2 and p27 co-localised in primordial follicles (1-3 GCs), suggesting that GCs in these follicles may be present in G0/early G1 phase. De-colocalisation was evident when p27 levels decreased in GCs at transitional stage (4-7 GCs), while CCND2 levels were still high, indicating proliferative activity. CCND2 levels were then decreased from primary stage, where both factors were barely co-localised. Since p27 loss was evident as GCs started to proliferate, it is proposed that p27 degradation is one of the earliest key defining events that allow GC proliferation. This is supported by previous findings in cell line models where degradation of p27 is a requirement to allow G1 cell cycle progression (Nakayama, 2004).

The presence of CCND2/p27 complexes was found in day 4 ovaries but was majorly reduced in day 16 ovaries. Since p27 presence was reduced in larger follicles, it is likely that the complexes are not required in proliferative GCs to facilitate cell cycle progression. Therefore, the main role of CCND2/p27 complexes is non-catalytic and probably involved in the maintenance of GCs in primordial follicles. However, their catalytic activity was not studied in this thesis and therefore it would be worth considering for future experiments.

It has been reported that dissociation of the complexes is triggered by mitogen stimulation, where the whole complex is translocated to the cytoplasm and p27 is degraded (Susaki E 1 2007). The increase in CCND2 levels and the phosphorylation on the Thr^{280} residue have been reported as the consequence of mitogen stimulation, together contributing to the translocation and dissociation of the complexes in the cytoplasm (Susaki E 1 2007). In this thesis, the absence of nuclear p27 was observed from the transitional follicle stage, becoming more evident at the primary stage, therefore, the dissociation of CCND2/p27 complexes in GCs is likely to be part of the process of PFA. Based on this, it is likely the initiation of PFA relies on the extracellular mitogen/s that trigger the increase in *Ccnd2* expression levels. Since SMAD3 has been detected to be bound to *Ccnd2* gene, the last Chapter of this thesis has focused on this aspect in detail.

6.2.3 CCND2 is a positive regulator while p27 is a negative regulator of PFA

Ccnd2$^{-/-}$ mice exhibit arrested follicle growth around the secondary stage with follicles surrounded by a decreased number of GCs (Sicinski, 1996). The high presence of CCND2 protein until primary stage observed in the image analysis in Chapter 3 suggests that CCND2 is essential to enhance GC proliferation during early follicle development and therefore, absence of CCND2 protein in primordial follicles delays initiation of GC proliferation and impairs the GC number in growing follicles. As described above, increased levels of Ccnd2 mRNA and protein allows p27 degradation and G1 cell cycle progression (Susaki E 1 2007). Therefore, it is likely that maintenance of basal CCND2 levels in GCs is necessary to eventually re-enter cell cycle. Extracellular mitogen/s may then increase these basal levels, initiating GC proliferation and follicle growth. In this thesis, SMAD3 regulation of *Ccnd2* gene has been proposed to maintain *Ccnd2* levels transcriptionally. However, post-translational regulation is also crucial at this point. For example, activation of PI3K pathway via AKT and mTOR has been reported to prevent CCND2 protein degradation via the inhibition of GSK3, which phosphorylates CCND2 and allows its degradation (Morales & de Plata, 2012). Interestingly, the mTOR pathway has recently been implicated in the maintenance of GC proliferation in primordial follicles (Zhang et al, 2014). It can be further suggested that CCND2 levels may be lost (by degradation) in GCs with limited mTOR and therefore the absence of sufficient CCND2 levels does not allow PFA.

p27$^{-/-}$ mice exhibited increased follicle formation and overactivation of primordial follicles (Rajareddy et al, 2007). Since CCND2/p27 complexes were observed in GCs from primordial follicles, the accelerated GC proliferation and PFA observed in *p27*$^{-/-}$ mice supports the proposed hypothesis that CCND2/p27 complexes are non-catalytic whereas p27 acts mainly as negative regulator. Therefore, it can be postulated that adequate p27 protein levels in GCs of primordial follicles may allow the formation of non-catalytic complexes that prevents premature initiation of GC proliferation.

Altogether, it can be proposed that the ratio of CCND2 and p27 proteins may be key determinants of GC cycle arrest.

6.2.4 FOXL2 does not interact with SMAD3 in primordial follicles but may maintain high levels of p27 protein in GCs

FOXL2 has been proposed to interact with SMAD3 and regulate the expression of common genes, such as the *Follistatin* gene in the mouse pituitary (Blount et al, 2009). In the ovary, FOXL2 was found to be specific to GCs and also to contribute to maintain high levels of p27 in primordial follicles by the transcriptional regulation of the gene in mice (Garcia-Ortiz et al, 2009; Mork et al, 2011). These aspects were supported by the findings of Chapter 3, where FOXL2 was detectable on the promoter of *p27* gene in day 4 ovaries. As explained above, high p27 levels may be important for the CCND2/p27 complex formation in GCs and maintenance of the G0/early G1 phase, therefore, although FOXL2 may not directly interact with SMAD3, it likely plays an independent role in regulating GCs of primordial follicles. FOXL2 expression levels were detected throughout all stages of follicle development and binding to *p27* was also observed in day 16 ovaries, indicating that FOXL2 is an important transcriptional regulator in other stages of growth. In fact, FOXL2 binding to *Ccnd2* was only detected in day 16 ovaries, therefore, it is likely that FOXL2 represses *Ccnd2* gene after PFA as a mechanism to avoid excessive upregulation of *Ccnd2* (e.g by an increase in TGFβ signalling)(Bentsi-Barnes et al, 2010).

6.2.5 Increased TGFβ signalling upregulates *Ccnd2* levels and triggers PFA

The last chapter of this thesis is focused on SMAD3 regulation of target genes under different conditions of TGFβ signalling and its relationship on early follicle growth. SMAD3 is the canonical transcriptional regulator of TGFβ signalling and its regulation of target genes such as *Myc* and *p15* is well-known to be involved in the maintenance of mitotic arrest (Joan et al, 2001). In contrast, TGFβ signalling has also been involved in triggering EMT via non-canonical signalling (Zhang, 2009).

Association between PFA and EMT has been speculated, since a partial transition from epithelial to stromal-like phenotype has been observed in GCs as they initiate proliferation (Childs & McNeilly, 2012; Mora et al, 2012a). TGFβ signalling in primordial follicles is functioning probably at basal levels, consistent with the fact that *Alk5* receptor expression was observed in day 4 ovaries (observed in Chapter 3). If TGFβ signalling is active in primordial follicles and TGFβ can drive EMT in GCs, it was proposed in this thesis that increased TGFβ signalling is the trigger of PFA, probably via canonical and non-canonical mechanisms. *In vivo* studies in mice have demonstrated that circulating TGFβ in serum is short lived and therefore a short pulse is enough to trigger an effect on follicle development (Bristol-Gould et al, 2006). Therefore, a short exposure to increase TGFβ1 ligand was used in the *in vitro* experiments in this thesis, in parallel with a short inhibition of TGFβ signalling with an inhibitor of the ALK5 receptor, A 83-01. The effect of these treatments was analysed by the changes in SMAD3 phosphorylation, binding to target genes, regulation of their expression and finally, effect on follicle growth. It was observed that SMAD3 phosphorylation was induced and depleted with the TGFβ1 ligand and the inhibitor, respectively. Moreover, SMAD3 binding to *Ccnd2* and *Myc* remained unaffected with the ligand but was reduced with the inhibitor. Despite the unchanged binding of SMAD3 binding to target genes, *Myc* and *Ccnd2* expression were upregulated, suggesting that non-canonical mechanisms involving SMAD3 binding may contribute to this upregulation. Several TFs acting as co-partners of SMAD3 are known to differently modulate SMAD3 regulation of target genes (Figure 5.17C). Therefore, it is possible that non-canonical TGFβ activation of these SMAD3 co-partners induces an upregulation of *Myc* and *Ccnd2* genes. In support of this, activation of the non-canonical mediators p-ERK1/2 and p-AKT was detected, suggesting MAPK and PI3K signalling pathways cooperate with SMAD3 signalling during PFA.

When follicle growth was evaluated, a subtle increase in the proportion of transitional follicles when compared to controls was observed in the TGFβ1 ligand-treated group. No effect in the proportions of primary or large primary follicles was observed. In contrast, treatment with A 83-01 inhibitor resulted in delayed GC proliferation and impaired germ cell cyst breakdown, as higher number of MOFs were observed, implying that the target cells for TGFβ treatment are the GCs and not the oocytes. Therefore, it was proposed that upregulation of cell cycle genes as a consequence of increased TGFβ signalling in primordial follicles may enhance GCs from some primordial follicles to re-enter cell cycle and initiate PFA. To evaluate the effect of the treatments in follicle growth, ovaries were left for two additional days in culture. A lack of effect in growing follicles suggested that TGFβ stimulation in GCs mainly targets primordial rather than growing GCs. The initiation of proliferation of primordial GCs is slow in physiological conditions. In fact, a previous report by Hirshfield in [3]thymidine-infused rats showed that only 11% of small follicles containing at least one proliferative GC were detected in a period of 48h (Hirshfield, 1991). Moreover, once a GC is active on the cell cycle, it took an average of 24 hours to complete a whole cycle in growing follicles (Hirshfield, 1991). A more recent study using *in vivo* labelling and tracing with *Sohl1*$^{-/-}$ cKO mice (expressed in primordial oocytes) reported that primordial follicles need 7-8 days to develop into primary follicles. Therefore, it is then unlikely that GCs from primordial follicles performed more than two cell divisions after two days of induced activation with TGFβ1 and therefore, it explains why only increased proportion of transitional follicles (up to 7 GCs) were observed after culture.

The observed effect of increased TGFβ signalling in PFA is supported by previous reports that focused on the potential sources of activating/inhibitory signals, where a positive effect (enhanced growth) from growing follicles was observed when located in close proximity with primordial follicles (Da Silva-Buttkus et al, 2009). Since it is well known that growing follicles produce several TGFβ ligands such as GFD9 and activins (Elvin et al, 1999a; Lee et al, 2004; Mizunuma et al, 1999; Nilsson & Skinner, 2003)) it can be postulated that when a "responsive" primordial follicle (e.g supplied with sufficient levels of CCND2/p27) is close to a growing follicle, it may be stimulated by the secreted ligand and activate.

6.2.6 Canonical TGFβ signalling is inhibited after PFA

The nuclear exclusion of SMAD3 in GCs from growing follicles observed in the image analysis and the decreased gene expression levels of *Alk5* receptor in day 8 ovaries (when compared with day 4 ovaries), indicate that the canonical TGFβ/SMAD2/3 signalling is reduced in activated/growing follicles (Figure 6.1). Sustained secretion of TGFβ ligands (e.g from the growing follicles in close proximity) may cause an overactivation of canonical TGFβ signalling that immediately triggers endogenous negative regulation of SMADs in GCs such as SMAD7 or STRAP (Datta & Moses, 2000). Interestingly, increased nuclear SMAD3 and CCND2 staining was observed in some GCs from transitional follicles (Chapter 3), suggesting that at this stage the levels of canonical TGFβ signalling may reach their maximum. As a consequence, the activated non-canonical pathways such as the observed p-ERK1/2 (Chapter 5) can contribute to the inhibitory phosphorylation of Smad3. Activation of p38 or the inhibitory phosphorylation by K4-6 can also participate in this inhibition, as previously reported in other models (Isao et al, 2004; Matsuura et al, 2005a). Since sustained exposure to elevated levels of TGFβ ligand induces GC apoptosis (Chuan-Wei et al, 2001), inhibition of canonical TGFβ signalling seems to be an essential event to allow further follicle growth, and therefore, the canonical and non-canonical mechanisms of inhibition are worthy of further investigation in this context (Figure 6.1).

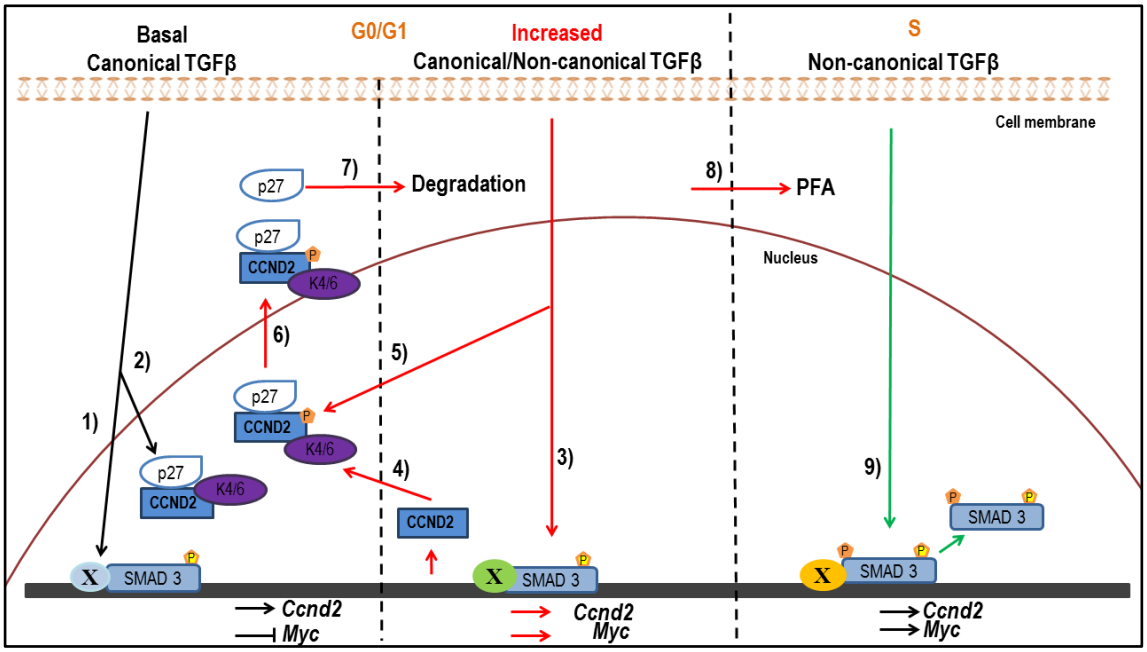

Figure 6.1. Hypothetical model of CCND2/K4-6/p27 complex dynamics and TGFβ regulation in GCs during PFA. (1) Basal TGFβ levels transcriptionally regulate *Ccnd2* and *Myc* genes. (2)This allows the maintenance of CCND2/K4-6/p27 complexes in the nucleus of GCs in G0/G1 phase. (3) After increased TGFβ levels, induction of *Ccnd2* and *Myc* genes facilitates G1 progression. (4) CCND2 levels increase and (5) phosphorylation of CCND2 protein via canonical and non-canonical mechanisms, allows the complex to (6) translocate to the cytoplasm and eventually (7) driving p27 towards degradation to finally, (8) ensure GC transition to S phase and subsequent PFA. (9) After PFA, inhibition of canonical TGFβ signalling is necessary to control proliferation (by self-regulatory mechanisms or inhibitory phosphorylation of Smad3 from non-canonical pathways), releasing the binding of SMAD3 from the promoter of *Ccnd2* and *Myc*. X represents any number of unknown SMAD3 binding partners at basal and increased TGFβ levels, that may participate in the modulation of the expression of *Ccnd2* and *Myc* target genes.

6.3 General conclusion

From the results in this thesis and along with previous findings, it can be concluded that PFA may be an event regulated by both endogenous competence and extracellular signalling, that will determine the order in which follicles activate. If the time that individual follicles activate is dictated by the time GCs specify from their precursors (Capel et al, 2012) a repertoire of factors, in between them, the right balance of CCND2, p27 and complexes may make them more "sensitive" or "responsive" to extracellular signalling. Moreover the location of the source of the "activating" extracellular signal may also determine the sequence of PFA, for instance, their proximity to sources of growth factors (e.g growing follicles) that may facilitate the passage through R1 and R2 from the G1 phase of the cell cycle, respectively. The molecular pathways regulating Ccnd2 levels transcriptionally and post-translationally may play an important role during PFA. This thesis has focused on the regulation at transcriptional level, where SMAD3 binding to *Ccnd2* gene maintains its levels in GCs at G0/early G1 phase and upregulates them with the cooperation of additionally activated non-canonical mediators after a short increase in TGFβ extracellular signalling. This likely facilitates the passage of GCs to S phase, allowing cell cycle progression. After this stage, inhibition of the canonical TGFβ signalling while maintenance of non-canonical pathways may be necessary to control cell cycle progression in growing follicles (Figure 6.2). This switch from maintenance to activation explains the different effects reported about TGFβ treatment in primordial follicles and provides new molecular insight about how changes in TGFβ levels could probably induce a partial EMT-like phenotypical change in GCs.

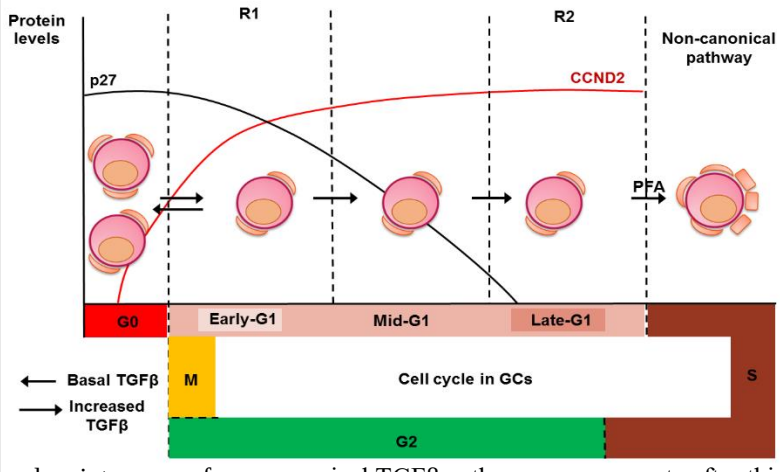

Figure 6.2. PFA depends on TGFβ levels. GCs from primordial follicles remain in G0/early G1 phase under basal conditions of TGFβ signalling. Increase in TGFβ signalling upregulates CCND2 expression and facilitates passage through S phase (PFA). Inhibition of canonical and maintenance of non-canonical TGFβ pathways may operate after this time to ensure GC proliferation.

6.4 Limitations

The main limitation in this thesis is the use of the mouse model. Although early follicle growth in mice shows similar dynamics with human (Zheng et al, 2014b), differences in growth rates, size and follicle competence exist between them (Griffin et al, 2006). Moreover, since mice are poly-ovulatory and humans are mono-ovulatory, specific molecular pathways may operate differently between species. Therefore, the use of nonhuman primate and finally human ovary culture models is essential to validate the information obtained in mice. In addition, the mouse model used in this thesis focuses at pre-pubertal age. Although the mechanisms may be similar in small follicles in older ages, further work should be done to investigate whether the proposed mechanisms are also found in post-pubertal tissue. Concerning technical limitations, obtaining starting material from ovarian tissue has been the main difficulty. Since the use of whole ovaries have been used as a model in order to preserve the molecular biology of the intact tissue, a minimal number of animals was used for the experimental design. This was sometimes a limitation for the number of replicates per treatment/sample used, and reduced the statistical power in some occasions. Moreover, the low amount of chromatin, RNA, protein obtained from uncultured and cultured ovaries and the limited number of middle cross-sections from cultured ovaries also limited the range of factors that could be analysed. Another limitation has been the number of target genes that could be analysed; for instance, the poor DNA recovery after the ChIP procedure only provided enough material for *Ccnd2* and *Myc* genes. It is entirely possible that SMAD3 binding to other cell cycle genes are increased or decreased after the treatments, providing a more defined scenario of the canonical/non-canonical activation in TGFβ-treated ovaries. In addition, although primers for ChiP-qPCR were designed to amplify regions enriched in SMAD3 binding domains, the impossibility of designing good primers flanking only the repressive binding domains (TIE) and activating binding domains (SBE) was not possible, which would have provided a better idea of the repressive or activating effect of the TGFβ treatment/inhibition by the change in SMAD3 binding to this regions. With regards to the optimisation of the treatments in the ovary culture, only two short time points and a single dose (for both TGFβ1 and inhibitor) were chosen based on the treatments with the cell line. However, the selection of two additional time points (e.g 4 hours and 24 hours) would have been appropriate to map the differences in expression and follicle growth after longer treatments. Moreover, the addition of ovaries treated with a sustained TGFβ signalling (e.g 24 hours) for the assessment of follicle growth would have also allowed

results to be compared with previous reports that argue the inhibitory role of sustained TGFβ1 treatment.

6.5 Future work

This work has established the foundations of a new model of TGFβ regulation in the neonatal ovary and has used molecular tools and approaches to test the effect of this regulation on PFA. It also proposes a molecular model of PFA that relies on the balance between individual follicle competence (such as expression of *Ccnd2* and presence of CCND2/K4-6/p27 complexes) and the exposure to extracellular ligands (such as TGFβ ligands). The ovary culture model employed in this thesis can be used to test this hypothesis further. Therefore, the next directions for the future work are described below:

Cell cycle dynamics

Since p27 is expressed in all mitotically arrested GCs from the fetal ovary (Gustin et al, 2016) and CCND2 is proposed to be the trigger that allows GC exit from G0/G1 phase, the following experiments can be performed:

1) Immunofluorescence staining and detailed quantification of the ratio of intensities of CCND2 and p27 in somatic cells surrounding GCs from primordial follicles can be performed to determine the moment where CCND2 increases its levels. This may identify a relationship between expression levels and location in the ovary, and also complement and provide new information to the existing evidence of the possible source/s of activation (e.g growing follicles)(Da Silva-Buttkus et al, 2009).

2) IPs and/or PLA assay after treatment with TGFβ ligand or TGFβ inhibitor, to determine in which conditions CCND2/p27 complexes are maintained and dissociated, also studying the catalytic or non-catalytic activity of the detected complexes by using kinase assays (Warner et al, 1999).

Effect of different ligands on follicle activation and growth

This work has focused on the effect of TGFβ1 ligand at the molecular and morphological levels in early follicle development. However, future work may include the use of other TGFβ ligands (such as GDF9) either alone or in combination with other ligands.

For instance, since the use of PTEN inhibitors has shown impaired rate of GC proliferation and follicle atresia, the use of a combination of short treatment with TGFβ ligands followed by treatment with PTEN inhibitors may help determine whether the initial increase in TGFβ ligands facilitates follicles to enhance GC proliferation and grow normally.

The ligands that show an effect in any aspect of PFA can then be tested in other ovary culture models in mice (such as the neonatal ovary fragment culture) or in other species such as nonhuman primates (Telfer & Zelinski, 2013). Finally, the potential candidates can be validated in human tissues in *vitro*, by using approaches such as the culture of ovarian cortical biopsies alongside a vital dye (neutral dye) for a more accurate determination of their effect on PFA (Soleimani & De Sutter, 2011).

SMAD gene regulation, binding partners and non-canonical pathway activation

The molecular techniques employed in this thesis can be used on a" –omic" scale in order to get a more detailed scenario of the molecular events operating in primordial follicles and PFA. The treatment model (short stimulation with TGFB1 ligand), can be used together with next-generation sequencing after ChIP (ChIP-Seq) and RNA sequencing (RNA-Seq) to map the different SMAD3 target genes in primordial follicles under basal conditions and to identify a snapshot of the key molecular changes after a short stimulation with TGFβ1. Moreover, the activation of different pathways (canonical and non-canonical) can also be studied by analysing the phospho-proteome of the ovaries under these treatments by non-targeted Mass Spectrometry (MS/MS), which will facilitate the identification of factors from other pathways that, in conjunction with Smads, play a role in cell cycle regulation during PFA.

6.6 Scientific and clinical implications

The information obtained from this thesis and the proposed future work provides additional knowledge to the biology of the ovary, however, it also benefits other areas of research. Since understanding the mechanisms that regulate exit from the cell cycle still remains unresolved in many cell types, any novel molecular information related to the initiation of cell proliferation in GCs may also provide new insights in other systems, such as the activation and proliferation of beta-pancreatic cells (recently known to be dependent on CCND2) (Stamateris et al, 2016) or the development of some cancerous phenotypes by a TGFβ-driven EMT, such as the case of epithelial cells during mammary gland involution (Guo et al, 2017). With regards to ovary research, the identification of specific factors operating in primordial GCs may allow the development of transgenic cKO mice with promoters to be used as locus for Cre recombinase in primordial GCs, as with the already used GC marker FOXL2.

The clinical implications of the present and future work are numerous. For instance, the knowledge of potential candidates that specifically target both the GCs and oocytes of primordial follicles and enhance/inhibit their activation may allow the development of specific small inhibitory molecules that "protect" the primordial follicles. This may give the opportunity to both young and adult women to preserve their ovarian reserve during cancer treatment or during the normal process of aging. Moreover, the identified candidates (if produced in sufficient amounts in body fluids) can be also employed as direct biomarkers of ovarian reserve, to complement or replace the currently used methods (AFC and determination of serum AMH). Finally, the relationship between these candidates and primordial follicle quality may also add another dimension to the assessment of the ovarian reserve, and allow an early diagnosis of the reproductive potential of women with specific fertility conditions such as POI and PCOS.

References

Abel, M. H., Wootton, A. N., Wilkins, V., Huhtaniemi, I., Knight, P. G. & Charlton, H. M. (2000) The effect of a null mutation in the follicle-stimulating hormone receptor gene on mouse reproduction. *Endocrinology*, 141(5), 1795-803.

Acmaz, G., Albayrak, E., Acmaz, B., Baser, M., Soyak, M., Zararsiz, G. & IpekMuderris, I. (2013) Level of Anxiety, Depression, Self- Esteem, Social Anxiety, and Quality of Life among the Women with Polycystic Ovary Syndrome. *SCIENTIFIC WORLD JOURNAL*.

Adhikari, D. & Liu, K. (2009) Molecular mechanisms underlying the activation of mammalian primordial follicles. *Endocrine reviews*, 30(5), 438.

Alarcón, C., Zaromytidou, A.-I., Xi, Q., Gao, S., Yu, J., Fujisawa, S., Barlas, A., Miller, A. N., Manova-Todorova, K., Macias, M. J., Sapkota, G., Pan, D. & Massagué, J. (2009) Nuclear CDKs Drive Smad Transcriptional Activation and Turnover in BMP and TGF-β Pathways. *Cell*, 139(4), 757-769.

Albanese, C., Johnson, J., Watanabe, G., Eklund, N., Vu, D., Pestell, R. G. & Arnold, A. (1995) Transforming p21 ras mutants and c- Ets- 2 activate the cyclin D1 promoter through distinguishable regions. *Journal of Biological Chemistry*, 270(40), 23589-23597.

Anttonen, M., Pihlajoki, M., Andersson, N., Georges, A., Hôte, D., Vattulainen, S., Färkkilä, A., Unkila-Kallio, L., Veitia, R. A. & Heikinheimo, M. (2014) FOXL2, GATA4, and SMAD3 co-operatively modulate gene expression, cell viability and apoptosis in ovarian granulosa cell tumor cells. *PloS one*, 9(1), e85545.

Arcellana-Panlilio, M. Y., Egeler, R. M., Ujack, E., Magliocco, A., Stuart, G. C. E., Robbins, S. M. & Coppes, M. J. (2002) Evidence of a role for the INK4 family of cyclin-dependent kinase inhibitors in ovarian granulosa cell tumors. *Genes, Chromosomes and Cancer*, 35(2), 176-181.

Arden, K. C. & Biggs, W. H., 3rd (2002) Regulation of the FoxO family of transcription factors by phosphatidylinositol-3 kinase-activated signaling. *Arch Biochem Biophys*, 403(2), 292-8.

Attisano, L. & Wrana, J. L. (2013) Signal integration in TGF- β, WNT, and Hippo pathways. *F1000prime reports*, 5, 17.

Baghirova, S., Hughes, B. G., Hendzel, M. J. & Schulz, R. (2015) Sequential fractionation and isolation of subcellular proteins from tissue or cultured cells. *MethodsX*, 2, 440-445.

Bagui TK , M. S., Haura E , Pledger WJ . (2003) P27Kip1 and p21Cip1 are not required for the formation of active D cyclin-cdk4 complexes. *Molecular Cell Biology*, 23(20), 7285-90.

Baird, D. T., Balen, A., Escobar-Morreale, H. F., Evers, J. L. H., Fauser, B., Franks, S., Glasier, A., Homburg, R., La Vecchia, C., Crosignani, P. G., Devroey, P., Diedrich, K., Fraser, L., Gianaroli, L., Liebaers, I., Sunde, A., Tapanainen, J. S., Tarlatzis, B., Van Steirteghem, A. & Veiga, A. (2012) Health and fertility in World Health Organization group 2 anovulatory women. *Human Reproduction Update.*

Benayoun, B. A. & Veitia, R. A. (2009) A post- translational modification code for transcription factors: sorting through a sea of signals. *Trends in Cell Biology*, 19(5), 189-197.

Bentsi-Barnes, I. K., Kuo, F.-T., Barlow, G. M. & Pisarska, M. D. (2010) Human forkhead L2 represses key genes in granulosa cell differentiation including aromatase, P450scc, and cyclin D2. *Fertility and Sterility*, 94(1), 353-356.

Bernard, D. J. (2004) Both SMAD2 and SMAD3 mediate activin-stimulated expression of the follicle-stimulating hormone beta subunit in mouse gonadotrope cells. *Molecular Endocrinology*, 18(3), 606-23.

Bhowmick, N. A., Ghiassi, M., Bakin, A., Aakre, M., Lundquist, C. A., Engel, M. E., Arteaga, C. L. & Moses, H. L. (2001) Transforming growth factor- beta1 mediates epithelial to mesenchymal transdifferentiation through a RhoA- dependent mechanism. *Molecular biology of the cell*, 12(1), 27.

Blain, S. W. (2008) Switching cyclin D- Cdk4 kinase activity on and off. *Cell cycle (Georgetown, Tex.)*, 7(7), 892.

Block (1952) Quantitative morphological investigations of the follicular system in women; variations at different ages. *Acta Anatomica (Basel)*, 14(1-2), 108-23.

Block (1953) A quantitative morphological investigation of the follicular system in newborn female infants. *Acta Anatomica (Basel)*, 17(3), 201-6

Blount, A. L., Schmidt, K., Justice, N. J., Vale, W. W., Fischer, W. H. & Bilezikjian, L. M. (2009) FoxL2 and Smad3 coordinately regulate follistatin gene transcription. *Journal of Biological Chemistry*, 284(12), 7631-45.

Bouchard, C., Kiermaier, A., Eilers, M., Dittrich, O., Dohmann, K., Menkel, A. & Lüscher, B. (2001) Regulation of cyclin D2 gene expression by the Myc/ Max/ Mad network: Myc- dependent TRRAP recruitment and histone acetylation at the cyclin D2 promoter. *Genes and Development*, 15(16), 2042-2047.

Bowles, J. & Koopman, P. (2007) Retinoic acid , meiosis and germ cell fate in mammals. *Development (Cambridge, England)*, 134(19), 3401-11.

Brambillasca, F., Guglielmo, M., Coticchio, G., Mignini Renzini, M., Dal Canto, M. & Fadini, R. (2013) The current challenges to efficient immature oocyte cryopreservation. *Journal of Assisted Reproduction and Genetics*, 30(12), 1531-9.

Braw-Tal, R. (2002) The initiation of follicle growth: the oocyte or the somatic cells? *Molecular Cell Endocrinoly*, 187(1-2), 11-8.

Bristol-Gould, S. K., Kreeger, P. K., Selkirk, C. G., Kilen, S. M., Cook, R. W., Kipp, J. L., Shea, L. D., Mayo, K. E. & Woodruff, T. K. (2006) Postnatal regulation of germ cells by activin: The establishment of the initial follicle pool. *Developmental Biology*, 298(1), 132-148.

Browne, J. A., Liu, X., Schnaper, H. W. & Hayashida, T. (2013) Serine- 204 in the linker region of Smad3 mediates the collagen- I response to TGF- β in a cell phenotype- specific manner. *Experimental Cell Research*.

Brunet, A., Bonni, A., Zigmond, M. J., Lin, M. Z., Juo, P., Hu, L. S., Anderson, M. J., Arden, K. C., Blenis, J. & Greenberg, M. E. (1999) Akt promotes cell survival by phosphorylating and inhibiting a Forkhead transcription factor. *Cell*, 96(6), 857-68.

Bullejos, M. & Koopman, P. (2004) Germ cells enter meiosis in a rostro- caudal wave during development of the mouse ovary. *Molecular Reproduction and Development*, 68(4), 422-428.

Burns KH 1 , Y. C., Kumar TR , Matzuk MM . (2001) Analysis of ovarian gene expression in follicle-stimulating hormone beta knockout mice. *Endocrinology*, 142(7), 2742-51.

Campos-Junior, P. H. A., Marinho Assuncao, C., Carvalho, B. C., Batista, R. I. T. P., Garcia, R. M. G. & Viana, J. H. M. (2012) Follicular populations, recruitment and atresia in the ovaries of different strains of mice. *Reproductive biology*, 12(1), 41.

Capel, B., Mork, L., Maatouk, D. M., McMahon, J., McMahon, A. P. & Zhang, P. (2012) Temporal differences in granulosa cell specification in the ovary reflect distinct follicle fates. *Human Reproduction*, 27.

Carlsson, I., Scott, J., Visser, J., Ritvos, O. & Hovatta, O. (2006) Anti- Müllerian hormone inhibits initiation of growth of human primordial ovarian follicles in vitro. *Human Reproduction*, 21(9), 2223-7.

Casanovas, O., Miró, F., Estanyol, J. M., Itarte, E., Agell, N. & Bachs, O. (2000) Osmotic stress regulates the stability of cyclin D1 in a p38(SAPK2)- dependent manner. *Journal of Biological Chemistry*, 275(45), 35091-35097.

Castrillon, D. H., Miao, L., Kollipara, R., Horner, J. W., Depinho, R. A. & DePinho, R. A. (2003) Suppression of Ovarian Follicle Activation in Mice by the Transcription Factor Foxo3a. *Science*, 301(5630), 215-218.

Chalhoub, N. & Baker, S. J. (2009) PTEN and the PI3- Kinase Pathway in Cancer. *Annual Review of Pathology,* 4, 127-150.

Chegini, N., Flanders KC. (1992) Presence of transforming growth factor-beta and their selective cellular localization in human ovarian tissue of various reproductive stages. *Endocrinology*, 130(3), 1707-15.

Cheng, M., Olivier, P., Diehl, J. A., Fero, M., Roussel, M. F., Roberts, J. M. & Sherr, C. J. (1999) The p21 Cip1 and p27 Kip1 CDK ' inhibitors' are essential activators of cyclin D- dependent kinases in murine fibroblasts. *EMBO Journal*, 18(6), 1571-1583.

Childs, A. J. & Anderson, R. A. (2009) Activin A selectively represses expression of the membrane-bound isoform of Kit ligand in human fetal ovary. *Fertility and Sterily*, 92(4), 1416-9.

Childs, A. J., Cowan, G., Kinnell, H. L., Anderson, R. A., Saunders, P. T. K. & Clarke, H. (2011) Retinoic Acid Signalling and the Control of Meiotic Entry in the Human Fetal Gonad. *PLoS one*, 6(6).

Childs, A. J. & McNeilly, A. S. (2012) Epithelial -to-Mesenchymal Transition in Granulosa Cells : A Key to Activation of Follicle Growth? *Biology of Reproduction,* 86 (5).

Choi, Y., Yuan, D. & Rajkovic, A. (2008) Germ cell- specific transcriptional regulator sohlh2 is essential for early mouse folliculogenesis and oocyte- specific gene expression. *Biology of reproduction*, 79(6), 1176.

Christopher, B. (2000) Immunolocalization of transforming growth factor-beta1 during follicular development and atresia in the mouse ovary. *Endocr J*, 47(4), 475-80.

Chuan-Wei, J., Chun-Hau, C., Chun-Chieh, C., Jia-Yun, C., Yi-Hsien, S. & Ruey-Hwa, C. (2001) TGF-β induces apoptosis through Smad- mediated expression of DAP- kinase. *Nature Cell Biology*, 4(1), 51.

Clarke, D. C., Brown, M. L., Erickson, R. A., Shi, Y. & Liu, X. (2009) Transforming growth factor beta depletion is the primary determinant of Smad signaling kinetics. *Molecular and cellular biology*, 29(9), 2443.

Compston, J. (2001) Sex Steroids and Bone.*Physiological Reviews*, 81 (1), 419-447.

Conery, A. R., Cao, Y., Thompson, E. A., Townsend, C. M., Ko, T. C. & Luo, K. (2004) Akt interacts directly with Smad3 to regulate the sensitivity to TGF-beta-induced apoptosis. *Nature Cell Biology*, 6(4).

Coutts, S. M., Childs, A. J., Fulton, N., Collins, C., Bayne, R. A., McNeilly, A. S. & Anderson, R. A. (2008) Activin signals via SMAD2/3 between germ and somatic cells in the human fetal ovary and regulates kit ligand expression. *Developmental Biology*, 314(1), 189-99.

Cox, R. T. & Spradling, A. C. (2003) A Balbiani body and the fusome mediate mitochondrial inheritance during Drosophila oogenesis. *Development (Cambridge, England)*, 130(8), 1579.

Crisponi, L., Deiana, M., Loi, A., Chiappe, F., Uda, M., Amati, P., Bisceglia, L., Zelante, L., Nagaraja, R., Porcu, S., Ristaldi, M. S., Marzella, R., Rocchi, M., Nicolino, M., Lienhardt-Roussie, A., Nivelon, A., Verloes, A., Schlessinger, D., Gasparini, P., Bonneau, D., Cao, A. & Pilia, G. (2001) The putative forkhead transcription factor FOXL2 is mutated in blepharophimosis/ptosis/epicanthus inversus syndrome. *Nature Genetics*, 27(2), 159-66.

Da Silva-Buttkus, P., Jayasooriya, G. S., Mora, J. M., Mobberley, M., Ryder, T. A., Baithun, M., Stark, J., Franks, S. & Hardy, K. (2008) Effect of cell shape and packing density on granulosa cell proliferation and formation of multiple layers during early follicle development in the ovary. *Journal of Cell Science*, 121(23), 3890-3900.

Da Silva-Buttkus, P., Marcelli, G., Franks, S., Stark, J. & Hardy, K. (2009) Inferring biological mechanisms from spatial analysis: Prediction of a local inhibitor in the ovary. *Proceedings of the National Academy of Sciences of the United States of America*, 106(2), 456-461.

Datta, P. K. & Moses, H. L. (2000) STRAP and Smad7 synergize in the inhibition of transforming growth factor beta signaling. *Molecular and cellular biology*, 20(9), 3157-67.

Davies, M., Robinson, M., Smith, E., Huntley, S., Prime, S. & Paterson, I. (2005) Induction of an epithelial to mesenchymal transition in human immortal and malignant keratinocytes by TGF- β1 involves MAPK, Smad and AP- 1 signalling pathways. *Journal of Cellular Biochemistry*, 95(5), 918-931.

de Bruin, J. P., Dorland, M., Spek, E. R., Posthuma, G., van Haaften, M., Looman, C. W. N. & Velde, E. R. (2002) Ultrastructure of the Resting Ovarian Follicle Pool in Healthy Young Women. *Biology of Reproduction*, 66(4), 1151-1160.

De Vos, M., Devroey, P. & Fauser, B. C. J. M. (2010) Primary ovarian insufficiency. *The Lancet*, 376(9744), 911-921.

De Vos, M., Smitz, J. & Woodruf, T. (2015) Fertility preservation in women with cancer (vol 384, pg 1302, 2014). *The Lancet*, 385(9971), 856-856.

Derynck, R. & Akhurst, R. J. (2007) Differentiation plasticity regulated by TGF-β family proteins in development and disease. *Nature Cell Biology*, 9(9), 1000-1004.

Devine, P. J., Payne, C. M., McCuskey, M. K. & Hoyer, P. B. (2000) Ultrastructural Evaluation of Oocytes During Atresia in Rat Ovarian Follicles 1. *Biology of Reproduction*, 63(5), 1245-1252.

Di Pasquale, E., Beck-Peccoz, P. & Persani, L. (2004) Hypergonadotropic ovarian failure associated with an inherited mutation of human bone morphogenetic protein-15 (BMP15) gene. *The American Journal of Human Genetics*, 75(1), 106-11.

Diehl, J. A., Cheng, M., Roussel, M. F. & Sherr, C. J. (1998) Glycogen synthase kinase-3beta regulates cyclin D1 proteolysis and subcellular localization. *Genes and Development*, 12(22), 3499-511.

Ding, C. C., Thong, K. J., Krishna, A. & Telfer, E. E. (2010) Activin A inhibits activation of human primordial follicles in vitro. *Journal of Assisted Reproduction and Genetics*, 27(4), 141-7.

Ding, X., Zhang, X., Mu, Y., Li, Y. & Hao, J. (2013) Effects of BMP4/SMAD signaling pathway on mouse primordial follicle growth and survival via up-regulation of Sohlh2 and c-kit. *Molecular Reproduction and Development*, 80(1), 70-8.

Dole, G., Nilsson, E. E. & Skinner, M. K. (2008) Glial-derived neurotrophic factor promotes ovarian primordial follicle development and cell-cell interactions during folliculogenesis. *Reproduction*, 135(5), 671-82.

Dong, J., Albertini, D. F., Nishimori, K., Kumar, T. R., Lu, N. & Matzuk, M. M. (1996) Growth differentiation factor-9 is required during early ovarian folliculogenesis. *Nature*, 383(6600), 531-5.

Drummond, A. E., Minh Tan, J.-F., Ethier, M., Dyson, J. K. & Findlay, J. K. (2002) Expression and localization of activin receptors, Smads, and βglycan to the postnatal rat ovary. *Endocrinology*, 143(4), 1423-1433.

Dumesic, D. A. & Richards, J. S. (2013) Ontogeny of the ovary in polycystic ovary syndrome. *Fertility and Sterility*, 100(1), 23-38.

Durlinger, A. L., Gruijters, M. J., Kramer, P., Karels, B., Ingraham, H. A., Nachtigal, M. W., Uilenbroek, J. T., Grootegoed, J. A. & Themmen, A. P. (2002a) Anti-Mullerian hormone inhibits initiation of primordial follicle growth in the mouse ovary. *Endocrinology*, 143(3), 1076-84.

Durlinger, A. L., Kramer, P., Karels, B., de Jong, F. H., Uilenbroek, J. T., Grootegoed, J. A. & Themmen, A. P. (1999) Control of primordial follicle recruitment by anti-Mullerian hormone in the mouse ovary. *Endocrinology*, 140(12), 5789-96.

Durlinger, A. L., Visser, J. A. & Themmen, A. P. (2002b) Regulation of ovarian function: the role of anti-Mullerian hormone. *Reproduction*, 124(5), 601-9.

Edlund, S., Lee, S. Y., Grimsby, S., Zhang, S., Aspenström, P., Heldin, C.-H. & Landström, M. (2005) Interaction between Smad7 and beta- catenin: importance for transforming growth factor beta- induced apoptosis. *Molecular And Cellular Biology*, 25(4), 1475-1488.

Edson, M. A., Nagaraja, A. K. & Matzuk, M. M. (2009) The Mammalian Ovary from Genesis to Revelation. *Endocrine Reviews*, 30(6), 624-712.

Elvin, J. A., Clark, A. T., Wang, P., Wolfman, N. M. & Matzuk, M. M. (1999a) Paracrine actions of growth differentiation factor- 9 in the mammalian ovary. *Molecular endocrinology (Baltimore, Md.)*, 13(6), 1035.

Elvin, J. A., Yan, C., Wang, P., Nishimori, K. & Matzuk, M. M. (1999b) Molecular characterization of the follicle defects in the growth differentiation factor 9-deficient ovary. *Molecular Endocrinology*, 13(6), 1018-34.

Eppig, J. (2001) Oocyte control of ovarian follicular development and function in mammals. *Reproduction*, 122(6), 829-838.

Eppig, J. J., Brien, M. & Wigglesworth, K. (1996) Mammalian oocyte growth and development in vitro. *Molecular Reproduction and Development*. 44(2), 260-73.

Eppig, J. J. & Brien, M. J. (1996) Development in vitro of mouse oocytes from primordial follicles. *Biology of reproduction*, 54(1), 197.

Eppig, J. J., Wigglesworth, K. & Pendola, F. L. (2002) The Mammalian Oocyte Orchestrates the Rate of Ovarian Follicular Development. *Proceedings of the National Academy of Sciences of the United States of America*, 99(5), 2890-2894.

Faddy, M. J. (2000) Follicle dynamics during ovarian ageing. *Molecular Cell Endocrinology*, 163(1-2), 43-8.

Faddy, M. J. & Gosden, R. G. (1996) A model conforming the decline in follicle numbers to the age of menopause in women. *Human Reprodruction*, 11(7), 1484-6.

Faddy, M. J., Gosden, R. G., Gougeon, A., Richardson, S. J. & Nelson, J. F. (1992) Accelerated disappearance of ovarian follicles in mid-life: implications for forecasting menopause. *Human reproduction (Oxford, England)*, 7(10), 1342.

Felici, A., Wurthner, J. U., Parks, W. T., Ruh-Yu Giam, L., Reiss, M., Karpova, T. S., Mcnally, J. G. & Roberts, A. B. (2003) TLP , a novel modulator of TGF - β signaling , has opposite effects on Smad2 - and Smad3 - dependent signaling. *EMBO Journal*, 22(17), 4465-4477.

Fenwick, M. A. & Hurst, P. R. (2002) Immunohistochemical localization of active caspase-3 in the mouse ovary: growth and atresia of small follicles. *Reproduction (Cambridge, England)*, 124(5), 659.

Fenwick, M. A., Mansour, Y. T., Franks, S. & Hardy, K. (2011) Identification and Regulation of Bone Morphogenetic Protein Antagonists Associated with Preantral Follicle Development in the Ovary. *Endocrinology*, 152(9), 3515-3526.

Fenwick, M. A., Mora, J. M., Mansour, Y. T., Baithun, C., Franks, S. & Hardy, K. (2013) Investigations of TGF-beta Signaling in Preantral Follicles of Female Mice Reveal Differential Roles for Bone Morphogenetic Protein 15. *Endocrinology*, 154(9), 3423-3436.

Findlay , J. K., Hutt, K. J., Hickey, M. & Anderson, R. A. (2015) What is the "ovarian reserve"? *Fertility and Sterility*.

Fink, S. P., Mikkola, D., Willson, J. K. V. & Markowitz, S. (2003) TGF- beta- induced nuclear localization of Smad2 and Smad3 in Smad4 null cancer cell lines. *Oncogene*, 22(9), 1317.

Forabosco, A. & Sforza, C. (2007) Establishment of ovarian reserve : a quantitative morphometric study of the developing human ovary. *Fertility and Sterility*, Vol.88(3), 675-683.

Fortune Joanne E. , Yang Ming Y. ,and Muruvi Wanzirai (2011). I*n vitro* and i*n vivo* regulation of follicular formation and activation in cattle. *Reproduction, Fertility and Development*, 23(1), 15–22.

Foster, D. A., Yellen, P., Xu, L. & Saqcena, M. (2011) Regulation of G1 cell cycle progression: Distinguishing the restriction point from a nutrient-sensing cell growth checkpoint(s). *Genes and Cancer*, 1(11), 1124-1131.

Frank, B., Daniel, V., Jean, D., Marc, F. & Reiner, A. V. (2007) Potential targets of FOXL2, a transcription factor involved in craniofacial and follicular development, identified by transcriptomics. *Proceedings of the National Academy of Sciences*, 104(9), 3330.

Franks, S., Stark, J. & Hardy, K. (2008) Follicle dynamics and anovulation in polycystic ovary syndrome. *Human Reproduction Update*, 14(4), 367-378.

Gallagher, JC., (2007) Effect of early menopause on bone mineral density and fractures. *Menopause*, 14 (3 Pt 2), 567-71.

Gallardo, T., John, G., Lane, S. & Contreras, C. (2007) Genomewide Discovery and Classification of Candidate Ovarian Fertility Genes in the Mouse. *Genetics*, 177(1), 179-94.

Galloway, S. M., McNatty, K. P., Cambridge, L. M., Laitinen, M. P., Juengel, J. L., Jokiranta, T. S., McLaren, R. J., Luiro, K., Dodds, K. G., Montgomery, G. W., Beattie, A. E., Davis, G. H. & Ritvos, O. (2000) Mutations in an oocyte-derived growth factor gene (BMP15) cause increased ovulation rate and infertility in a dosage-sensitive manner. *Nature Genetics*, 25(3), 279-83.

Gao, S., Alarcón, C., Sapkota, G., Rahman, S., Chen, P.-Y., Goerner, N., Macias, M. J., Erdjument-Bromage, H., Tempst, P. & Massagué, J. (2009) Ubiquitin Ligase Nedd4L Targets Activated Smad2/ 3 to Limit TGF-β Signaling. *Molecular Cell*, 36(3), 457-468.

Garcia-Ortiz, J. E., Pelosi, E., Omari, S., Nedorezov, T., Piao, Y., Karmazin, J., Uda, M., Cao, A., Cole, S. W., Forabosco, A., Schlessinger, D. & Ottolenghi, C. (2009) Foxl2 functions in sex determination and histogenesis throughout mouse ovary development. *BMC Developmental Biology*.

Gigli, I., Cushman, R. A., Wahl, C. M. & Fortune, J. E. (2005) Evidence for a role for anti-Müllerian hormone in the suppression of follicle activation in mouse ovaries and bovine ovarian cortex grafted beneath the chick chorioallantoic membrane. *Molecular Reproduction and Development*, 71(4), 480-488.

Ginzinger, D. G. (2002) Gene quantification using real- time quantitative PCR: An emerging technology hits the mainstream. *Experimental Hematology*, 30(6), 503-512.

Gittens, J. E. & Kidder, G. M. (2005) Differential contributions of connexin37 and connexin43 to oogenesis revealed in chimeric reaggregated mouse ovaries. *Journal of Cell Science*, 118(Pt 21), 5071-8.

Gougeon, A., Ecochard, R. & Thalabard, J. C. (1994) Age-related changes of the population of human ovarian follicles: increase in the disappearance rate of non-growing and early-growing follicles in aging women. *Biology of reproduction*, 50(3), 653.

Griffin, J., Emery, B. R., Huang, I., Peterson, C. M. & Carrell, D. T. (2006) Comparative analysis of follicle morphology and oocyte diameter in four mammalian species (mouse, hamster, pig, and human). *Journal of experimental and clinical assisted reproduction*, 3, 2.

Gueripel, X., Benahmed, M. & Gougeon, A. (2004) Sequential gonadotropin treatment of immature mice leads to amplification of transforming growth factor beta action, via upregulation of receptor-type 1, Smad 2 and 4, and downregulation of Smad 6. *Biolofy of Reproduction*, 70(3), 640-8.

Guo, K., Li, C.-h., Wang, X.-y., He, D.-j. & Zheng, P. (2016) Germ stem cells are active in postnatal mouse ovary under physiological conditions. *MHR: Basic science of reproductive medicine*, 22(5), 316-328.

Guo, Q., Betts, C., Pennock, N., Mitchell, E., Schedin, P. & Turtoi, A. (2017) Mammary Gland Involution Provides a Unique Model to Study the TGF- β Cancer Paradox. *Journal of Clinical Medicine*, 6(1).

Gupta, S. K., Bhandari, B., Shrestha, A., Biswal, B. K., Palaniappan, C., Malhotra, S. S. & Gupta, N. (2012) Mammalian zona pellucida glycoproteins: structure and function during fertilization. *Cell Tissue Research*, 349(3), 665-678.

Gustin, S. E., Hogg, K., Stringer, J. M., Rastetter, R. H., Pelosi, E., Miles, D. C., Sinclair, A. H., Wilhelm, D. & Western, P. S. (2016) WNT / β - catenin and p27 / FOXL2 differentially regulate supporting cell proliferation in the developing ovary. *Developmental Biology*, 412(2), 250-60.

Hansen, K. R., Hodnett, G. M., Knowlton, N. & Craig, L. B. (2011) Correlation of ovarian reserve tests with histologically determined prim ordial follicle number. *Fertility and Sterility*, 95(1), 170-175.

Hansen, K. R., Knowlton, N. S., Thyer, A. C., Charleston, J. S., Soules, M. R. & Klein, N. A. (2008) A new model of reproductive aging: the decline in ovarian non-growing follicle number from birth to menopause. *Human. Reproduction.*, 23(3), 699-708.

Harikae, K., Miura, K., Shinomura, M., Matoba, S., Hiramatsu, R., Tsunekawa, N., Kanai-Azuma, M., Kurohmaru, M., Morohashi, K.-I. & Kanai, Y. (2013) Heterogeneity in sexual bipotentiality and plasticity of granulosa cells in developing mouse ovaries. *Journal of cell science*, 126(Pt 13), 2834-44.

Heldin, C.-H., Landström, M. & Moustakas, A. (2009) Mechanism of TGF- β signaling to growth arrest, apoptosis, and epithelial– mesenchymal transition. *Current Opinion in Cell Biology*, 21(2), 166-176.

Henderson SA , E. R. (1968) Chiasma frequency and maternal age in mammals. *Nature*, 218(5136), 22-28.

Hernandez ,SF.,Vahidi, NA., Park, S., Weitzel, R. P., Tisdale, J., R. Rueda, B. & Erin, F. W. (2015) Characterization of extracellular DDX4- or Ddx4- positive ovarian cells. *Nature Medicine*, 21(10), 1114.
Hill, C. S. (2008) Nucleocytoplasmic shuttling of Smad proteins. *Cell Research*, 19(1), 36-46.

Hirshfield, A. (1991) Development of mammalian follicles in the ovary. *International Review of Citology*, 124, 43-101.

Hirshfield, A. N. (1992) Heterogeneity of cell populations that contribute to the formation of primordial follicles in rats. *Biology of reproduction*, 47(3), 466.

Holaska, J. M., Wilson, K. L. & Mansharamani, M. (2002) The nuclear envelope, lamins and nuclear assembly. *Current Opinion in Cell Biology*, 14(3), 357-364.

Horie, K., Takakura, K., Taii, S., Narimoto, K., Noda, Y., Nishikawa, S., Nakayama, H., Fujita, J. & Mori, T. (1991) The expression of c-kit protein during oogenesis and early embryonic development. *Biology of Reproduction*, 45(4), 547-52.

Hough, C., Radu, M. & Doré, J. J. E. (2012) TGF- Beta Induced Erk Phosphorylation of Smad Linker Region Regulates Smad Signaling, *PLoS One*, 7(8), e42513.

Huang, J. Y. J., Tulandi, T., Holzer, H., Tan, S. L. & Chian, R.-C. (2008) Combining ovarian tissue cryobanking with retrieval of immature oocytes followed by in vitro maturation and vitrification: an additional strategy of fertility preservation. *Fertility and Sterility*, 89(3), 567-572.

Imamura, T., Takase, M., Nishihara, A., Oeda, E., Hanai, J.-I., Kawabata, M. & Miyazono, K. (1997) Smad6 inhibits signalling by the TGF -β superfamily. *Nature,* 389(6651), p.622.

Ingman, W. V., Robker, R. L., Woittiez, K. & Robertson, S. A. (2006) Null mutation in transforming growth factor beta1 disrupts ovarian function and causes oocyte incompetence and early embryo arrest. *Endocrinology*, 147(2), 835-45.

Isao, M., Natalia, G. D., Guannan, W., Dongming, H., Jianyin, L. & Fang, L. (2004) Cyclin- dependent kinases regulate the antiproliferative function of Smads. *Nature*, 430(6996), 226.

Ishida, N., Hara, T., Kamura, T., Yoshida, M., Nakayama, K. & Nakayama, K. I. (2002) Phosphorylation of p27(Kip1) on serine 10 is required for its binding to CRM1 and nuclear export. *Journal of Biological Chemistry*, 277(17), 14355-14358.

Itoh, F., Asao, H., Sugamura, K., Heldin, C. H., ten Dijke, P. & Itoh, S. (2001) Promoting bone morphogenetic protein signaling through negative regulation of inhibitory Smads. *EMBO Journal*, 20(15), 4132-42.

Itóh, S., Landström, M., Hermansson, A., Itoh, F., Heldin, C. H., Heldin, N. E. & Ten Dijke, P. (1998)

Transforming growth factor beta1 induces nuclear export of inhibitory Smad7. *The Journal of biological chemistry*, 273(44),29195-29201.

Jae, Y. Y., Shin, I. & Arteaga, C. L. (2005) Type I transforming growth factor β receptor binds to and activates phosphatidylinositol 3- kinase. *Journal of Biological Chemistry*, 280(11), 10870-10876.

Jagarlamudi, K., Liu, L., Adhikari, D., Reddy, P., Idahl, A., Ottander, U., Lundin, E. & Liu, K. (2009) Oocyte- Specific Deletion of Pten in Mice Reveals a Stage- Specific Function of PTEN/ PI3K Signaling in Oocytes in Controlling Follicular Activation. *PLoS One*, 4(7).

Jian, X., Samy, L. & Rik, D. (2009) TGF- β- induced epithelial to mesenchymal transition. *Cell Research*, 19(2), 156.

Jirawatnotai, S., Moons, D. S., Stocco, C. O., Franks, R., Hales, D. B., Gibori, G. & Kiyokawa, H. (2003) The cyclin- dependent kinase inhibitors p27Kip1 and p21Cip1 cooperate to restrict proliferative life span in differentiating ovarian cells. *The Journal of biological chemistry*, 278(19), 17021.

Joakimsen, O., Bønaa, K. H., Stensland-Bugge, E. & Jacobsen, B. K. (2000) Population-based study of age at menopause and ultrasound assessed carotid atherosclerosis: The Tromsø Study. *Journal of Clinical Epidemiology*, 53(5), 525-530.

Joan, S., Celio, P., Peter, S., Manuela, S., Martin, E. & Joan, M. (2001) TGFβ influences Myc, Miz- 1 and Smad to control the CDK inhibitor p15INK4b. *Nature Cell Biology*, 3(4), 400.

John, G. B., Gallardo, T. D., Shirley, L. J. & Castrillon, D. H. (2008) Foxo3 is a PI3K-dependent molecular switch controlling the initiation of oocyte growth. *Developmental Biology.*, 321(1), 197-204.

John, G. B., Shidler, M. J., Besmer, P. & Castrillon, D. H. (2009) Kit signaling via PI3K promotes ovarian follicle maturation but is dispensable for primordial follicle activation. *Developmental Biology.*, 331(2), 292-299.

Johnson, J., Jacqueline, C., Tomoko, K., James, K. P. & Jonathan, L. T. (2004) Germline stem cells and follicular renewal in the postnatal mammalian ovary. *Nature*, 428(6979), 145.

Jonas, A. N. & John, L. C. (2003) Myc pathways provoking cell suicide and cancer. *Oncogene*, 22(56), 9007.

Jones, G. L., Hall, J. M., Lashen, H. L., Balen, A. H. & Ledger, W. L. (2011) Health-Related Quality of Life Among Adolescents with Polycystic Ovary Syndrome. *JOGNN*, 40(5), 577-588.

Joseph, J. V., Conroy, S., Tomar, T., Eggens-Meijer, E., Bhat, K., Copray, S., Walenkamp, A. M. E., Boddeke, E., Balasubramanyian, V., Wagemakers, M., Dunnen,

W. F. A. D. & Kruyt, F. A. E. (2014) TGF- β is an inducer of ZEB1- dependent mesenchymal transdifferentiation in glioblastoma that is associated with tumor invasion. *Cell Death and Disease*, 5(10), e1443.

Joshi, S., Davies, H., Sims, L., Levy, S. & Dean, J. (2007) Ovarian gene expression in the absence of FIGLA, an oocyte- specific transcription factor. *BMC Developmental Biology*, 7(1), 67.

Joyce, I. M., Clark, A. T., Pendola, F. L. & Eppig, J. J. (2000a) Comparison of recombinant growth differentiation factor-9 and oocyte regulation of KIT ligand messenger ribonucleic acid expression in mouse ovarian follicles. *Biology of Reproduction*, 63(6), 1669-75.

Joyce, I. M., Clark, A. T., Pendola, F. L. & Eppig, J. J. (2000b) Comparison of Recombinant Growth Differentiation Factor- 9 and Oocyte Regulation of KIT Ligand Messenger Ribonucleic Acid Expression in Mouse Ovarian Follicles 1. *Biology of Reproduction*, 63(6), 1669-1675.

Kalluri, R. & Weinberg, R. (2009) The basics of epithelial - mesenchymal transition. *Journal Of Clinical Investigation*, 119(6), 1420-1428.

Kamalanathan, S., Sahoo, J. & Sathyapalan, T. (2013) Pregnancy in polycystic ovary syndrome. *Indian Journal of Endocrinology and Metabolism*, 17(1), 37-43.

Karkanaki, A., Praras, N., Katsikis, I., Kita, M. & Panidis, D. (2007) Is the Y chromosome all that is required for sex determination? *Hippokratia*, 11(3), 120.

Kawamura, K., Cheng, Y., Suzuki, N., Deguchi, M., Sato, Y., Takae, S., Ho, C., Kawamura, N., Tamura, M., Hashimoto, S., Sugishita, Y., Morimoto, Y., Hosoi, Y., Yoshioka, N., Ishizuka, B. & Hsueh, A. (2013) Hippo signaling disruption and Akt stimulation of ovarian follicles for infertility treatment. *Proceedings of the National Academy of Sciences of the United States of America*, 110(43), 17474-17479.

Kerr, J., Duckett, R., Myers, M., Britt, K., Mladenovska, T. & Findlay, J. (2006) Quantification of healthy follicles in the neonatal and adult mouse ovary: evidence for maintenance of primordial follicle supply. *Reproduction*, 132(1), 95-109.

Kezele, P., Nilsson, E. E. & Skinner, M. K. (2005) Keratinocyte growth factor acts as a mesenchymal factor that promotes ovarian primordial to primary follicle transition. *Biology of Reproduction*, 73(5), 967-73.

Kida, A., Kakihana, K., Kotani, S., Kurosu, T. & Miura, O. (2007) Glycogen synthase kinase-3β and p38 phosphorylate cyclin D2 on Thr280 to trigger its ubiquitin/ proteasome- dependent degradation in hematopoietic cells. *Oncogene*, 26(46), 6630.

Kimura, F., Bonomi, L. M. & Schneyer, A. L. (2011) Follistatin regulates germ cell nest breakdown and primordial follicle formation. *Endocrinology*, 152(2), 697-706.

Knowlton, A. A. & Lee, A. R. (2012) Estrogen and the cardiovascular system. *Pharmacology and Therapeutics*, 135(1), 54-70.

Koopman P , G. J., Vivian N , Goodfellow P , Lovell-Badge R . (1991) Male development of chromosomally female mice transgenic for Sry. *Nature*, 351(6322), 117-121.
Kretzschmar, M., Doody, J., Timokhina, I. & Massague, J. (1999) A mechanism of repression of TGF beta /Smad signaling by oncogenic Ras. *Genes & Development*, 13(7), 804-816.

Kuliev, A., Zlatopolsky, Z., Kirillova, I., Spivakova, J. & Cieslak Janzen, J. (2011) Meiosis errors in over 20,000 oocytes studied in the practice of preimplantation aneuploidy testing. *Reproductive BioMedicine Online*, 22(1), 2-8.

Kumar, T. R., Wang, Y., Lu, N. & Matzuk, M. M. (1997) Follicle stimulating hormone is required for ovarian follicle maturation but not male fertility. *Nature Genetics*, 15(2), 201-4.

Kuo, F.-T., Fan, K., Ambartsumyan, G., Menon, P., Ketefian, A., Bentsi-Barnes, I. K. & Pisarska, M. D. (2011) Relative expression of genes encoding SMAD signal transduction factors in human granulosa cells is correlated with oocyte quality. *Journal of Assisted Reproduction and Genetics*, 28(10), 931-938.

Kurisaki, A., Kose, S., Yoneda, Y., Heldin, C. H. & Moustakas, A. (2001) Transforming growth factor -beta induces nuclear import of Smad3 in an importin -beta1 and Ran - dependent manner. *Molecular biology of the cell*. 12(4), 1079-91.

Kuwayama, M., Vajta, G., Kato, O. & Leibo, S. P. (2005) Highly efficient vitrification method for cryopreservation of human oocytes. *Reproductive BioMedicine Online*, 11(3), 300-308.

Labaer, J., Garrett, M. D., Stevenson, L., Slingerland, J., Sandhu, C., Chou, H., Fattaey, A. & Harlow, E. (1997) New functional activities for the p21 family of CDK inhibitors. *Genes and Development*, 11(7), 847-862.

Lamouille, S. & Derynck, R. (2007) Cell size and invasion in TGF-beta- induced epithelial to mesenchymal transition is regulated by activation of the mTOR pathway. *The Journal of cell biology*, 178(3), 437.

Laronda, M., Duncan, F., Hornick, J., Xu, M., Pahnke, J., Whelan, K., Shea, L. & Woodruff, T. (2014) Alginate encapsulation supports the growth and differentiation of human primordial follicles within ovarian cortical tissue. *Official Publication of ALPHA, Scientists in Reproductive Medicine*, 31(8), 1013-1028.

Lau, L. F. & Nathans, D. (1987) Expression of a set of growth - related immediate early genes in BALB/c 3T3 cells: coordinate regulation with c-fos or c-myc. *Proceedings of the National Academy of Sciences of the United States of America*, 84(5):1182-6.

Lawson, K. A., Dunn, N. R., Roelen, B. A., Zeinstra, L. M., Davis, A. M., Wright, C. V., Korving, J. P. & Hogan, B. L. (1999) Bmp4 is required for the generation of primordial germ cells in the mouse embryo. *Genes and Development*, 13(4), 424-36.

Le Bouffant, R., Guerquin, M. J., Duquenne, C., Frydman, N., Coffigny, H., Rouiller-Fabre, V., Frydman, R., Habert, R. & Livera, G. (2010) Meiosis initiation in the human ovary requires intrinsic retinoic acid synthesis. *Human Reproduction*, 25(10), 2579-2590.

Lee, M. K., Pardoux, C., Hall, M. C., Lee, P. S., Warburton, D., Qing, J., Smith, S. M. & Derynck, R. (2007) TGF - beta activates Erk MAP kinase signalling through direct phosphoryl ation of ShcA. *EMBO Journal*, 26(17), 3957-67.

Lee, W. S., Otsuka, F., Moore, R. K. & Shimasaki, S. (2001) Effect of bone morphogenetic protein-7 on folliculogenesis and ovulation in the rat. *Biology of Reproduction*, 65(4), 994-9.

Lee, W. S., Yoon, S. J., Yoon, T. K., Cha, K. Y., Lee, S. H., Shimasaki, S., Lee, S. & Lee, K. A. (2004) Effects of bone morphogenetic protein-7 (BMP-7) on primordial follicular growth in the mouse ovary. *Molecular Reproduction and Development*, 69(2), 159-63.

Lei, L. & Spradling, A. C. (2013) Mouse primordial germ cells produce cysts that partially fragment prior to meiosis. *Development (Cambridge, England)*, 140(10), 2075.

Levine, J., Canada, A. & Stern, C. J. (2010) Fertility preservation in adolescents and young adults with cancer. *Journal of clinical oncology : official journal of the American Society of Clinical Oncology*, 28(32), 4831.

Li, J., Kawamura, K., Cheng, Y., Liu, S., Klein, C., Liu, S., Duan, E.-K. & Hsueh, A. J. W. (2010) Activation of dormant ovarian follicles to generate mature eggs. *Proceedings of the National Academy of Sciences of the United States of America*, 107(22), 10280.

Li, Q., Pangas, S. A., Jorgez, C. J., Graff, J. M., Weinstein, M. & Matzuk, M. M. (2008) Redundant roles of SMAD2 and SMAD3 in ovarian granulosa cells in vivo. *Molecular Cell Biology*, 28(23), 7001-11.

Li, S., Maruo, T., Ladines-Llave, C. A., Kondo, H. & Mochizuki, M. (1994) Stage-limited expression of myc oncoprotein in the human ovary during follicular growth, regression and atresia. *Endocrine Journal*, 41(1), 83-92.

Li, T. Y., Colley, D., Barr, K. J., Yee, S. P. & Kidder, G. M. (2007) Rescue of oogenesis in Cx37-null mutant mice by oocyte-specific replacement with Cx43. *Journal of Cell Science*, 120(Pt 23), 4117-25.

Lin, X., Duan, X., Liang, Y.-Y., Su, Y., Wrighton, K. h., Long, J., Hu, M., Davis, C. m., Wang, J., Brunicardi, F. c., Shi, Y., Chen, Y.-G., Meng, A. & Feng, X.-H. (2016) PPM1A Functions as a Smad Phosphatase to Terminate TGFβ Signaling. *Cell*, 166(6), 1597.

Lin, Y., Gill, M. E., Koubova, J. & Page, D. C. (2008) Germ cell- intrinsic and -extrinsic factors govern meiotic initiation in mouse embryos. *Science (New York, N.Y.)*, 322(5908), 1685.

Ling, N., Ying, S. Y., Ueno, N., Shimasaki, S., Esch, F., Hotta, M. & Guillemin, R. (1986) Pituitary FSH is released by a heterodimer of the beta-subunits from the two forms of inhibin. *Nature*, 321(6072), 779-82.

Lintern-Moore, S. & Moore, G. P. (1979) The initiation of follicle and oocyte growth in the mouse ovary. *Biology of reproduction*, 20(4), 773.

Liu, K. (2010) Molecular mechanisms underlying the activation of mammalian primordial follicles. *Endocrine Journal*, 57, S288-S288.

Liu, L., Liu, X., Ren, X., Tian, Y., Chen, Z., Xu, X., Du, Y., Jiang, C., Fang, Y., Liu, Z., Fan, B., Zhang, Q., Jin, G., Yang, X. & Zhang, X. (2016) Smad2 and Smad3 have differential sensitivity in relaying TGFβ signaling and inversely regulate early lineage specification. *Scientific Reports*, 6, 1317-1323.

Liu, L., Rajareddy, S., Reddy, P., Du, C., Jagarlamudi, K., Shen, Y., Gunnarsson, D., Selstam, G., Boman, K. & Liu, K. (2007) Infertility caused by retardation of follicular development in mice with oocyte- specific expression of Foxo3a. *Development*, 134(1), 199-209.

Liu, Y. X. & Hsueh, A. J. (1986) Synergism between granulosa and theca-interstitial cells in estrogen biosynthesis by gonadotropin-treated rat ovaries: studies on the two-cell, two-gonadotropin hypothesis using steroid antisera. *Biology of Reproduction*, 35(1), 27-36.

Livak, K. J. & Schmittgen, T. D. (2001) Analysis of relative gene expression data using real- time quantitative PCR and the 2(- Delta Delta C(T)) Method. *Methods (San Diego, Calif.)*, 25(4), 402.

Looyenga, B. D. & Hammer, G. D. (2007) Genetic removal of Smad3 from inhibin- null mice attenuates tumor progression by uncoupling extracellular mitogenic signals from the cell cycle machinery. *Molecular endocrinology (Baltimore, Md.)*, 21(10), 2440.

López-Novoa, J. M. & Nieto, M. A. (2009) Inflammation and EMT: an alliance towards organ fibrosis and cancer progression. *EMBO Molecular Medicine*, 1(6-7), 303-314.

Maatouk, D. M., Dinapoli, L., Alvers, A., Parker, K. L., Taketo, M. M. & Capel, B. (2008) Stabilization of β- catenin in XY gonads causes male -to- female sex -reversal. *Human Molecular Genetics*, 7(19), 2949-2955.

Maehama, T. & Dixon, J. E. (1998) The tumor suppressor, PTEN/ MMAC1, dephosphorylates the lipid second messenger, phosphatidylinositol 3,4,5- trisphosphate. *The Journal of biological chemistry*, 273(22), 13375.

Malven PV , S. C. (1966) A luteolytic action of prolactin in hypophysectomized rats. . *Endocrinology*, 79(2), 268-74.

Mamsen, L. S., Brøchner, C. B., Byskov, A. G. & Møllgard, K. (2012) The migration and loss of human primordial germ stem cells from t he hind gut epithelium towards the gonadal ridge. *The Innternational Journal of Developmental Biology*, 56(10-12), 771-8.

Martins da Silva, S. J., Bayne, R. A., Cambray, N., Hartley, P. S., McNeilly, A. S. & Anderson, R. A. (2004) Expression of activin subunits and receptors in the developing human ovary: activin A promotes germ cell survival and proliferation before primordial follicle formation. *Developmental Biology*, 266(2), 334-45.

Massague, J. (1998) TGF-beta signal transduction. *Annual Review of Biochemistry*, 67, 753-91.

Massague, J. (2012) TGFbeta signalling in context. *Nature Reviews Molecular Cell Biology*, 13(10), 616-30.

Massague, J., Seoane, J. & Wotton, D. (2005) Smad transcription factors. *Genes and Development*, 19(23), 2783-2810.

Mathew, L. C., Christopher, J. M. & Michael, F. O. (2004) RAS and RHO GTPases in G1- phase cell- cycle regulation. *Nature Reviews Molecular Cell Biology*, 5(5), 355.

Matsuda-Minehata, F., Inoue, N., Goto, Y. & Manabe, N. (2006) The regulation of ovarian granulosa cell death by pro- and anti- apoptotic molecules. *Journal of Reprouction and Development*,52(6), 695-705.

Matsuura, I., Wang, G., He, D. & Liu, F. (2005b) Identification and characterization of ERK MAP kinase phosphorylation sites in Smad3. *Biochemistry*, 44(37), 12546.

Matzuk MM , F. M., Su JG , Hsueh AJ , Bradley A . (1992) Functional analysis of activins during mammalian development. *Nature*, 374(6520), 354-6.

McGee, E. A. & Hsueh, A. J. W. (2000) Initial and cyclic recruitment of ovarian follicles. *Endocrine Reviews*, 21(2), 200-14.

McLaughlin, M., Kinnell, H. L., Anderson, R. A. & Telfer, E. E. (2014) Inhibition of phosphatase and tensin homologue (PTEN) in human ovary in vitro results in increased activation of primordial follicles but compromises development of growing follicles. *Molecular Human Reproduction*, 20(8), 736-744.

McLaughlin, M. & Telfer, E. E. (2010) Oocyte development in bovine primordial follicles is promoted by activin and FSH within a two- step serum- free culture system. *Reproduction*, 139(6), 971-978.

Medrano, J. V., Ramathal, C., Nguyen, H. N., Simon, C. & Reijo Pera, R. A. (2012) Divergent RNA- binding Proteins, DAZL and VASA, Induce Meiotic Progression in Human Germ Cells Derived in Vitro. *STEM CELLS*, 30(3), 441-451.

Meloche, S. & Pouysségur, J. (2007) The ERK1/ 2 mitogen- activated protein kinase pathway as a master regulator of the G1- to S- phase transition. *Oncogene*, 26(22), 3227.

Memon, M. A., Anway, M. D., Covert, T. R., Uzumcu, M. & Skinner, M. K. (2008) Transforming growth factor beta (TGFbeta1, TGFbeta2 and TGFbeta3) null-mutant phenotypes in embryonic gonadal development. *Molecular Cell Endocrinology*, 294(1-2), 70-80.

Merkwitz, C., Lochhead, P., Tsikolia, N., Koch, D., Sygnecka, K., Sakurai, M., Spanel-Borowski, K. & Ricken, A. M. (2011) Expression of KIT in the ovary, and the role of somatic precursor cells. *Progress in Histochemistry and Cytochemistry*, 46(3), 131-84.

Meyyappan, M., Wong, H., Hull, C. & Riabowol, K. T. (1998) Increased expression of cyclin D2 during multiple states of growth arrest in primary and established cells. *Molecular and cellular biology*, 18(6), 3163.

Mihm, M. & Evans, A. (2008) Mechanisms for Dominant Follicle Selection in Monovulatory Species: A Comparison of Morphological, Endocrine and Intraovarian Events in Cows, Mares and Women. *Reproduction in Domestic Animals*, 43, 48-56.

Mizunuma, H., Liu, X., Andoh, K., Abe, Y., Kobayashi, J., Yamada, K., Yokota, H., Ibuki, Y. & Hasegawa, Y. (1999) Activin from secondary follicles causes small preantral follicles to remain dormant at the resting stage. *Endocrinology*, 140(1), 37-42.

Moons, D. S., Jirawatnotai, S., Tsutsui, T., Franks, R., Parlow, A. F., Hales, D. B., Gibori, G., Fazleabas, A. T. & Kiyokawa, H. (2002) Intact follicular maturation and defective luteal function in mice deficient for cyclin- dependent kinase- 4. *Endocrinology*, 143(2), 647.

Mora, J. M., Fenwick, M. A., Castle, L., Baithun, M., Ryder, T. A., Mobberley, M., Carzaniga, R., Franks, S. & Hardy, K. (2012) Characterization and Significance of Adhesion and Junction-Related Proteins in Mouse Ovarian Follicles. *Biology of Reproduction*, 86(5).

Morales, N. & de Plata, C. (2012) Role of AKT/ mTORC1 pathway in pancreatic beta-cell proliferation. *Colomb. Medica*, 43(3), 235-43.

Mork, L., Maatouk, D. M., McMahon, J. A., Guo, J. J., Zhang, P., McMahon, A. P. & Capel, B. (2011) Temporal Differences in Granulosa Cell Specification in the Ovary Reflect Distinct Follicle Fates in Mice 1. *Biology of Reproduction*, 86(2).

Moustakas, A., Souchelnytskyi, S. & Heldin, C. H. (2001) Smad regulation in TGF-beta signal transduction. *Journal of Cell Science*, 114(Pt 24), 4359-69.

Mu, X., Wen, J., Guo, M., Wang, J., Li, G., Wang, Z., Wang, Y., Teng, Z., Cui, Y. & Xia, G. (2013) Retinoic acid derived from the fetal ovary initiates meiosis in mouse germ cells. *Journal of Cellular Physiology*, 228(3), 627-639.

Mu, Y., Gudey, S. & Landström, M. (2012) Non - Smad signaling pathways. *Cell Tissue Research*, 347(1), 11-20.

Myers, M., Mansouri-Attia, N., James, R., Peng, J. & Pangas, S. A. (2013) GDF9 modulates the reproductive and tumor phenotype of female inha-null mice. *Biology of Reproduction*, 88(4), 86.

Myers, M., Middlebrook, B. S., Matzuk, M. M. & Pangas, S. A. (2009) Loss of inhibin alpha uncouples oocyte-granulosa cell dynamics and disrupts postnatal folliculogenesis. *Developmental Biology*, 334(2), 458-67.

Nagarajan, R. P., Zhang, J., Li, W. & Chen, Y. (1999) Regulation of Smad7 promoter by direct association with Smad3 and Smad4. *The Journal of biological chemistry*, 274(47), 33412.

Nandedkar, T. D. & Dharma, S. J. (2001) Expression of bcl xs and c- myc in atretic follicles of mouse ovary. *Reproductive BioMedicine Online*, 3(3), 221-225.

Nelson, L. M. (2009) Primary Ovarian Insufficiency. *The New England Journal of Medicine*, 360(6), 606-614.

Nicolás, F. J., De Bosscher, K., Schmierer, B., Hill, C. S., Nicolás, F. J. & De Bosscher, K. (2004) Analysis of Smad nucleocytoplasmic shuttling in living cells. *Journal of Cell Science*, 17(Pt 18), 4113-25.

Nilsson, E., Parrott, J. A. & Skinner, M. K. (2001) Basic fibroblast growth factor induces primordial follicle development and initiates folliculogenesis. *Molecular and Cellular Endocrinology*, 175(1), 123-130.

Nilsson, E. E., Detzel, C. & Skinner, M. K. (2006) Platelet-derived growth factor modulates the primordial to primary follicle transition. *Reproduction*, 131(6), 1007-15.

Nilsson, E. E., Doraiswamy, V. & Skinner, M. K. (2003) Transforming growth factor beta isoform expression during bovine ovarian antral follicle develop ment. *Molecular Reproduction and Development*, 66(3), 237-46.

Nilsson, E. E. & Skinner, M. K. (2003) Bone morphogenetic protein-4 acts as an ovarian follicle survival factor and promotes primordial follicle development. *Biology of Reproduction*, 69(4), 1265-72.

Nilsson, E. E. & Skinner, M. K. (2004) Kit ligand and basic fibroblast growth factor interactions in the induction of ovarian primordial to primary follicle transition. *Molecular and Cellular Endocrinology*, 214(1-2), 19-25.

Nyboe Andersen, A. & Erb, K. (2006) Register data on assisted reproductive technology (ART) in Europe including a detailed description of ART in Denmark. Oxford, UK.

Okamura, Y., Myoumoto, A., Manabe, N., Tanaka, N., Okamura, H. & Fukumoto, M. (2001) Protein tyrosine kinase expression in the porcine ovary. *Molecular Human Reproduction*, 7(8), 723-729.

Onichtchouk, D., Dosch, R. & Gawantka, V. (1999) Silencing of TGF- beta signalling by the pseudoreceptor BAMBI. *Nature*, 401(6752), 480-5.

Otsuka, F. & Shimasaki, S. (2002) A negative feedback system between oocyte bone morphogenetic protein 15 and granulosa cell kit ligand: its role in regulating granulosa cell mitosis. *Proc Natl Acad Sci U S A*, 99(12), 8060-5.

Ozdamar, B., Bose, R., Barrios-Rodiles, M., Wang, H.-R., Zhang, Y. & Wrana, J. L. (2005) Regulation of the polarity protein Par6 by TGFbeta receptors controls epithelial cell plasticity. *Science (New York, N.Y.)*, 307(5715), 1603.

Pangas, S. A. (2012a) Bone morphogenetic protein signaling transcription factor (SMAD) function in granulosa cells. *Molecular and Cellular Endocrinology*, 356(1-2), 40-47.

Pangas, S. A. (2012b) Regulation of the ovarian reserve by members of the transforming growth factor beta family. *Molecular Reproduction and Development*, 79(10), 666-79.

Pangas, S. A., Choi, Y., Ballow, D. J., Zhao, Y. G., Westphal, H., Matzuk, M. M. & Rajkovic, A. (2006) Oogenesis requires germ cell-specific transcriptional regulators Sohlh1 and Lhx8. *Proc. Natl. Acad. Sci. U. S. A.*, 103(21), 8090-8095.

Pangas, S. A., Li, X., Umans, L., Zwijsen, A., Huylebroeck, D., Gutierrez, C., Wang, D., Martin, J. F., Jamin, S. P., Behringer, R. R., Robertson, E. J. & Matzuk, M. M. (2008) Conditional deletion of Smad1 and Smad5 in somatic cells of male and female gonads leads to metastatic tumor development in mice. *Molecular Cell Biology*, 28(1), 248-57.

Pangas, S. A., Rademaker, A. W., Fishman, D. A. & Woodruff, T. K. (2002) Localization of the activin signal transduction components in normal human ovarian follicles: implications for autocrine and paracrine signaling in the ovary. *J Clin Endocrinol Metab*, 87(6), 2644-57.

Park, Y., Maizels, E. T., Feiger, Z. J., Alam, H., Peters, C. A., Woodruff, T. K., Unterman, T. G., Lee, E. J., Jameson, J. L., Hunzicker-dunn, M. & Hunzicker-Dunn, M. (2005) Induction of cyclin D2 in rat granulosa cells requires FSH- dependent relief from FOXO1 repression coupled with positive signals from Smad. *The Journal of biological chemistry*, 280(10), 9135.

Pellestor, F., Andréo, B., Arnal, F., Humeau, C. & Demaille, J. (2003) Maternal aging and chromosomal abnormalities: new data drawn from in vitro unfertilized human oocytes. *Human Genetics*, 112(2), 195-203.

Pepling, M. E. & Spradling, A. C. (1998) Female mouse germ cells form synchronously dividing cysts. *Development (Cambridge, England)*, 125(17), 3323.

Pepling , M. E. & Spradling , A. C. (2001) Mouse Ovarian Germ Cell Cysts Undergo Programmed Breakdown to Form Primordial Follicles. Developmental Biology.

Pepling, M. E., Wilhelm, J. E., Hara, A. L., Gephardt, G. W. & Spradling, A. C. (2007) Mouse Oocytes within Germ Cell Cysts and Primordial Follicles Contain a Balbiani Body. *Proceedings of the National Academy of Sciences of the United States of America*, 104(1), 187-192.

Persani, L. (2011) Genetic defects of ovarian TGF- β- like factors and premature ovarian failure. *J Endocrinol Invest*, 34(3), 244.

Persson, H., Gray, H. E. & Godeau, F. (1985) Growth- dependent synthesis of c- myc-encoded proteins: Early stimulation by serum factors in synchronized mouse 3T3 cells. *Molecular and Cellular Biology*, 5(11), 2903-2912.

Pesce, M., Wang, X., Wolgemuth, D. J. & Schöler, H. R. (1998) Differential expression of the Oct - 4 transcription factor during mouse germ cell differentiation. *Mechanisms of Development*, 71(1-2), 89-98.

Peters, H., Byskov, A. G., Lintern-Moore, S., Faber, M. & Andersen, M. (1973) The effect of gonadotrophin on follicle growth initiation in the neonatal mouse ovary. *Journal of Reproduction and Fertility*, 35(1), 139-41.

Polani, P. & Crolla, J. (1991) A test of the production line hypothesis of mammalian oogenesis. *Human Genetics*, 88(1), 64-70.

Putowski LT 1 , S. M., Zielewicz J , Kaminski K , Jakowicki JA . (1997) The relevance of c-myc to the physiology of the human ovary. *Gynecol Endocrinol*. 11(1):5-10.

Qin, Y., Jiao, X., Simpson, J. L. & Chen, Z.-J. (2015) Genetics of primary ovarian insufficiency: new developments and opportunities. *Human Reproduction Update*, 21(6), 787-808.

Rabinovici, J., Spencer, S. J., Doldi, N., Goldsmith, P. C., Schwall, R. & Jaffe, R. B. (1992) Activin-A as an intraovarian modulator: actions, localization, and regulation of the intact dimer in human ovarian cells. *J Clin Invest*, 89(5), 1528-36.

Rajareddy, S., Reddy, P., Du, C., Liu, L., Jagarlamudi, K., Tang, W., Shen, Y., Berthet, C., Peng, S. L., Kaldis, P. & Liu, K. (2007) p27(kip1) (Cyclin-Dependent kinase inhibitor 1B) controls ovarian development by suppressing follicle endowment and activation and promoting follicle atresia in mice. *Molecular Endocrinology*, 21(9), 2189-2202.

Rajkovic, A., Pangas, S. A., Ballow, D., Suzumori, N. & Matzuk, M. M. (2004) NOBOX deficiency disrupts early folliculogenesis and oocyte- specific gene expression. *Science (New York, N.Y.)*, 305(5687), 1157.

Ray, A., James, M. K., Blain, S. W., Larochelle, S. & Fisher, R. P. (2009) P27 Kip1 inhibits cyclin D- cyclin- dependent kinase 4 by two independent modes. *Molecular and Cellular Biology*, 29(4), 986-999.

Reddy, P., Shena, L. J., Ren, C., Boman, K., Lundin, E., Ottander, U., Lindgren, P., Liu, Y. X., Sun, Q. Y. & Liu, K. (2005) Activation of Akt (PKB) and suppression of FKHRL1 in mouse and rat oocytes by stem cell factor during follicular activation and development. *Developmental Biology*, 281(2), 160-170.

Reddy, P., Zheng, W. J. & Liu, K. (2010) Mechanisms maintaining the dormancy and survival of mammalian primordial follicles. *Trends Endocrinol. Metab*, 21(2), 96-103.

Richardson, S., Senikas, V. & Nelson, J. (1988) Follicular depletion during the menopausal transition : Evidence for accelerated loss and ultimate exhaustion. *J Clin Endocrinol Metab*, 65(6), 1231-7.

Robker, R. L. & Richards, J. S. (1998) Hormone- induced proliferation and differentiation of granulosa cells: a coordinated balance of the cell cycle regulators cyclin D2 and p27Kip1. *Molecular endocrinology (Baltimore, Md.)*, 12(7), 924.

Rosairo, D , Kuyznierewicz, I., Findlay J , Drummond A . (2008) Transforming growth factor - β : its role in ovarian follicle development. Reproduction, 136(6), 799-809.

Rosen, M. P., Johnstone, E., McCulloch, C. E., Schuh-Huerta, S. M., Sternfeld, B., Reijo-Pera, R. A. & Cedars, M. I. (2012) A characterization of the relationship of ovarian reserve markers with age. *Fertility and sterility*, 97(1), 238.

Rosendahl, M., Greve, T. & Andersen, C. (2013) The safety of transplanting cryopreserved ovarian tissue in cancer patients: a review of the literature. *Official Publication of ALPHA, Scientists in Reproductive Medicine*, 30(1), 11-24.

Ross, A., Munger, S. & Capel, B. (2007) Bmp7 regulates germ cell proliferation in mouse fetal gonads. *Sex Dev*, 1(2), 127-37.

Runyan, C. E., Hayashida, T., Hubchak, S., Schnaper, H. W., Curley, J. F. & Runyan, C. E. Role of SARA (SMAD anchor for receptor activation) in maintenance of epithelial cell phenotype. *Journal of Biological Chemistry*, 284(37), 25181-9.

Salpeter, S., Klochendler, A., Weinberg-Corem, N., Porat, S., Granot, Z., Shapiro, A., Magnuson, M., Eden, A., Grimsby, J., Glaser, B. & Dor, Y. (2011) Glucose Regulates Cyclin D2 Expression in Quiescent and Replicating Pancreatic beta - Cells Through Glycolysis and Calcium Channels. *Endocrinology*, 152(7), 2589-2598.

Samy, L., Jian, X. & Rik, D. (2014) Molecular mechanisms of epithelial– mesenchymal transition. *Nature Reviews Molecular Cell Biology*, 15(3), 178.

Satyanarayana, A. & Kaldis, P. (2009) Mammalian cell-cycle regulation: several Cdks, numerous cyclins and diverse compensatory mechanisms. *Oncogene*, 28(33), 2925.

Schmidt, D., Ovitt, C. E., Anlag, K., Fehsenfeld, S., Gredsted, L., Treier, A. C. & Treier, M. (2004) The murine winged-helix transcription factor Foxl2 is required for granulosa cell differentiation and ovary maintenance. *Development*, 131(4), 933-42.

Schmierer, B., Tournier, A. L., Bates, P. A. & Hill, C. S. (2008) Mathematical modeling identifies Smad nucleocytoplasmic shuttling as a dynamic signal-interpreting system. *Proceedings of the National Academy of Sciences of the United States of America*, 105(18), 6608-13.

Schneider, D., Tarantola, M. & Janshoff, A. (2011) Dynamics of TGF- β induced epithelial-to- mesenchymal transition monitored by Electric Cell- Substrate Impedance Sensing. *BBA - Molecular Cell Research*, 1813(12), 2099-2107.

Schuster, N. & Krieglstein, K. (2002) Mechanisms of TGF-β-mediated apoptosis. *Cell Tissue Research*, 307(1), 1-14.

Seoane, J., Le, H.-V., Shen, L., Anderson, S. A. & Massagué, J. (2004) Integration of Smad and Forkhead Pathways in the Control of Neuroepithelial and Glioblastoma Cell Proliferation. *Cell*, 117(2), 211-23.

Seoane, J., Pouponnot, C., Staller, P., Schader, M., Eilers, M. & Massague, J. (2001) TGF beta influences Myc, Miz- 1 and Smad to control the CDK inhibitor p15(INK4b). *Nature Cell Biology*, 3(4), 400-408.

Sharum, I., Granados-Aparici, S., Warrander , F., Tournant , F. & Fenwick, M. (2016) S*trap* regulates early follicle development in the mouse ovary. *Reproduction*, 153(2), 221-231.

Sherr, C. J. & Roberts, J. M. (1999) CDK inhibitors: positive and negative regulators of G1-phase progression. *Genes and Development*, 13(12), 1501.

Shi, Y., Wang, Y.-F., Jayaraman, L., Yang, H., Massagué, J. & Pavletich, N. P. (1998) Crystal Structure of a Smad MH1 Domain Bound to DNA: Insights on DNA Binding in TGF-β Signaling. *Cell*, 94(5), 585-594.

Shimada, M. (2012) Regulation of oocyte meiotic maturation by somatic cells. *Reproductive Medicine and Biology*, 11(4), 177-184.

Shimasaki, S., Zachow, R. J., Li, D., Kim, H., Iemura, S., Ueno, N., Sampath, K., Chang, R. J. & Erickson, G. F. (1999) A functional bone morphogenetic protein system in the ovary. *Proceedings of the National Academy of Sciences of the United States of America*, 96(13), 7282-7.

Sicinski, P. (1996) Cyclin D2 is an FSH- responsive gene involved in gonadal cell proliferation and oncogenesis. *Nature*, 384(6608), 470.

Silva, J. R., van den Hurk, R., de Matos, M. H., dos Santos, R. R., Pessoa, C., de Moraes, M. O. & de Figueiredo, J. R. (2004) Influences of FSH and EGF on primordial follicles during in vitro culture of caprine ovarian cortical tissue. *Theriogenology*, 61(9), 1691-704.

Siqin, W., Cihan, C., Maria, J. M.-A., Natalie Von Der, L., Fuad, B., Vincent, B., Martin, E., Javier, L. & Lars-Gunnar, L. (2003) Myc represses differentiation- induced p21CIP1 expression via Miz- 1- dependent interaction with the p21 core promoter. *Oncogene*, 22(3), 351.

Sleer, L. S. & Taylor, C. C. (2007) Cell- Type Localization of Platelet- Derived Growth Factors and Receptors in the Postnatal Rat Ovary and Follicle 1. *Biology of Reproduction*, 76(3), 379-390.

Soleimani, R. & De Sutter, P. (2011) In situ identification of follicles in ovarian cortex as a tool for quantifying follicle density, viability and developmental potential in strategies to preserve female fertility. *Human reproduction (Oxford, England)*, 26(4), 955.

Solloway, M. J., Dudley, A. T., Bikoff, E. K., Lyons, K. M., Hogan, B. L. & Robertson, E. J. (1998) Mice lacking Bmp6 function. *Developmental Genetics*, 22(4), 321-39.

Soyal, S. M., Amleh, A. & Dean, J. (2000) FIGα, a germ cell- specific transcription factor required for ovarian follicle formation. *Development*, 127(21), 4645-4654.

Spoerke, J. M., Brien, C., Huw, L., Koeppen, H., Fridlyand, J., Brachmann, R. K., Haverty, P. M., Pandita, A., Mohan, S., Sampath, D., Friedman, L. S., Ross, L., Hampton, G. M., Amler, L. C., Shames, D. S. & Lackner, M. R. (2012) Phosphoinositide 3- Kinase (PI3K) Pathway Alterations Are Associated with Histologic Subtypes and Are Predictive of Sensitivity to PI3K Inhibitors in Lung Cancer Preclinical Models. *Clinical Cancer Research*, 18(24), 6771-6783.

Stamateris, R., Sharma, R., Kong, Y., Ebrahimpour, P., Panday, D., Ranganath, P., Zou, B., Levitt, H., Parambil, N., Donnell, C., García-Ocaña, A. & Alonso, L. (2016) Glucose Induces Mouse [Beta]- Cell Proliferation via IRS2, MTOR, and Cyclin D2 but Not the Insulin Receptor. *Diabetes*, 65(4), 981.

Sun L 1 , T. L., Yang F , Luo Y , Li X , Deng HW , Dvornyk V . (2012) Meta-analysis suggests that smoking is associated with an increased risk of early natural menopause. *Menopause*, 19(2), 126-32.

Susaki, E., Nakayama, KI (2004) Multiple Mechanisms for p27 Kip1 Translocation and Degradation. *Cell Cycle*, 6(24), 3015-20.

Susaki, E., Nakayama, K. & Nakayama, K. I. (2007) Cyclin D2 translocates p27 out of the nucleus and promotes its degradation at the G0-G1 transition. *Molecular and cellular biology*, 27(13), 4626-4640.

Suszko, M. I., Balkin, D. M., Chen, Y. & Woodruff, T. K. (2005) Smad3 mediates activin-induced transcription of follicle-stimulating hormone beta-subunit gene. *Molecular Endocrinology*, 19(7), 1849-58.

Suszko, M. I., Lo, D. J., Suh, H., Camper, S. A. & Woodruff, T. K. (2003) Regulation of the rat follicle-stimulating hormone beta-subunit promoter by activin. *Molecular Endocrinology*, 17(3), 318-32.

Suzuki, N., Yoshioka, N., Takae, S., Sugishita, Y., Tamura, M., Hashimoto, S., Morimoto, Y. & Kawamura, K. (2015) Successful fertility preservation following ovarian tissue vitrification in patients with primary ovarian insufficiency. *Human reproduction (Oxford, England)*, 30(3), 608-15.

Sylviane, D., Stéphane, H. & Jean-Michel, G. (1999) A short amino- acid sequence in MH1 domain is responsible for functional differences between Smad2 and Smad3. *Oncogene*, 18(8), 1643.

Taylor, C. C. (2000) Platelet- derived growth factor activates porcine thecal cell phosphatidylinositol- 3- kinase- Akt/ PKB and ras- extracellular signal- regulated kinase- 1/ 2 kinase signaling pathways via the platelet- derived growth factor- beta receptor. *Endocrinology*, 141(4), 1545.

Telfer, E. E., McLaughlin, M., Ding, C. & Thong, K. J. (2008) A two- step serum- free culture system supports development of human oocytes from primordial follicles in the presence of activin. *Human Reproduction*, 23(5), 1151-1158.

Telfer, E. E. & Zelinski, M. B. (2013) Ovarian follicle culture: advances and challenges for human and nonhuman primates. *Fertility and Sterility*, 99(6), 1523-1533.

Thomas, F. H. & Vanderhyden, B. C. (2006a) Oocyte- granulosa cell interactions during mouse follicular development: regulation of kit ligand expression and its role in oocyte growth. *Reproductive biology and endocrinology*,4, 19.

Tingen, C. M., Bristol-Gould, S. K., Kiesewetter, S. E., Wellington, J. T., Shea, L. & Woodruff, T. K. (2009) Prepubertal Primordial Follicle Loss in Mice Is Not Due to Classical Apoptotic Pathways 1. *Biology of Reproduction*, 81(1), 16-25.

Tojo, M., Hamashima, Y., Hanyu, A., Kajimoto, T., Saitoh, M., Miyazono, K., Node, M. & Imamura, T. (2005) The ALK- 5 inhibitor A- 83- 01 inhibits Smad signaling and epithelial-to- mesenchymal transition by transforming growth factor-β. *Cancer Science*, 96(11), 791-800.

Tomic, D., Brodie, S. G., Deng, C., Hickey, R. J., Babus, J. K., Malkas, L. H. & Flaws, J. A. (2002) Smad 3 May Regulate Follicular Growth in the Mouse Ovary 1. *Biology of Reproduction*, 66(4), 917-923.

Tomic, D., Miller, K., Kenny, H., Woodruff, T., Hoyer, P. & Flaws, J. (2004) Ovarian Follicle Development Requires Smad3. *Molecular Endocrinology*, 18(9), 2224-2240.

Toshihiko, O., Koutarou, N., Jiro, K., Katsuhiro, T., Akie, M., Kumi, I., Asako, S.-S., Atsushi, N., Satoru, M., Hiroyuki, A., Hiroshi, K., Atsushi, M. & Toshio, K. (2014) A novel cell- cycle- indicator, mVenus-p27K−, identifies quiescent cells and visualizes G0–G1 transition. *Scientific Reports*, 4.

Tran, S., Lamba, P., Wang, Y. & Bernard, D. J. (2011) SMADs and FOXL2 synergistically regulate murine FSHβ transcription via a conserved proximal promoter element. *Molecular Endocrinology*, 25(7), 1170-1183.

Tran, T. N., Brettingham-Moore, K., Duong, C. P., Mitchell, C., Clemons, N. J. & Phillips, W. A. (2013) Molecular changes in the phosphatidylinositide 3- kinase (PI3K) pathway are common in gastric cancer. *Journal of Surgical Oncology*, 108(2), 113-120.

Tuck, A. R., Robker, R. L., Norman, R. J., Tilley, W. D. & Hickey, T. E. (2015) Expression and localisation of c-kit and KITL in the adult human ovary. *Journal of ovarian research*, 8(1), 31.

Uda, M., Ottolenghi, C., Crisponi, L., Garcia, J. E., Deiana, M., Kimber, W., Forabosco, A., Cao, A., Schlessinger, D. & Pilia, G. (2004) Foxl2 disruption causes mouse ovarian failure by pervasive blockage of follicle development. *Human Molecular Genetics*, 13(11), 1171-81.

Vale, W., Rivier, J., Vaughan, J., McClintock, R., Corrigan, A., Woo, W., Karr, D. & Spiess, J. (1986) Purification and characterization of an FSH releasing protein from porcine ovarian follicular fluid. *Nature*, 321(6072), 776-9.

van der Stege JG 1 , G. H., van Zadelhoff SJ , Lambalk CB , Braat DD , van Kasteren YM , van Santbrink EJ , Apperloo MJ , Weijmar Schultz WC , Hoek A . (2008) Decreased androgen concentrations and diminished general and sexual well-being in women with premature ovarian failure, *Menopause*, 15(1), 23-31.

van Dorp, W., Mulder, R. L., Kremer, L. C. M., Hudson, M. M., van Den Heuvel-Eibrink, M. M., van Den Berg, M. H., Levine, J. M., van Dulmen-Den Broeder, E., Di Iorgi, N., Albanese, A., Armenian, S. H., Bhatia, S., Constine, L. S., Corrias, A., Deans, R., Dirksen, U., Gracia, C. R., Hjorth, L., Kroon, L., Lambalk, C. B., Landier, W., Levitt, G., Leiper, A., Meacham, L., Mussa, A., Neggers, S. J., Oeffinger, K. C., Revelli, A., van Santen, H. M., Skinner, R., Toogood, A., Wallace, W. H. & Haupt, R. (2016) Recommendations for Premature Ovarian Insufficiency Surveillance for Female Survivors of Childhood, Adolescent, and Young Adult Cancer: A Report From the International Late Effects of Childhood Cancer Guideline Harmonization Group in Collaboration With the PanCareSurFup Consortium. *Journal of clinical oncology : official journal of the American Society of Clinical Oncology*, 34(28), 3440.

Varelas, X., Sakuma, R., Samavarchi-Tehrani, P., Peerani, R., Rao, B. M., Dembowy, J., Yaffe, M. B., Zandstra, P. W. & Wrana, J. L. (2008) TAZ controls Smad nucleocytoplasmic shuttling and regulates human embryonic stem - cell self - renewal. *Nature Cell Biology*, 10(7), 837-48.

Veitch, G. I., Gittens, J. E., Shao, Q., Laird, D. W. & Kidder, G. M. (2004) Selective assembly of connexin37 into heterocellular gap junctions at the oocyte/granulosa cell interface. *Journal of Cell Science*, 117(Pt 13), 2699-707.

Vitt, UA, Hayashi M, Hsueh AJ. (2000) In vivo treatment with GDF-9 stimulates primordial and primary follicle progression and theca cell marker CYP17 in ovaries of immature rats. *Endocrinology*, 141(10), 3814-20.

Wandji, S. A., Srsen, V., Voss, A. K., Eppig, J. J. & Fortune, J. E. (1996) Initiation in vitro of growth of bovine primordial follicles. *Biology of Reproduction*, 55(5), 942-948.

Wang, Z., Mu, X., Guo, M., Wang, Y., Teng, Z., Mao, G. P., Niu, W., Feng, L., Zhao, L. H. & Xia, G. (2014a) Transforming Growth Factor- beta Signaling Participates in the Maintenance of the Primordial Follicle Pool in the Mouse Ovary. *Journal Of Biological Chemistry*, 289(12), 8299-8311.

Wang, Z., Niu, W., Wang, Y., Teng, Z., Wen, J., Xia, G. & Wang, C. (2015) Follistatin288 Regulates Germ Cell Cyst Breakdown and Primordial Follicle Assembly in the Mouse Ovary. *PloS One*, 10(6), e0129643.

Wang, Z., Xie, Y., Zhang, L., Zhang, H., An, X., Wang, T. & Meng, A. (2008) Migratory Localization of Cyclin D2 - Cdk4 Complex Suggests a Spatial Regulation of the G1 - S Transition. *Cell Structure and Function*, 33(2), 171-83.

Warner, B., Blain, S., Seoane, J. & Massague, J. (1999) Myc Downregulation by Transforming Growth Factor beta Required for Activation of the p15 super(Ink4b) G sub(1) Arrest Pathway. *Molecular and Cellular Biology*, 19(9), 5913-5922.

Watanabe , Y., Itoh, S., Goto, T., Ohnishi, E., Inamitsu, M., Itoh, F., Satoh, K., Wiercinska, E., Yang, W., Shi, L., Tanaka, A., Nakano, N., Mommaas, A. M., Shibuya, H., Ten Dijke, P. & Kato, M. (2010) TMEPAI , a Transmembrane TGF - β - Inducible Protein , Sequesters Smad Proteins from Active Participation in TGF - β Signaling. *Molecular Cell*, 7(1), 123-34.

Webber, L., Davies, M., Anderson, R., Bartlett, J., Braat, D., Cartwright, B., Cifkova, R., Keizer - Schrama, S., Hogervorst, E., Janse, F., Liao, L., Vlaisavljevic, V., Zillikens, C. & Vermeulen, N. (2016) ESHRE guideline: management of women with premature ovarian insufficiency.

Webber, L., Stubbs, S., Stark, J., Trew, G., Margara, R., Hardy, K. & Franks, S. (2003) Formation and early development of follicles in the polycystic ovary. *The Lancet*, 362(9389), 1017-1021.

Weenen, C., Laven, J. S. E., Von Bergh, A. R. M., Cranfield, M., Groome, N. P., Visser, J. A., Kramer, P., Fauser, B. C. J. M. & Themmen, A. P. N. (2004) Anti-Müllerian hormone expression pattern in the human ovary: potential implications for initial and cyclic follicle recruitment. *Molecular human reproduction*, 10(2), 77.

White, Y. A. R., Woods, D. C., Takai, Y., Ishihara, O., Seki, H. & Tilly, J. L. (2012) Oocyte formation by mitotically active germ cells purified from ovaries of reproductive - age women. *Nature Medicine*, 18(3), 413-21.

Wilkes, M. C., Murphy, S. J., Garamszegi, N. & Leof, E. B. (2003) Cell- Type- Specific Activation of PAK2 by Transforming Growth Factor β Independent of Smad2 and Smad3. *Molecular and Cellular Biology*, 23(23), 8878-8889.

Wurthner, J. U., Frank, D. B., Felici, A., Green, H. M., Cao, Z., Schneider, M. D., McNally, J. G., Lechleider, R. J. & Roberts, A. B. (2001) Transforming Growth Factor -β Receptor - associated Protein 1 Is a Smad4 Chaperone. *Journal of Biological Chemistry*. 276(22), 19495-19502.

Xiao, Z., Watson, N., Rodriguez, C., Lodish, H. F., Lodish, H. F. & Lodish, H. F. (2001) Nucleocytoplasmic Shuttling of Smad1 Conferred by Its Nuclear Localiz ation and Nuclear Export Signals. *Journal of Biological Chemistry*, 276(42), 39404-39410.

Xie, L., Law, B. K., Chytil, A. M., Brown, K. A., Aakre, M. E. & Moses, H. L. (2004) Activation of the Erk Pathway Is Required for TGF-β1- Induced EMT In Vitro. *Neoplasia*, 6(5), 603-610.

Xing, G. & Xiao-Fan, W. (2008) Signaling cross- talk between TGF- β/ BMP and other pathways. *Cell Research*, 19(1), 71.

Xu, L., Kang, Y., Çöl, S. & Massagué, J. (2002) Smad2 Nucleocytoplasmic Shuttling by Nucleoporins CAN /Nup214 and Nup153 Feeds TGFβ Signaling Complexes in the Cytoplasm and Nucleus. *Molecular Cell*, 10(2), 271-82.

Xu, L., Massagué, J., Alarcón, C. & Çöl, S. (2003) Distinct Domain Utilization by Smad3 and Smad4 for Nucleoporin Intera ction and Nuclear Import. *Journal of Biological Chemistry*, 278(43), 42569-42577.

Yamaguchi, T., Kurisaki, A., Yamakawa, N., Minakuchi, K. & Sugino, H. (2006) FKBP12 functions as an adaptor of the Smad7– Smurf1 complex on activin type I receptor. *Journal of Molecular Endocrinology*, 36(3), 569-579.

Yamamura, S., Matsumura, N., Mandai, M., Huang, Z., Oura, T., Baba, T., Hamanishi, J., Yamaguchi, K., Kang, H. S., Okamoto, T., Abiko, K., Mori, S., Murphy, S. K. & Konishi, I. (2012) The activated transforming growth factor- beta signaling pathway in peritoneal metastases is a potential therapeutic target in ovarian cancer. *International Journal of Cancer*, 130(1), 20-28.

Yamashita, M., Fatyol, K., Jin, C., Wang, X., Liu, Z. & Zhang, Y. E. (2008) TRAF6 Mediates Smad - Independent Activation of JNK and p38 by TGF -β. *Molecular Cell*, 31(6), 918-24.

Yan, C., Wang, P., DeMayo, J., DeMayo, F. J., Elvin, J. A., Carino, C., Prasad, S. V., Skinner, S. S., Dunbar, B. S., Dube, J. L., Celeste, A. J. & Matzuk, M. M. (2001) Synergistic roles of bone morphogenetic protein 15 and growth differentiation factor 9 in ovarian function. *Molecular Endocrinology*, 15(6), 854-66.

Yang, P. & Roy, S. K. (2004) Follicle stimulating hormone-induced DNA synthesis in the granulosa cells of hamster preantral follicles involves activation of cyclin-dependent kinase-4 rather than cyclin d2 synthesis. *Biology of reproduction*, 70(2), 509.

Yao, H. H., Matzuk, M. M., Jorgez, C. J., Menke, D. B., Page, D. C., Swain, A. & Capel, B. (2004) Follistatin operates downstream of Wnt4 in mammalian ovary organogenesis. *Developmental Dynanimcs*, 230(2), 210-5.

Yen, A. & Pardee, A. B. (1978) Arrested states produced by isoleucine deprivation and their relationship to the low serum produced arrested state in Swiss 3T3 cells. *Experimental Cell Research*, 114(2), 389-395.

Zarate-Garcia, L., I. R. Lane, S., A. Merriman, J. & T. Jones, K. (2016) FACS- sorted putative oogonial stem cells from the ovary are neither DDX4- positive nor germ cells. *Scientific Reports*, 6.

Zhang, H. & Bradley, A. (1996) Mice deficient for BMP2 are nonviable and have defects in amnion/chorion and cardiac development. *Development*, 122(10), 2977-86.

Zhang, H., Risal, S., Gorre, N., Busayavalasa, K., Li, X., Shen, Y., Bosbach, B., Brännström, M. & Liu, K. (2014) Somatic Cells Initiate Primordial Follicle Activation and Govern the Development of Dormant Oocytes in Mice. *Current Biology*.

Zhang, H., Zheng, W., Shen, Y., Adhikari, D., Ueno, H. & Liu, K. (2012) Experimental evidence showing that no mitotically active female germline progenitors exist in postnatal mouse ovaries. *Proceedings of the National Academy of Sciences of the United States of America*, 109(31), 12580.

Zhang, Y. E. (2009) Non- Smad pathways in TGF- beta signaling. *Cell research*, 19(1), 128.

Zhao, J., Taverne, M. A., van Der Weijden, G. C., Bevers, M. M. & van Den Hurk, R. (2001) Effect of activin A on in vitro development of rat preantral follicles and localization of activin A and activin receptor II. *Biology of reproduction*, 65(3), 967.

Zheng, W., Zhang, H. & Liu, K. (2014a) The two classes of primordial follicles in the mouse ovary: their development, physiological functions and implications for future research. *Molecular human reproduction*, 20(4), 286.

Zheng, W. J., Zhang, H., Gorre, N., Risal, S., Shen, Y. & Liu, K. (2014b) Two classes of ovarian primordial follicles exhibit distinct developmental dynamics and physiological functions. *Human Molecular Genetics.*, 23(4), 920-928.

Zhu, J., Lin, S. J., Zou, C., Makanji, Y., Jardetzky, T. S. & Woodruff, T. K. (2012) Inhibin alpha-subunit N terminus interacts with activin type IB receptor to disrupt activin signaling. *Journal of Biological Chemistry*, 287(11), 8060-70.

Zhu, Y., Richardson, J. A., Parada, L. F. & Graff, J. M. (1998) Smad3 Mutant Mice Develop Metastatic Colorectal Cancer. *Cell*, 94(6), 703-714.

Zi, Z., Feng, Z., Chapnick, D. A., Dahl, M., Deng, D., Klipp, E., Moustakas, A. & Liu, X. (2011) Quantitative analysis of transient and sustained transforming growth factor- β signaling dynamics. *Molecular Systems Biology*, 7(1), n/a-n/a.

Zou, K., Yuan, Z., Yang, Z., Luo, H., Sun, K., Zhou, L., Xiang, L., Shi, L., Yu, Q., Zhang, Y., Hou, R. & Wu, J. (2009) Production of offspring from a germline stem cell line derived from neonatal ovaries. *Nature Cell Biology*, 11(5), 631-636.

Yvonne A R White ; Dori C Woods ; Yasushi Takai ; Osamu Ishihara ; Hiroyuki Seki ; Jonathan L Tilly. Oocyte formation by mitotically-active germ cells purified from ovaries of reproductive age women. *Nature Medicine*, 18(3), 413–421.

Appendices

Appendix 1. Proportion of small follicles in day 4, day 8 and day 16 ovaries and steps for immature mouse ovary embedding in paraffin. A) Proportions were calculated using the largest cross-section of a single ovary. B) After dehydration with increasing gradients of ethanol, ovaries were placed in metal molds and solutions were replaced with a Pasteur pipette. Once the paraffin was melted, ovaries were embedded by using a plastic pipette and a plastic cassette lid was rapidly placed onto the metal mold and covered with more paraffin. All metal molds with paraffin were incubated for 15 minutes and allowed to cool down in ice.

A)

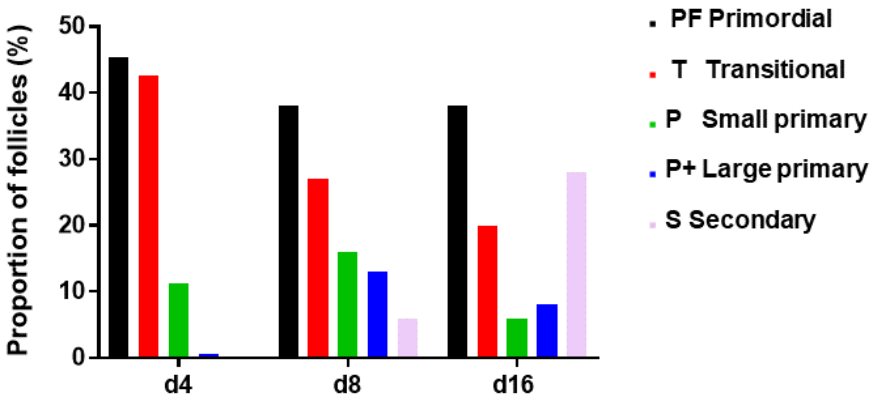

B)

SOLUTION	TIME
70% Ethanol	20 min
90% Ethanol	20 min
100% Ethanol	20 min
100% Ethanol	20 min
100% Ethanol	20 min
HistoChoice	60 min
HistoChoice	30 min
Paraffin	60 min

Appendix 2. Optimisation of starting material and chromatin shearing from neonatal mouse ovaries for ChIP-qPCR.

The amount of starting material used, the crosslinking process with the formaldehyde and the sonication of the chromatin require considerable optimisation for small ovary samples. In order to optimise the amount of starting material, a variable number of ovaries were initially used with a fixed crosslinking time (30 minutes) and sonication (three times during 10 seconds for day 16 and two times for day 4) (A and B). Highly sheared chromatin with a fragment size range of 100-400bp was obtained in all samples from day 16 ovaries (A) while larger fragments were observed from day 4 ovary samples, suggesting extra sonication may be needed (B). As sufficient chromatin was observed in samples of two day 4 ovaries, extra sonication was applied (additional 5 seconds) (C) and the range was comparable to that of a single day 16 ovary sample with more sonication (three times for 10 seconds).

A second optimisation using two different lysis buffers (tissue vs. cell/nuclear lysis buffers, from Magna ChIP™ G Tissue kit, Millipore and EZ- Magna ChIP™ G kit, Millipore respectively) and two different sonication methods (bioruptor, Diagenode vs vibra cell 150 probe, Sonics) were initially used with samples of day 8 ovaries to compare the lysis power and sonication efficiency (D and E). Additionally, different sonication times and amplitudes with samples of day 8 ovaries were also performed to ensure maximum chromatin shearing between the desired fragment size range (F and G). Although transcription factor binding sites can be located in other regions apart from the promoter, they are usually located between 200 and 1000bp upstream the open reading frame (ORF) of the target genes(Chun-Ping et al, 2016). However, ideal fragment size range for ChIP experiments is from 100-300bp (Benjamin et al, 2011). Poorly sonicated chromatin is usually observed when using 50% maximum amplitude (fragment size 700-2000 bp; F). In contrast, when using 100% maximum amplitude, large fragments are not present (G) and the most abundant fragments are obtained in a range from 200 to 400 bp

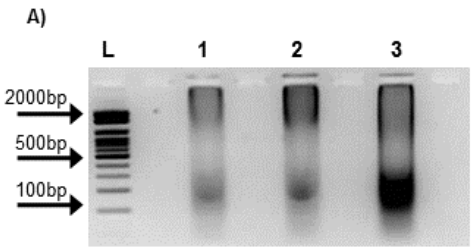

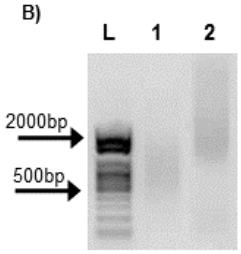

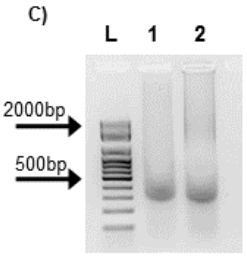

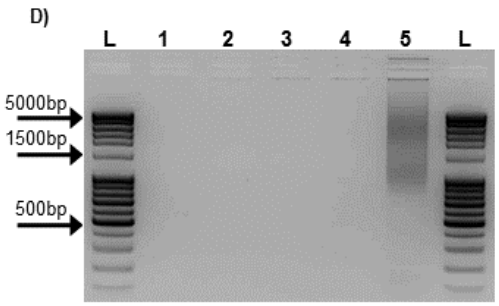

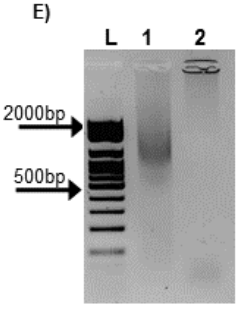

Number	Second intervals
6	10x3
7	10x4
8	10x5
9	10x6
10	10x7
11	10x8

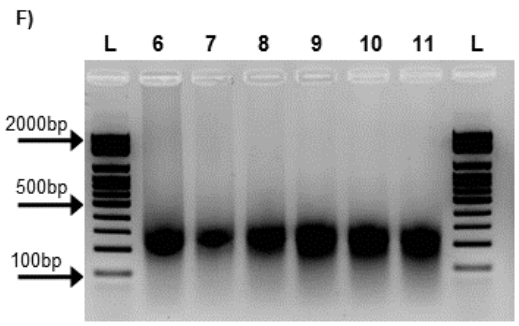

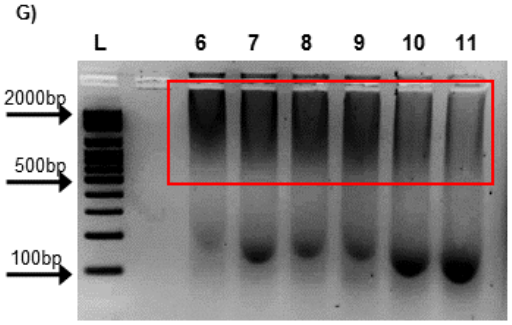

Appendix 3. Promoter sequence for *Ccnd2, p27, Myc, Follistatin* and *FSHb* genes.

Binding sites for FOXL2 (Tran et al, 2011) and binding sites for FOXL2 and SMADs (TRANSFAC® software) are highlighted in yellow and green, respectively. Primers designed to cover all possible binding sites are detailed in the tables below.

FOXL2 binding site (FBE1 ATTTT, FBE2 TTTGT, FBE3 CTAAACAA)
SMAD binding site (SBE AGACA, GTCTG, CAGACA, GGCGG TIE GNNTTGGtGa)

Ccnd2 promoter

CCTCCCGAGCCATTTCCTAGAAAGCTGTATCAATGTGGCCACGCTCCGCGCAGACACCTAGGGCGGCT
TGTCAGCAGATGCAGGGGCGAGGAAGCGGGTTTTTCCTGCGTGGCCGAGGCCCGCGGAGGAACCGCTG
CTAGCCCTGCCCCCGGTCTGGGGCCGCTCTGAGAGGCTGGCCGCGTTGCCCAATGGCGCCCCCAAGAA
CAGAAAGGTTTCTGCAGGAGGGTCATATTCTACTAGGCTTAAGAAGCACCCCTTTCTCCAACATCCAC
CCCTTCCTCCTCTTCCTCTCCACGCACGTGGCTCGGGGCGGACAACAGCTTGAAAGTTATCAGGAGTC
TAAGCTTGAGGGGCATAACCTTTATCCCTGGTTTGGCGAGGTTGCAATTTTCTCAAATAAGCCTTTCC
TTGTTCCTCATTTAGGGGTCTACTTCTAAGTTATCTGAACTCATCCACATGGTAAATCTATCTACCTG
AATCTTGAATAATGGGCTGTTTTTCTGATCACATTGCAAGCCTCCGAAGTTAGAGAGCACACACGTAC
ACACCCTTTATGCCCCCATGGTATGCCTACAGAATGTCAGAAAGGATAATCAATAGGAATCCATGGGG
TTTGTGGGTTCCCCTATCCGAGGCCCCTAGCATGCGGGGCTGGATGGGGAGAGGGCCTCGGAGAAGTA
GGGAGAGGGGTTGGGGGTGGGGAGCGGGGATCGTGTTTGAAGTTTGGTCAGGCCAGCTGCTGTGCTCC
TTAATAACAAGAGGGAAGGGGGGGGGGAGAGGGAGGGAAAGATTGAAAGGAGGGGAGGGACGCTAGAG
GAGGGGAGGAAAGGGGGAGGAGGAACCTGAGAGGGGGAGGAGATCTAACTGCCCTTCCAGCTTGCGTC
AC

Primer set	**Primers sequence (5'→ 3')**	**Annealing Temperature (ATºC)**	**bp**
Ccnd2.1	F:TTCTGCAGGAGGGTCATATTCT R:AATGAGGAACAAGGAAAGGCTT	57	207
Ccnd2.2	F:GTTAGAGAGCACACACGTACAC R:TGTTATTAAGGAGCACAGCAGC	59	233

p27 promoter

CTTTTTCAAAATTTAGTGTCTGGGACGGCTCTAAAGAGAGGCTTGGGAGAGCACTGGGGGTTTTCAAT
CTCGAGATCCTACGGTGGAAGCGCTTGGATTCAGAAACACCCTGATAAGAGCGGTCAGTCCTGGCTTC
TTTTTGAAACCGCCTCCTGGCCTGTCCTACATAGCAGAGACTTCTGGGGGTCAGGCTAAGCGGCCGATT
CCGCACCCCAGCTAAGGCACCCTGCCGGTGGGGGTGGGTGGGCTGCCCCAGGCCCTGAGCAAGGTTTC
CTGAACTTTGCGCATAGCGCTCCTCCATTCCCACCTCGGCGAATCGAGGTGGCTGAACTAGCCACCGA
AGCTCCTAATAAGCCGCCAGCGACCTCGGAGCCACTGGTCCAGGCCCTAGGTTTCGCGGGCAAAGACC
TGGAGGTGCAGTCGGGAGCGGTGACGCTGCCAGCCAGCTCTGCGCCGGGACCTAGATCCCCGGGTCCC
TGCCTGCGCGGCTGGCCCCTCCCCAGCTCTCCGGCCGTTTGGCTAGTTTGTTTGTCTTATTTTTAATTT
TCTCCGGGGCCAGCCAGAGCAGGTTTGTTGGCAGTCGTACACCTCCGGTAGTCACGCGACCAGCCAAT
GTCCTGGCGGCGCTACGGGGAGGCGGCTCGGGAGCGCGGAGAGCGGCGGCGCCGCGCCCCGGGCCACC
TTAAGAGCGCGCTCGCCAGCCTGGGCGGAGCGGCTCCCGGCGCCGAGACCAATGGAGCTCCTCCTCTG
TTTAAATAGACTTGCAGTGTCAATAATCTTCTTCTTCGTCAGCCTCCCTTCCACCGCCATATTGGGCA
ACTAAAAAAGAAGGGGGGCTCGTGCTTTTGGGGTGTTTTTCCCCCCTCATCCCTTGTCCCGACTCACT
CGCGGCTCCGAGACTGCGCGGCGGCAAGGTTTGGAGAGGGGCTGGTTCGCGGGACACACGGCTCGCCC
CAGCCTACGCTCCGACTGTTTGCCACCTCCTCCTGCCTCCTCCCCTCCCTTCCCCGCCCTCCAGTACA
CTTGATCACTGAAGCCTCGAGCTGCGCGGCGGCTGGGGTGTCCCTGCGCCTCTCTTCCCCAGACCTGC
GCGCTACTGCGGCTCGGGCGGTCGCTCGCCTGGCTCTGCTCCATTTGACTGTCTGTGTGCAGTCGCAG
AACTTCGAAGAGGGTTTTGCGCTCCATCCGTGGCGTTTCGCTTTTGTTCGGTTTTGTTGTTTATTTCA
TTTTTTTTTTTTCCGGA

Primer set	Primers sequence (5'→ 3')	Annealing Temperature (ATºC)	bp
p27.1	F:GTCAGTCCTGGCTTCTTTTTGA R:ATTAGGAGCTTCGGTGGCTAGT	60	231
p27.2	F: TTAGTGTCTGGGACGGCTCTAA R: GACCCCAGAAGTCTCTGCTATG	60	175
p27.3	F: AGAGCAGGTTTGTTGGCAGT R:AGAGGAGGAGCTCCATTGGT	-	188
p27.4	F: ACTGTTTGCCACCTCCTCCT R: AGTTCTGCGACTGCACACAG	60	182

Myc promoter

TCTAGAACCAATGCACAGAGCAAAAGACTCATGTTTCTGGTTGGTTAATAAGCTAGATTATCGTGTAT
ATATAAAGTGTGTATGTATACGTTTGGGGATTGTACAGAATGCACAGCGTAGTATTCAGGAAAAAGGA
AACTGGGAAATTAATGTATAAATTAAAATCAGCTTTTAATTAGCTTAACACACACATACGAAGGCAAA
AATGTAACGTTACTTTGATCTGATCAGGGCCGACTTTTTTTTTTAAGTGCATAATTACGATTCCAGTA
ATAAAAGGGGAAAGCTTGGGTTTGTCCTGGGAGGAAGGGGTTAACGGTTTTCTTTATTCTAGGGTCTC
TGCAGGCTCCCCAGATCTGGGTTGGCAATTCACTCCTCCCCCTTTCTGGGAAGTCCGGGTTTTCCCCA
ACCCCCCAATTCATGGCATATTCTCGCGTCTAGCCTTGATTTCCCCACCCCAGCTCCTAAACCAGAGT
CTGCTGCAAACTGGCTCCACAGGGGCAAAGAGGATTTGCCTCTTGTGAAAACCGACTGTGGCCCTGGA
ACTGTGTGGAGGTGTATGGGGTGTAGACCGGCAGAGACTCCTCCCGGAGGAGCCGGTAGAGCGCACCC
GCCGCCACTTTACTGGACTGCGCAGGGAGACCTACAGGGGAAAGAGCCGCCTCCACACCACCCGCCGG
TGGAAGTCCGAACCGGAGGTGCTGGAGTGTGTGTGTGGGGGGGGGGGGGGGAATCTGCCTTTTGGCAG
CAAATTGGGGGGGGGGTCGTTCTGGAAAGAATGTGCCCAGTCAACATAACTGTACGACCAAAGGCAAA
ATACACAATGCCTTCCCCGCGAGATGGAGTGGCTGTTTATCCCTAAGTGGCTCTCCAAGTATACGTGG
CAGTGAGTTGCTGAGCAATTTTAATAAAATTCCAGACATCGTTTTTCCTGCATAGACCTCATCTGCGG
TTGATCACCCTCTATCACTCCACACACTGAGCGGGGGCTCCTAGATAACTCATTCGTTCGTCCTTCCC
CCTTTCTAAATTCTGTTTTCCCCAGCCTTAGAGAGACGCCTGGCCGCCCGGGACGTGCGTGACGCGGT
CCAGGGTACATGGCGTATTGTGTGGAGCGAGGCAGCTGTTCCACCTGCGGTGACTGATATACGCAGGG
CAAGAACACAGTTCAGCCGAGCGCTGCGCCCGAACAACCGTACAGAAAGGGAAAGGACTAGCGCGCGA
GAAGAGAAAATGGTCGGGCGCGCAGTTAATTCATGCTGCGCTATTACTGTTTACACCCCGGAGCCGGA
GTACTGGACTGCGGGCTGAGGCTCCTCCTCCTCTTTCCCCGGCTCCCCACTAGCCCCCTCCCGAGTTC
CCAAAGCAGAGGGCGGGGAAACGAGAGGAAGGAAAAAAATAGAGAGAGGTGGGGAAGGGAGAAAGAGA
GGTTCTCTGGCTAATCCCCGCCCACCCGCCCTTTATATTCCGGGGGTCTGCGCGGCCGAGGACCCCTG
GCTGCGCTGCTCTCAGCTGCCGGGTCCGACTCGCCTCACTCAG

Primer set	**Primers sequence (5'► 3')**	**Annealing Temperature (ATºC)**	**bp**
Myc.1	F:CGAGATGGAGTGGCTGTTT R:TGTGTGGAGTGATAGAGGGT	57	207
Myc.2	F:GCGCTATTACTGTTTACACCC R: CCTCTCTTTCTCCCTTCCC	57	233
Myc.3	F:GGCATATTCTCGCGTCTAGC R:TGAAGACAAACGGATGAACAGT	60	154

Follistatin promoter (2000bp upstream)

ATAGTGGTGGGGACATAGGAAGGTGAATAACAAACTTCCTCAGTAGTACATCACAGCATAAGTATCTC
TGAGTAAAGAAGAAAACAGTTCAACTTTGAAATTCTGCCGTTAAGTGGCGGCTCCTGCAAGGGGGACA
GTTTGCTATTAATTGTTAATGTCGCCTACCATTAGAGGGCACTAAACAACTCCACATTAATGCGTTGG
AGGGAAGAGAAAAGGAAGCGAGGAAAGGGGAGGGAGAGTATGGGCAGAGTTCGGGGAGAGGGAGGGGA
GACCGAAGCCGGGAAGGGCTGGGAAAAAGAGATGTGGGGAGTGGGAGGAGGGAGGAGGGAGGAGGGAG
GAAAAAGCCTGAAGAGGAAGGAGACTGACAAACGGGCAGACAGACAGAAACAGACAAAATGAATCTGG
CAAGATTAAGAAGGATGTGAAGCCCCAGAGCCGTCTAAAGTGAGCAAAAAGCCGGCTCTCCCGGGTCA
CCCACTCCCCTCCCCGCCGCTCCGTCCTCATGACTGTAATTATAAAGCGAAAAGCGGCGGCGAGGTCA
CCCGTTTTTACCAGCCTGCTGCACCGAATGCGCGCGGTGCAGGTGCGGCGGCCGCGGGGCTTTGTGAT
TCATGCCCACTTTCAAAGCGGGGCTTGGGCCCGTCTGAGAGGCACCCAAACAACTGTCTTCTAATATT
AGCACGGCTGTATTTCGGGATCTATTATAGTCTGTCCAGACAGATCCCATTGTAATGGGACCTTTTAT
TAAAAGATTAGCACTATCTCCTGCAGTTGGTGGAAAAAAATCTGTTATCACTGAGTTATTTGCAGTTG
TGGAGGGGGTAGGAGGAGGGTGATGGAAGATGGGGGTGGGAGGATGAGAGGAGGACCGGGGGGGGGGG
GCGCTAGGGCTGGGGCTAGAGAAGAAGGGCGAATTTGAAATCCGTAAGAGCAAATCCCAATGACCTGG
GAATGTCCAAGAATTTTGTCTGTTTTGTTCGCTGTTTGTTGTCGTTCGGGCTTCAGAAGCGAAAAGAA
TAGAAATTTAAAAGGCAGCTTTGAAATAAACAATATAGCCTTTTCCGTGAAGTAATCGTTTTATATAA
AAGGAAATATCGCCTCCTCAGTTTCATTCAGCCGTGCCAGAAAATGTTATAAATGAGAAGACCCGCCA
ACTTTCGGCGAAGAATGCCAGGCATTGCACTCAATAAACTGAGGCTGCAGAAGTTCATTATCATGGTG
CAATCTTTTTTTTAAATAAGAGAGAGAGAGAGAGAGAGAGAGGAGTCGGGACAGAAACTGGGGCGT
CTCGGAGCGGGGGAGGAGGGGGGCAGACCGCCTACGTCGGCGCCCCCGCTCGGGGCTGCGACTCCAGA
CGCGACGAAGTGAAAGGGGAGAAAAGAAAGGGAGAGGGCGAGACTGCCGGGGGCGGCCGGCTCCGAGG
TGTTAAACATTTTTGTTTGCTTCTGACTTGTGGAGCCCGAGGGCCGCGTCTCCGCAGCGCTCGGCCCG
GGTGGAAGGTGCCCGGGGGTCGGGGTTCTTAGCAACCTACTCCAGGCTGGGGGGGGAGGGGGCGCGGG
AGGGAGTGGGAGGCGGGGGAGCTGGCAGGGTGGCCGCAAAGTAAGACACGTAAGAGACCTCGGGACAC
AAAACGTCTCCGGGACCCCGCGCCAAGGCTCTGCAGGGAGGCTCCTGAAACTGCTCCCCCGGGCATTG
AAGCAGCTCAGGGATCCTGCGGCGGGTTGCAGAAGTCTCATCCCGGAGCCCTGGAGCAGAGGTGCTGG
GGACCCATTCCCGGGGTCCTCCGGGGTCCCCGCGCTCCGCCGGCCGCCTCCTCCAGCGCCCTCACTCA
CACGCGCACACGCACACACGCGCGCACACACACACTCGCACGCCACCCCGGGCGCGCCGGCTCCGAGC
GGCGGCGTGCAGGACTGAAGTGGATGTTCCTCCCCACCCCCGACGCGTCGCCCCCAGCCCCCGCCCCT
GCCTCCTTCCCCCCTCCCCTCCCGCTCCTACGCAAATAAGAACTCGGCGATTCCCCTCCTGCCGCTTT
GATTTCGGGCACCTCCGACAGATAATTGGGAAGGGTTTCCAGAAGGTGGGAAATGTCACCTGATTCAC
ACTGAACTTTTAAAAGCTCCCCACCCCCAAAGAGCCGGCACACCCTCGGTCGCGGCCGCCCTCCCACA
GCCCCACACACTGGGAGACCGCCCACCGCAAACCTCGGAGACCCCCGTCTAGATTTAAAGCGCGGCTG
CGCCCGGCTTCT

Gene	Primers Sequence (5'➔ 3')	Annealing Temperature (ATºC)	bp
Follistatin1	F:ACCTCCGACAGATAATTGGGAA R:CGCGCTTTAAATCTAGACGGG	59	190
Follistatin2	F:GCACCCAAACAACTGTCTTCTA R:CCCTCCACAACTGCAAATAACT	59	170
Follistatin3	F:AAGAGCAAATCCCAATGACCTG R:TGAATGAAACTGAGGAGGCGAT	59	189
Follistatin4	F:ATAAATGAGAAGACCCGCCAAC R:CAGTTTCTGTCCCGACTCCT	59	150
Follistatin5	F:GGCTCCGAGGTGTTAAACATTT R:TCTTACGTGTCTTACTTTGCGG	59	201

FSHb promoter (2295bp upstream)

ACCTGCCCTCCCACCACACCTGCCCTCCAACCACACCTGCCCTCCTACCACACCTGCCCTCCTACCAC
ACTTGTCCACCTACCACACCTGCCCTCCCAACCACACCTGCCCTCCCACCACACCTGCACTCCAACCA
CACCTGCCCACCTACCACACTTGTCCACCTACCACACCTGCCCTCCCAACCACACCTGCCCTCCAACC
ACACCTGTCCACCTACCACACCTGCCCTCCCAACCACACCTGCCCTCCAACCACACCTGTCCACCTAC
CACACCTGCCCTCTCATCACACCTGCCCACCTAGGACACCTGTTCATTAACCACTGAGCTCTATCTTT
CTGCTTGATTGGGGATTGAGCTCCCCCATGGTCCTGCCTAAAAGTAGAACCTCCATATACACTCTAAA
ACCATCTGTACTCTTGTCTTTAGAGACACTCAAAAATCTCTCTGGGTTTTCACTCTATATAAACATCC
CATCTCCATGTGAGCATTCATTTATTTCTTCCTCTTAAAAGTAAAAATAAATATAAAACTATTTTTAC
TCTACTTCTGCACTGCTCAATTATATATTTTTCTTGCTAATACTTATAAGAAAATTCTTAAAGAAGTT
ATCTATGTTCACTACATGTCACTTCCTCTCCCCTGACATGTGAGCCAAATGCTGCATAAAAGAAGGGC
TCAGAGTTATATAACATATCTTGAGATCTAATCCTTAGCTAGAGAAGTTGAATGGATGGAAGCTATAA
CCTAGTATTTGTTTAAAAGGTTGAGAAGAGATAACATGTACCTGACTTCTAGGAGACGATATTCTCCT
CAATTCATACACTACTCAATGACACTTCTCAACTTCATTTGGATAGAAGAAAGGAAGAAGAAAACAAA
GAGGATGAGGAAGAAGATTCATTGTATCCTTGAAATAGTAGTATTGGAGTTTAACCATCTTCAACTAT
TCTATTCTCATTCTCTGTTCTCTTCAGTCAAGATATGTCTCTAAATCTAGATTCACCAGTCTATGTAA
GTGTATTATAGACACATCACAGTCAACATATCTATACAGAATGTCTTAGGTTTTCCAAAATGCACATC
CTTAACCATTCCATCTTTAGACTCATCCTCACCTTTCTTCCATACTCAACATCAATCCAGCAGAAATG
TTCTTTCTAGTTTCAAAATATATCCAGAGTAATAGCATGACTCATAACATCCATTGTTCCCACATTGG
CCCAAACAAACACCATGCCTCACCTGTGTTACTACAAACCATCTTAGTAATATCTTCCTGCTTCTACC
GTGTTTCTCTTAGCAACAAAGAAATGAGAAGGATTCCTTTGAAGCAGATTATAAAACTCTCTACTTAA
AATCCTACAGTGGACCAAATCACACAGAGTGAAAATTGAAATACTTACATTGGGCTCTAAGTTCTATT
ACATTTCTGACATGCTCCCCTAACATTTTTACACTATTGATCCTTGTTTCTAATCATATTATTAATAA
ATGAATATTACAAATTAATAAATGAGTTAAACAGCCTCATTCTCTATAGAGTTCACAGAATCCTGATA
GAAATGGGTATATGAATAACTACAATCAGAAAGAGATTATAACTCTCCTTACCATTGGCCCTAAATTA
GAGGTGAAGCACCTCTGTGTGGTAAAGTTTCAAGAACTTTGTGGGAAAGAAAAGACAGAAAAGAAGCA
AGGGCATTGGTGACAGAGAGGACATCACATGCAGAGATCTGGAGGAACCCATCAGTATCATAATTAGG
GAATATTTAGGGAATTACAATTTCTGATGCTCTTCACAAAGCATCAGAAAAAGGGGGGTTGAGATCAG
GAGAACTGAATGTGGTCATAAAGAAAGACACAGCCCATAGGAACAAGATGCAGAAGTACTTCCTATTT
GTTCATACACTTGGAGTGTTCAGTCTGTTCTTGGATCAATTAAGACATATTTTGGTTTACCTTCGCAA
TGGAGCCAAAGCAATGTTCAGAAAGGATTCTGAGTTCGCCAAGTTAAAGATCAGAAAGAATAGTCTAG
ACTCTAGAGTCACATTTAATTTACAAGGTGAGGGAGTGGGTGTGCTGCCATATCAGATTCGGTTTGTA
CAGAAACCATCATCACTGATAGCATTTTCTGCTCTGTGGCATTTAGACTGCTTTGGCGAGGCTTGATC
TCCCTGTCCGTCTAAACACAATGATTCCCTTTCAGCAGGCTTTATGTTGGTATTGGTCATGTTAACACCC
AGTAAATCCACAGGGTTTTAAGTTTGTATAAAAGATGAGGTGTAACTTGAC

Gene	Primers sequence (5'→3')	Annealing Temperature (ATºC)	bp
FSH.1	F: CCACTGAGCTCTATCTTTCTGC R: TTGAGCAGTGCAGAAGTAGAGT	59	242
FSH.2	F: AAAGGATTCTGAGTTCGCCAAG R: TTAGACGGACAGGGAGATCAAG	59	198

Appendix 4. RNA quality and integrity of samples from day 4 , 8 and 16 mouse ovaries (A) and day 4 cultured ovaries (B) under control (C), TGFβ1 ligand (T), A 83-01 inhibitor (I) and A 83-01 inhibitor +TGFβ1 (BO). Concentration and RIN number of all RNA samples used for gene expression analysis, determined with the Agilent Bio-analyser. An example of the electropherogram of a good sample (sample 1) is shown.

A)

RNA sample	**1**	**2**	**3**	**4**	**5**	**6**	**7**	**8**	**9**	**10**
Day	4	4	4	4	4	8	8	8	8	8
RIN	9.5	9.7	10	9.5	9.5	7.8	9.8	9	9.7	9.4
Concentration (ng/µl)	13.5	15.6	3.15	6.3	15.3	16.8	9.8	8	6	11

RNA sample	**11**	**12**	**13**	**14**	**15**
Day	16	16	16	16	16
RIN	6.2	9.1	9.8	-	-
Concentration (ng/µl)	34	28.7	40.6	20	20

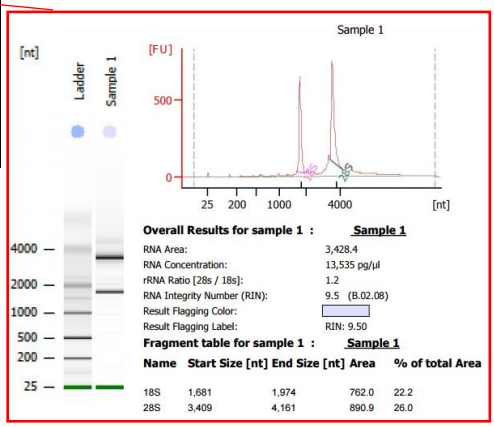

B)

RNA sample	**1**	**2**	**3**	**4**	**5**	**6**	**7**	**8**	**9**	**10**
Treatment	C	C	C	C	C	T	T	T	T	T
RIN	9.9	9.5	9.3	9.8	N/A	9.9	10	9.7	9.9	9.2
Concentration (ng/µl)	1.1	15.7	18.7	36	7.8	36	2.7	10.5	5.04	15

RNA sample	**11**	**12**	**13**	**14**	**15**	**16**	**17**	**18**	**19**	**20**
Treatment	I	I	I	I	I	BO	BO	BO	BO	BO
RIN	10	8.7	9	9.9	10	2.5	N/A	9.3	9.6	9.4
Concentration (ng/µl)	34	13.9	8.5	10.2	15.8	0.4	9.3	13.8	15.1	11.3

Appendix 5. cDNA quality assessment with the reference gene *Htrp1* of retro-transcribed RNA samples from day 4, 8 and 16 ovary samples and day 4 cultured ovaries. Day 4 (1-5), day 8 (6-10) and day 16 (11-15). Day 4 cultured ovaries: control (1-5), TGFβ1 ligand (6-10), A 83-01 inhibitor (11-15) and A 83-01 inhibitor +TGFβ1 (16-20).

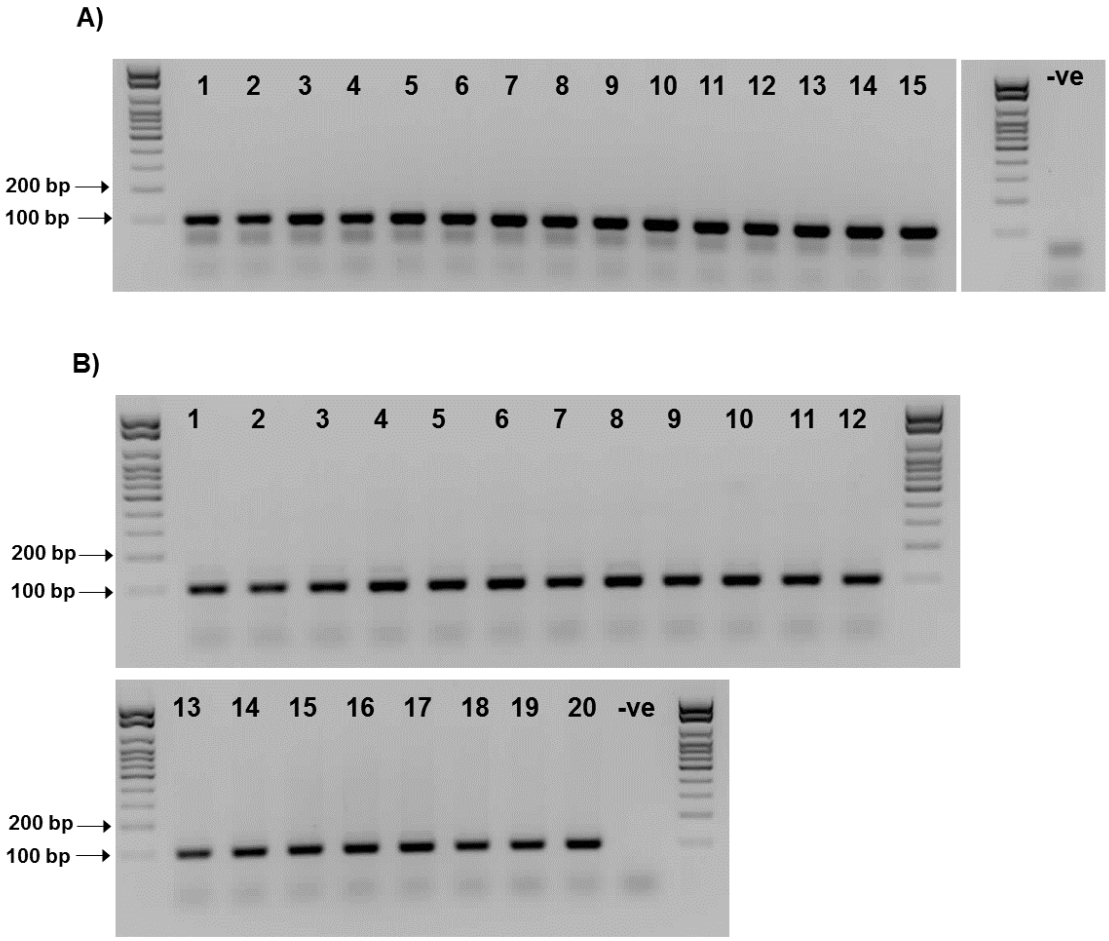

Appendix 6. Antibody specificity and chromatin shearing. In A) a western blot with SMAD2/3 and FOXL2 antibodies used for ChIP (day 4, 8 and 16 ovary samples) showing the expected bands. In B), immunoprecipitation with SMAD2/3 antibody shows IP specificity. C) shows sheared chromatin from day 4 and day 16 ovary samples used in chapter 3. D) shows sheared chromatin from day 4 and day 16 ovary samples (n=5) used in chapter 5. E) shows sheared chromatin from day 4 cultured ovaries (n=5) under control (D), TGFβ1 ligand (T), A 83-01 inhibitor (I) and A 83-01 inhibitor +TGFβ1 (BO) treatments.

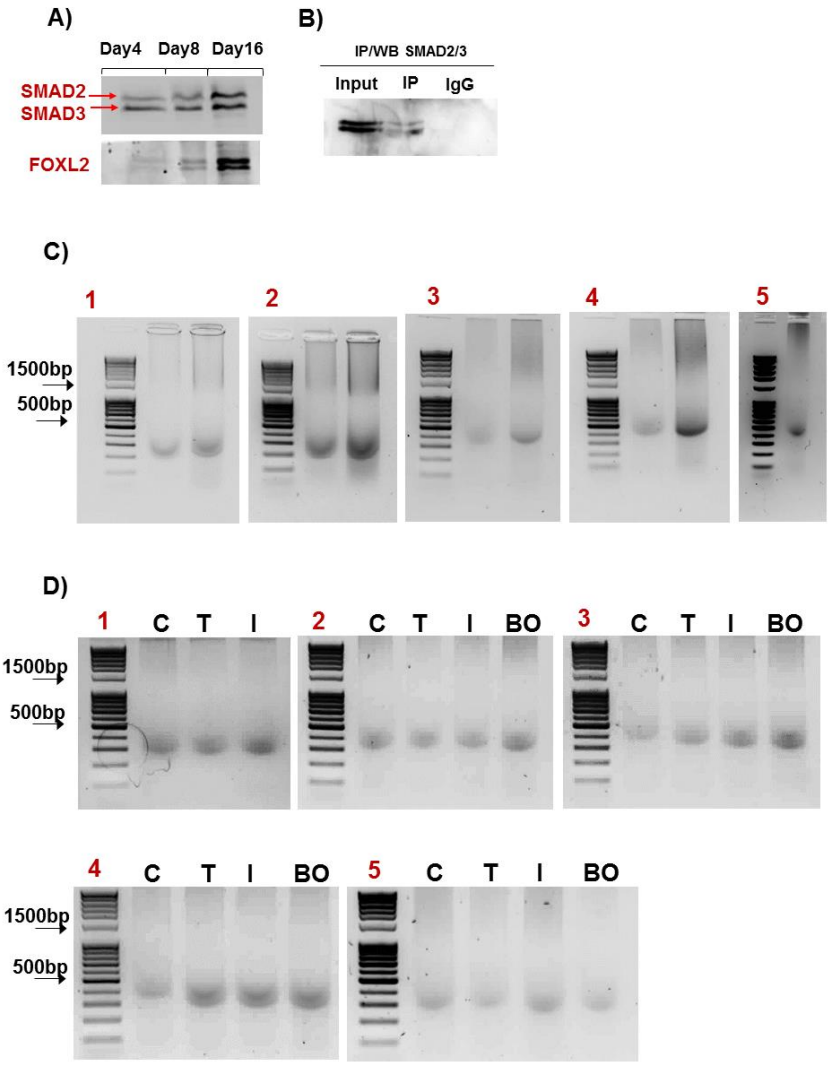

Appendix 7. Composition of protein extraction buffers A, B and C for subcellular fractionation of proteins in day 4 and day 16 ovaries (Baghirova et al, 2015).

Buffer	Composition
A	NaCl 150mM HEPES (pH 7.4) 50mM Digitonin (Sigma, D141) 25 μg/mL Hexylene glycol (Sigma, 112100) 1M
B	NaCl 150mM HEPES (pH 7.4) 50mM Igepal (Sigma, I7771) 1%v/v Hexylene glycol (Sigma, 112100) 1M
C	NaCl 150 mM HEPES (pH 7.4) 50 mM Sodium deoxycholate 0.5% w:v Sodium dodecyl sulfate 0.1% w:v Hexylene glycol 1 M

Appendix 8. Western blot showing CCND2, p27 and beta-actin (loading control) protein expression in NIH3T3 cells. Graphs show the individual blots from three independent experiments (n=3) where cells were serum-deprived for 24 hours and then stimulated with 10%FCS for the stated times (hours). OD values for each protein are normalised against beta-actin.

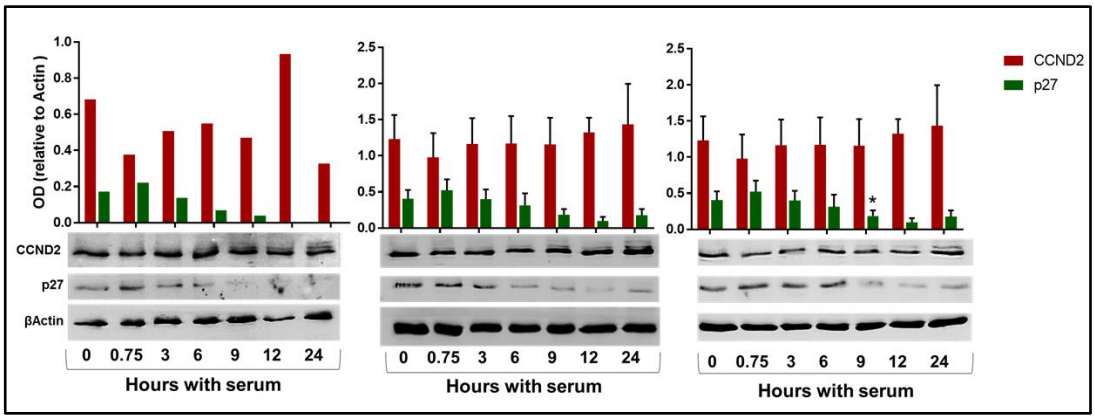

Appendix 9. Relative mRNA levels of *p15* in day 4, day 8 and day 16 ovaries (A) and in day 4 cultured ovaries treated with TGFβ1 ligand and A 83-01 inhibitor (B).

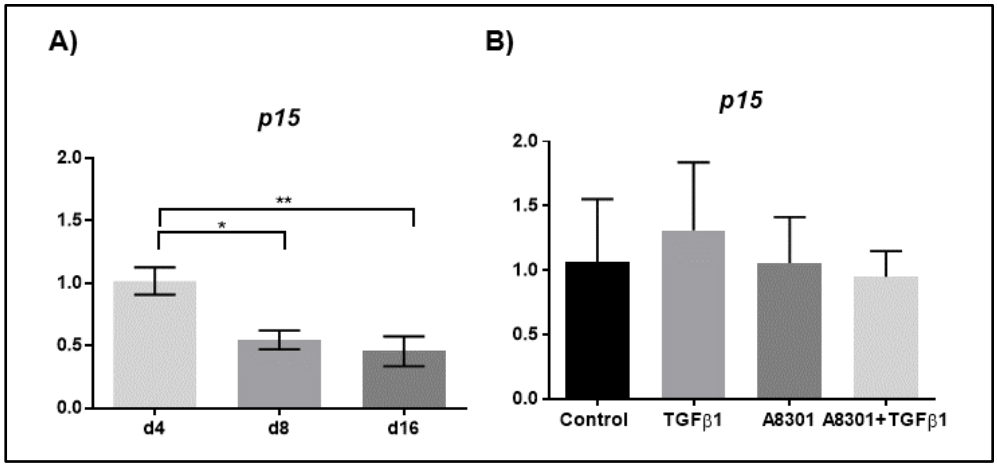

Appendix 10. Diagram of Co-immunoprecipitation protocol with p27 and CCND2 antibodies. Assuming p27 is present only in complex but CCND2 can be present alone, when p27 antibody is used for the IP, only CCND2 in complex is detected (A). When CCND2 antibody is used for the IP, both CCND2 in complex and alone is bound, but only p27 in complex is detected (B).

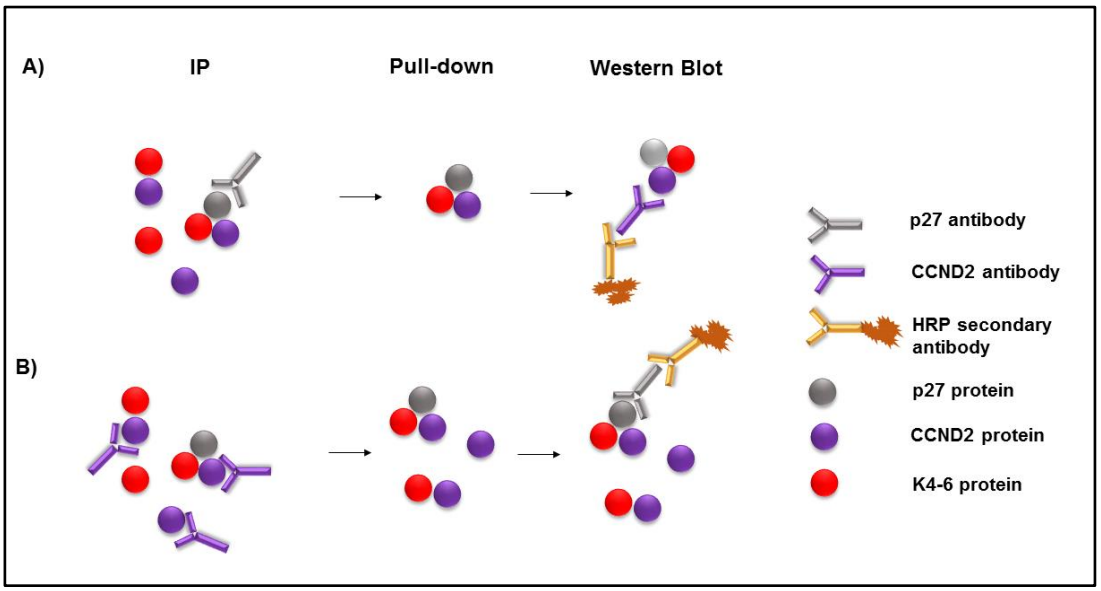

Appendix 11. Literature search from PubMed database based on the search terms "TGF-beta-1" and "ovary". From 210 papers identified after the search, individual papers were excluded based on the relevance to the topic and culture models. Selected papers are shown on the table and classified according to the culture system and dose used for TGFβ1 ligand

Search term	TGFβ1 ligand amount	GC/follicle culture	Non-GC culture	Ovary culture
TGF-beta-1 AND ovary	≥10ng/ml	(Rodrigues et al, 2014) (Fang et al, 2014) (Méndez et al, 2006)	(Kohan-Ivani et al, 2016; Pan et al, 2015) (Kohan-Ivani et al, 2016)	(Wang et al, 2014b) (2008; Rosairo D 2008) (Schindler et al, 2010)
	≤5ng/ml	(Yao et al, 2010) (Liang et al, 2013) (Yin et al, 2014) (Cheng et al, 2015) (Fazzini et al, 2006)	(Yao et al, 2014)	(2008; Rosairo D 2008)

Appendix 12. Western Blot showing SMAD3 phosphorylation in PHM1 cells treated with A 83-01 inhibitor. PHM1 cells were exposed for different time points to 1µM and 10µM of A83-01 inhibitor. Non-labelled lane corresponds to the ladder, where the 63kDa band is shown.

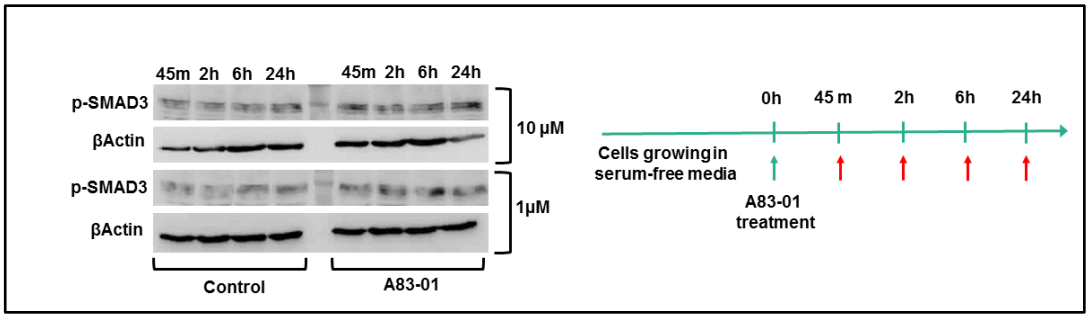

Appendix 13. Positive correlation between oocyte area (µm^2) and oocyte diameter (µm) in small follicles in the mouse ovary. Two representative sections are counted from the control group of day 4 cultured ovaries.

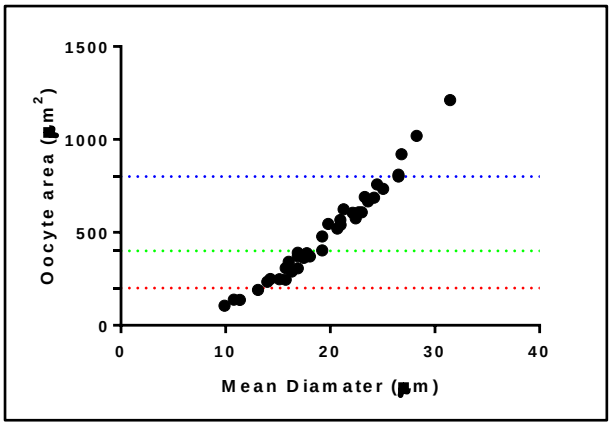

Appendix 14. Nfat and Calcineurin expression in juvenile mouse ovaries. Conventional PCR amplification of the different Nfats (C1, C2, C3 and C4) and Calcineurin (CA, CB and CC) isoforms are shown in day 4 and day 8 ovaries (A) together with GDF9 as control. Western blotting for Calcineurin in day 4, day 8 and day 16 ovaries shows protein expression in all ovary ages (B).

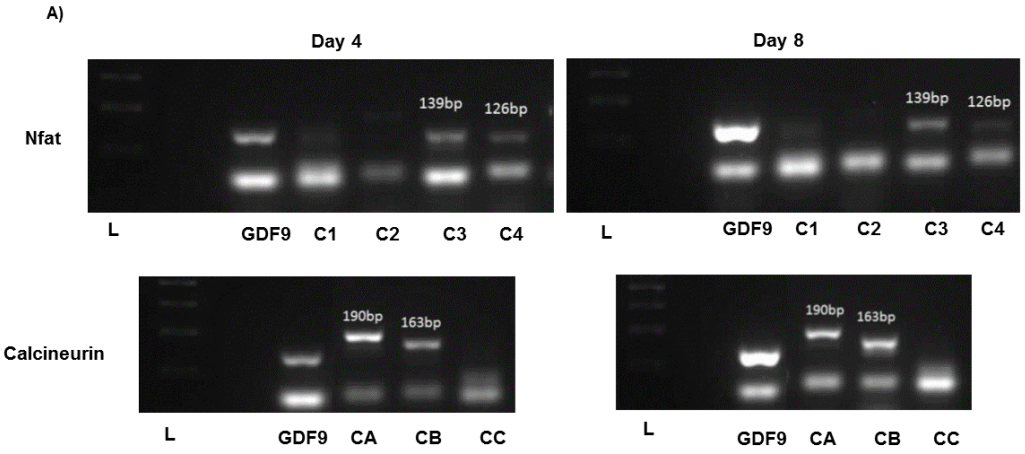

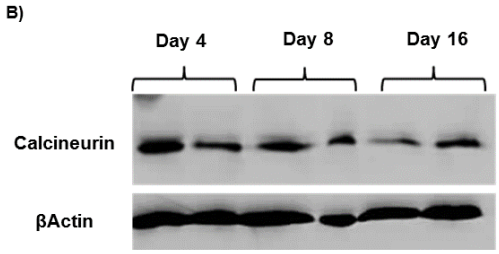

Appendix 15. Permission obtained for the use of Figure 1.4.

OXFORD UNIVERSITY PRESS LICENSE
TERMS AND CONDITIONS
Jul 19, 2017

This Agreement between The University of Sheffield -- Sofia Granados Aparici ("You") and Oxford University Press ("Oxford University Press") consists of your license details and the terms and conditions provided by Oxford University Press and Copyright Clearance Center.

License Number	4147750061154
License date	Jul 14, 2017
Licensed content publisher	Oxford University Press
Licensed content publication	Human Reproduction
Licensed content title	A new model of reproductive aging: the decline in ovarian non-growing follicle number from birth to menopause
Licensed content author	Hansen, Karl R.; Knowlton, Nicholas S.
Licensed content date	Jan 12, 2008
Type of Use	Thesis/Dissertation
Institution name	
Title of your work	TGFβ signalling and cell cycle regulation during early follicle development
Publisher of your work	n/a
Expected publication date	Jul 2017
Permissions cost	0.00 GBP
Value added tax	0.00 GBP
Total	0.00 GBP
Requestor Location	The University of Sheffield The Jessop Wing, Level 4 Tree Root Walk Sheffield, South Yorkshire S10 2SF United Kingdom Attn: The University of Sheffield
Publisher Tax ID	GB125506730
Billing Type	Invoice
Billing Address	The University of Sheffield The Jessop Wing, Level 4 Tree Root Walk

	Sheffield, United Kingdom S10 2SF Attn: The University of Sheffield
Total	0.00 GBP

Terms and Conditions